

# **Chemotactic factors underlying tumor infiltration by immunocompetent cells in human colorectal cancer**

## **Inauguraldissertation**

Zur

Erlangung der Würde eines Doktors der Philosophie

vorgelegt der

Philosophisch-Naturwissenschaftlichen Fakultät

Der Universität Basel

von

**Cremonesi Eleonora**

aus Italien, Lodi

Basel, 2017

Original document stored on the publication server of the University of Basel  
[edoc.unibas.ch](http://edoc.unibas.ch)



This work is licensed under a [Creative Commons Attribution-NonCommercial 4.0 International License](http://creativecommons.org/licenses/by-nc/4.0/).

Genehmigt von der Philosophisch-Naturwissenschaftlichen  
Fakultät

auf Antrag von

Prof. Dr. Christoph Hess

Prof. Dr. med. Giandomenica Iezzi

Prof. Dr. med. Alfred Zippelius

Basel, 22.03.2016

Prof. Dr. J Schibler

Dekan

During my PhD training I have extensively investigated the role of chemotactic factors involved in the recruitment of beneficial immune cells in human colorectal cancer (CRC).

This thesis consists of an **introduction** highlighting the clinical relevance of immune cell infiltration in CRC, and providing an overview of CRC microenvironment determinants and their possible influence on immune cell migration. A complete description of **methods** used and **results** obtained is then included. Finally, major findings and their implications are reviewed in the **discussion**.

The results of this study have been included in a manuscript currently under preparation.

Beside my main research project, I have also been involved in additional projects of our group addressing the prognostic significance of a number of immune cells markers in human CRC, including interleukin-17A (IL-17), granulocyte macrophage colony-stimulating factor (GM-CSF), tumor necrosis factor receptor superfamily, member 4 (TNFRSF4, also known as OX40) and programmed death-ligand 1(PD-L1), and the development of innovative tridimensional systems for culturing human CRC cells in vitro. Publications resulting from these studies are included in the **appendix**.

*To my family...*



## **Summary**

Colorectal cancer (CRC) is a common digestive tract malignancy and a major cause of cancer mortality. Several studies have convincingly shown that CRC infiltration by immunocompetent cells and, in particular, cytotoxic CD8<sup>+</sup> T cells (CTLs), IFN- $\gamma$ -producing T-helper 1 cells (Th1), Foxp3<sup>+</sup> regulatory T cells (Tregs), and CD16<sup>+</sup> MPO<sup>+</sup> neutrophils, is significantly associated with prolonged patient survival. However, the chemotactic factors driving these cell populations into the tumor site, their cellular sources and their microenvironmental triggers remain to be elucidated.

During my PhD training I have investigated the chemokine/chemokine receptor network promoting CRC infiltration by immune cells associated to favorable prognosis.

In particular, I addressed:

1. The expression of immune cell markers and their correlation with chemokine expression in primary CRC tissues;
2. The identification of chemokine receptors relevant for CRC infiltration by beneficial immune cells;
3. The chemokine sources in CRC;
4. The microenvironmental stimuli triggering chemokine production in CRC tissues;
5. The effects of chemokine production on immune cell recruitment into CRC.

The expression of a panel of genes encoding 39 chemokines and 7 markers specific for defined immune cell populations was assessed by quantitative PCR array in 62 samples of freshly excised primary CRC and autologous healthy colonic tissue. Correlations between expression of chemokine genes and immune cell markers were then evaluated.

Furthermore, chemokine receptor profiles were analysed by flow cytometry on cell suspensions obtained upon digestion of clinical specimens or on corresponding cell populations from autologous peripheral blood. Based on chemokine receptor expression on

tumor infiltrating cells and correlations between expression of chemokines and immune cell markers, I could identify for each immune cell subset a putative “chemokine signature”:

- 1) CCL3, CCL5, CCL8 CXCL9, CXCL10 and CXCL12, associated with recruitment of cytotoxic CTLs;
- 2) CCL5, CCL22, CXCL9, and CXCL12 correlating with infiltration by Th1;
- 3) CCL22 and CXCL12 potentially attracting Tregs;
- 4) CXCL2 and CXCL5 promoting chemotaxis of CD16<sup>+</sup> MPO<sup>+</sup> neutrophils.

I have further investigated potential chemokine sources and stimuli leading to chemokine release within CRC tissues. I found that CRC cells purified from primary tumor specimens express many of the genes encoding identified immune cell recruiting chemokines, including CCL3, CCL5, CXCL2, CXCL5, CXCL9 and CXCL10. In vitro experiments showed that chemokine production by CRC cells is triggered upon their exposure to microbial stimuli, such as Toll-like receptor agonists, or CRC-associated bacteria, including *Fusobacterium nucleatum*, *Bacteroides Fragilis*, *Bacteroides vulgatus*, and *Escherichia Coli*, thus suggesting that components of the gut flora may critically influence chemokine production in CRC tissues. This was indeed confirmed by “in vivo” experiments showing that chemokine gene expression in xenografts, generated upon injection of human CRC cells in immunodeficient NSG mice, appeared to be related to the presence of commensal bacteria. In particular, chemokine gene expression levels in intracecal xenografts, were found to be  $\geq 10$  fold higher as compared to those of subcutaneous xenografts, and they were significantly reduced upon antibiotic treatment of tumor bearing mice.

Most importantly, a correlation between extent of immune cell infiltration and bacterial load was also observed in human CRC samples. Indeed, CRC samples characterized by high expression of chemokine and immune cell markers, displayed significantly higher bacterial loads, as assessed by analysis of bacterial 16S ribosomal RNA, as compared to samples

showing low chemokine expression and immune cell infiltration. In addition, a significant correlation between bacterial load and expression of the Th1 marker IRF1, CCL3 and CCL5, was also detected.

Our *in vitro* and *in vivo* results cumulatively suggest that bacteria-induced chemokine production by tumor cells may lead to tumor infiltration by beneficial immune cells. Consistent with this hypothesis, in preliminary “*in vitro*” experiments, I found that supernatants of bacteria-stimulated CRC cells promote chemotaxis of CTLs and Th1 cells to a higher extent than untreated tumor cells.

Additional “*in vivo*” studies are clearly warranted. In particular, I plan to evaluate intratumoral recruitment of CRC-derived CTLs and Th1 cells upon adoptively transfer into intracecal xenografts-bearing mice.

Bacterial species or strains mostly contributing to high chemokine expression and immune cell infiltration in human CRC samples also remain to be identified. Microbiome analysis of CRC samples characterized by high or low immune cell infiltration might be envisaged in future studies.

The results of the present work together with the proposed additional studies will contribute to the understanding of the interplay occurring between gut flora and immune system in CRC, and may pave the way towards innovative treatments aimed at modifying the gut flora in order to promote CRC infiltration by beneficial immune cell subsets.

# Table of content

<b>Summary</b> .....	1
<b>I. INTRODUCTION</b> .....	<b>6</b>
1.Human colorectal cancer .....	7
1.1 Epidemiology and etiopathogenesis .....	7
1.2 Staging and prognosis.....	9
1.3 Current treatment guidelines .....	10
2.CRC immune contexture .....	11
2.1 Definition of immune contexture .....	11
2.2 Impact of immune contexture in CRC.....	12
3. Immune cell trafficking in CRC .....	13
3.1 Chemokines and chemokine receptors .....	13
3.2 Role of chemokines in leukocyte trafficking.....	17
3.3 Gut homing receptors .....	17
3.4 Prognostic significance of chemokine expression in colorectal cancer.....	18
4. Pathophysiology of CRC microenvironment .....	18
4.1 Physiology of normal colonic mucosa .....	18
4.2 The gut microbiota .....	20
4.3 Interactions between gut flora and normal colonic epithelium .....	21
4.4 Physiopathology of gut epithelium in CRC.....	25
<b>II. AIM OF THE STUDY</b> .....	<b>28</b>
<b>III. MATERIALS AND METHODS</b> .....	<b>30</b>
1. Clinical specimen collection and processing.....	31

2. Cell lines.....	31
3. Bacteria.....	31
4. Flow cytometry.....	32
5. Real-time reverse transcription PCR assays.....	33
6. CRC cell stimulation with TLR agonists and bacteria .....	34
7. Migration assay .....	35
8. Generation of CRC xenografts .....	35
9. Statistical analysis .....	36
<b>IV. RESULTS.....</b>	<b>37</b>
1. Expression of immune cell markers in primary CRC.....	38
2. Chemokine gene expression in primary CRC .....	41
3. Correlations between expression of immune cell markers and chemokine genes in CRC.....	41
4. Chemokine receptor expression on CRC infiltrating beneficial immune cells .....	42
5. Chemokine signatures underling immune cell recruitment in CRC.....	47
6. Chemokine sources in primary CRC .....	47
7. Effects of microbial stimulation on chemokine production by CRC cells in vitro.....	49
8. Effects of microbial stimulation on chemokine production in vivo .....	52
9. Effects of chemokine production on immune cell recruitment into CRC tissues.....	54
<b>V. DISCUSSION AND OUTLOOK .....</b>	<b>56</b>
1. Discussion .....	57
2. Outlook.....	62
<b>VI. BIBLIOGRAPHY .....</b>	<b>64</b>
<b>VII. APPENDIX .....</b>	<b>74</b>

# **I. INTRODUCTION**

# **1.Human colorectal cancer**

## **1.1 Epidemiology and etiopathogenesis**

Colorectal cancer (CRC) is the third most frequent type of cancer worldwide. In 2012 about 1,361,000 new CRC cases (9.7% of total cancer incidence) and approximately 694,000 deaths (8.5% of total cancer deaths) were globally reported [Ferlay J. et al., 2013]. The highest incidence is reported in westernized countries [Center MM., et al., 2009]. In particular, in Europe 447,136 new cases of CRC have been reported in 2012 [Ferlay J., et al., 2015]. Notably, in Switzerland, CRC causes 1600 deaths per year (National Institute for epidemiology and cancer registration, NICER, Switzerland).

Risk factors include smoking, alcohol intake and increased body weight [Kuipers E., et al 2015]. Furthermore, chronic colitis due to inflammatory bowel disease (IBD) is also associated with an increased risk of CRC. However, IBD explains only 1% of CRC in westernized population [Jess T., et al., 2012].

CRC results from the accumulation of genetic and epigenetic mutations transforming the normal colonic epithelium initially into benign neoplasia (adenoma), and, subsequently, invasive adenocarcinoma. The steps involved in this process are described in the classic tumor progression model proposed by Fearon and Vogelstein [Fearon & Vogelstein, 1990], (Figure I.1).

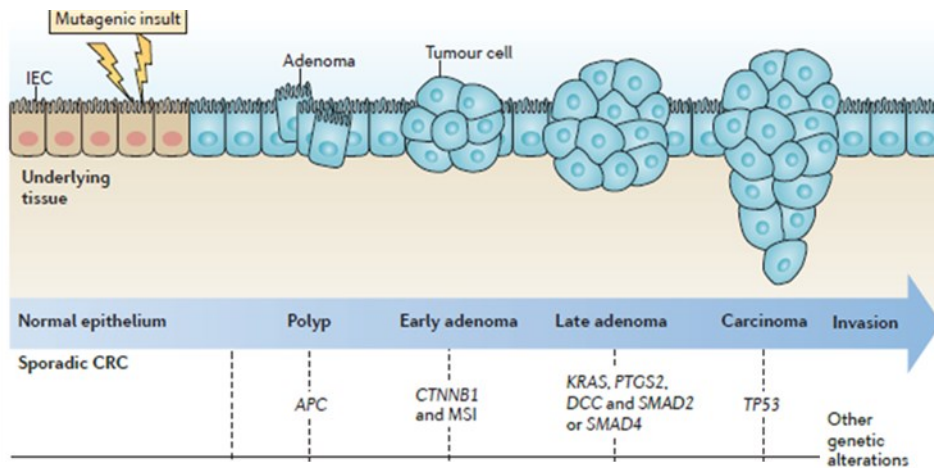


**Figure I.1:** Adenoma to carcinoma sequences [West NR, et al. 2015].

Two major types of genomic instability are recognized as alternative mechanisms of CRC carcinogenesis. The most common, present in 65-70% of CRCs, is represented by chromosomal instability (CIN) defined by the presence of multiple structural or numerical chromosome changes in tumor cells. Instead, 15% of CRCs have a near-diploid chromosome set, but present instability in at least 2 of five standard microsatellite markers (so called microsatellite instability, MSI). Furthermore, approximately 20% of CRCs harbor epigenomic instability, either as global hypomethylation or as CpG island methylator phenotype (CIMP) [Walther A., et al., 2009].

Most cases (88%-94%) of CRC are sporadic, i.e. develop upon acquisition of somatic mutations. However, 5– 10% of CRC consist of hereditary cancer syndromes. Two main autosomal-dominant forms are recognized: 1) hereditary non-polyposis colorectal cancer (HNPCC), also known as Lynch syndrome, caused by germ line mutations of mismatch repair (MMR) genes, mainly MLH1, MSH2 and MSH6; 2): familial adenomatous polyposis (FAP) caused by germ line mutation of APC gene [Cunningham D., et al., 2010].



## 1.2 Staging and prognosis

Pathologic evaluation of resected CRC specimens plays a pivotal role in prognostication and patient management [Brenner H., et al., 2014]. The method currently used to assess prognostic differences among patients is the tumor-node-metastasis (TNM) staging system, established by the American Joint Committee on Cancer (AJCC), based on evaluation of tumor size (T), lymph node involvement (N) and presence of distant metastases (M) (Figure 2). Five-year survival rates are estimated approximately around 90% for patients in stage I, 80%, for patients in stage II, 60% in stage III and only <10% in stage IV [O'Connell JB., et al., 2004].

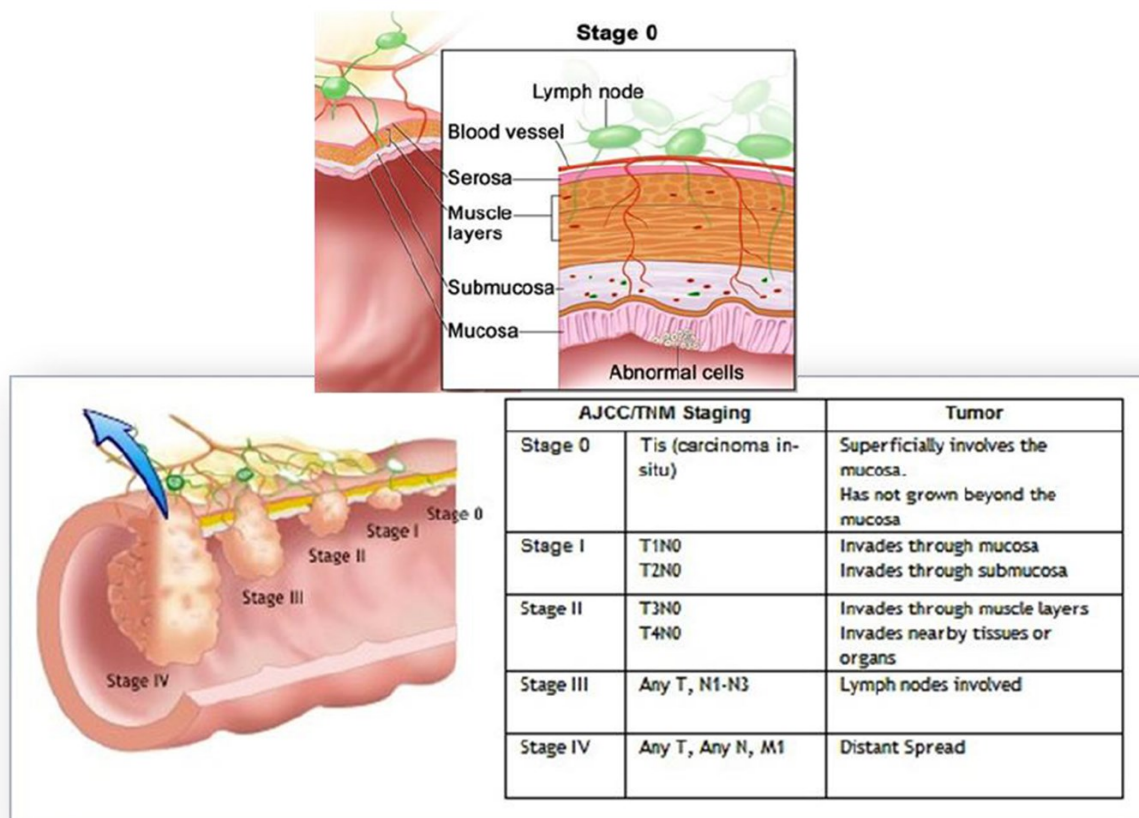


**Figure 2:** CRC development and TNM staging system.

However, TNM system does not precisely predict clinical outcome. Indeed, patients with early stage CRC still have approximately a 20-30% risk of recurrence [Cunningham D., et al., 2010]. Furthermore, there is significant variation in patients' outcome also within the same

tumor stage [Maguire, et al., 2014]. The possibility to identify high risk patients who may benefit of additional systemic therapies through the evaluation of additional prognostic factors represents therefore an essential clinical need.

Numerous putative prognostic molecular and immunohistochemical biomarkers have been proposed [Walther A., et al., 2009 and Zlobec I., et al., 2008]. Importantly, KRAS mutation status has been found to predict responsiveness to treatment with anti-epidermal growth factor receptor EGFR antibodies [Walther A., et al., 2009]. However, the potential use of additional putative markers in clinical practice is still under evaluation [Brenner H., et al., 2014].

### **1.3 Current treatment guidelines**

In general, the first line of CRC treatment is surgery, aiming at removing the tumor and corresponding lymphatic vessels [Kuipers E., et al 2015]. Usually, patients with stage I -II tumors do not receive any additional therapy. Instead, when the tumor has spread in to the lymph nodes (stage III), surgery is combined with adjuvant or neo-adjuvant chemotherapy, in particular with 5-Fluorouracil (5-FU), in combination with Oxaliplatin or Irinotecan. For stage IV disease, in which tumor has involved distant organs (metastatic CRC), combined chemotherapies are administered together with targeted therapies, such as monoclonal antibodies specific for EGFR or vascular endothelial growth factor (VEGF), or small molecule-based multikinase inhibitors [Kuipers E., et al 2015]. Response rates to systemic therapies remain limited, usually not exceeding 20% of treated patients [Brenner H., et al., 2014]. The identification of novel and more effective therapeutic approaches would therefore be desirable. Recently, the potential efficacy of therapeutic antibodies targeting immunological checkpoints, including CTLA4, PD-1 and PD-L1, has also started to be evaluated in clinical trials [Le DT., et al., 2015 and Singh PP., 2015].

## **2.CRC immune contexture**

### **2.1 Definition of immune contexture**

The term “immune contexture” refers to the analysis of location, density and functional orientation, of different tumor infiltrating immune cell populations [Fridman WH., et al., 2012] (Figure I.3).

Since a long time, histopathological analysis has provided evidence that tumors are infiltrated by different types of immune cells, including lymphocytes, macrophages and granulocytes. Immune infiltrates are heterogeneous between tumor types, and largely vary from patient to patient.

Only in the last decade, however, the prognostic significance of specific tumor infiltrating immune cell types has been recognized. Comprehensive gene expression and immunohistochemical analysis in large cohorts of different types of human tumors, annotated with clinico-pathological data, have revealed that tumor infiltration by defined immune cell types, their localization within the tumor, and their expression of specific cytokines/chemokines, predict patient survival more precisely than TNM staging, thus possibly representing a superior prognostic factor [Fridman WH., et al., 2012].

The immune contexture has therefore been proposed as additional prognostic tool. Its robustness in clinical practice is currently being evaluated by a consortium of experienced pathologists worldwide [Galon, et al., 2012].

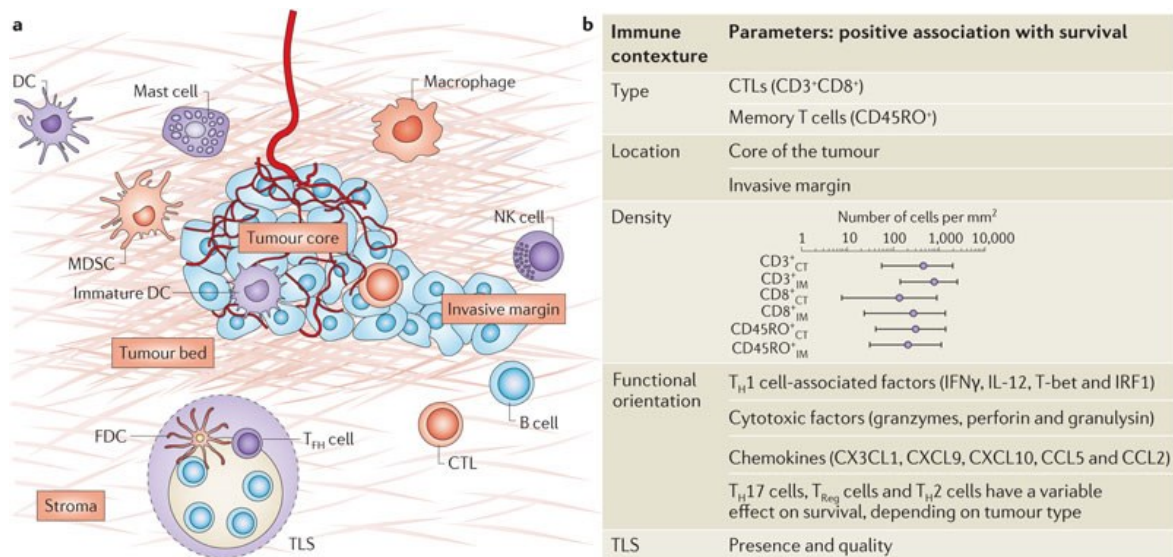


**Figure I.3:** The immune contexture [Fridman WH., et al., 2012].

## **2.2 Impact of immune contexture in CRC**

CRC is the first tumor type for which the immune contexture has been proven to critically impact survival. In particular, Galon and collaborators have reported that high infiltration by CD8<sup>+</sup>CD45RO<sup>+</sup> T cells, and IFN- $\gamma$  producing Th1 cells correlates with good prognosis [Galon J., et al., 2006 , Tosolini M., et al., 2011 and Camus M., et al., 2009]. More surprisingly, high infiltration by Foxp3<sup>+</sup> regulatory cells has also be found to predict better survival [Salama P., et al., 2009 and Frey DM., et al., 2010]. In addition, the presence of CD16<sup>+</sup> MPO<sup>+</sup> cells is also associated with favorable prognosis [Sconocchia G., et al., 2010; Hirt C., et al., 2013]. In contrast, the role of IL-17-producing CD4<sup>+</sup> T cells (Th17) is still controversial. In a study, based on a small sample cohort (50-200), high expression of IL-17 has been found to be associated with unfavorable prognosis [Tosolini M., et al., 2011]. More recently, however, in a recent study from our group, based on the analysis of a cohort including more than 1400 CRC samples, no association with clinical outcome has been found [ Amicarella F., et al., 2015], (Table I.1).

<u>Type of cells</u>	<u>Prognostic significance</u>	<u>References</u>
CD3+CD45RO+ CD8+IFN-g+	Good	Galon et al., Science 2006
CD8 +TIA-1+	Good	Zlobec et al., PLOS One, 2011
CD4+ IFN- $\gamma$ +(Th1)	Good	Tosolini et al., Cancer Research, 2011
CD4+FOXP3+ T-regs	Good	Salama et al., J Clin Oncol, 2009; Frey-Droeser et al., Int. J. Cancer 2010
CD4+IL-17+(Th17)	Bad Neutral	Tosolini et al., Cancer Research 2011 Amicarella et al. Gut, 2015
CD16+MPO+	Good	Sconocchia et al., Int. J. Cancer 2011; Hirt C., et al., Oncoimmunology 2013.

**Table I.1:** Prognostic significance of immune cell subsets in CRC.

Mechanisms underlying heterogeneity of tumor infiltration by immune cells in different tumors remain to be elucidated. In particular, factors promoting migration of individual immune cell populations into the tumor remain to be clarified.

### **3. Immune cell trafficking in CRC**

#### **3.1 Chemokines and chemokine receptors**

Chemokines are chemotactic cytokines which control migratory patterns and positioning of various cell types [Griffith JW. et al., 2014]. Tumors are known to secrete chemokines playing a crucial role in the recruitment of different types of proinflammatory leukocytes into the tumor microenvironment as well as in many additional biological processes, such as tumor growth, survival, migration and angiogenesis [Wang D., et al., 2009 and Balkwill F., 2004].

More than 40 different chemokines have been identified so far which can be divided in four groups, based on the position of the last cysteine residue: CXC ( $\alpha$ -family), CC ( $\beta$ -family), C ( $\gamma$ -family), and CX3C ( $\delta$ -family) [Esche C., et al., 2005] (Figure I.4).



CCL11, CCL20, CCL22, which are constitutively expressed and can also be upregulated upon inflammation. In humans, genes encoding inflammatory chemokines are located in chromosomes 4 and 17, whereas those encoding homeostatic chemokines are located individually or in miniclusters in different chromosomes [Zlotnik A., et al., 2012]. Notably, as a result of chromosomal instability, chemokine genes localized in chromosomes 7, 16 and 19, frequently undergo amplifications, whereas chemokine genes localized in chromosome 4 and 17 are deleted [Bindea G., et al., 2013].

Chemokines mediate their biological effects by binding to corresponding receptors. Chemokine receptors are members of the class A rhodopsin-like family of seven transmembrane domain G protein-coupled receptors (GPCRs) [Borroni EM., et al., 2010]. Chemokine receptor activation begins with extracellular ligand binding (Figure I.5) which triggers interaction with intracellular quiescent GDP-bearing trimeric G-proteins. This results in exchange of GDP for GTP, causing the G-protein to dissociate into G-alpha and G-beta/gamma subunits. The latter subunit in turn activates enzymes such as phospholipase C and phosphoinositide-3-kinase, which convert phosphatidylinositol-4,5-diphosphate (IP<sub>2</sub>) into phosphatidylinositol-1,4,5-triphosphate (IP<sub>3</sub>) and diacylglycerol (DAG). IP<sub>3</sub> stimulates the influx of calcium ions, and DAG activates protein kinase C (PKC) isoforms. The intracellular environment is thus prepared for a cascade of phosphorylation events involving a series of kinases (e.g., mitogen-activated protein kinase and protein tyrosine kinase) and small GTPases (e.g., Ras and Rho) ultimately mediating cellular functions such as adhesion, chemotaxis, degranulation, and respiratory burst [Chensue SW., et al., 2001].

On the other side, chemokine receptors undergo desensitization and regulation. Upon ligation, chemokine receptors may be internalized and then degraded or recycled, leaving the membrane temporarily unresponsive to further ligand stimulation [Chensue SW., et al., 2001]. In particular, the C-terminal region contains target residues that may be phosphorylated by GPCR kinases, thus allowing the binding of regulatory molecules called arrestins, ultimately

causing uncoupling and desensitization. An additional mechanism of regulation occurs through direct inactivation of G-protein activity by GTPases, known as RGS (regulators of G-protein signaling) proteins [Chensue SW, et al., 2001].

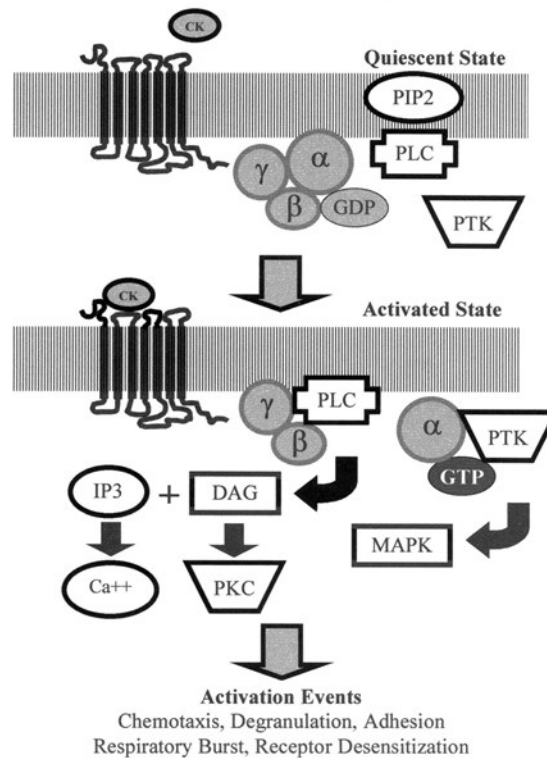


**Figure I.5:** Chemokine receptor ligation and activation events. [Chensue SW., et al., 2001].

So called 'atypical chemokine receptors' [Mantovani A., et al., 2006], have also emerged as important regulators of chemokine function. These receptors, which are characterized by inability to signal following ligand binding, have been shown to be able to scavenge chemokines and therefore to influence chemokine responses in vivo [Graham GJ., et al., 2012]. Four atypical receptors, DARC, CCXCKR and CXCR7 and D6, have been identified so far [Graham GJ., 2009].



### **3.2 Role of chemokines in leukocyte trafficking**

Chemokines and chemokine receptors play a crucial role in the complex series of interactions between leukocytes and endothelial cells, eventually leading to the extravasion of leukocytes from the circulation into tissues. Transitory leukocyte attachment to the endothelium is initially mediated by the interaction of adhesion molecules, such as integrins and selectins, with their ligands on endothelial cells. However, only engagement of chemokine receptors, expressed on leukocytes, with corresponding chemokines on endothelial cells induces the arrest of leukocytes under shear flow, and subsequently promotes the diapedesis of the cells through the vascular endothelium and their localization into specific microenvironments [Masopust D., Schenkel JM., 2013 and Griffith JW., et al., 2014 and Habtezion A., et al., 2016].

### **3.3 Gut homing receptors**

Distinct homing receptor patterns mediate immune cell recruitment into different anatomical compartments. In particular, in the absence of inflammation, T cell recruitment into the lamina propria of small intestine, is largely dependent on the expression of the integrin  $\alpha 4\beta 7$  and the chemokine receptor CCR9 whose corresponding ligands, mucosal vascular addressin cell-adhesion molecule 1(MAdCAM-1) and CCL25, are expressed in the gut lamina propria and on epithelial cells [Mora JR., et al., 2006 and Habtezion A., et al., 2016]. However, CCL25 expression decreases from the proximal to the distal small intestine [Stenstad H., et al., 2007] and it is poor in the colon [Papadakis KA., et al., 2000]. Indeed, CCR9 expression does not appear to be required for T cell trafficking into the colon [Papadakis KA., et al., 2000].

CCR6 and its ligand CCL20 have also been shown to significantly contribute to recruitment of T cells, and in particular of Th17 cells, into the small and large intestine, upon

inflammation [Wang C., et al., 2009]. Colon tissues from patients with IBD express higher levels of CCL20 than uninflamed tissues [Kaser A., et al., 2004]. Furthermore, antibodies against CCL20 has been shown to block adhesion of T and B cells to inflamed microvessels in mice with dextran sodium sulfate (DSS)-induced colitis [Teramoto K., et al., 2005]. Finally, CXCR4 and its widely expressed ligand CXCL12 may also participate in lymphocyte localization in the gut [Oyama T., et al., 2007].

### **3.4 Prognostic significance of chemokine expression in colorectal cancer**

In humans CRC expression of defined chemokines, including CXCL16 [Hojo S., et al., 2007], CXCL9, CXCL10 [Mlecnik B., et al., 2010], CXCL13 [Bindea G., et al., 2013], CCL18 [Yuan R., et al., 2013], and CCL21 [Zou Y., et al., 2013], has been reported to correlate with good prognosis. In contrast, expression of CCL7 [Cho YB., et al., 2012], CXCL1 [Wang D., et al., 2006 and Ogata H., et al., 2010], CXCL5 [Kawamura M., et al., 2012], CXCL8 [Rubie C., et al., 2007], and CXCL12 [Wang SC., et al., 2010 and Kim J., et al., 2005 and 2006] has been found to be associated with unfavorable clinical outcome, Mechanisms underlying these associations remain to be clarified. Importantly, the nature of the cell populations responding to these chemokines and potential chemokine sources have not been elucidated yet.

## **4. Pathophysiology of CRC microenvironment**

### **4.1 Physiology of normal colonic mucosa**

The normal colonic mucosa is composed by a single cell layered epithelium, formed by four types of intestinal epithelial cells (IEC), including absorptive enterocytes, mucus-producing goblet cells, antimicrobial peptides (AMP)-producing Paneth cells, and hormone-producing enteroendocrine cells, and by the underlying lamina propria, infiltrated by different type of

immune cells, including dendritic cells, macrophages, innate lymphoid cells, T lymphocytes, and plasma cells [Abreu MT., 2010].

IEC display a polarized structure characterized by an apical and basolateral surface facing the intestinal lumen and the lamina propria, respectively. The epithelial layer is overlaid by a mucous stratum, composed of secretory mucins (MUCs), mainly MUC2, produced by goblet cells, which creates a barrier impermeable to commensal bacteria and other microorganisms present in the gut lumen [Abreu MT., 2010] (Figure I.6). The integrity of the barrier is also maintained by the presence of adherent and tight junctions holding epithelial cells together and regulating the selective para-cellular permeability to solutes and water [Sánchez de Medina F., et al., 2014].

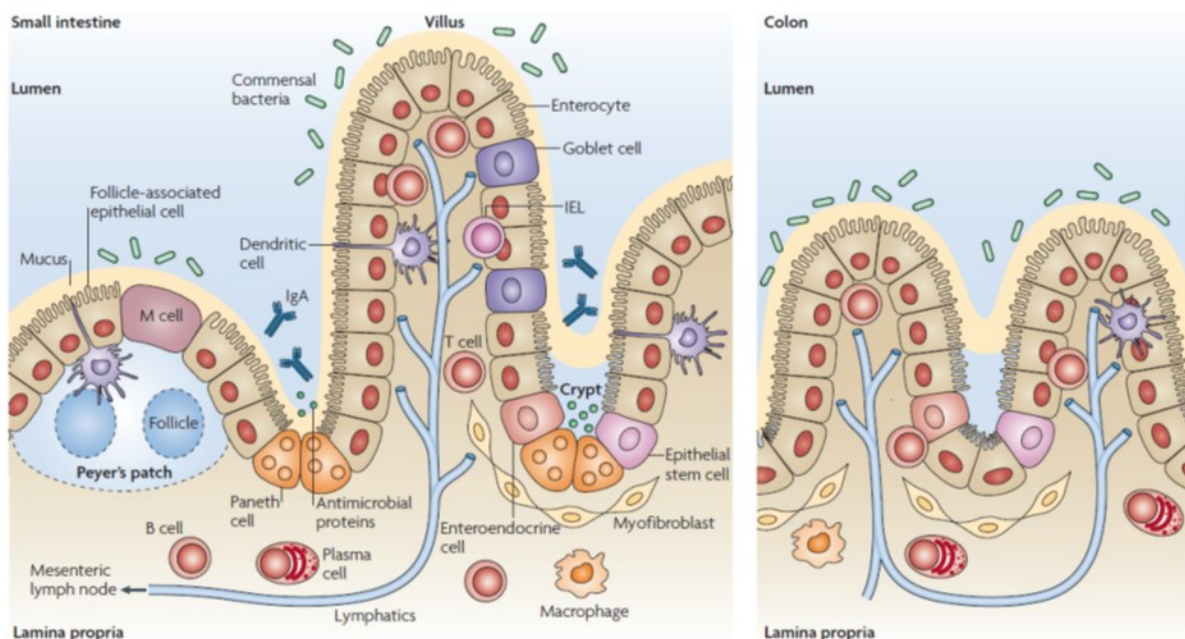


**Figure I.6:** Anatomy of the intestinal immune system [Abreu MT., 2010].

## **4.2 The gut microbiota**

The gastrointestinal tract is heavily colonized by a vast number of microorganisms, mostly bacteria, viruses, and fungi, referred to as the gut microbiota or microflora, living in peaceful coexistence with their host [Sekirov I., et al., 2010]. Bacteria represent a major component of the gut flora. The number of bacterial cells present in the mammalian gut shows a continuum going from  $10^1$  to  $10^3$  bacteria per gram of content in the stomach and duodenum, progressing to  $10^4$  to  $10^7$  bacteria per gram in the jejunum and ileum and culminating in  $10^{11}$  to  $10^{12}$  cells per gram in the colon. Indeed the colon alone is estimated to contain over 70% of all the microbes in the human body [O'Hara AM., et al., 2006]. The majority of the gut flora is composed of strict anaerobes. Although, more than 50 bacterial phyla have been recognized, two only, Bacteroides and Firmicutes, appear to be dominant, whereas Proteobacteria, Verrucomicrobia, Actinobacteria, are present in minor proportions [Donaldson GP., et al., 2016] (Figure I.7).

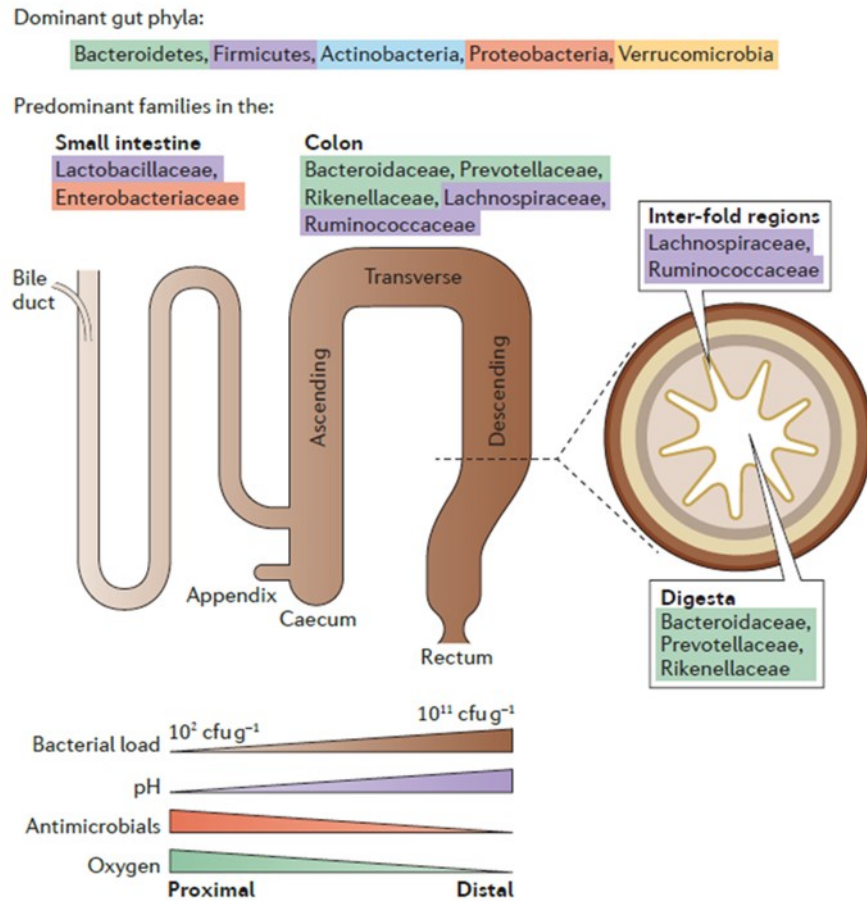


**Figure I.7:** Spatial and temporal aspects of intestinal microbiota composition [Sekirov I., et al., 2010].

Microbial colonization of human gut begins at birth, upon the passage through the birth canal where the fetus is exposed to a complex microbial population. Indeed, the intestinal microbiota of newborns has been found to be very similar to the vaginal microbiota of their mothers [Mandar R., et al., 1996].

However, subsequently, the gut microbiota composition is shaped by additional factors, such as diet and exposure to antibiotics [Sekirov I., et al., 2010].

### **4.3 Interactions between gut flora and normal colonic epithelium**

Under normal conditions, interaction between normal colonic epithelial cells and gut microbiota is limited and highly regulated. IEC can sense the presence of gut microbiota or

their products into the gut lumen thanks to the expression of Pattern recognition receptors (PRR) recognizing specific molecular patterns related to commensals, pathogens or cellular damage. Several functionally distinct classes of PRR [Medzhitov R., 2007] including, among others, Toll-like receptors (TLR), nucleotide binding oligomerization domain (NOD)-like receptors (NLR), and RNA helicases (RIG-I (retinoid acid-inducible gene-I) [Fukata M and Arditi M., 2013], are expressed by IEC. In particular, in the intestine and in the colon the recognition of commensal bacteria and pathogens is largely mediated by TLRs [Abreu MT., 2010].

TLRs are type 1 integral membrane glycoproteins [Martin MU., 2002], and are characterized by an extracellular leucine-rich repeat (LRR) domain and an intracellular Toll/IL-1 receptor (TIR) domain [Hashimoto C., 1988]. Thirteen mammalian TLRs have been described; classified into two subfamilies based on their localization. Cell surface TLRs, including TLR1, TLR2, TLR4, TLR5, TLR6, and TLR10; and intracellular TLRs, localized in the endosome including TLR3, TLR7, TLR8, TLR9, TLR11, TLR12, and TLR13 [Kawasaki T and Kawai T., 2014]. TLRs play a central role as primary sensor of invading pathogens and inducers of host antimicrobial defense. Cell surface TLRs recognize microbial membrane components, such as lipids, lipoproteins, and proteins, whereas intracellular TLRs sense exogenous or endogenous nucleic [Blasius AL. and Beutler B., 2010] (Table I.2).

TLRs	Ligands			
	Exogenous	Endogenous	Synthetic analogs	Fully synthetic molecules
TLR1	Lipopeptides (Bacteria and Mycobacteria) Soluble factors ( <i>Neisseria meningitidis</i> )		Triacyl lipopeptides	
TLR2	Lipoprotein/lipopeptides (Gram-positive bacteria, Mycoplasma, Mycobacteria, Spirochetes) Peptidoglycan (Gram-positive bacteria) Lipoteichoic acid (Gram-positive bacteria) Phenol-soluble modulin ( <i>Staphylococcus epidermidis</i> ) Heat-killed bacteria ( <i>Listeria monocytogenes</i> ) Porins ( <i>Neisseria</i> ) Atypical lipopolysaccharides ( <i>Leptospira interrogans</i> , <i>Porphyromonas gingivalis</i> ) Soluble factors ( <i>Neisseria meningitidis</i> ) Glycolipids ( <i>Treponema maltophilia</i> ) Outer membrane protein A ( <i>Klebsiella pneumoniae</i> ) Glycoinositolphospholipids ( <i>Trypanosoma cruzi</i> ) Phospholipomannan ( <i>Candida albicans</i> ) Structural viral proteins (Herpes simplex virus, Cytomegalovirus) Hemagglutinin (Measles virus) Lipoarabinomannan (Mycobacteria) Zymosan ( <i>Saccharomyces</i> )	HSP60 HSP70 HSP96 HMGB1 Hyaluronic acid	Diacyl and triacyl lipopeptides	
TLR3	Single-stranded viral RNA (ssRNA) and double-stranded RNA (dsRNA; Viruses)	mRNA	Poly(I:C) Poly(I:C <sub>12</sub> U)	
TLR4	Lipopolysaccharide (Gram-negative bacteria) HSP60 ( <i>Chlamydia pneumoniae</i> ) Envelope proteins (Respiratory syncytial virus and mouse mammary tumor virus) Fusion protein (syncytial virus) Glycoinositolphospholipids ( <i>Trypanosoma cruzi</i> ) Taxol (Plant product)	HSP22 HSP60 HSP70 HSP96 HMGB1 $\beta$ -defensin 2 Extra domain A of fibronectin Hyaluronic acid Heparan sulfate Fibrinogen Surfactant-protein A	Lipid A mimetics (Monophosphoryl lipid A, aminoalkyl glucosamine 4-phosphate)	E6020 E5531 E5564
TLR5	Flagellin (Gram-positive or Gram-negative bacteria)		Discontinuous 13-amino acid peptide CBLB502	
TLR6	Diacyl lipopeptides (Mycoplasma) Lipoteichoic acid (Gram-positive bacteria) Phenol-soluble modulin ( <i>Staphylococcus epidermidis</i> ) Zymosan ( <i>Saccharomyces</i> ) Heat-labile soluble factor (Group B <i>streptococcus</i> )		Diacyl lipopeptides	
TLR7	Single-stranded RNA (Viruses)	Endogenous RNA	Oligonucleotides	Imidazoquinolines (Imiquimod, Resiquimod) Guanosine nucleotides (Loxoribine, Isatoribine) Bropirimine
TLR8	Single-stranded RNA (Viruses)	Endogenous RNA		Imidazoquinolines (Resiquimod)
TLR9	Unmethylated CpG motifs (Bacteria and viruses) Hemozoin ( <i>Plasmodium</i> )	Endogenous DNA	CpG oligodeoxynucleotides (CPG 7909, CPG 10101, 1018 ISS)	
TLR10	Unknown, may interact with TLR2 and TLR1			
TLR11	Profiling-like molecule ( <i>Toxoplasma gondii</i> )			

**Table I.2:** Toll-like receptors and their main ligands [modified from Manaval B., et al., 2011].

The activity of TLR agonists occurs through binding to the corresponding TLR receptors. In particular, most Toll-like receptors (TLRs) except for TLR3 induce nuclear factor (NF)- $\kappa$ B activation through the myeloid differentiation primary response gene 88 (MyD88) pathway. In contrast, TLR3 exclusively induces IRF3 activation through the TIR-domain-containing adapter-inducing interferon (IFN) -  $\beta$  (TRIF) pathway (Figure I.8), [Fukata M and Arditì M, 2013].

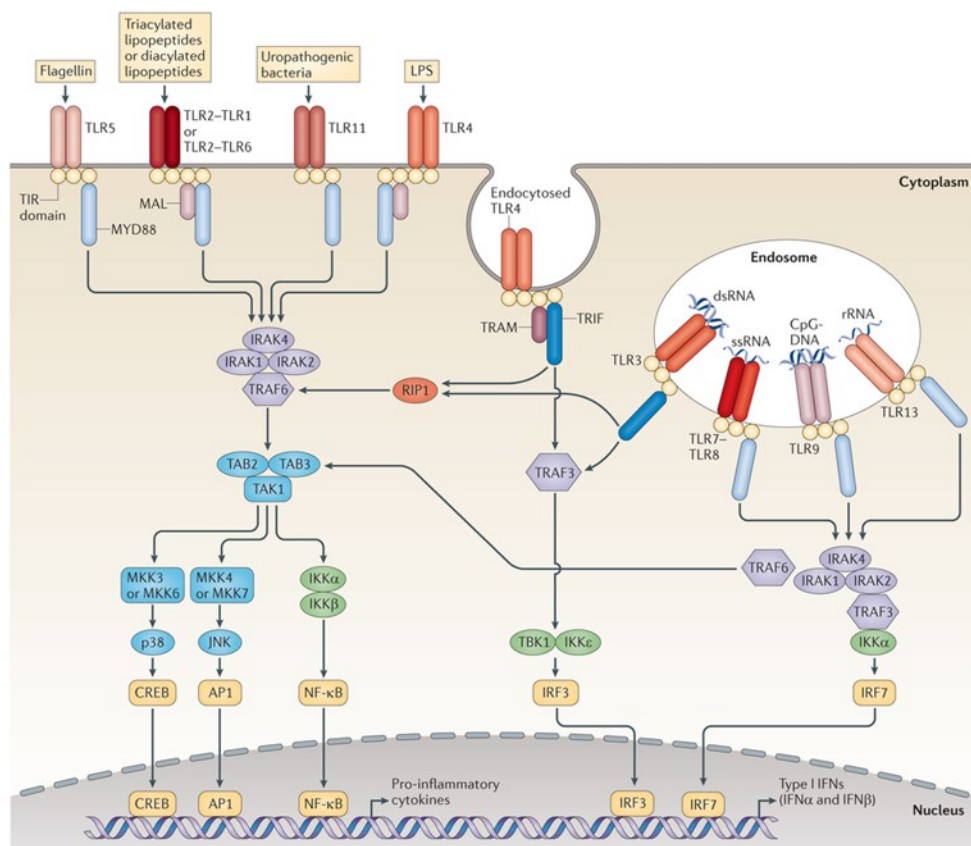


**Figure I.8:** Mammalian TLR signalling pathways [O' Neill L., et al., 2013].

Under homeostatic conditions, colonic IECs express low levels of TLR2, TLR4 and high levels of TLR3 and TLR5 [Abreu MT., et al., 2001 and Otte JM., et al., 2004]. Notably, some TLRs, such as TLR5 are expressed only at the basolateral surface, whereas others, such as TLR9, are expressed at both apical and basolateral surface. However, also in the latter case,



TLR function appears to be polarized inasmuch as basolateral TLR engagement has been shown to trigger activation of NF- $\kappa$ B pathway, whereas apical engagement leads to its inhibition. These evidences are consistent with the hypothesis that inflammatory responses should only occur upon formation of a breach in the epithelial barrier [Abreu MT., 2010].

In the presence of inflammation, TLRs expression on IEC is increased. In particular, TLR4 expression is up regulated by inflammatory cytokines such as, interferon- $\gamma$  (IFN- $\gamma$ ) and tumor necrosis factor (TNF). Notably, high TLR4 expression has been reported in inflammatory bowel disease [Abreu MT., et al., 2002 and 2010].

On the other hand, TLR2 and TLR4 functions are negatively regulated by Toll-interacting protein (TOLLIP) [Abreu MT., 2010] an intracellular protein that inhibits TLR2 and TLR4 signaling through its effect on IL-1R-associated kinases (IRAKs) [Burns K., et al., 2000]. Interestingly, IECs from patients affected by inflammatory bowel disease fail to upregulate TOLLIP, a finding suggesting that lack of TOLLIP may lead to chronic inflammation [Abreu MT., 2010].

TLR triggering by microbial stimuli results in a number of protective functions, including induction of IEC proliferation upon epithelial cells injury, release of antimicrobial peptides, and induction of IgA secretion by B cells [Abreu MT., 2010].

#### **4.4 Physiopathology of gut epithelium in CRC**

Recent evidence has proved that genetic mutations eventually leading to CRC development cause an early alteration of the epithelial barrier, due to decreased mucus production and loss of tight junctions [Grivennikov S., et al., 2012]. Commensal bacteria and their products may then translocate across the epithelium into the lamina propria, and trigger TLRs expressed on the basolateral surface of IEC and on immune cells. This results in the release of pro-inflammatory factors, ultimately promoting tumor progression (Figure I.9).

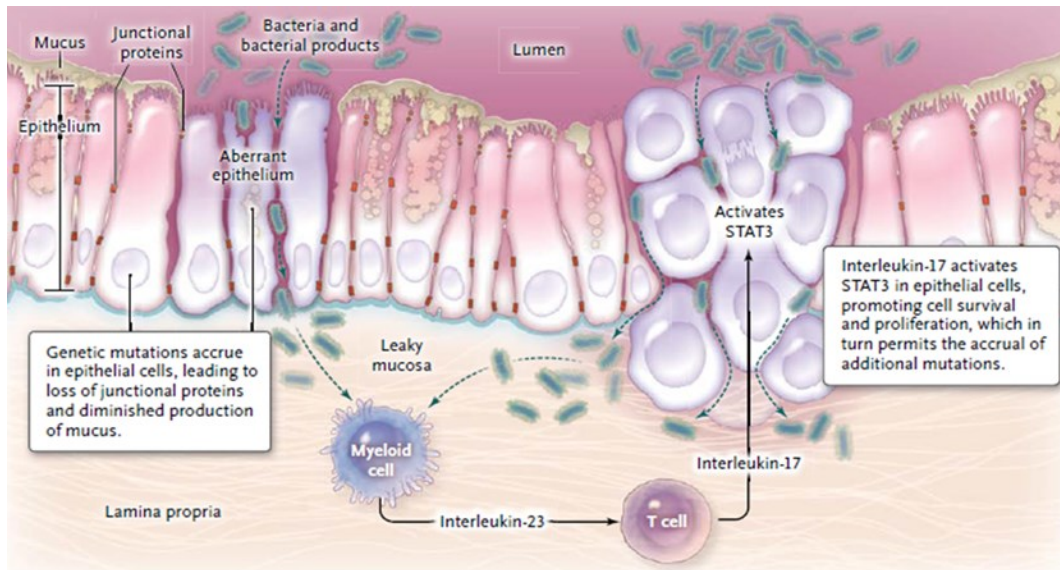


**Figure I.9:** Inflammatory Model of the Initiation of Colorectal Cancer [Gallimore AM. and Godkin A., 2013].

Indeed, mice grown under germ free condition or deficient for TLRs or MYD88 show reduced tumor development [Rakoff-Nahoum S., et al., 2007], thus suggesting that TLR engagement by microbial stimuli promotes tumor growth.

Interestingly, in humans, defined bacteria species have been found to be abundant in CRC tissues [Castellarin M., et al., 2012]. In particular, *Fusobacterium nucleatum* (*F. nucleatum*), an invasive anaerobic bacterium common in dental plaque and generally associated with periodontitis [Castellarin M., et al., 2012], has been found to be overrepresented in CRC as compared to corresponding healthy colonic mucosa [Castellarin M., et al., 2012 and Kostic AD., et al., 2013]. The significance of this association is still unclear. On the one hand, *F. nucleatum* has been shown to directly promote CRC cell proliferation in vitro upon activation of WNT signaling [Rubinstein MR., et al., 2013] and tumor development in vivo [Kostic AD., et al., 2013]. On the other hand, it might suppress antitumor immune responses by promoting recruitment of myeloid derived suppressor cells [Kostic AD., et al., 2013] and by inhibiting the activities of NK and T cell through its interaction with the inhibitor receptor TIGIT [Gur C., et al 2015].

Paradoxically, TLR stimulation has also been shown to result in the induction of effective anti-tumor immunity [Rhee SH., et al., 2008]. However, underlying mechanisms are not fully understood. In particular, whether TLR triggering may also lead to production of chemokines possibly recruiting effector immune cell populations remains to be thoroughly evaluated.

## **II. AIM OF THE**

## **STUDY**

CRC infiltration by specific immune cells, including CTLs, Th1 cells, and, most surprisingly, T regs and CD16<sup>+</sup> MPO<sup>+</sup> neutrophils, is associated with good prognosis. However, the chemotactic factors driving these cell populations into the tumor site, their cellular sources and their microenvironmental triggers remain to be elucidated. My PhD work aimed at investigating the chemokine/chemokine receptor network promoting CRC infiltration by immunocompetent cells associated to favorable clinical outcome.

In particular I have addressed:

1. Expression of immune cell markers and their correlation with chemokine expression in primary CRC tissues;
2. Identification of chemokine receptors relevant for CRC infiltration by beneficial immune cells;
3. Chemokine sources in CRC;
4. Microenvironmental stimuli triggering chemokine production in CRC tissues;
5. Effects of chemokine production on immune cell recruitment into CRC tissues.

# **III. MATERIALS AND**

# **METHODS**

## **1. Clinical specimen collection and processing**

Clinical specimens were collected from consenting patients undergoing surgical treatment at Basel University Hospital, St. Claraspital in Basel, Kantonsspital Olten, Kantonsspital St. Gallen, and Ospedale Civico di Lugano. Tumor or healthy tissue fragments were snap frozen for RNA extraction or treated by enzymatic digestion in order to obtain single cell suspensions. Briefly, tissues were minced and digested in Dulbecco's Modified Eagle Medium (DMEM) supplemented with 2 mg/ml collagenase IV (Worthington Biochemical Corporation) and 0.2 mg/ml DNase I (Sigma-Aldrich) for 1 hour at 37°C. Single cell suspensions were then filtered through cell strainers (100, 70, and 40 µm diameter, sequentially) and used for flow cytometric analysis. In addition, peripheral blood mononuclear cells (PBMCs) from healthy donors (HD PB) or from CRC patients (CRC PB) were isolated by Ficoll-Hypaque (Histopaque-1077, Sigma-Aldrich) density gradient centrifugation and subsequently used for flow cytometry characterization.

The use of human samples in this study has been approved by the local ethical committee.

## **2. Cell lines**

LS180, HT29 and Colo2015 human CRC cell lines were purchased from the European Collection of Cell Cultures, and maintained in RPMI 1640 (GIBCO) or, for HT29, McCoy's 5A medium (Sigma-Aldrich), supplemented with 10% fetal bovine serum, GlutaMAX-I and kanamycin (GIBCO). All cell lines were used at early passages.

## **3. Bacteria**

*Fusobacterium nucleatum* (subsp. *Nucleatum*, ATCC 25586), *Bacteroides vulgatus* (Eggerth and Gagnon, ATCC 8482), and *Bacteroides fragilis* (non enterotoxigenic strain 9343, ATCC 25285), were kindly provided by Dr. Nina Khanna, Department of Biomedicine, University of Basel. They were cultured under anaerobic conditions. *Escherichia coli* (Castellani and

Chalmers, ATTC 25922) was purchased from American type culture collection (ATCC) and cultured in Tryptic Soy Agar/Broth (BD). All bacteria were used upon heat-inactivation at 90° for 1 hour.

#### **4. Flow cytometry**

For the analysis of surface markers, PBMCs from CRC patients, and single cell suspensions obtained from freshly excised clinical specimens of CRC and corresponding tumor-free colonic mucosa were incubated with fluorochrome-conjugated antibodies for 15 minutes at 4 °C. For the analysis of intracellular markers, cells were fixed and permeabilized (Intracellular Fixation & Permeabilization Buffer Set, eBioscience) and stained intracellularly with specific antibodies for 30 minutes at room temperature (RT). Antibodies used are listed in Table III.1

<b>Specificity</b>	<b>clone</b>	<b>company</b>
<b>CD3</b>	SK7	BD Biosciences
<b>CD4</b>	SK3	BD Biosciences
<b>CD8</b>	SK1	BD Biosciences
<b>CD16</b>	3G8	BD Biosciences
<b>CD66b</b>	G10F5	Biolegend
<b>CCR3</b>	5 E8	BD Biosciences
<b>CCR4</b>	205410	R&D Systems
<b>CCR5</b>	2D7	BD Biosciences
<b>CCR6</b>	R6H1	eBioscience
<b>CCR9</b>	BBC3M4	eBioscience
<b>CXCR1</b>	42705	R&D Systems
<b>CXCR2</b>	48311	R&D Systems
<b>CXCR3</b>	1C6	BD Biosciences
<b>CXCR4</b>	12G5	BD Biosciences
<b>CX3CR1</b>	528728	R&D Systems
<b>TLR1</b>	GD2.F4	eBioscience
<b>TLR2</b>	TL2.1	eBioscience
<b>TLR3</b>	TLR3.7	eBioscience
<b>TLR4</b>	HTA125	eBioscience
<b>TLR5</b>	624915	R&D Systems
<b>TLR6</b>	86B1153.2	IMGENEX
<b>TLR7</b>	533707	R&D Systems
<b>TLR8</b>	44C143	IMGENEX
<b>TLR9</b>	eB72-1665	eBioscience
<b>TLR10</b>	3C10C5	eBioscience

**Table III.1:** List of antibody used in this study



Stained cells were analyzed by FACSCalibur flow cytometer (BD Biosciences). Tumor cells, as identified by the expression of EpCAM+, were sorted by magnetic microbeads (MACS® MicroBeads from Miltenyi Biotec) from single cell suspensions obtained upon digestion of freshly excised CRC samples. The purity of tumor cells was > 98%, as evaluated by flow cytometry.

### **5. Real-time reverse transcription PCR assays**

Total RNA was extracted from stored CRC tissues or sorted cell populations using NucleoSpin RNA (MACHEREY-NAGEL) and reverse transcribed using the Moloney Murine Leukemia Virus Reverse Transcriptase (M-MLV RT, Invitrogen). Quantitative Real-Time PCR was performed in the ABI prism™ 7700 sequence detection system, using TaqMan Universal Master Mix and No AmpErase UNG (both from Applied Biosystems).

Commercially available primer sequences used are summarized in Table III.2.

<b>Gene name</b>	<b>code/seq</b>	<b>company</b>
<b>CCL1</b>	Hs00171072_m1	AppliedBiosystems
<b>CCL2</b>	Hs00234140_m1	"
<b>CCL3</b>	Hs00234142_m1	"
<b>CCL4</b>	Hs99999148_m1	"
<b>CCL5</b>	Hs00982282_m1	"
<b>CCL7</b>	Hs00171147_m1	"
<b>CCL8</b>	Hs00271615_m1	"
<b>CCL11</b>	Hs00237013_m1	"
<b>CCL13</b>	Hs00234646_m1	"
<b>CCL14-15</b>	Hs00361122_m1	"
<b>CCL16</b>	Hs00171123_m1	"
<b>CCL17</b>	Hs00171074_m1	"
<b>CCL18</b>	Hs00268113_m1	"
<b>CCL19</b>	Hs00171149_m1	"
<b>CCL20</b>	Hs00171125_m1	"
<b>CCL21</b>	Hs99999110_m1	"
<b>CCL22</b>	Hs00171080_m1	"
<b>CCL23</b>	Hs00270756_m1	"
<b>CCL24</b>	Hs00171082_m1	"
<b>CCL25</b>	Hs00171144_m1	"
<b>CCL26</b>	Hs00171146_m1	"
<b>CCL27</b>	Hs00171157_m1	"

<b>CCL28</b>	Hs00219797_m1	"
<b>CXCL1</b>	Hs00236937_m1	"
<b>CXCL2</b>	Hs00236966_m1	"
<b>CXCL3</b>	Hs00171061_m1	"
<b>CXCL4</b>	Hs00236998_m1	"
<b>CXCL5</b>	Hs00171085_m1	"
<b>CXCL6</b>	Hs00237017_m1	"
<b>CXCL7</b>	Hs00234077_m1	"
<b>CXCL8</b>	Hs00174103_m1	"
<b>CXCL9</b>	Hs00171065_m1	"
<b>CXCL10</b>	Hs99999049_m1	"
<b>CXCL11</b>	Hs00171138_m1	"
<b>CXCL12</b>	Hs00171022_m1	"
<b>CXCL13</b>	Hs00757930_m1	"
<b>CXCL14</b>	Hs01557413_m1	"
<b>CXCL16</b>	Hs00222859_m1	"
<b>CX3CL1</b>	Hs00171086_m1	"
<b>IRF1</b>	Hs00971960_m1	"
<b>FOXP3</b>	Hs01085834_m1	"
<b>CD16A/B</b>	Hs00275547_m1	"
<b>IL17A</b>	Hs99999082_m1	"
<b>T-bet</b>	Hs00203436_m1	"
<b>CD33</b>	HS01076281_m1	"
<b>CD8</b>	CTCGGCCCTGAGCAACTC (Forward)	Microsynth
	GGCTTCGCTGGCAGGA (Reverse)	"
	ATGTACTTCAGCCACTTCGTGCCGGTC (Probe)	"
<b>IFN<math>\gamma</math></b>	AGCTCTGCATCGTTTTGGGTT (Forward)	"
	GTTCCATTATCCGCTACATCTGAA (Reverse)	"
	TCTTGGCTGTTACTGCCAGGACCCA (Probe)	"
<b>16S</b>	TCCTACGGGAGGCAGCAGT (Forward)	"
	GGACTACCAGGGTATCTAATCCTGTT (Reverse)	"
	CGTATTACCGCGGCTGCTGGCAC (Probe)	"

**Table III.2:** List of primers used in this study

## **6. CRC cell stimulation with TLR agonists and bacteria**

Cells from LS180, HT29 and Colo205 CRC cell lines, were plated in 24-well plates (Sigma-Aldrich) (350'000 cells/well in 0.5 ml) in RPMI 1640 and then stimulated at 37°C with a panel of TLR agonists, including Lipopolysaccharides (LPS, 1000ng/ml from *Escherichia coli* O111:B4, Sigma-Aldrich), polyinosinic-polycytidylic acid (poly(I:C), 10 $\mu$ g/ml, Invivogen), synthetic diacylated lipoprotein (FSL-1, 1 $\mu$ g/ml, Invivogen), and purified

flagellin from *S. Typhimurium* (100ng/ml, Invivogen), or with heat-inactivated bacteria, including *Fusobacterium nucleatum*, *Escherichia Coli*, *Bacteroides vulgatus*, and *Bacteroides Fragilis* (bacteria: cell ratio = 30:1). After 4 hours, cells were collected for RNA extraction and used for the analysis of chemokine expression. Supernatants were collected from parallel cultures after an overnight incubation and used for migration assays.

## **7. Migration assay**

Following gradient centrifugation, CD8<sup>+</sup> T cells and neutrophils were sorted from peripheral blood of healthy donors by magnetic microbeads (MACS® MicroBeads from Miltenyi Biotec, and EasyStep enrichment kit from StemCell Technologies, respectively,) according to manufacturer's instructions. The purity of both cell populations was >98%, as confirmed by flow cytometry. Chemotaxis assays were performed using 96-well transwell plates with 5- $\mu$ m pore size membranes (Corning Costar). Supernatants from LS180 cells, left untreated or treated with different bacteria strains for an overnight period, were added to the lower chambers (250  $\mu$ l/ well). CD8<sup>+</sup> T cells and neutrophils ( $1.5 \times 10^4$  / well in 80  $\mu$ l) were placed in the upper chamber and allowed to migrate for 90 min at 37°C. Numbers of cell migrated into the lower chamber were quantified by flow cytometry. Extent of cell migration was expressed as migration index, calculated as numbers of cells migrated towards supernatants / number of cells migrated towards control medium.

## **8. Generation of CRC xenografts**

In vivo experiments were performed collaboration with Prof. Dr. Borsig Lubor, Institute of Physiology, University of Zurich.

NSG mice (NOD.Cg-Prkdcscid Il2rgtm1Wjl/SzJ) were initially purchased from Charles River Germany, and then bred and maintained in our mouse facility. Eight-week old mice were

injected subcutaneously or intracecally with LS180 cells ( $3 \times 10^5$ / mouse), resuspended in a 1:1 mixture of PBS and Matrigel (8.7 mg/ml, Corning Costar).

For intracecal injection, mice were anesthetized with 10 % Ketamine (0.65 ml/kg intraperitoneum, i.p. Streuli Pharma AG) and 2% Xylazine, (0.5 ml/kg, i.p. Streuli Pharma AG). After surgery, Meloxicam (2 mg/kg, i.p. Boehringer Ingelheim), as pain killer, was also administered. Tumor growth was weekly monitored by palpation. In some experiments, starting from day 10 after injection, a randomized group of intracecally injected mice was treated with Ampicillin Sodium Salt (1 g/L, Amresco) and Vancomycin Hydrochloride (0.2 g/L, Bio Basic Canada), administered in the drinking water. Subcutaneously injected mice were sacrificed 24 days after injection. Intracecally injected mice were sacrificed on day 31 after inoculation. Tumors were harvested and snap frozen for RNA extraction.

## **9. Statistical analysis**

The significance of differential expression of chemokines and immune cells markers in CRC specimens and corresponding healthy mucosa was tested by using Wilcoxon signed rank test. Correlations between chemokine expression and immune cell markers were evaluated using Spearman correlation assays. Differences in frequencies of chemokines receptor expression on CTLs, Th1 and Tregs and neutrophils from peripheral blood of healthy donors or CRC patients, and between tumor and control tissues were evaluated by Mann Whitney test. Chemokine induction in CRC cells in vitro and in vivo was analyzed using two-way ANOVA. Differences in migration rates were tested by one-way ANOVA. Statistical analysis was performed by using GraphPad Prism 5 software (GraphPad Software).

## **IV. RESULTS**

## **1. Expression of immune cell markers in primary CRC**

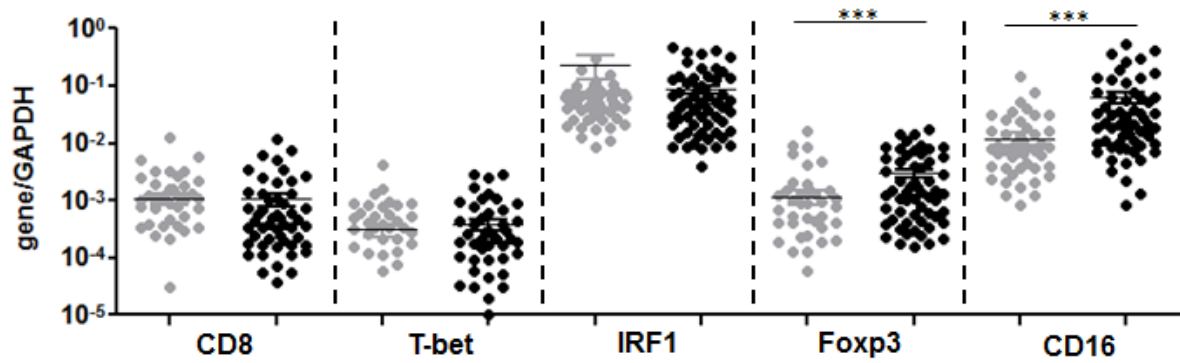
We first evaluated by RT-PCR the expression of genes encoding immune cell markers identifying specific immune cell populations predictive of favorable prognosis, including CD8 for CTLs [Galon J., et al., 2006], T-bet and IRF1 for Th1 [Tosolini M., et al., 2011], Foxp3 for Tregs [Salama P., et al., 2009 and Frey DM., et al., 2010], and CD16 for neutrophils [Droeser RA ., et al 2013], in a cohort of 62 CRC specimens and corresponding tumor-free colonic tissues. Clinical-pathological characteristics of patients included in the cohort are listed in Table IV.1.

<b>Patients Characteristics</b>	
<b>Age (mean)</b>	71.03
<b>Sex</b>	
Male n (%)	34 (54.8)
Female n (%)	28 (45.2)
<b>T stage</b>	
T1 n (%)	0
T2 n (%)	6 (9.7)
T3 n (%)	46 (74.2)
T4 n (%)	10 (16.1)
<b>N stage</b>	
N0 (%)	39 (62.9)
N1 (%)	14 (22.6)
N2 (%)	9 (14.5)

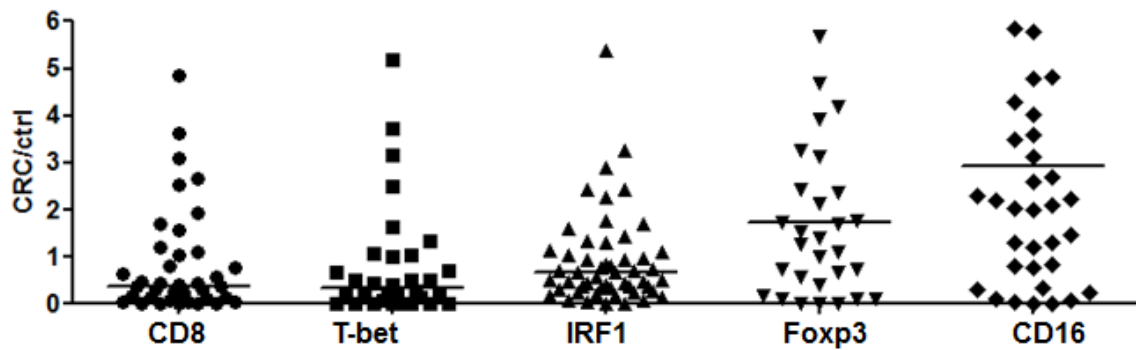
**Table IV.1:** Patient Characteristics (n=62)

Expression levels of Foxp3 and CD16 genes were significantly increased in CRC ( $p < 0.0001$ ), whereas expression of CD8, T-bet and IRF1 genes was comparable in CRC and control tissues (Figure IV.1A). However, in a subgroup of CRCs (up to  $n=15$ ) a marked upregulation of the expression of CD8, T-bet and IRF1 genes, as compared to matched control tissues, was also observed (Figure IV.1B). Correlations between different immune cell markers were also observed. As expected, expression of IRF-1 and T-bet genes, were strongly correlated. More surprisingly, expression of both IRF-1 and T-bet genes was associated with that of Foxp3 gene. Furthermore, a strong correlation between expression of CD8 and T-bet, Foxp3, and CD16 genes was also detected (Figure IV.1C).

A



B



C

	CD8		T-bet		IRF1		Foxp3		CD16	
	Spearman r	p Value	Spearman r	p Value	Spearman r	p Value	Spearman r	p Value	Spearman r	p Value
<b>CD8</b>			0.5101	<0.0001	0.2682	0.0366	0.4182	0.0008	0.4300	0.0005
<b>T-BET</b>	0.5101	<0.0001			0.4343	0.0005	0.6449	<0.0001	0.2566	0.0459
<b>IRF1</b>	0.2682	0.0366	0.4343	0.0005			0.6727	<0.0001	0.2588	0.0441
<b>Foxp3</b>	0.4182	0.0008	0.6449	<0.0001	0.6727	<0.0001			0.2501	0.0519
<b>CD16</b>	0.4300	0.0005	0.2566	0.0459	0.2588	0.0441	0.2501	0.0519		

**Figure IV.1:** Expression of immune cell markers genes in CRC tissue and corresponding tumor-free colonic tissues. Total cellular RNA was extracted from freshly excised CRC tissues (bold) and corresponding tumor-free colonic mucosa samples (gray) and reverse transcribed (n = 62). Expression of the indicated genes was analyzed by qRT-PCR, using GAPDH house-keeping gene as reference. **A.** Gene expression levels relative to GAPDH. **B.** Ratio between gene expression levels in CRCs and matched tumor-free tissues. Statistical significance was assessed by Wilcoxon signed rank test (\*\*\*)p<0.0001) **C.** Correlation between CD8; IRF1 and T-bet, Foxp3 and, CD16 were detected. Spearman r and relative p-values are indicated in the table. Significant correlation coefficients  $\geq 0.3$  are indicated in bold.

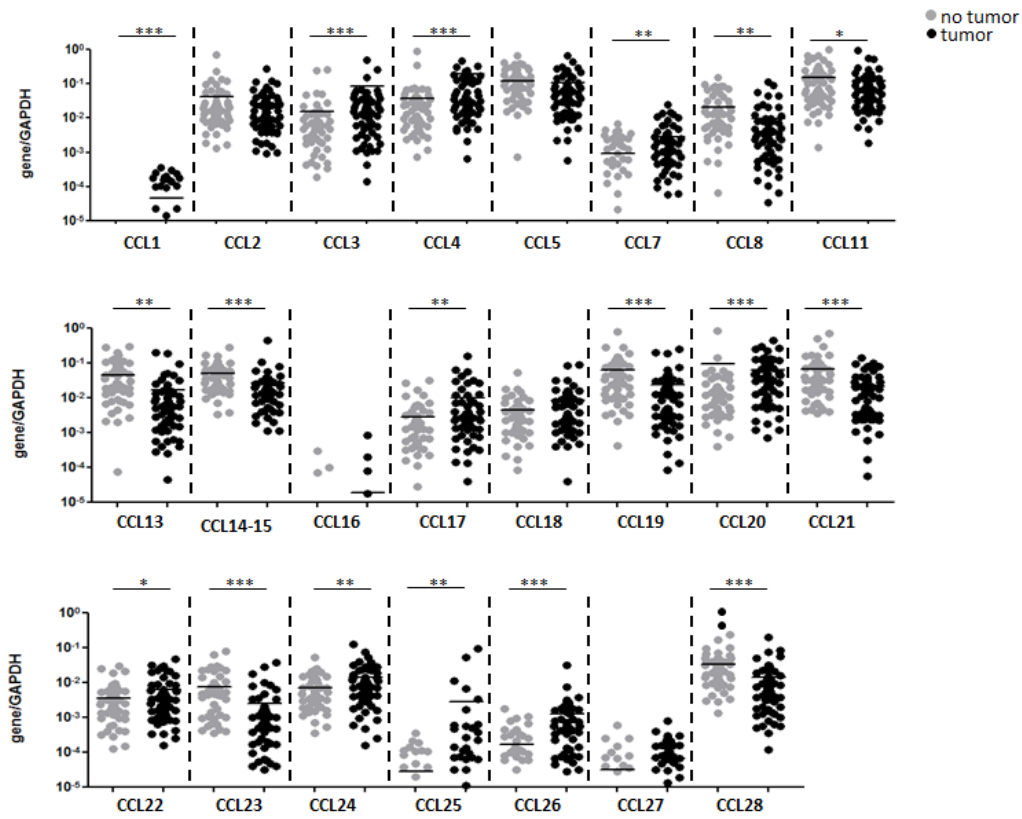


## **2. Chemokine gene expression in primary CRC**

We next evaluated the expression of a large panel of chemokine genes (Table III.2) in the same cohort of samples. All chemokines were found to be expressed in CRC, although at different levels. Notably, expression levels of CCL3, CCL4, CCL7, CCL17, CCL22, CCL24, CCL25, CCL26, CXCL1, CXCL2, CXCL3, CXCL4, CXCL5, CXCL6, CXCL7, CXCL8, CXCL9, CXCL10, CXCL11, and CXCL16 were significantly higher in CRC as compared to tumor-free colonic mucosa, whereas those of CCL8, CCL11, CCL13, CCL14-15, CCL19, CCL20, CCL21, CCL23, CCL28, CXCL12, and CXCL14 genes appeared to be downregulated (Figure IV.2 A, B).

Furthermore, when chemokine expression in tumors was normalized to that detected in corresponding tumor-free colonic tissues, a strong upregulation of a panel of chemokines including, CCL3-5, CCL7-8, CCL13, CCL20, CCL22, CXCL1-3, CXCL5, CXCL8-12, CXCL16, and CX3CL1, was observed in a subgroup of 11 samples (Figure IV.3). Importantly, these samples also displayed a higher expression of CD8, IRF1, T-bet, Foxp3 and CD16 genes (Figure IV.3).

A



B

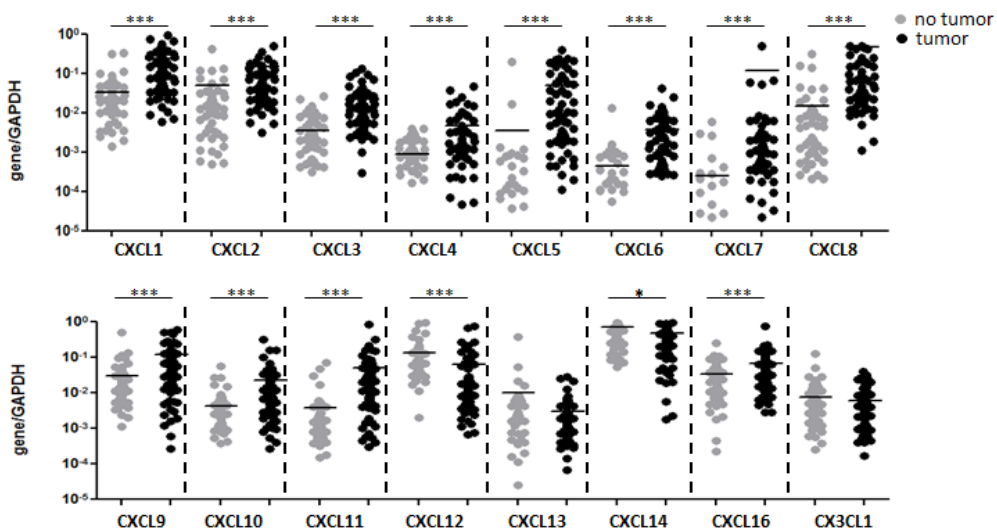


**Figure IV.2:** Chemokine gene expression in CRC and corresponding tumor-free colonic tissues. Total cellular RNA was extracted from freshly excised CRC tissues (n = 62) and corresponding tumor-free colonic tissues, and reverse transcribed. Specific gene expression was analyzed by qRT-PCR, using, as reference, GAPDH house-keeping gene. A. CCL family chemokines. B. CXC family chemokines and CX3CL1. Means are indicated by bars. Statistical significance was assessed by Wilcoxon signed rank test (\*p<0.05; \*\*p<0.01\*\*\*p<0.001;).

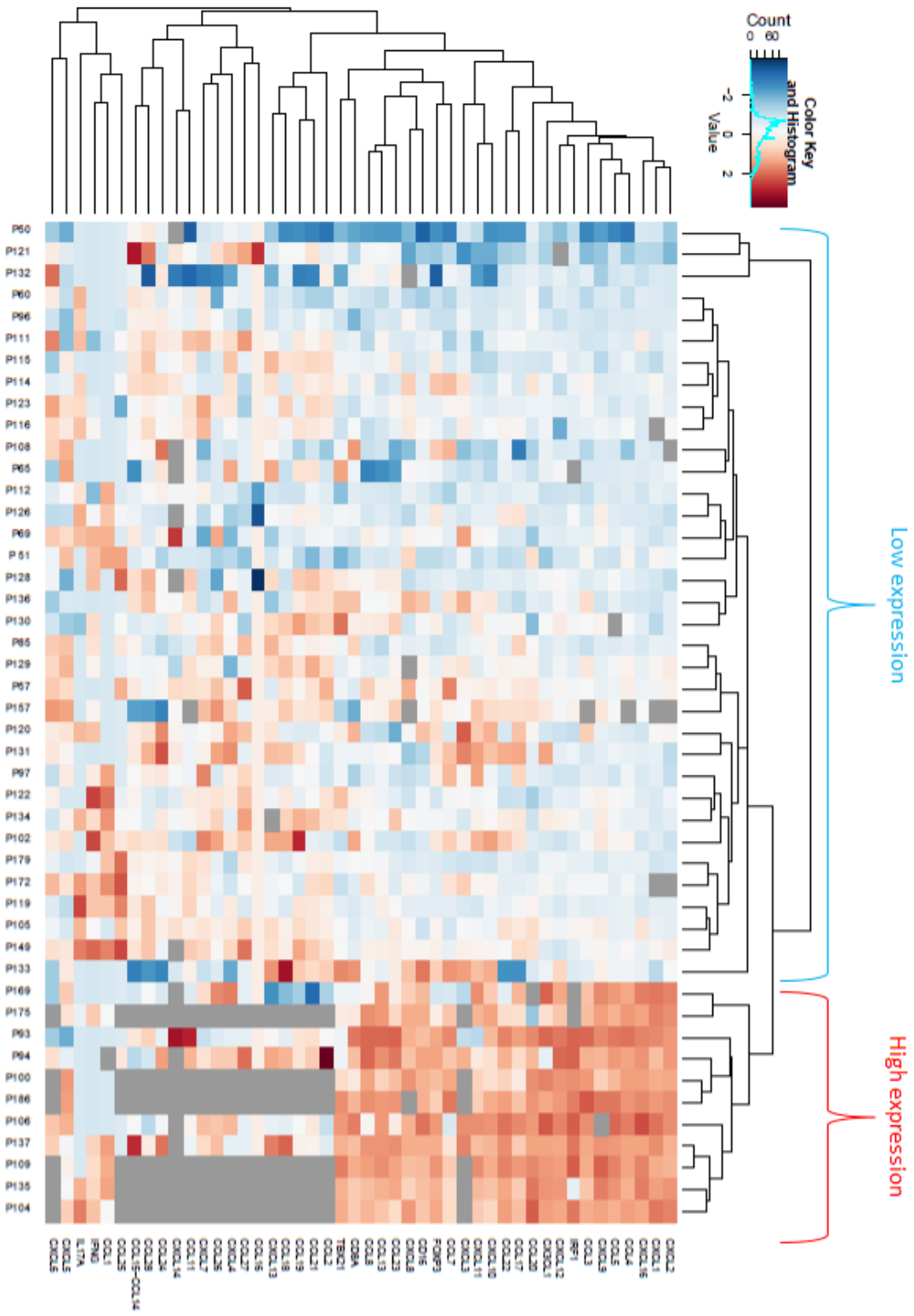


**Figure IV.3:** Chemokine gene expression in CRC and tumor-free colonic tissues. Total cellular RNA was extracted from freshly excised CRC tissues (n = 46) and corresponding tumor-free colonic tissues, and reverse transcribed. Specific gene expression was analyzed by qRT-PCR, using, as reference, GAPDH house-keeping gene.

### 3. Correlations between expression of immune cell markers and chemokine genes in CRC

Prompted by these results, we subsequently evaluated in greater detail correlations between expression of the identified chemokines and that of immune cell marker genes (Table VI.2).

Chemokines	CD8		T-bet		IRF1		Foxp3		CD16	
	Spearman r	p Value	Spearman r	p Value	Spearman r	p Value	Spearman r	p Value	Spearman r	p Value
CCL3	<b>0.4036</b>	<b>0.0015</b>	0.1247	0.3468	<b>0.3205</b>	<b>0.0133</b>	0.1519	0.2509	<b>0.6722</b>	<b>&lt;0.0001</b>
CCL4	<b>0.3454</b>	<b>0.0069</b>	0.0162	0.9021	0.0687	0.6017	-0.0533	0.6857	<b>0.6668</b>	<b>&lt;0.0001</b>
CCL5	<b>0.6544</b>	<b>&lt;0.0001</b>	<b>0.4252</b>	<b>0.0007</b>	<b>0.5578</b>	<b>&lt;0.0001</b>	<b>0.3399</b>	<b>0.0079</b>	<b>0.5505</b>	<b>&lt;0.0001</b>
CCL7	<b>0.3258</b>	<b>0.0104</b>	0.0736	0.5730	0.2613	0.0420	0.1244	0.3396	<b>0.5471</b>	<b>&lt;0.0001</b>
CCL8	<b>0.4632</b>	<b>0.0002</b>	0.1333	0.3056	0.2969	0.0202	0.2038	0.1152	<b>0.4972</b>	<b>&lt;0.0001</b>
CCL13	<b>0.4097</b>	<b>0.0010</b>	0.1364	0.2944	<b>0.3265</b>	<b>0.0102</b>	0.1764	0.1739	<b>0.4161</b>	<b>0.0009</b>
CCL20	-0.2528	0.0493	-0.2051	0.1128	-0.0933	0.4743	-0.1297	0.3192	-0.2001	0.1220
CCL22	<b>0.3754</b>	<b>0.0029</b>	<b>0.4432</b>	<b>0.0003</b>	<b>0.6803</b>	<b>&lt;0.0001</b>	<b>0.7033</b>	<b>&lt;0.0001</b>	<b>0.3362</b>	<b>0.0081</b>
CXCL1	-0.0238	0.8591	-0.1273	0.3411	-0.0580	0.6652	-0.0853	0.5243	<b>0.3377</b>	<b>0.0095</b>
CXCL2	0.1632	0.2170	0.0353	0.7907	0.0244	0.8546	-0.1205	0.3633	<b>0.5375</b>	<b>&lt;0.0001</b>
CXCL5	-0.0318	0.8075	-0.0446	0.7331	0.0298	0.8198	-0.0257	0.8441	<b>0.5318</b>	<b>&lt;0.0001</b>
CXCL8	-0.0823	0.5466	-0.0445	0.7445	-0.1070	0.4326	0.0365	0.7897	<b>0.3420</b>	<b>0.0099</b>
CXCL9	<b>0.5509</b>	<b>&lt;0.0001</b>	<b>0.4138</b>	<b>0.0010</b>	<b>0.5125</b>	<b>&lt;0.0001</b>	<b>0.3458</b>	<b>0.0068</b>	<b>0.5963</b>	<b>&lt;0.0001</b>
CXCL10	<b>0.4268</b>	<b>0.0006</b>	0.2867	0.0251	0.1835	0.1569	0.1431	0.2711	<b>0.6781</b>	<b>&lt;0.0001</b>
CXCL11	0.2075	0.1085	0.2361	0.0669	<b>0.3708</b>	<b>0.0033</b>	0.1436	0.2697	<b>0.6411</b>	<b>&lt;0.0001</b>
CXCL12	<b>0.5330</b>	<b>&lt;0.0001</b>	<b>0.3592</b>	<b>0.0045</b>	<b>0.5795</b>	<b>&lt;0.0001</b>	<b>0.4887</b>	<b>0.0001</b>	<b>0.4597</b>	<b>0.0002</b>
CXCL16	0.2864	0.0252	0.1562	0.2293	<b>0.4231</b>	<b>0.0007</b>	0.2046	0.1138	<b>0.4150</b>	<b>0.0009</b>
CX3CL1	0.2703	0.0351	<b>0.3134</b>	<b>0.0139</b>	<b>0.5272</b>	<b>&lt;0.0001</b>	<b>0.4085</b>	<b>0.0011</b>	<b>0.5902</b>	<b>&lt;0.0001</b>

**Table IV.2:** Correlation between gene encoding chemokine and immune cell markers. Total cellular RNA was extracted from freshly excised CRC tissues (n = 62) and corresponding healthy mucosa sampled at distance from the tumor and reverse transcribed. Specific gene expression was analyzed by qRT-PCR, using, as reference, GAPDH house-keeping gene expression. Correlation between CD8; IRF1 and T-bet, Foxp3 and, CD16 and chemokines were found. Spearman r and relative p-values are indicated in the table. Significant correlation coefficients  $\geq 0.3$  are indicated in bold.

CCL3 strongly correlated with CD16 and, to a lower extent, with CD8 and IRF1 gene expression. Similarly, CCL4 was strongly associated with CD16, and weakly with CD8 gene expression. CCL5 gene expression strongly correlated with CD8 and, IRF-1, and to a lower extent, with all other genes under investigation. CCL7, CCL8, and CCL13 were associated with expression of CD8 and CD16, and more weakly, with IRF1 gene. CCL20 only correlated with CD8. In contrast, CCL22 expression was associated with all markers, but most strongly with CD8. CXCL1, CXCL2, CXCL5 and CXCL8 were found to be only associated with CD16. CXCL9, CXCL10 and CXCL11 positively correlated with the

expression of CD16 and to a lower extent with that of T cell markers. CXCL12 expression also correlated with CD16 and all T cell markers. CXCL16 was associated with CD16 and IRF1, and weakly with CD8. Finally, expression of CX3CL1 correlated with CD16 and, to a lower extent, with that of all T cell marker genes.

#### **4. Chemokine receptor expression on CRC infiltrating beneficial immune cells**

We next investigated the molecular background underlying these associations. We hypothesized that chemokines associated with expression of specific immune cell markers, might have a role in recruiting the corresponding cell populations into tumor tissues. Therefore, we first verified whether CRC infiltrating CD8<sup>+</sup> lymphocytes, CD4<sup>+</sup> T helper cells, Tregs and CD16<sup>+</sup>CD66b<sup>+</sup> neutrophils (and corresponding cell populations in tumor-free colonic tissues and PBMCs) expressed corresponding chemokine receptors.

CRC infiltrating CD8<sup>+</sup> T cells expressed CCR5, (binding CCL3-5, CCL8 and CCL13), CXCR3, (the receptor of CXCL9 and CXCL10) and CXCR4 (specific for CXCL12) on a large fraction of cells, whereas CCR3 (binding CCL7) and CCR6 (the receptor of CCL20) were expressed on smaller subsets. Notably, frequencies of CCR5<sup>+</sup>, CCR6<sup>+</sup>, and CXCR4<sup>+</sup> cells were significantly increased within tissue infiltrating as compared to peripheral blood CD8<sup>+</sup> cells, whereas no significant differences were observed between CD8<sup>+</sup> cells infiltrating CRC or tumor-free colonic tissues nor between peripheral blood lymphocytes from patients and healthy donors. Unfortunately, expression of the gut homing receptor CCR9 (binding CCL25) could be evaluated only on three CRC samples displaying heterogeneous proportions of CD8<sup>+</sup> T cells. Remarkably, percentages of CCR9<sup>+</sup> /CD8<sup>+</sup> cells in PBMCs were significantly increased in patients as compared to healthy donors. In contrast, cells expressing CCR4 and CX3CR1, binding CCL22 and CX3CL1 respectively, were not detected (data not shown) (Figure IV.4).

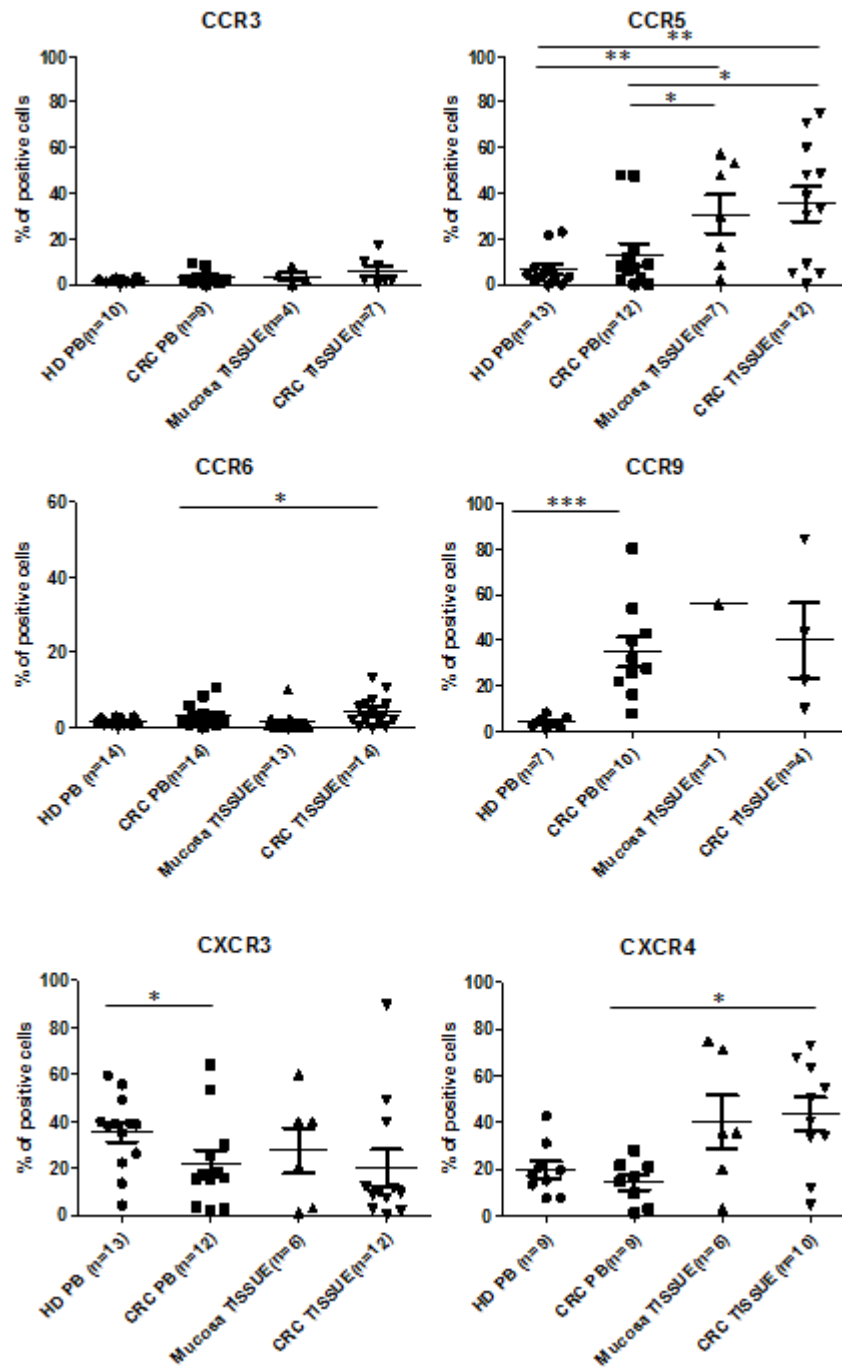


**Figure IV.4:** Chemokine receptor expression in CRC infiltrating CD8<sup>+</sup> T cells. PBMC from healthy donors or CRC patients, and single cell suspensions obtained from freshly excised clinical specimens of CRC and tumor free colonic tissues were surface stained with antibodies specific for CD8, in combination with the indicated chemokine receptors. Percentages of positive cells are shown. Means and standard deviation are indicated by bars. Statistical significance was assessed by Mann Whitney test (\*p<0.05; \*\*p<0.01; \*\*\*p<0.001).

Tumor infiltrating CD4<sup>+</sup> (Foxp3<sup>-</sup>) T helper cells mostly expressed CCR4, CCR5, CXCR3 and CXCR4. In addition, CCR3, CCR6 and CCR9 were also expressed in smaller cell fractions. In contrast to CD8<sup>+</sup> T cells, poor expression of CCR9 was detected on peripheral blood T-helper

cells. Frequencies of CCR3+, CCR4+, CCR5+ and CXCR4+ cells were significantly higher within tissue infiltrating as compared to PB T helper cells (Figure IV.5).

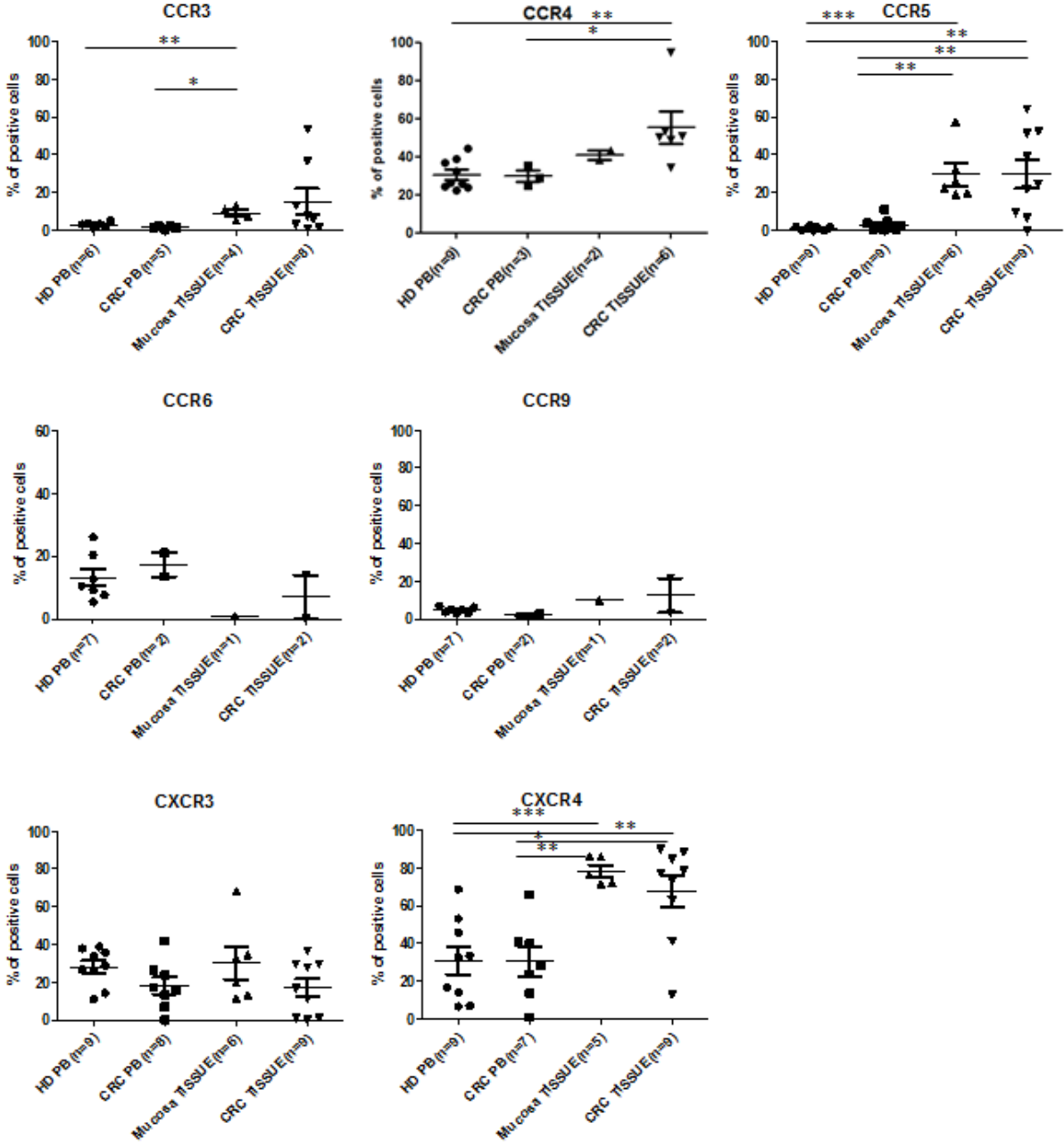


**Figure IV.5:** Chemokine receptor expression on CRC infiltrating CD4+ T helper cells. PBMC from healthy donors or CRC patients, and single cell suspensions obtained from freshly excised clinical specimens of CRC and tumor free colonic tissues were surface stained with antibodies specific for CD4, in combination with the indicated chemokine receptors, and intracellular staining for Foxp3 was then performed. Percentages of CD4+ Foxp3-positive cells are reported. Means and standard deviations are indicated by bars. Statistical significance was assessed by Mann Whitney test (\*p<0.05; \*\*p<0.01).

CRC infiltrating Tregs also showed prominent expression of CCR4, CCR5, CXCR3 and CXCR4, whereas only small fractions of cells expressed CCR3. Expression of CCR6 and CCR9, evaluated so far on two samples only, also appeared to be limited. Moreover, percentages of CCR5+ and CXCR4+ cells were significantly increased within tissue infiltrating as compared to peripheral blood Tregs, whereas no significant differences were observed between Tregs infiltrating CRC or tumor-free colonic tissues. (Figure IV.6).

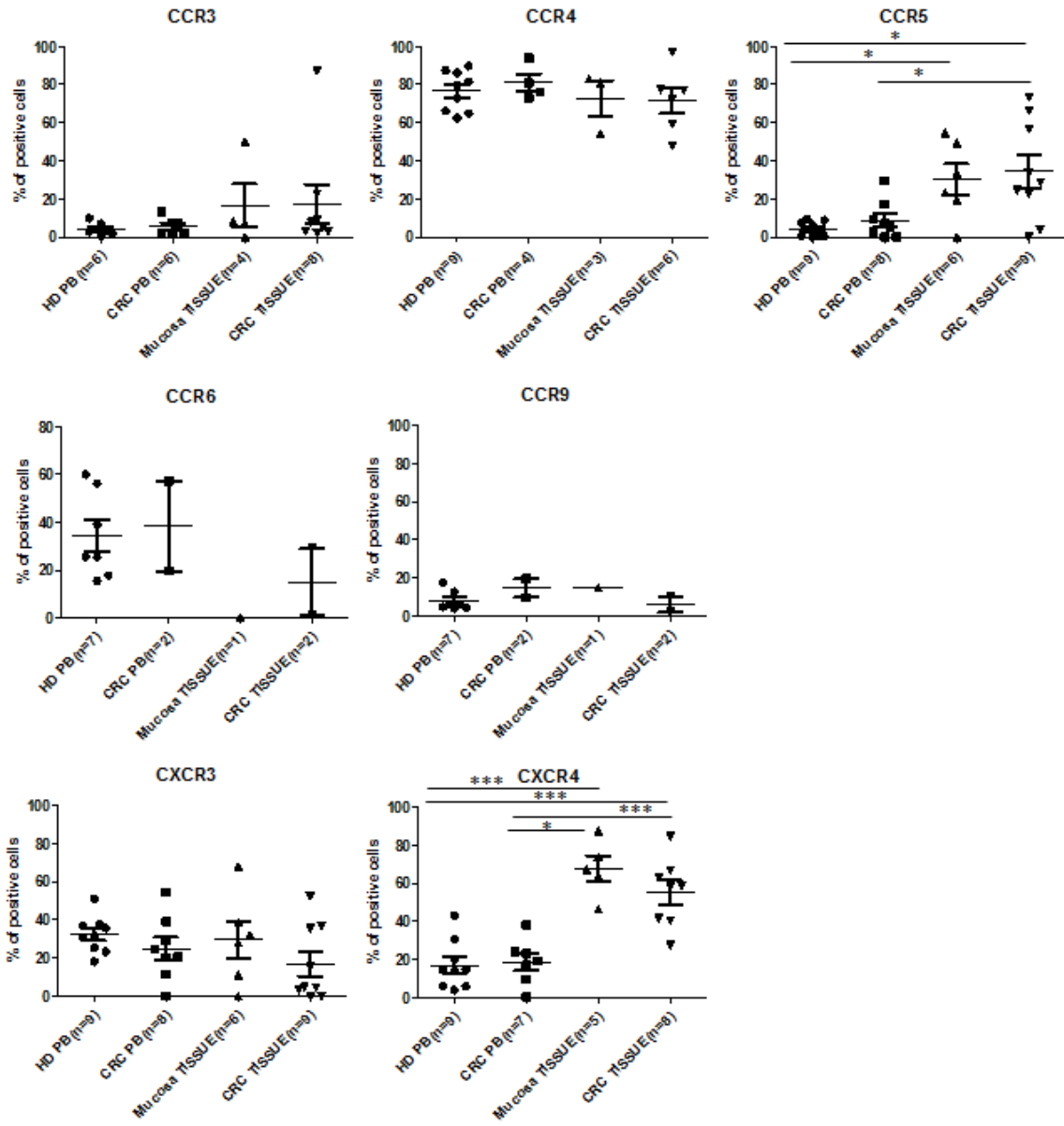


**Figure IV.6:** Chemokine receptor expression on CRC infiltrating Tregs. PBMCs from healthy donors or CRC patients, and single cell suspensions obtained from freshly excised clinical specimens of CRC and tumor free colonic tissues were surface stained with antibodies specific for CD4, in combination with the indicated chemokine receptors. Intracellular staining for Foxp3 was then performed. Percentages of CD4+ Foxp3+ positive cells are shown. Means and standard deviation are indicated by bars. Statistical significance was assessed by Mann Whitney test (\*p<0.05; \*\*\*p<0.001).



CD16+CD66b+ neutrophils in CRC and mucosa tissues similarly expressed CXCR1 (binding CXCL8) and CXCR2 (binding CXCL1, 2, CXCL5 and CXCL8) on a large cell fraction (approximately up to 60% of cells) This percentage however, appeared to be reduced as compared to that of positive cells among circulating neutrophils of both patients and healthy donors. In contrast, no expression of CCR3-5, CXCR3-4 and CXCR6 was detected in any neutrophil populations (Figure IV.7). Furthermore, we detected expression of CX3CR1 on a small neutrophil subset in peripheral blood of healthy donors (data not shown). We are currently evaluating CX3CR1 expression on circulating and tissue infiltrating neutrophils in patients.

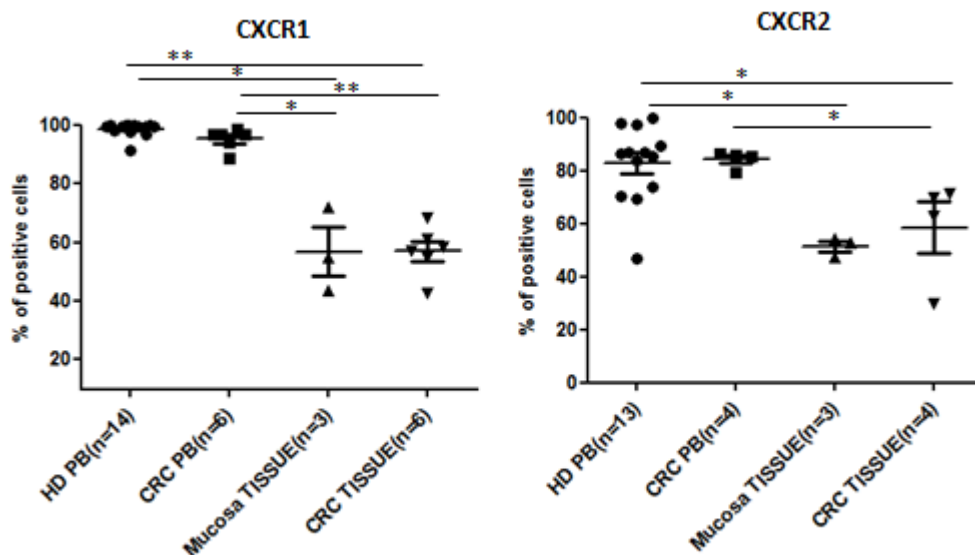


**Figure IV.7:** Chemokine receptor expression on CRC infiltrating CD16+CD66b+ neutrophils. Neutrophils from healthy donors or CRC patients (EasyStep enrichment kit), and single cell suspensions obtained from freshly excised clinical specimens of CRC and tumor free colonic tissues were surface stained with specific antibodies, in combination with the indicated chemokine receptors. Percentages of CD16+ CD66b+ positive cells are shown. Means and standard deviation are indicated by bars. Statistical significance was assessed by Mann Whitney test (\*P<0.05; \*\*P<0.01).

In summary, CRC infiltrating immune cell subsets were found to express receptors capable of sensing chemokines whose expression is positively associated with that of immune cell markers in CRC tissues, thus suggesting a role for these chemokines in immune cell recruitment.

## **5. Chemokine signatures underling immune cell recruitment in CRC**

Based on chemokine receptor expression profiles and correlations between expression of chemokines and immune cell markers, we could define for each immune cell subset a putative “chemokine signature” (Figure IV.8):

- for CD8+ cells: CCL3, CCL5, CCL8, CCL13, CXCL9, CXCL10 and CXCL12, (and to a minor extent CCL4 and CCL7);
- for Th1: CCL5, CCL22, CXCL9 and CXCL12, (and to a minor extent CCL3, CCL7 and CCL13);
- for Foxp3: CCL22 and CXCL12, (and to a minor extent CCL5 and CXCL9);
- for neutrophils: CXCL2 and CXCL5, (and to a minor extent CX3CL1).

	CCL7	CCL13	CCL8	CCL3	CCL5	CXCL9	CXCL10	CXCL12	CCL22	CXCL2	CXCL5	CX3CL1
CD8												
IRF1												
Foxp3												
CD16												

**Figure IV.8:** Schematic representation of putative chemokine signatures for individual immune cell subsets.

## **6. Chemokine sources in primary CRC**

We next investigated potential chemokine sources in CRC. Indeed, different cell types present within the CRC microenvironment including tumor, stromal, endothelial, and immune cells, may contribute to chemokine release. We first focused our attention on the major CRC component, i.e. the tumor cells. We analyzed by RT-PCR the expression of those chemokines found to be upregulated in CRC samples displaying high immune cell infiltration (see Figure

IV.3), on total CRC tissues and corresponding purified tumor cells, upon sorting based on expression of EpCAM marker. EpCAM<sup>+</sup> cells expressed CCL3, CCL4, CCL20, CXCL1 and CXCL2, at significantly higher levels than total CRC tissues, thus suggesting that tumor cells are a major source of these chemokines. Furthermore, expression of CCL5, CXCL5, CXCL8, CXCL9, CXCL10, CXCL11, CXCL12, and CX3CL1, was also detected in purified EpCAM<sup>+</sup> cells, but was not increased as compared to total CRC tissue, possibly indicating that these chemokines are also released by cells other than tumor cells. Finally, CCL7, CCL8, CCL13, and CCL22, were detected in CRC tissue but not in purified tumor cells (Figure IV.9). These results clearly indicated that tumor cells released a number of chemokines relevant for recruitment of CTLs, Th1, Tregs and neutrophils into CRC tissues.

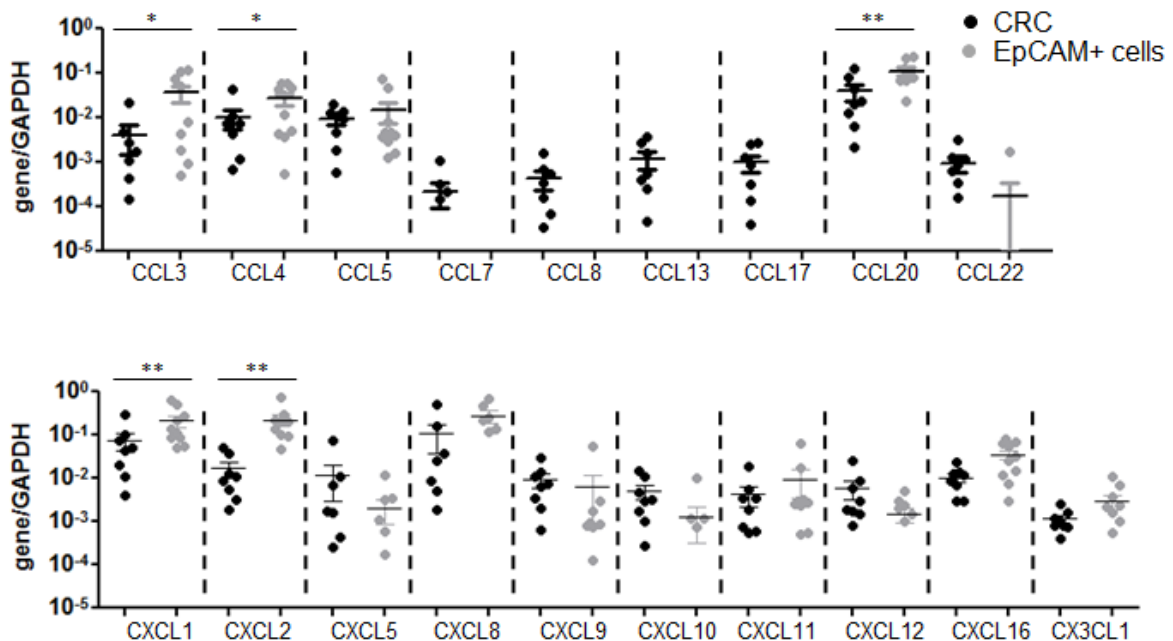


**Figure IV.9:** Chemokine expression in isolated EpCAM<sup>+</sup> cell and CRC tissue. Total cellular RNA was extracted from freshly excised CRC tissues (n= 10) and from EpCAM<sup>+</sup> cells (purity > 97%) sorted from corresponding colorectal cancer cell suspensions, obtained upon enzymatic digestion (n=10). Specific gene expression was analyzed by qRT-PCR, using, as reference, GAPDH house-keeping gene. Means are indicated by bars. Statistical significance was assessed by Mann Whitney test (\* p<0.05; \*\*p<0.01).

## 7. Effects of microbial stimulation on chemokine production by CRC cells in vitro

Subsequently, we sought to elucidate the stimuli leading to chemokine release by CRC cells. Given the peculiar features of the gut microenvironment, we hypothesized that chemokine production in CRC cells might be induced upon triggering of TLRs, expressed on tumor cells, by microbial stimuli derived from gut flora-, possibly translocated into the lamina propria across the altered gut epithelium [Grivennikov S., et al., 2012]. We therefore first evaluated TLR expression on CRC cells from clinical specimens by flow cytometry. TLR2, TLR3, TLR4 and TLR5 were found to be highly expressed both at surface and intracellularly, whereas TLR6, TLR8, TLR9 and TLR10 were expressed at lower levels. No significant expression of TLR1 and TLR7 was observed (Figure IV.10 A, B). Similar TLR expression profiles were detected on a panel of established CRC cell lines (Figure IV.10 C, D).

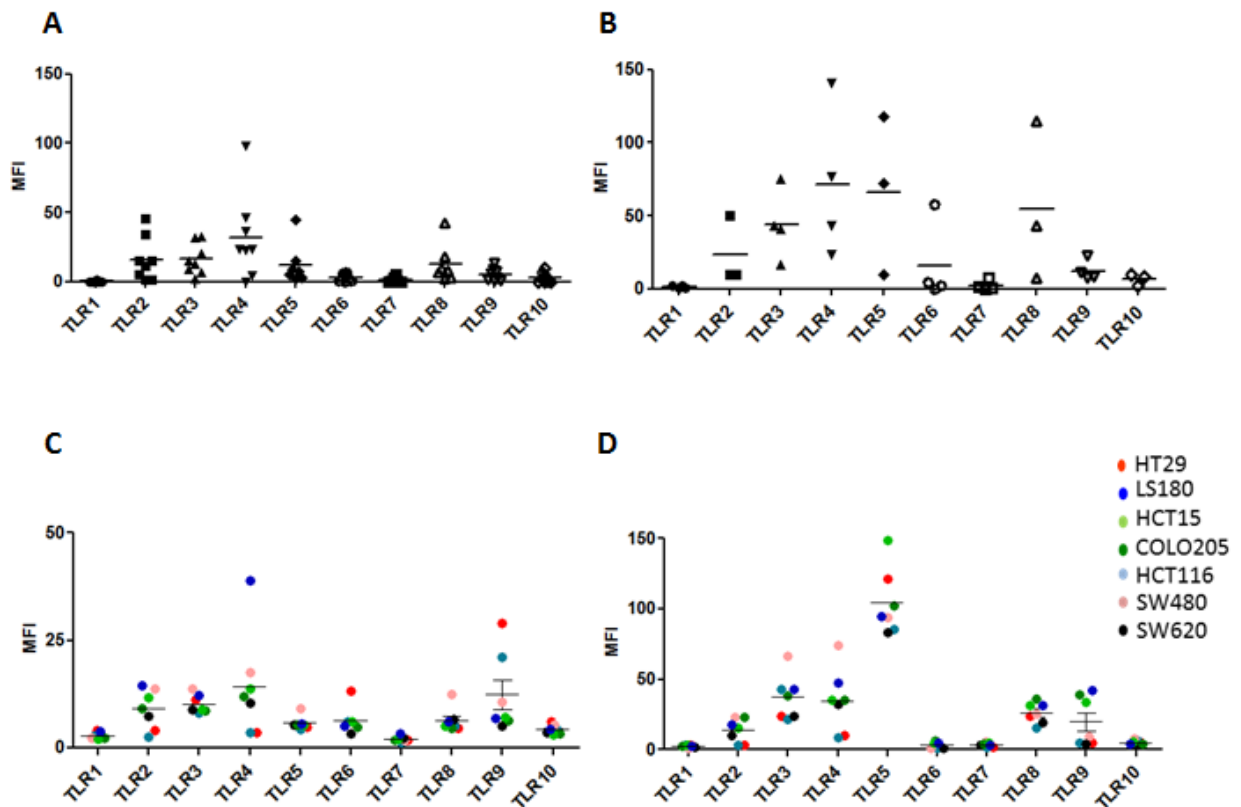


**Figure IV.10.** TLR expression on CRC cells. EpCAM + cells sorted from CRC clinical specimens (A, n=7; B, n=4) and CRC cells from established cell lines (C,D) were surface (A,C) and intracellularly (B,D) stained with antibodies specific for the indicated TLRs. MFI in individual samples or cell lines are shown. Means are indicated by bars.

We then investigated, the effects of stimulation by microbial products on CRC cells from established cell lines. Exposure of CRC cells to purified TLR agonists including Poly(I:C), LPS, Flagellin and FSL-1, binding TLR3, TLR4, TLR5, and TLR2/6 resulted in a significant upregulation of chemokine genes in all cell lines tested, although to different extents (Figure IV.11), thus indicating that TLRs expressed on CRC cells are functional.

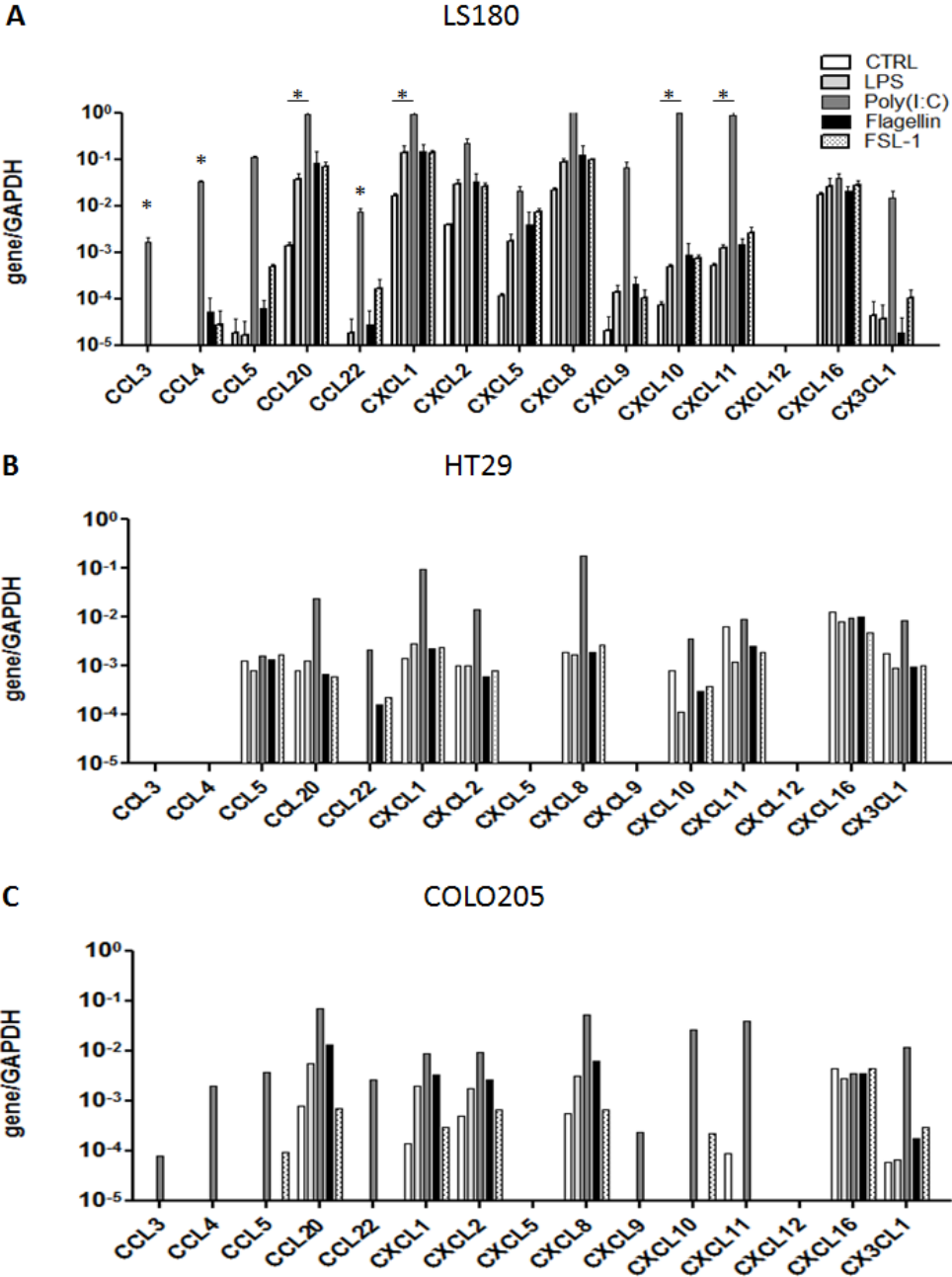
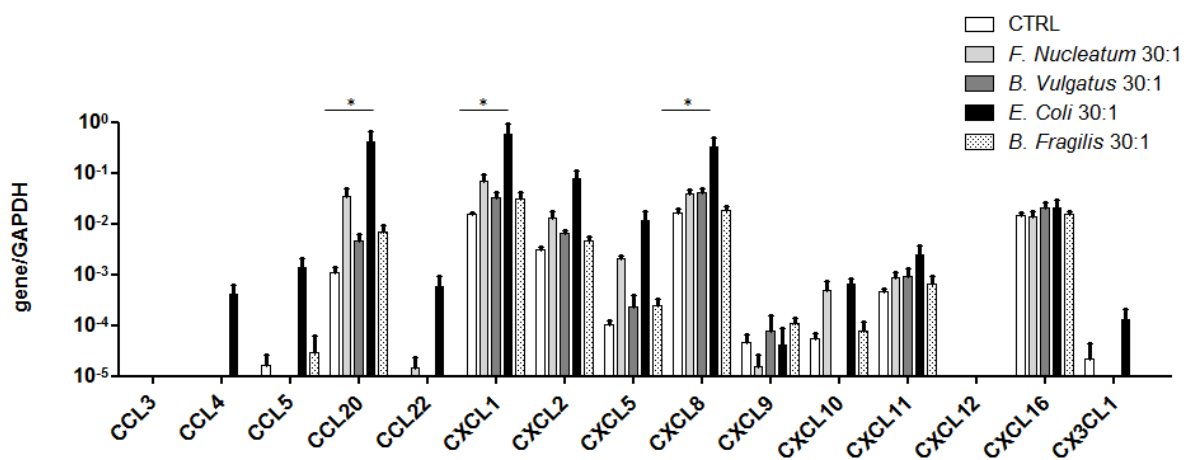


**Figure IV.11:** CRC cell from the indicated established cell lines were treated with LPS, Poly(I:C), Flagellin and FSL-1 at the indicated concentrations. Following four hours incubation, gene expression levels of the indicated chemokines were analyzed by RT-PCR, using GAPDH housekeeping gene as reference. Data from three independent experiments (A) and from one representative experiment (B, C) are shown. Statistical significance was assessed by two-way ANOVA test (\*= $p < 0.05$ ).

Most importantly, when CRC cells were cultured in the presence of different bacterial species known to be abundant in CRC tissues, including *Fusobacterium nucleatum*, *Escherichia Coli*, *Bacteroides vulgatus*, and *Bacteroides Fragilis* [Castellarin M., et al., 2012 and Kostic AD., et al., 2013] expression of genes encoding chemokines mediating recruitment of beneficial immune cell populations into CRC, was also observed (Figure IV.12). Thus, gut flora-derived microbial stimuli are capable of triggering chemokine gene expression in CRC cells in vitro.

A



B

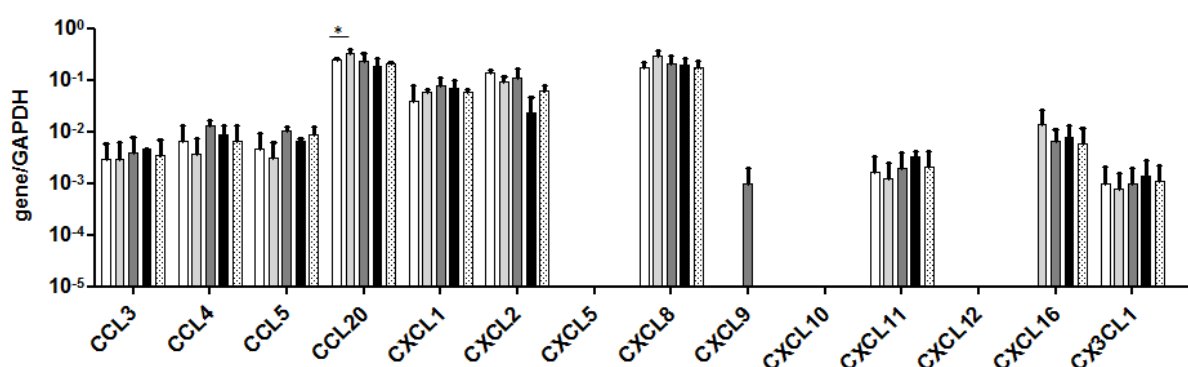


**Figure IV.12:** LS180 cells (A) and Primary CRC cells (B, n=1) were treated with heat-killed preparations of the indicated bacterial strains at the indicated bacteria/tumor cell ratio. After four hours culture, expression levels of the indicated chemokine genes were analyzed by RT-PCR, using GAPDH housekeeping gene as reference. Cumulative data from four independent experiments are shown (A). Statistical significance was assessed by two-way ANOVA test (\*= $p < 0.05$ ).

## **8. Effects of microbial stimulation on chemokine production in vivo**

In order to investigate the impact of the gut flora on chemokine production by CRC cells in vivo, we evaluated gene expression levels of the selected chemokine gene panel in tumor xenografts generated upon subcutaneous or intracecal injection of CRC cells from established cell lines in immunodeficient NSG mice. Whereas subcutaneous xenografts displayed chemokine gene expression levels comparable to those of in vitro cultured CRC cells, intracecal xenografts showed strong upregulation of a number of chemokines, including CCL5, CCL20, CXCL1, CXCL2, CXCL5, CXCL8, and CXCL10 (Figure IV.13). These results suggest that exposure to gut environment promotes chemokine gene expression in CRC cells.

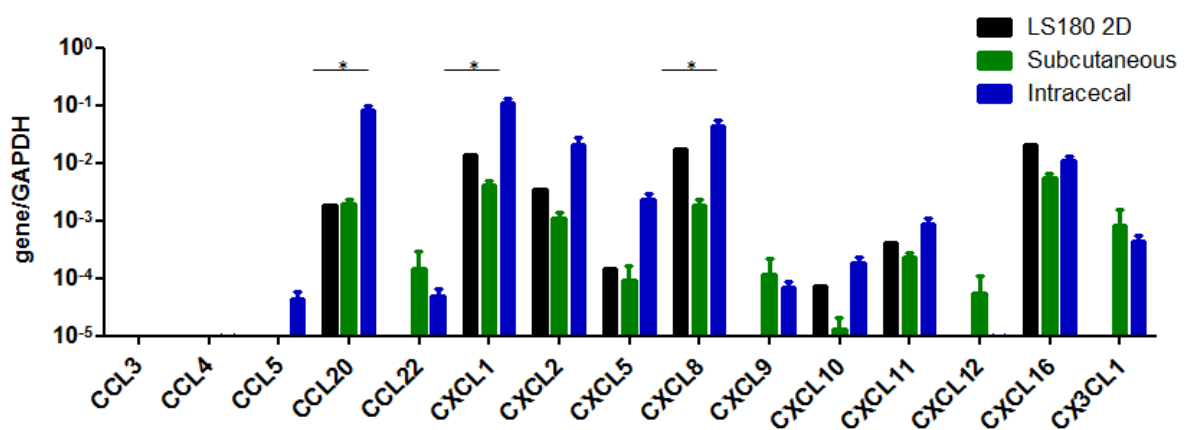


**Figure IV.13:** NSG mice were inoculated subcutaneously (n=8) or intracecally (n=14) with LS180 cells (10<sup>5</sup> cells/mouse). Following tumor development, xenografts were removed and expression levels of the indicated chemokine genes were analyzed by RT-PCR, using GAPDH housekeeping gene as reference, in comparison to those detectable in in vitro cultured LS180 cells. Statistical significance was assessed by two-way ANOVA test (\*= p<0.05).

To further verify whether gut commensal bacteria play a role in this phenomenon, we evaluated the effect of antibiotic administration to tumor bearing mice on chemokine expression detected in intracoecal xenografts. Strikingly, expression of different chemokine genes, including CCL5, CCL20, CXCL5, and CXCL10, was significantly reduced in intracecal xenografts of treated mice as compared to controls (Figure IV.14). Moreover,

expression levels of CCL5, CCL20 and CXCL5 genes significantly correlated with bacterial loads ( $r=0.671$   $p=0.002$ ;  $r=0.484$ ,  $p=0.042$ ;  $r=0.545$ ,  $p=0.019$ , respectively). Thus, gut commensal bacteria promote the expression of genes encoding chemokines putatively contributing to CRC infiltration by immune cells.

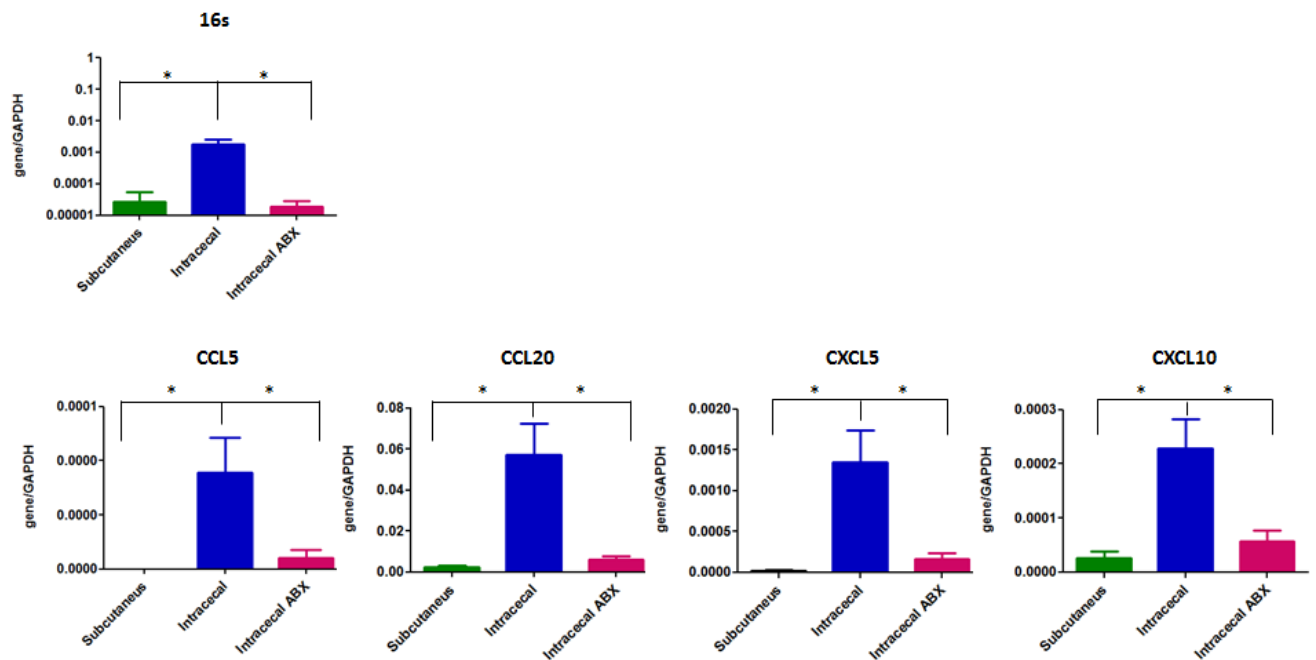


**Figure IV.14:** NSG mice were inoculated subcutaneously ( $n=4$ ) or intracinally ( $n=18$ ) with LS180 cells ( $10^5$  cells/mouse). Following tumor development, a group of mice ( $n=10$ ) bearing intracinal xenografts were treated with Ampicillin and Vancomycin for three weeks. Xenografts were then removed and expression levels of the indicated chemokine genes and bacterial 16s were analyzed by RT-PCR, using GAPDH housekeeping gene as reference. Statistical significance was assessed by Mann Whitney test ( $*=p<0.05$ ).



## 9. Effects of chemokine production on immune cell recruitment into CRC tissues

Next, we evaluated whether chemokines released by CRC cell upon bacteria stimulation promote immune cell migration in vitro. In particular, we tested chemotaxis of peripheral blood CD8<sup>+</sup> T cells, CD4<sup>+</sup> T cells (including T-regs), and neutrophils, towards supernatants of LS180 cells untreated or stimulated with CRC-associated bacteria (Figure IV.15).

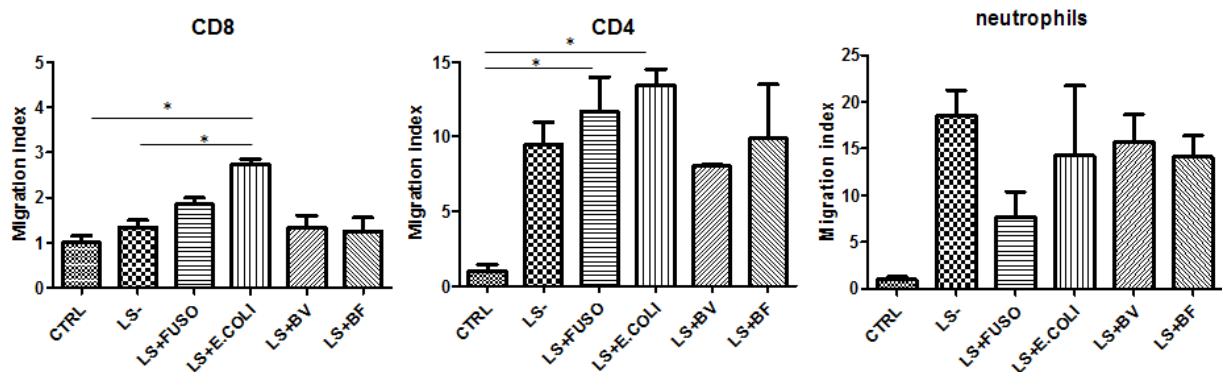


**Figure IV.15: A.** Migration of CTLs, CD4<sup>+</sup> T cells (including T-regs) and neutrophils purified from PBMCs of healthy donors, towards control medium or supernatants from LS180 untreated or exposed for an overnight period to the indicated bacteria. Means  $\pm$  SD from experimental triplicates are indicated. Statistical significance was assessed by one-way ANOVA test (\*=  $p < 0.05$ ).

Supernatants from untreated CRC cells induced vigorous migration of CD4<sup>+</sup> T cells and neutrophils but not of CD8<sup>+</sup> T cells. Upon stimulation with *Fusobacterium nucleatum* and *Escherichia Coli*, but not *Bacteroides Fragilis* nor *Bacteroides vulgatus*, increased migration of CD4<sup>+</sup> T cells and, to a lower extent, of CD8<sup>+</sup> T cells was observed. In contrast, chemotaxis of neutrophils was not increased but rather appeared to be slightly reduced upon bacteria stimulation. These data suggest that the capacity of CRC cells to recruit immune cells into tumor tissues might be modulated by commensal bacteria.

To gain insights into the potential impact of commensal bacteria on chemokine expression, and consequently immune cell infiltration in vivo, we evaluated bacterial loads in our cohort of human CRC samples (see Figure IV.3). Notably, CRC samples characterized by elevated chemokine expression and high immune cell infiltration displayed significantly higher bacterial loads as compared to poorly infiltrated samples (Figure IV.16A). Furthermore,

bacterial loads significantly correlated with expression levels of CCL3, CCL5 and IRF1 (Figure IV.16B), thus suggesting that bacterial stimulation may particularly favor recruitment of Th1 cells.

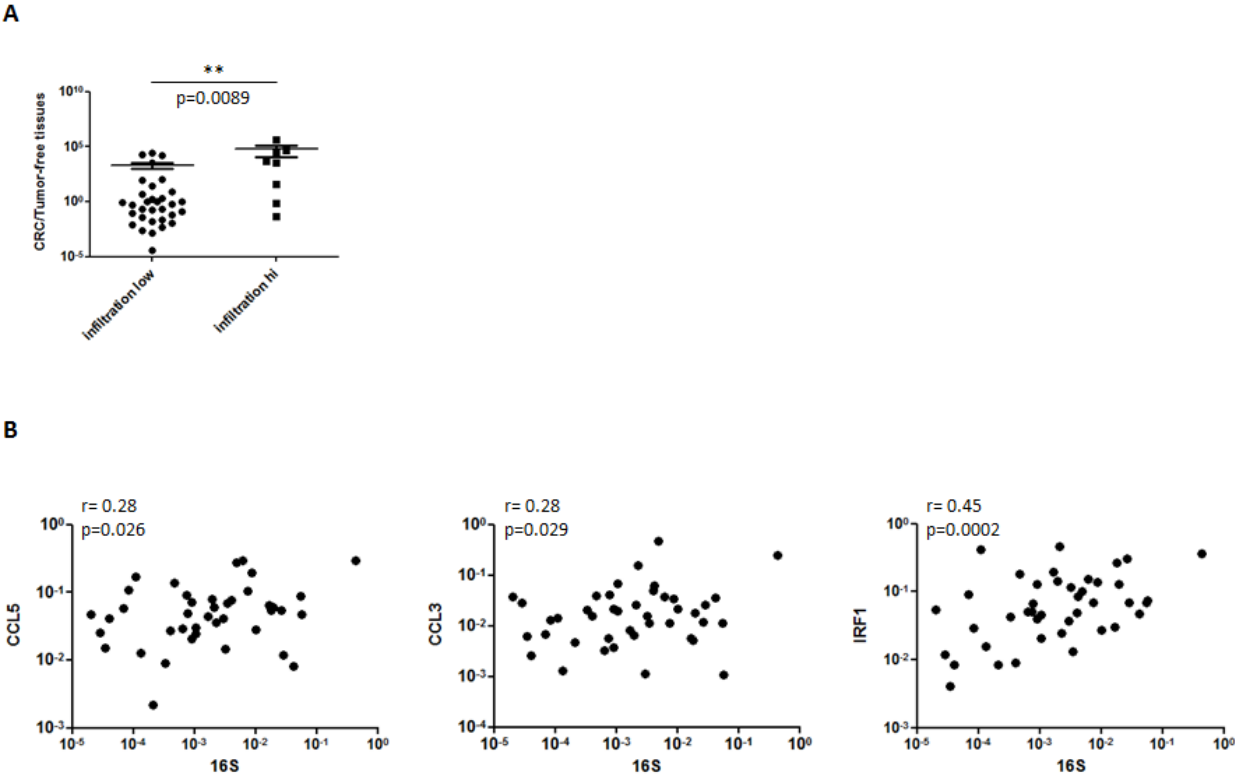


**Figure IV.16:** Bacterial loads were assessed on freshly excised CRC tissues and corresponding healthy mucosa. (n = 62) by evaluating 16s expression, by qRT-PCR, using, GAPDH as house-keeping gene. **A.** Ratio between 16s expression in tumors and corresponding healthy tissues. **B.** Correlations between expression of 16S and that of CCL3, CCL5, and IRF-1. Spearman r and relative p-values are indicated.

# **V. DISCUSSION AND**

# **OUTLOOK**

## **1. Discussion**

During the past decade it has been recognized that CRC infiltration by specific immune cell subsets, including CTLs, Th1 cells, Tregs, and CD16+MPO+ neutrophils, predicts good prognosis. However, mechanisms underlying tumor infiltration by these cell subsets remain to be elucidated. During my PhD I aimed at identifying chemotactic factors possibly involved in this phenomenon, their cellular sources and the stimuli eliciting their production within the CRC microenvironment.

Our data indicate that in CRC:

- a) defined “chemokine signatures” underlie CRC infiltration by specific immune cell subsets;
- b) tumor cells per se act as a source of chemokines promoting recruitment of beneficial immune cells;
- c) gut commensal bacteria modulate chemokine expression by tumor cells “in vitro” and in mouse xenografts;
- d) bacterial loads appear to be associated to chemokine expression and immune cell infiltration in human CRC samples.

### **a) “Chemokine signatures” underlying CRC infiltration by specific immune cell subsets**

The combined analysis of chemokine gene expression in tumor tissues, and its correlation with immune cell markers and chemokine receptor expression on infiltrating immune cells, including CTLs, Th1, Tregs and neutrophils, led us to the identification, of a prominent “chemokine signature” for each cell subset (Figure IV.8).

As expected, neutrophil-associated signature was completely distinct from that of T cell subsets. In contrast, CD8+ T cell and Th1 chemokine signatures largely overlapped, thus

indicating that these two subsets may be concomitantly recruited. Indeed, we observed a significant positive correlation between expression of CD8 and IRF-1 markers (Table IV.1).

Treg-associated signature also partially overlapped with that of CTLs and Th1 cells. Although unexpected, this finding is not surprising considering chemokine receptor expression profiles of CRC infiltrating Tregs, largely resembling those of Th1 and, to a lower extent, CTLs. Accordingly, Foxp3 expression in CRC tissues significantly correlated with that of both CD8 and IRF-1 genes (Table IV.1). Notably, in a melanoma model, recruitment of T regs has been shown to be dependent on release of CCL17 and CCL22 by tumor infiltrating CTLs [Spranger S., et al., 2013]. In our cohort, we did not find significant CCL22 production by tumor cells (see Figure IV.9). Intriguingly however, a significant correlation between expression of CD8 and CCL22 genes was observed (Table IV.2), possibly suggesting that CCL22 may be produced by CRC infiltrating CTLs. Further studies are warranted to verify whether CTLs may actually contribute to Tregs recruitment into CRC tissues through CCL22.

### **b) Tumor cells as source of immune cells recruiting chemokines**

Expression of immune cell recruiting chemokines in CRC tissue has been previously described [Mlecnik B., et al., 2010]. However, cellular sources remain to be defined. Here we show that tumor cells per se express a spectrum of chemokines potentially recruiting immune cell populations associated to a favorable prognosis (Figure IV.9). In particular, tumor cells appeared to express genes encoding CCL3, CCL4 and CCL20, promoting recruitment of CTLs and Th1 cells, and CXCL1 and CXCL2, attracting neutrophils. In contrast, expression of chemokine genes involved in the recruitment of Tregs, such as CCL22, although being detected in CRC tissues, was not observed in tumor cells.

Remarkably, CRC samples displayed heterogeneous chemokine gene expression levels possibly reflecting peculiar molecular characteristics of tumor cells or different microenvironmental conditions. Genomic alterations occurring in CRC cells have been

reported to result in either loss or amplification of chemokine genes [Bindea G., et al., 2013]. More recently, epigenetic silencing of Th1-type chemokines in CRC has also been described [Peng D., et al., 2015 and Nagarsheth N., et al., 2016].

Thus, differential genomic and epigenomic instability may at least partially explain the heterogeneity of chemokine gene expression across different samples. Accordingly, different CRC cell lines, although maintained under comparable culture conditions, displayed a certain degree of variability in chemokine production capacity (Figure IV.11). Importantly however, chemokine gene expression levels in xenografts generated by CRC cells from the same cell line varied according to the site of tumor cell inoculation (Figure IV.13), thus indicating that micro-environmental stimuli also play a relevant role in modulating chemokine gene expression.

### **c) Impact of gut commensal bacteria on chemokine expression by tumor cells**

CRC arise within a peculiar microenvironment which is normally populated by trillions of microorganisms. Upon cancer development, due to the loss of mucus production and of functional tight junctions, commensal bacterial translocate into the lamina propria [Grivennikov S., et al., 2012] and directly act on tumor cells. This phenomenon has been previously shown to induce pro-tumorigenic effects resulting either from direct interaction of bacteria with tumor cells [Rubinstein et al., 2013 and Arthur JC., et al, 2012] or from the release of protumorigenic cytokines by defined immune cell populations exposed to bacterial stimulation [Grivennikov S., et al., 2012].

Unexpectedly, we found that commensal bacteria also trigger in CRC cells the release of chemokines eventually leading to the recruitment of beneficial immune cells. Indeed, upon exposure to specific CRC-associated bacteria, chemokine expression was induced in CRC cell lines in vitro (Figure IV.12). Accordingly, in “in vivo” experiments significantly higher chemokine gene expression levels were detected in intracecal as compared to subcutaneous

xenografts (Figure IV.13). These differences were no longer evident upon antibiotic treatment of tumor bearing mice, thus indicating that chemokine gene expression by tumor cells requires the presence of commensal bacteria (Figure IV.14).

The potential contribution of individual bacterial species remains to be defined. Our “in vitro” experiments suggest that different species of CRC-associated bacteria may differentially modulate chemokine production by CRC cells. Indeed, whereas neutrophils recruiting chemokine gene expression was effectively induced in CRC cells by all tested bacterial strains, expression of T cell recruiting chemokine genes was mainly promoted by *Escherichia Coli* and *Bacteroides Fragilis* (Figure IV.12). Furthermore, only CRC cell stimulation with *Escherichia Coli* resulted in increased T cell chemotaxis in vitro (see Figure IV.15). It is tempting to speculate that the composition of gut flora in CRC patients may concur with the genetic characteristics of the tumor to determine extent and quality of immune cell infiltration.

Molecular mechanisms mediating the cross-talk between CRC cells and gut bacteria also remain to be elucidated. Colon epithelial cells are capable of sensing gut microorganism through PRRs, including TLRs. Our data suggest that TLR triggering on tumor cells may contribute to these phenomena. Indeed, we found TLRs expression on primary CRC cells (Figure IV.10). Furthermore, stimulation with purified TLR agonists resulted in marked induction of chemokine gene expression in CRC cells (Figure IV.11). However, further studies are warranted to precisely identify which TLRs, and, possibly, other PRRs are engaged by individual CRC associated bacterial species.

#### **d) Impact of gut bacteria and chemokines expression on CRC infiltration by immune cells**

Our in vitro and in vivo results, cumulatively suggest that bacteria-induced chemokine production by tumor cells may lead to tumor infiltration by beneficial immune cells.

Consistent with this hypothesis, in preliminary “in vitro” experiments, supernatants of bacteria-stimulated CRC cells promoted chemotaxis of CTLs and Th1 cells to a higher extent than those of untreated tumor cells (Figure IV.15). Moreover, in clinical CRC samples the extent of immune cell infiltration appeared to correlate with chemokine gene expression levels and bacterial loads (Figure IV.16). In particular, significant association between bacterial loads and expression of the Th1 marker IRF-1 and of Th1-recruiting chemokines was observed, thus possibly suggesting that bacteria might play a major role in the recruitment of Th1 cells.

This finding may appear counterintuitive in the light of our in vitro and in vivo results showing preferential production of myeloid cells recruiting chemokines by CRC cells upon bacterial stimulation. However, the cascade of events leading to recruitment of beneficial immune cells may comprise a number of different steps. We may hypothesize that bacteria may first promote the recruitment of neutrophils, and then stimulate them to release T cell recruiting chemokines. Additional “in vivo” studies in support of this concept are required.



## **2. Outlook**

We are currently establishing a suitable “in vivo” model to formally prove the role of gut bacteria in promoting CRC infiltration by immune cells. In particular, we envisage to evaluate recruitment of CRC-derived CD8<sup>+</sup> and Th1 cells, adoptively transferred following in vitro expansion into NSG mice, into intracecal tumor xenografts, generated upon inoculation of CRC cells from cell lines or from autologous primary tumors. To this aim, CTLs and Th1 cells from several CRC samples have already been expanded. Autologous primary CRC cells have also been xenografted in NSG mice in order to allow their in vivo expansion.

We plan to initially assess the effects of antibiotic treatment on intratumoral immune cell recruitment. Subsequently, the contribution of individual CRC-associated bacteria species to the modulation of immune cell recruitment will also be evaluated, upon colonization of tumor bearing mice with defined bacterial strains.

Bacterial species or strains mostly contributing to high chemokine expression and immune cell infiltration in human CRC samples still remain to be identified. Recent work has revealed that specific bacteria are overrepresented in CRC tissues as compared to corresponding non tumoral tissues [Castellari M., et al., 2012 and Kostic AD., et al., 2013]. However, their potential correlation with chemokine expression profiles and tumor infiltration by defined immune cell subsets has not been studied yet.

We envisage to perform microbiome analysis in homogenous small groups of CRC samples characterized by high or low immune cell infiltration. Identified bacterial species or strains will then be tested for their capacity to elicit chemokine production by tumor cells and to favor immune cell recruitment by using the in vivo model described above.

These studies might shed light on the interplay occurring between gut flora and immune system in CRC. Furthermore, they may pave the way towards innovative treatments aimed at modifying the gut flora in order to promote CRC infiltration by beneficial cell types. Notably

in a clinical trial administration of defined strains of probiotics, including *Bifidobacterium longum* and *Lactobacillus johnsonii* to CRC patients prior to tumor resection, resulted in increased numbers of tumor infiltrating T cells [Gianotti L., et al., 2010], thus suggesting a possible modulation of local immunity by the administered probiotics. However, phenotypes of infiltrating T cells have not been evaluated in detail. We plan to investigate the capacity of commercially available probiotics to elicit chemokine production by CRC cells in vitro and promote CRC infiltration by clinically relevant myeloid and T cell populations in vivo. Based on the result of these studies, administration of probiotics found to be effective in CRC patients undergoing surgery might eventually be envisaged.

## **VI. BIBLIOGRAPHY**

Abreu MT, Vora P, Faure E, Thomas LS, Arnold ET, Arditi M. Decreased expression of Toll-like receptor-4 and MD-2 correlates with intestinal epithelial cell protection against dysregulated proinflammatory gene expression in response to bacterial lipopolysaccharide. *J Immunol.* 2001.

Abreu MT, Arnold ET, Thomas LS, Gonsky R, Zhou Y, Hu B, Arditi M. TLR4 and MD-2 expression is regulated by immune-mediated signals in human intestinal epithelial cells. *J Biol Chem.*, 2002.

Abreu MT. Toll-like receptor signalling in the intestinal epithelium: how bacterial recognition shapes intestinal function. *Nat Rev Immunol.*, 2010.

Amicarella F, Muraro MG, Hirt C, Cremonesi E, Padovan E, Mele V, Governa V, Han J, Huber X, Drosler RA, Zuber M, Adamina M, Bolli M, Rosso R, Lugli A, Zlobec I, Terracciano L, Tornillo L, Zajac P, Eppenberger-Castori S, Trapani F, Oertli D, Iezzi G. Dual role of tumour-infiltrating T helper 17 cells in human colorectal cancer. *Gut.* 2015.

Balkwill F. Cancer and the chemokine network. *Nat Rev Cancer.*, 2004.

Bindea G, Mlecnik B, Tosolini M, Kirilovsky A, Waldner M, Obenauf AC, Angell H, Fredriksen T, Lafontaine L, Berger A, Bruneval P, Fridman WH, Becker C, Pagès F, Speicher MR, Trajanoski Z, Galon J. Spatiotemporal dynamics of intratumoral immune cells reveal the immune landscape in human cancer. *Immunity*, 2013.

Blasius AL, Beutler B. Intracellular toll-like receptors. *Immunity*, 2010.

Borroni EM, Mantovani A, Locati M, Bonecchi R. Chemokine receptors intracellular trafficking. *Pharmacol Ther.*, 2010.

Brenner H, Kloor M, Pox CP. Colorectal cancer. *Lancet*, 2014.

Burns K, Clatworthy J, Martin L, Martinon F, Plumpton C, Maschera B, Lewis A, Ray K, Tschopp J, Volpe F. Tollip, a new component of the IL-1RI pathway, links IRAK to the IL-1 receptor. *Nat Cell Biol.*, 2000.

Camus M, Tosolini M, Mlecnik B, Pagès F, Kirilovsky A, Berger A, Costes A, Bindea G, Charoentong P, Bruneval P, Trajanoski Z, Fridman WH, Galon J. Coordination of intratumoral immune reaction and human colorectal cancer recurrence. *Cancer Res.*, 2009.

Castellarin M, Warren RL, Freeman JD, Dreolini L, Krzywinski M, Strauss J, Barnes R, Watson P, Allen-Vercoe E, Moore RA, Holt RA. *Fusobacterium nucleatum* infection is prevalent in human colorectal carcinoma. *Genome Res.* 2012.

Center MM, Jemal A, Smith RA, Ward E. Worldwide variations in colorectal cancer. *CA Cancer J Clin.* 2009.

Chensue SW. Molecular machinations: chemokine signals in host-pathogen interactions. *Clin Microbiol Rev.* 2001.

Cho YB, Lee WY, Choi SJ, Kim J, Hong HK, Kim SH, Choi YL, Kim HC, Yun SH, Chun HK, Lee KU. CC chemokine ligand 7 expression in liver metastasis of colorectal cancer. *Oncol Rep.*, 2012.

Cunningham D, Atkin W, Lenz HJ, Lynch HT, Minsky B, Nordlinger B, Starling N. Colorectal cancer. *Lancet.* 2010.

Donaldson GP, Lee SM, Mazmanian SK. Gut biogeography of the bacterial microbiota. *Nat Rev Microbiol.* 2016.

Esche C, Stellato C, Beck LA. Chemokines: key players in innate and adaptive immunity. *J Invest Dermatol.*, 2005.

Fearon ER & Vogelstein B. A genetic model for colorectal tumorigenesis. *Cell*, 1990.

Ferlay J, Soerjomataram I, Ervik M, Dikshit R, Eser S, Mathers C, Rebelo M, Parkin DM, Forman D, Bray F. Cancer Incidence and Mortality Worldwide: IARC Cancer Base No. 11 (Internet). Lyon, France: Int Agency Res Cancer. Available from: <http://globocan.iarc.fr>, 2013.

Ferlay J, Soerjomataram I, Dikshit R, Eser S, Mathers C, Rebelo M, Parkin DM, Forman D, Bray F. Cancer incidence and mortality worldwide: sources, methods and major patterns in GLOBOCAN 2012. *Int J Cancer.* 2015.

Frey DM, Drosner RA, Viehl CT, Zlobec I, Lugli A, Zingg U, Oertli D, Kettelhack C, Terracciano L, Tornillo L. High frequency of tumor-infiltrating FOXP3(+) regulatory T cells predicts improved survival in mismatch repair-proficient colorectal cancer patients. *Int J Cancer.*, 2010.

Fridman WH, Pagès F, Sautès-Fridman C, Galon J. The immune contexture in human tumours: impact on clinical outcome. *Nat Rev Cancer.*, 2012.

Fukata M, Arditi M. The role of pattern recognition receptors in intestinal inflammation. *Mucosal Immunol.*, 2013.

Gallimore AM, Godkin A. Epithelial barriers, microbiota, and colorectal cancer. *N Engl J Med.*, 2013.

Galon J, Costes A, Sanchez-Cabo F, Kirilovsky A, Mlecnik B, Lagorce-Pagès C, Tosolini M, Camus M, Berger A, Wind P, Zinzindohoué F, Bruneval P, Cugnenc PH, Trajanoski Z, Fridman WH, Pagès F. Type, density, and location of immune cells within human colorectal tumors predict clinical outcome. *Science*, 2006.

Galon J, Pagès F, Marincola FM, Angell HK, Thurin M, Lugli A, Zlobec I, Berger A, Bifulco C, Botti G, Tatangelo F, Britten CM, Kreiter S, Chouchane L, Delrio P, Arndt H, Asslaber M, Maio M, Masucci GV, Mihm M, Vidal-Vanaoclocha F, Allison JP, Gnjatic S, Hakansson L, Huber C, Singh-Jasuja H, Ottensmeier C, Zwierzina H, Laghi L, Grizzi F, Ohashi PS, Shaw PA, Clarke BA, Wouters BG, Kawakami Y, Hazama S, Okuno K, Wang E, O'Donnell-Tormey J, Lagorce C, Pawelec G, Nishimura MI, Hawkins R, Lapointe R, Lundqvist A, Khleif SN, Ogino S, Gibbs P, Waring P, Sato N, Torigoe T, Itoh K, Patel PS, Shukla SN, Palmqvist R, Nagtegaal ID, Wang Y, D'Arrigo C, Kopetz S, Sinicrope FA, Trinchieri G, Gajewski TF, Ascierto PA, Fox BA. Cancer classification using the Immunoscore: a worldwide task force. *J Transl Med.*, 2012.

Gianotti L, Morelli L, Galbiati F, Rocchetti S, Coppola S, Beneduce A, Gilardini C, Zonenschain D, Nespoli A, Braga M. A randomized double-blind trial on perioperative administration of probiotics in colorectal cancer patients. *World J Gastroenterol.* 2010.

Graham GJ. D6 and the atypical chemokine receptor family: novel regulators of immune and inflammatory processes. *Eur J Immunol.*, 2009.

Graham GJ, Locati M, Mantovani A, Rot A, Thelen M. The biochemistry and biology of the atypical chemokine receptors. *Immunol Lett.*, 2012.

Griffith JW, Sokol CL, Luster AD. Chemokines and chemokine receptors: positioning cells for host defense and immunity. *Annu Rev Immunol.* 2014.

Grivennikov Sergei I., Wang Kepeng, Mucida Daniel, Stewart Andrew, Schnabl Bernd, Jauch Dominik, Taniguchi Koji, Guann-Yi Yu., Österreicher Christoph H., Hung Kenneth E, Datz Christian, Feng Ying, Fearon Eric R., Oukka Mohamed, Tessarollo Lino, Coppola Vincenzo, Yarovinsky Felix, Cheroutre Hilde, Eckmann Lars, Trinchieri Giorgio & Karin Michael. Adenoma-linked barrier defects and microbial products drive IL-23/IL-17-mediated tumour growth. *Nature* 2012.

Gur C, Ibrahim Y, Isaacson B, Yamin R, Abed J, Gamliel M, Enk J, Bar-On Y, Stanietsky-Kaynan N, Copenhagen-Glazer S, Shussman N, Almogy G, Cuapio A, Hofer E, Mevorach D, Tabib A, Ortenberg R, Markel G, Miklić K, Jonjic S, Brennan CA, Garrett WS, Bachrach G, Mandelboim O. Binding of the Fap2 protein of *Fusobacterium nucleatum* to human inhibitory receptor TIGIT protects tumors from immune cell attack. *Immunity*. 2015.

Habtezion A, Nguyen LP, Hadeiba H, Butcher EC. Leukocyte Trafficking to the Small Intestine and Colon. *Gastroenterology*. 2016

Hashimoto, C., Hudson, K. L. & Anderson, K. V. The Toll gene of *Drosophila*, required for dorsal–ventral embryonic polarity, appears to encode a transmembrane protein. *Cell*, 1988.

Hirt C, Eppenberger-Castori S, Sconocchia G, Iezzi G, Tornillo L, Terracciano L, Spagnoli GC, Droeser RA. Colorectal carcinoma infiltration by myeloperoxidase-expressing neutrophil granulocytes is associated with favorable prognosis. *Oncoimmunology*, 2013.

Hojo S, Koizumi K, Tsuneyama K, Arita Y, Cui Z, Shinohara K, Minami T, Hashimoto I, Nakayama T, Sakurai H, Takano Y, Yoshie O, Tsukada K, Saiki I. High-level expression of chemokine CXCL16 by tumor cells correlates with a good prognosis and increased tumor-infiltrating lymphocytes in colorectal cancer. *Cancer Res.*, 2007.

Jess T, Simonsen J, Jørgensen KT, Pedersen BV, Nielsen NM, Frisch M. Decreasing risk of colorectal cancer in patients with inflammatory bowel disease over 30 years. *Gastroenterology*. 2012.

Kaser A, Ludwiczek O, Holzmann S, Moschen AR, Weiss G, Enrich B, Graziadei I, Dunzendorfer S, Wiedermann CJ, Mürzl E, Grasl E, Jasarevic Z, Romani N, Offner FA, Tilg H. Increased expression of CCL20 in human inflammatory bowel disease. *J Clin Immunol*. 2004.

Kawamura M, Toiyama Y, Tanaka K, Saigusa S, Okugawa Y, Hiro J, Uchida K, Mohri Y, Inoue Y, Kusunoki M. CXCL5, a promoter of cell proliferation, migration and invasion, is a novel serum prognostic marker in patients with colorectal cancer. *Eur J Cancer*, 2012.

Kawasaki T, Kawai T. Toll-like receptor signaling pathways. *Front Immunol*. 2014.

Keeley, Mehrad, and Strieter. Chemokines as mediators of neovascularization. *Arterioscler. Thromb. Vasc. Biol*. 2008.

Kim J, Takeuchi H, Lam ST, Turner RR, Wang HJ, Kuo C, Foshag L, Bilchik AJ, Hoon DS. Chemokine receptor CXCR4 expression in colorectal cancer patients increases the risk for recurrence and for poor survival. *J Clin Oncol.*, 2005.

Kim J, Mori T, Chen SL, Amersi FF, Martinez SR, Kuo C, Turner RR, Ye X, Bilchik AJ, Morton DL, Hoon DS. Chemokine receptor CXCR4 expression in patients with melanoma and colorectal cancer liver metastases and the association with disease outcome. *Ann Surg.*, 2006.

Kostic AD, Chun E, Robertson L, Glickman JN, Gallini CA, Michaud M, Clancy TE, Chung DC, Lochhead P, Hold GL, El-Omar EM, Brenner D, Fuchs CS, Meyerson M, Garrett WS. *Fusobacterium nucleatum* potentiates intestinal tumorigenesis and modulates the tumor-immune microenvironment. *Cell Host Microbe*, 2013.

Kuipers, Grady, Lieberman, Seufferlein, Sung, Boelens, van de Velde and Watanabe. Colorectal cancer. *Nature Reviews Disease Primers*. 2015.

Le DT, Uram JN, Wang H, Bartlett BR, Kemberling H, Eyring AD, Skora AD, Luber BS, Azad NS, Laheru D, Biedrzycki B, Donehower RC, Zaheer A, Fisher GA, Crocenzi TS, Lee JJ, Duffy SM, Goldberg RM, de la Chapelle A, Koshiji M, Bhaijee F, Hübner T, Hruban RH, Wood LD, Cuka N, Pardoll DM, Papadopoulos N, Kinzler KW, Zhou S, Cornish TC, Taube JM, Anders RA, Eshleman JR, Vogelstein B, Diaz LA Jr. PD-1 Blockade in Tumors with Mismatch-Repair Deficiency. *N Engl J Med*. 2015.

Le Y, Zhou Y, Iribarren P, Wang J. Chemokines and chemokine receptors: their manifold roles in homeostasis and disease. *Cell Mol Immunol.*, 2004.

Lee HJ, Song IC, Yun HJ, Jo DY, Kim S. CXC chemokines and chemokine receptors in gastric cancer: from basic findings towards therapeutic targeting. *World J Gastroenterol.*, 2014.



- Maguire A, Sheahan K. Controversies in the pathological assessment of colorectal cancer. *World J Gastroenterol.*, 2014.
- Manavalan B, Basith S, Choi S. Similar Structures but Different Roles - An Updated Perspective on TLR Structures. *Front Physiol.*, 2011.
- Mandar R, Mikelsaar M. Transmission of mother's microflora to the newborn at birth. *Biol Neonate*, 1996.
- Mantovani A, Bonecchi R, Locati M. Tuning inflammation and immunity by chemokine sequestration: decoys and more. *Nat Rev Immunol.*, 2006.
- Martin MU, Wesche H. Summary and comparison of the signaling mechanisms of the Toll/interleukin-1 receptor family. *Biochim Biophys Acta.*, 2002.
- Masopust D, Schenkel JM. The integration of T cell migration, differentiation and function. *Nat Rev Immunol.* 2013.
- Medzhitov R. Recognition of microorganisms and activation of the immune response. *Nature.* 2007.
- Mlecnik B, Tosolini M, Charoentong P, Kirilovsky A, Bindea G, Berger A, Camus M, Gillard M, Bruneval P, Fridman WH, Pagès F, Trajanoski Z, Galon J. Biomolecular network reconstruction identifies T-cell homing factors associated with survival in colorectal cancer. *Gastroenterology*, 2010.
- Mora JR, von Andrian UH. T-cell homing specificity and plasticity: new concepts and future challenges. *Trends Immunol.* 2006.
- O'Connell JB, Maggard MA, Ko CY. Colon cancer survival rates with the new American Joint Committee on Cancer sixth edition staging. *J Natl Cancer Inst.* 2004.
- Ogata H, Sekikawa A, Yamagishi H, Ichikawa K, Tomita S, Imura J, Ito Y, Fujita M, Tsubaki M, Kato H, Fujimori T, Fukui H. GRO $\alpha$  promotes invasion of colorectal cancer cells. *Oncol Rep.*, 2010.
- O'Hara AM, and, Shanahan F. The gut flora as a forgotten organ. *EMBO*, 2006.

Oyama T, Miura S, Watanabe C, Hokari R, Fujiyama Y, Komoto S, Tsuzuki Y, Hosoe N, Nagata H, Hibi T. CXCL12 and CCL20 play a significant role in mucosal T-lymphocyte adherence to intestinal microvessels in mice. *Microcirculation*. 2007.

O'Neill Luke A. J., Golenbock Douglas & Bowie Andrew G. The history of Toll-like receptors — redefining innate immunity. *Nature Reviews Immunology*, 2013.

Otte JM, Cario E, Podolsky DK. Mechanisms of cross hyporesponsiveness to Toll-like receptor bacterial ligands in intestinal epithelial cells. *Gastroenterology*. 2004 .

Papadakis KA, Prehn J, Nelson V, Cheng L, Binder SW, Ponath PD, Andrew DP, Targan SR. The role of thymus-expressed chemokine and its receptor CCR9 on lymphocytes in the regional specialization of the mucosal immune system. *J Immunol*. 2000.

Peng D, Kryczek I, Nagarsheth N, Zhao L, Wei S, Wang W, Sun Y, Zhao E, Vatan L, Szeliga W, Kotarski J, Tarkowski R, Dou Y, Cho K, Hensley-Alford S, Munkarah A, Liu R, Zou W. Epigenetic silencing of TH1-type chemokines shapes tumor immunity and immunotherapy. *Nature*. 2015.

Rakoff-Nahoum S, Medzhitov R. Regulation of spontaneous intestinal tumorigenesis through the adaptor protein MyD88. *Science*. 2007

Rhee SH, Im E, Pothoulakis C. Toll-like receptor 5 engagement modulates tumor development and growth in a mouse xenograft model of human colon cancer. *Gastroenterology*. 2008

Rostène William, Kitabgi Patrick & Mélik Parsadaniantz Stéphane. Chemokines: a new class of neuromodulator? *Nature Reviews Neuroscience*, 2007.

Rubie C, Frick VO, Pfeil S, Wagner M, Kollmar O, Kopp B, Graber S, Rau BM, Schilling MK. Correlation of IL-8 with induction, progression and metastatic potential of colorectal cancer. *World J Gastroenterol.*, 2007.

Rubinstein MR, Wang X, Liu W, Hao Y, Cai G, Han YW. *Fusobacterium nucleatum* promotes colorectal carcinogenesis by modulating E-cadherin/ $\beta$ -catenin signaling via its FadA adhesin. *Cell Host Microbe*. 2013.

Salama P, Phillips M, Grieu F, Morris M, Zeps N, Joseph D, Platell C, Iacopetta B. Tumor-infiltrating FOXP3<sup>+</sup> T regulatory cells show strong prognostic significance in colorectal cancer. *J Clin Oncol.*, 2009.

Sánchez de Medina F, Romero-Calvo I, Mascaraque C, Martínez-Augustin O. Intestinal inflammation and mucosal barrier function. *Inflamm Bowel Dis.*, 2014

Sconocchia G<sup>1</sup>, Zlobec I, Lugli A, Calabrese D, Iezzi G, Karamitopoulou E, Patsouris ES, Peros G, Horcic M, Tornillo L, Zuber M, Drosner R, Muraro MG, Mengus C, Oertli D, Ferrone S, Terracciano L, Spagnoli GC. Tumor infiltration by FcγRIII (CD16)<sup>+</sup> myeloid cells is associated with improved survival in patients with colorectal carcinoma. *Int J Cancer.* 2011.

Sekirov I, Russell SL, Antunes LC, Finlay BB. Gut microbiota in health and disease. *Physiol Rev.*, 2010.

Singh, Sharma, Krishnan, and Lockhart Immune checkpoints and immunotherapy for colorectal cancer *Gastroenterol. Rep.* 2015.

Stenstad H, Svensson M, Cucak H, Kotarsky K, Agace WW. Differential homing mechanisms regulate regionalized effector CD8αβ<sup>+</sup> T cell accumulation within the small intestine. *Proc Natl Acad Sci U S A.* 2007.

Teramoto K, Miura S, Tsuzuki Y, Hokari R, Watanabe C, Inamura T, Ogawa T, Hosoe N, Nagata H, Ishii H, Hibi T. Increased lymphocyte trafficking to colonic microvessels is dependent on MAdCAM-1 and C-C chemokine mLARC/CCL20 in DSS-induced mice colitis. *Clin Exp Immunol.* 2005.

Tosolini M, Kirilovsky A, Mlecnik B, Fredriksen T, Mangu S, Bindea G, Berger A, Bruneval P, Fridman WH, Pagès F, Galon J. Clinical impact of different classes of infiltrating T cytotoxic and helper cells (Th1, th2, treg, th17) in patients with colorectal cancer. *Cancer Res.*, 2011.

Walther A, Johnstone E, Swanton C, Midgley R, Tomlinson I, Kerr D. Genetic prognostic and predictive markers in colorectal cancer. *Nat Rev Cancer.* 2009.

Wang C, Kang SG, Lee J, Sun Z, Kim CH. The roles of CCR6 in migration of Th17 cells and regulation of effector T-cell balance in the gut. *Mucosal Immunol.* 2009.

Wang D, Wang H, Brown J, Daikoku T, Ning W, Shi Q, Richmond A, Strieter R, Dey SK, DuBois RN. CXCL1 induced by prostaglandin E2 promotes angiogenesis in colorectal cancer. *J Exp Med.*, 2006.

Wang D, Dubois RN, Richmond A. The role of chemokines in intestinal inflammation and cancer. *Curr Opin Pharmacol.*, 2009.

Wang SC, Lin JK, Wang HS, Yang SH, Li AF, Chang SC. Nuclear expression of CXCR4 is associated with advanced colorectal cancer. *Int J Colorectal Dis.*, 2010.

West NR, McCuaig S, Franchini F, Powrie F. Emerging cytokine networks in colorectal cancer. *Nat Rev Immunol.* 2015.

Yuan R, Chen Y, He X, Wu X, Ke J, Zou Y, Cai Z, Zeng Y, Wang L, Wang J, Fan X, Wu X, Lan P. CCL18 as an independent favorable prognostic biomarker in patients with colorectal cancer. *J Surg Res.*, 2013.

Zlotnik A, Yoshie O. The chemokine superfamily revisited. *Immunity*, 2012.

Zlobec I, Lugli A. Prognostic and predictive factors in colorectal cancer. *J Clin Pathol.* 2008 .

Zou Y, Chen Y, Wu X, Yuan R, Cai Z, He X, Fan X, Wang L, Wu X, Lan P. CCL21 as an independent favorable prognostic factor for stage III/IV colorectal cancer. *Oncol Rep.*, 2013.

## **VII. APPENDIX**



## Clinical impact of programmed cell death ligand 1 expression in colorectal cancer

Raoul A. Droeser<sup>a,b,\*,h</sup>, Christian Hirt<sup>a,b,h</sup>, Carsten T. Viehl<sup>a</sup>, Daniel M. Frey<sup>a</sup>, Christian Nebiker<sup>a,b</sup>, Xaver Huber<sup>a</sup>, Inti Zlobec<sup>c</sup>, Serenella Eppenberger-Castori<sup>d</sup>, Alexander Tzankov<sup>d</sup>, Raffaele Rosso<sup>e</sup>, Markus Zuber<sup>f</sup>, Manuele Giuseppe Muraro<sup>b</sup>, Francesca Amicarella<sup>b</sup>, Eleonora Cremonesi<sup>b</sup>, Michael Heberer<sup>b</sup>, Giandomenica Iezzi<sup>b</sup>, Alessandro Lugli<sup>c</sup>, Luigi Terracciano<sup>d</sup>, Giuseppe Sconocchia<sup>g</sup>, Daniel Oertli<sup>a</sup>, Giulio C. Spagnoli<sup>b</sup>, Luigi Tornillo<sup>d</sup>

<sup>a</sup> Department of Surgery, University Hospital of Basel, Switzerland

<sup>b</sup> Institute for Surgical Research and Hospital Management ICFS, Department of Biomedicine, University of Basel, Switzerland

<sup>c</sup> Institute of Pathology, University of Bern, Switzerland

<sup>d</sup> Institute of Pathology, University of Basel, Switzerland

<sup>e</sup> Department of Surgery, Ospedale Regionale di Lugano, Switzerland

<sup>f</sup> Department of Surgery, Kantonsspital Olten, Switzerland

<sup>g</sup> Institute of Translational Pharmacology, National Council Research, Rome, Italy

Available online 13 March 2013

### KEYWORDS

Human colorectal cancer  
PD-L1  
Prognostic factors  
Overall survival  
Tissue microarrays

**Abstract Background:** Programmed cell death 1 (PD-1) receptor triggering by PD ligand 1 (PD-L1) inhibits T cell activation. PD-L1 expression was detected in different malignancies and associated with poor prognosis. Therapeutic antibodies inhibiting PD-1/PD-L1 interaction have been developed.

**Materials and methods:** A tissue microarray ( $n = 1491$ ) including healthy colon mucosa and clinically annotated colorectal cancer (CRC) specimens was stained with two PD-L1 specific antibody preparations. Surgically excised CRC specimens were enzymatically digested and analysed for cluster of differentiation 8 (CD8) and PD-1 expression.

**Results:** Strong PD-L1 expression was observed in 37% of mismatch repair (MMR)-proficient and in 29% of MMR-deficient CRC. In MMR-proficient CRC strong PD-L1 expression correlated with infiltration by CD8<sup>+</sup> lymphocytes ( $P = 0.0001$ ) which did not express PD-1. In univariate analysis, strong PD-L1 expression in MMR-proficient CRC was significantly associated with early T stage, absence of lymph node metastases, lower tumour grade, absence of

\* Corresponding author: Address: Department of Surgery, University of Basel, Spitalstrasse 21, CH-4031 Basel, Switzerland. Tel.: +41 61 265 25 25; fax: +41 61 265 72 50.

E-mail address: [rdroeser@uhbs.ch](mailto:rdroeser@uhbs.ch) (R.A. Droeser).

<sup>h</sup> These authors contributed equally to this work.

vascular invasion and significantly improved survival in training ( $P = 0.0001$ ) and validation ( $P = 0.03$ ) sets. A similar trend ( $P = 0.052$ ) was also detectable in multivariate analysis including age, sex, T stage, N stage, tumour grade, vascular invasion, invasive margin and MMR status. Interestingly, programmed death receptor ligand 1 (PDL-1) and interferon (IFN)- $\gamma$  gene expression, as detected by quantitative reverse transcriptase polymerase chain reaction (RT-PCR) in fresh frozen CRC specimens ( $n = 42$ ) were found to be significantly associated ( $r = 0.33$ ,  $P = 0.03$ ).

**Conclusion:** PD-L1 expression is paradoxically associated with improved survival in MMR-proficient CRC.

© 2013 Elsevier Ltd. All rights reserved.

## 1. Introduction

Tumour-infiltrating lymphocytes (TILs) are widely considered to reflect primary host immune response against solid tumours. Recent reports have demonstrated a direct correlation between colorectal cancer (CRC) patient survival and tumour infiltration by cluster of differentiation 8 (CD8) positive T lymphocytes expressing typical activation markers.<sup>1,2</sup> However, the immune system is characterised by the presence of a number of inhibitory mechanisms preventing ‘excessive’ lymphocyte activation.<sup>3</sup> In particular, programmed cell death receptor 1 (PD-1; CD279) is typically expressed by activated lymphocytes.<sup>4</sup> Its engagement by specific ligands, including PD ligand 1 (PD-L1; B7-H1; CD274) and PD ligand 2 (PD-L2; B7-DC; CD273), induces down-regulation of antigen-stimulated lymphocyte proliferation<sup>5,6</sup> and cytokine production,<sup>6,7</sup> ultimately resulting in lymphocyte ‘exhaustion’ and in the induction of immunological tolerance.<sup>6,8–10</sup>

PD-L1 is constitutively expressed by T and B cells, macrophages and dendritic cells (DC) and is up-regulated upon activation by interferons (IFN).<sup>8,9</sup> PD-L1 is also expressed on additional cell types including endothelial, pancreatic and muscle cells.<sup>4</sup> In contrast, PD-L2 expression is much more restricted and typically detectable in activated DC and macrophages.<sup>9</sup> Importantly, up-regulation of the expression of PD-1 ligands in malignant cells has been suggested to play a central role in tumour-immune system interaction<sup>5,11</sup> since, by triggering PD-1, cancer cells might shut down specific immune responses. Indeed, the expression of PD ligands on tumour cells was shown to suppress the cytolytic activity of CD8<sup>+</sup> T-cells.<sup>12,13</sup>

PD-L1 and, to a lesser extent, PD-L2, have been reported to be expressed by tumour cells of different origins, including glioblastoma, ovarian and renal cell carcinomas, squamous cell carcinoma of the head and neck, oesophageal and non-small cell lung cancers.<sup>5,14–18</sup> A strong correlation between expression of PD ligands on tumour cells and severe prognosis has been observed in oesophageal cancer and in renal cell carcinoma.<sup>15,17</sup> Capitalising on this background, PD-1/PD-L1 blockade by anti PD-1 or anti PD-L1 monoclonal antibodies has been envisaged as an appealing option to activate the

host immune system to eradicate tumours. Recently, promising results of phase I clinical trials involving patients bearing a variety of malignancies have been published.<sup>19–21</sup>

Expression of PD-L1 in human CRC has not been addressed so far. In this study we used a tissue microarray (TMA)<sup>22</sup> including 1420 well documented, clinically annotated CRC specimens<sup>23</sup> to investigate the expression of PD-L1 in CRC and its clinical significance.

## 2. Materials and methods

### 2.1. Tissue microarray construction

The TMA used for this study includes 1420 unselected, non-consecutive, primary, sporadic CRCs treated between 1987 and 1996, and 71 normal mucosa specimens from the Institute of Pathology of the University of Basel (Switzerland), the Institute of Clinical Pathology, Basel (Switzerland) and the Institute of Pathology of the Stadtspital Triemli, Zürich (Switzerland). TMA was constructed with materials collected from the Tissue Biobank of the Institute of Pathology, University Hospital Basel. This institution performs translational research with the approval of the EKBB (Ethics Committee Beider Basel) in compliance with ethical standards and patient confidentiality. Construction of this TMA has been previously described in detail.<sup>23</sup> Briefly, formalin-fixed, paraffin-embedded tissue blocks from resected CRC were obtained. Tissue cylinders with a 0.6 mm diameter were punched from representative tissue areas of each donor tissue block and brought into one recipient paraffin block (30 × 25 mm). Each TMA spot included at least 50% tumour cells.

### 2.2. Immunohistochemistry

Four micron sections of TMA blocks were transferred to an adhesive-coated slide system (Instrumedics Inc., Hackensack, NJ, United States of America (USA)). Standard indirect immunoperoxidase procedures were used for immunohistochemistry (IHC; ABC-Elite, Vector Laboratories, Burlingame, CA, USA). Briefly, slides were dewaxed and rehydrated in distilled water. Endogenous peroxidase activity was

blocked using 0.5% H<sub>2</sub>O<sub>2</sub>. The sections were treated with 10% normal goat serum (DakoCytomation, Carpinteria, CA, USA) for 20 min and incubated with primary antibodies at room temperature. Two primary PD-L1 (CD274) specific reagents were used: a monoclonal antibody (mAb, clone 27A2, MBL, Woburn, MA, USA)<sup>24</sup> and a polyclonal preparation (ab82059, Abcam, Cambridge, United Kingdom (UK)).<sup>25</sup> Subsequently, sections were incubated with peroxidase-labelled secondary antibody (DakoCytomation, Glostrup, Denmark) for 30 min at room temperature. For visualisation of the antigen, the sections were immersed in 3-amino-9-ethylcarbazole plus substrate-chromogen (DakoCytomation) for 30 min and counterstained with Gill's haematoxylin. Data used for the analysis of correlations with the expression of other immune markers such as CD8, PD-1, T-intracellular antigen-1 (TIA-1) and Fork Head box P3 (FOXP3) were in part available from previous studies.<sup>26,27</sup>

Two independent observers, blinded to any prior information on clinicopathological features of the patients' samples, examined the immunohistochemical slides. Percentages of PD-L1 positive tumour cells and staining intensity were evaluated for each punch. Staining intensity was scored as previously reported.<sup>24</sup> Outcome analysis was mainly based on staining intensity because in the case of PD-L1 positivity nearly all tumour cells were stained, and tumours with weak or moderate expression were collectively classified as 'low' PD-L1 positive (Fig. 1).<sup>24</sup>

### 2.3. Flow cytometric analyses

Following the Basel Institutional Review Board approval (63/07), tissues from surgically removed CRC and adjacent normal mucosa were minced, centrifuged, and resuspended in RPMI 1640 medium supplemented with 5% foetal calf serum, 2 mg/ml collagenase IV, 0.1 mg/ml hyaluronidase V and 0.2 mg/ml DNase I (Sigma–Aldrich, Basel, Switzerland). Following a 12-h digestion, cell suspensions were filtered and centrifuged. Mononuclear cells were isolated by Ficoll-Hypaque gradient separation, stained with CD8 (clone RPA-T8) and PD-1 (clone MIH4) specific fluorochrome-conjugated monoclonal antibodies (Becton–Dickinson, San Jose, CA, USA), and analysed by flow cytometry using a 2-laser BD FACSCalibur (Becton–Dickinson, San Jose, CA, USA). Propidium iodide (PI) positive cells were excluded from the analysis. Results were analysed by Cell Quest (Becton–Dickinson, San Jose, CA, USA) and Flow Jo (Tree Star, Ashland, OR, USA) computer softwares.

### 2.4. Clinicopathological features and mismatch repair status

Available clinicopathological data included age, sex, pathological tumour stage (pT) stage, pathological

lymph node stage (pN) stage, tumour grade, vascular invasion, tumour border configuration and disease-specific survival. Tumour border configuration was evaluated using the original H&E slides of the resection specimens corresponding to each tissue microarray punch. Any disagreement between the numbers of available tissue punches and clinicopathological features shown was due to the fact that occasionally specific clinicopathological data were not available. CRCs were stratified according to DNA mismatch repair (MMR) status as described elsewhere.<sup>28,29</sup> Briefly, MMR-proficient tumours were defined as those simultaneously expressing MutL homolog 1 (MLH1), mutS homolog 2 (MSH2) and mutS homolog 6 (MSH6), while MMR-deficient tumours were defined as those lacking expression of at least one of these markers. Based on these features, 1197 CRCs could be classified as MMR-proficient and 223 as MMR-deficient. 47.6% of the patients were male and 34.9% of them were bearing right-sided tumours. Rectal tumours accounted for 34.4% of the cases and the mean tumour diameter was 4.75 cm. The predominant tumour stage was pT3 (64.8%) with over 50% of the samples pN0 (52.2%) and G1 or G2 (87.2%). Vascular invasion was present in 27.7% of the tumours and the overall 5-year survival was 56.4%. Clinicopathological data of the different CRC subsets are summarised in Table 1.

### 2.5. Quantitative real-time PCR

Total cellular RNA was extracted from CRC surgical specimens ( $n = 42$ ) and reverse transcribed as previously described.<sup>30</sup> cDNAs were then amplified in the presence of primers and probes specific for glyceraldehyde 3-phosphate dehydrogenase (GAPDH) house-keeping gene,<sup>31</sup> IFN- $\gamma$ <sup>30</sup> or PD-L1 genes (Assays-on-demand, Applied Biosystems, Rotkreuz, Switzerland) by using a 7300 Real Time PCR system (Applied Biosystems) according to manufacturer's recommendation. Specific gene expression was quantified by using GAPDH gene as reference.<sup>32</sup>

### 2.6. Statistical analysis

Differences in clinic-pathological features between negative, low and strong intensity PD-L1 positive CRCs were analysed using  $\chi^2$  or Fisher's exact tests, while differences in the number of infiltrating immune cells were investigated by using the non-parametric Wilcoxon Rank Sum test. Correlation analyses were performed using Spearman's rank correlation coefficient and agreement was calculated by Cohen's kappa statistics. Survival analysis was performed using one third of the total MMR-proficient collective as training set and the remaining two thirds as validation set. PD-L1 expression levels had a dichotomous character: absent or low



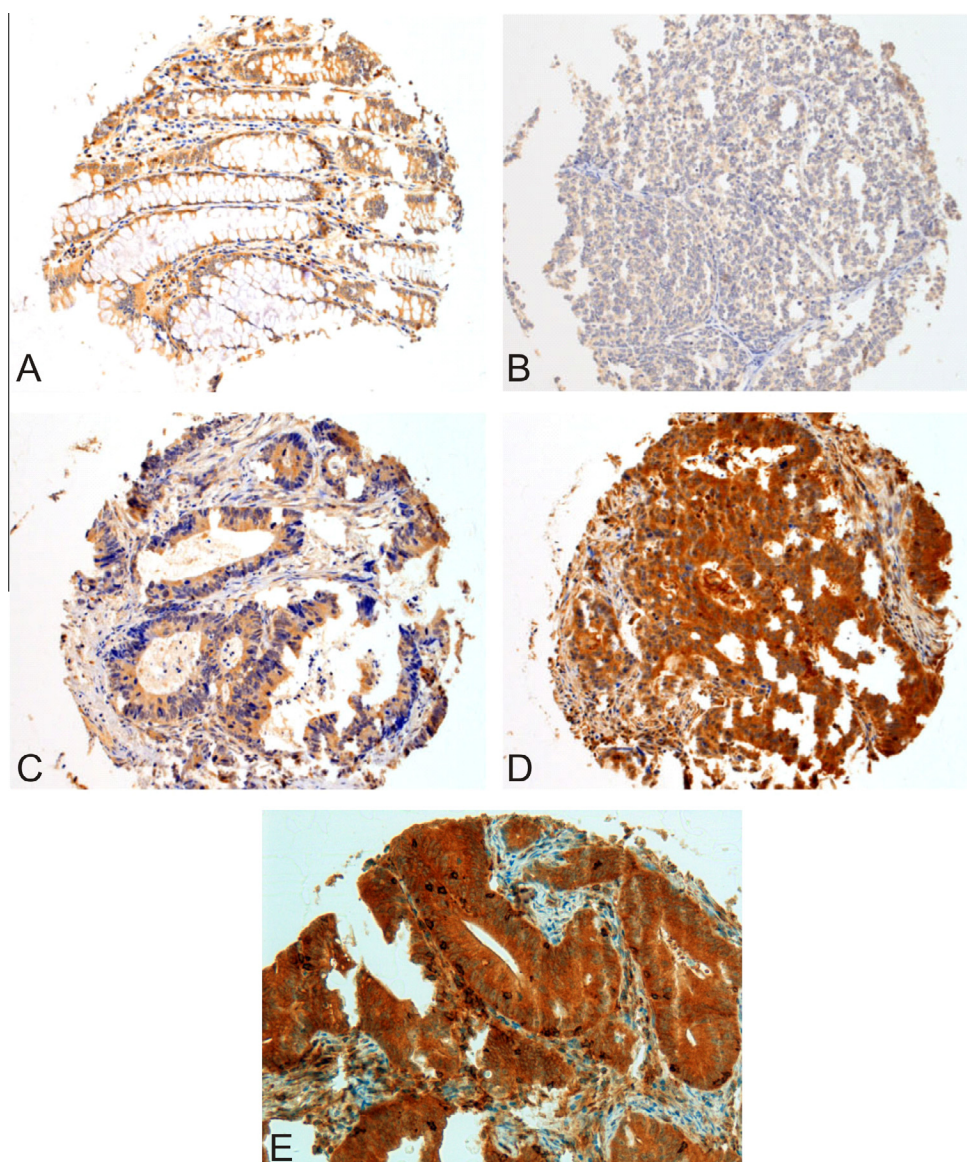


Fig. 1. Programmed cell death ligand 1 (PD-L1) staining in healthy colon mucosa and in colorectal cancer (CRC). Normal colon mucosa (panel A) and CRC samples (panels B–D) were stained with a PD-L1 specific monoclonal antibody (clone 27A2). Tumour punches are representative of negative (panel B), low (panel C) and high (panel D) PD-L1 specific staining intensities. Zoom (20 $\times$ ) of strong PD-L1 expression by tumour cells with high number of PDL-1 positive tumour infiltrating cells is shown in panel E.

or, high. The survival analysis was performed with the Kaplan–Meier method and the two curves were compared with the log rank test. Subsequently, the PD-L1 expression status was entered into uni- and multivariate Cox regression analysis. Hazard ratios (HR) and 95% confidence intervals (CI) were used to determine the prognostic effect of PD-L1 expression on survival time. The MMR-deficient CRC was analysed as a separate cohort.

Regarding tumour infiltrating cells detected as continuous variables, following proof of significant correlation with survival by univariate Cox regression, we used classification and regression trees analysis to calculate threshold values utilised to draw Kaplan–Meier curves.<sup>34</sup> Analyses were performed using SPlus software

(Version 6.1, Insightful Corporation, Seattle, WA, USA). Data reporting was performed according to the REMARK criteria.<sup>35</sup>

Correlations between the expression of different genes, as detected by quantitative reverse transcriptase polymerase chain reaction (RT-PCR) were evaluated by using Spearman's correlation coefficient ( $r$ ) and  $P$  values  $<0.05$  were considered statistically significant.

### 3. Results

#### 3.1. Immunohistochemical detection of PD-L1

Representative stainings of the tissues under investigation, as observed upon incubation with 27A2 mAb

specific for PD-L1, are shown in Fig. 1. PD-L1 was detectable in epithelial cells from normal colonic mucosa (Fig. 1A), and, importantly, in cancer cells (Fig. 1C–E).

In 433 MMR-proficient CRC (36%) a strong positivity (Fig. 1D) was observed, whereas in 723 and 41 cases, respectively, PD-L1 expression was low (Fig. 1C), or absent (Fig. 1B). Among the 223 MMR-deficient cases a strong positivity was observed in 62 cases (29%), whereas in 143 and 6 cases, respectively, PD-L1 expression was low or absent. Comparable stainings were also observed following incubation with polyclonal ab82059 antibody (Abcam, Cambridge, UK). This second staining was analysed by a second specialised investigator. The resulting combined inter-observer and inter-testing Kappa value of  $0.29 \pm 0.049$  indicated a fairly significant ( $P < 0.001$ ) agreement between experiments, antibodies and observers.

### 3.2. Correlation of PD-L1 expression with clinicopathological features

In univariate analysis, strong PD-L1 expression was associated with early T stage ( $P = 0.002$ ; OR = 2.14, CI = 0.87–5.22), absence of lymph node metastasis ( $P = 0.015$ ; OR = 2.29, CI = 1.16–4.54), lower tumour grade ( $P = 0.002$ ; OR = 2.33, CI = 0.91–5.98) and absence of vascular invasion ( $P = 0.017$ ; OR = 2.49, CI = 1.29–4.77) in MMR-proficient CRC (Table 2). Similar results were also observed upon TMA staining with the second reagent used in our study (data not shown).

### 3.3. PD-L1 expression correlates with high CD8<sup>+</sup> T-cell infiltration in MMR-proficient CRC

PD-L1 interaction with PD-1 expressed by activated T-cells has been shown to promote the induction of lymphocyte ‘exhaustion’.<sup>6,8,9</sup> Therefore, in order to evaluate the immunological context of PD-L1 expression, we analysed correlations with the expression of CD8, PD-1, TIA-1 and FOXP3 markers.<sup>26,27</sup>

Interestingly, in MMR-proficient CRC a direct correlation between PD-L1 expression in tumour cells and absolute numbers per punch of CD8<sup>+</sup> tumour-infiltrating lymphocytes, as detected in >1000 specimens,<sup>27</sup> was observed. In particular, CD8<sup>+</sup> infiltration was significantly ( $P = 0.0024$ ) higher in weakly to moderately (low) PD-L1 positive tumours than in negative cases and even higher ( $P = 0.0006$ ) in strongly positive tumours, as compared to low positivity CRC (Fig. 2A). Indeed, except for two cases, all CRCs with low PD-L1 expression displayed a CD8<sup>+</sup> infiltration by <10 cells per punch. In contrast, no significant correlation between PD-L1 expression and CRC infiltration by cells expressing TIA-1, a granule-associated cytotoxic protein typically detectable in activated cytotoxic T cells<sup>36</sup> or CRC infiltration by FOXP3<sup>+</sup> cells,<sup>26,27</sup> could

Table 1  
Summary of patient characteristics ( $n = 1420$ ).

Clinicopathological features		Frequency N (%)
Age ( $n = 1420$ )	Mean (range)	69.9 (30–96)
Gender ( $n = 1414$ )	Female	741 (52.4)
	Male	673 (47.6)
Tumour location ( $n = 1400$ )	Left-sided	430 (30.7)
	Right-sided	488 (34.9)
	Rectum	482 (34.4)
pT stage ( $n = 1387$ )	pT1	62 (4.5)
	pT2	203 (14.6)
	pT3	899 (64.8)
	pT4	223 (16.1)
pN stage ( $n = 1363$ )	pN0	711 (52.2)
	pN1	358 (26.3)
	pN2	294 (21.6)
Tumour grade ( $n = 1385$ )	G1	31 (2.2)
	G2	1177 (85.0)
	G3	177 (12.8)
Histological subtype ( $n = 1420$ )	Mucinous	119 (8.4)
	Other	1301 (91.6)
Vascular invasion ( $n = 1385$ )	Absent	1002 (72.4)
	Present	383 (27.7)
Tumour border configuration ( $n = 1384$ )	Pushing	513 (37.1)
	Infiltrating	871 (62.9)
Mismatch repair (MMR) status ( $n = 1420$ )	Proficient	1197 (84.3)
	Deficient	223 (15.7)
	Five-year survival rate (95% confidence interval (CI))	56.4 (54–59)

be observed (data not shown). Notably, PD-1 expression was detectable in small numbers of CRC infiltrating lymphocytes and in only 5% of all cases.<sup>27</sup> These data indicate that PD-L1 expression in MMR-proficient CRC cells is paradoxically associated with tumour infiltration by CD8<sup>+</sup> T cells which do not express the PD-1 co-receptor. No significant association was found between CD8<sup>+</sup> T cell infiltration and PD-L1 expression in MMR-deficient cases.

### 3.4. Ex vivo analysis of PD-1 expression on CD8 positive lymphocytes in CRC and normal colon mucosa

To further characterise CRC immune infiltrates we performed an *ex vivo* analysis of CD8<sup>+</sup> CRC infiltrating lymphocytes in freshly excised tumour tissues and corresponding normal mucosa ( $n = 7$ ). In accordance with TMA staining data (see above), this flow cytometry study confirmed that PD-1 expression in infiltrating CD8<sup>+</sup> lymphocytes is extremely limited in both CRC ( $3.5 \pm 2.4\%$ ) and normal mucosa ( $1.6 \pm 1\%$ ; Fig. 2B and C).

### 3.5. Prognostic significance of PD-L1 expression

Median overall survival was 32 and 23 months for patients with MMR-proficient tumours with high

Table 2

Association between programmed cell death ligand 1 (PD-L1) specific staining and clinico-pathological features in mismatch repair (MMR)-proficient colorectal cancer patients ( $n = 1197$ ).

		Frequency $N$ (%)			$P$ -value
		PD-L1 Negative	PD-L1 Low	PD-L1 Strong	
Age ( $n = 1141$ ) (years)	Mean (min, max)	67.7 (40–83)	70.4 (30–96)	69.6 (36–96)	0.201
Tumour diameter ( $n = 1088$ ) (mm)	Mean (min, max)	54.3 (4–100)	48.3 (5–150)	45.5 (5–120)	0.008
Gender ( $n = 1143$ )	Female	22 (53.7)	335 (49.7)	217 (50.7)	0.858
	Male	19 (46.3)	339 (50.3)	211 (49.3)	
Tumour location ( $n = 1129$ )	Left-sided	27 (65.9)	455 (68.3)	321 (76.1)	0.017
	Right-sided	14 (34.2)	211 (31.7)	101 (23.9)	
Histologic type ( $n = 1197$ )	Mucinous	8 (19.5)	55 (7.6)	20 (4.6)	<0.001
	Other	33 (80.5)	668 (92.4)	413 (95.4)	
pT stage ( $n = 1117$ )	T1–2	6 (14.6)	120 (18.3)	113 (26.8)	0.002
	T3–4	35 (85.4)	535 (81.7)	308 (73.2)	
pN stage ( $n = 1098$ )	N0	14 (35.9)	321 (49.8)	233 (56.3)	0.015
	N1–2	25 (64.1)	324 (50.2)	181 (43.7)	
Tumour grade ( $n = 1117$ )	G1–2	35 (85.4)	565 (86.5)	394 (93.1)	0.002
	G3	6 (14.6)	88 (13.5)	29 (6.9)	
Vascular invasion ( $n = 1118$ )	Absent	22 (53.7)	463 (70.8)	314 (74.2)	0.017
	Present	19 (46.3)	191 (29.2)	109 (25.8)	
Tumour border configuration ( $n = 1118$ )	Pushing	32 (78.1)	521 (79.7)	337 (79.7)	0.969
	Infiltrating	9 (21.9)	133 (20.3)	86 (20.3)	
Five-year survival rate ( $n = 1054$ )	(95% confidence interval (CI))	35.6 (21–50)	49.7 (45–54)	62.4 (57–67)	<0.001

PD-L1 expression and no or low PD-L1 expression, respectively. This difference was significant in univariate analysis ( $P = 0.003$ ; HR = 0.84 (0.79–0.88); Table 3). A training set consisting of about 1/3 of the MMR-proficient CRC cases was also stained with the second polyclonal antibody preparation. With either staining high PD-L1 expression levels positively correlated with improved overall survival ( $P = 0.0001$  and  $P = 0.008$ , respectively; Fig. 3A and B). The remaining samples were stained with only one antibody. In this validation set, similar significant results were observed ( $P = 0.035$ ; Fig. 3C). Several randomisations of the overall MMR-proficient cohort were tested and all results were found to be comparable.

In MMR-deficient CRC no significant correlation between PD-L1 expression and survival could be observed (data not shown).

In multivariate Cox regression analysis including age, gender, T stage, N stage, tumour grade, vascular invasion, invasive margin and MMR status, a trend ( $P = 0.052$ ) suggesting a correlation between high PD-L1 expression in tumour cells and improved survival in CRC could still be observed (Table 3). These uni- and multivariate results indicate a significant, moderate correlation (HR = 0.85) between high expression of PD-L1 and good prognosis.

### 3.6. PD-L1 expression in tumour infiltrating cells

PD-L1 expression in non-cancerous interstitial cells was usually limited (cell/punch range: 0–44; median/mean: 0 cell/punch), as tested in a more restricted test

group of MMR-proficient CRC ( $n = 424$ ). However, classification and regression tree analysis<sup>33,34</sup> helped to define a cut-off (22 cells/punch) that identified a small (2.5%) percentage of cases with relatively high PD-L1 positive cell infiltration. Patients bearing these tumours also had a significantly ( $P = 0.006$ ) improved survival as compared with patients bearing tumours with lower interstitial numbers of PD-L1 positive cells (Figs. 1E and 3B). This correlation was confirmed by Cox regression analyses based on dichotomous values ( $P = 0.0001$ ; HR = 0.78, CI = 0.71–0.84) or on continuous values ( $P = 0.026$ ; HR = 0.97, CI = 0.96–0.98).

### 3.7. Correlation between IFN- $\gamma$ and PDL-1 gene expression in CRC

Detection of programmed death receptor ligand 1 (PDL-1) expression in melanoma cells has recently been suggested to mirror IFN- $\gamma$  gene expression by tumour infiltrating lymphocytes.<sup>37</sup> In order to verify whether a similar association could also be postulated in CRC, the expression of PDL-1 and IFN- $\gamma$  genes was quantitatively evaluated in surgically excised tumour specimens ( $n = 42$ ). Indeed, we found that expression of PDL-1 and IFN- $\gamma$  genes were significantly correlated ( $P = 0.03$ ,  $r = 0.33$ ).

## 4. Discussion

The aim of this study was to analyse the expression of PD-L1 in a large series of CRC samples and to evaluate its clinical relevance. Here we report that untransformed



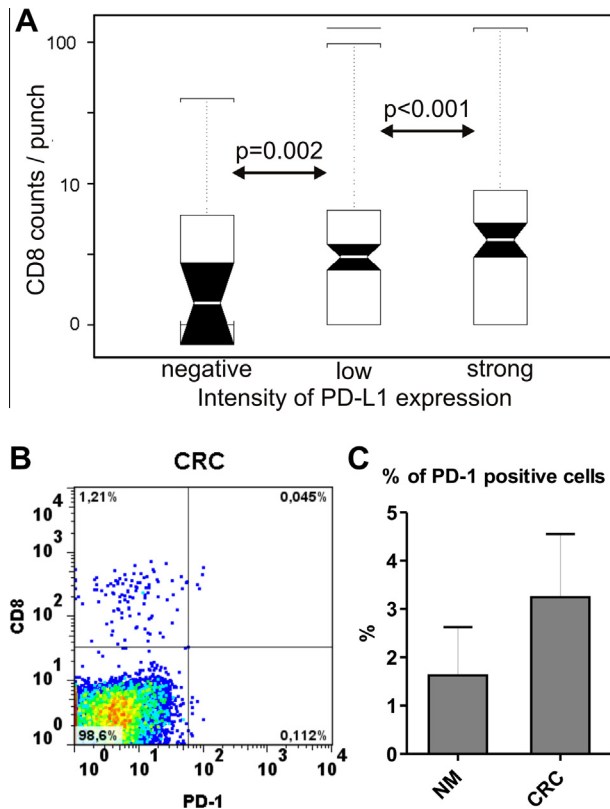


Fig. 2. CD8<sup>+</sup> T-cell infiltration in colorectal cancer (CRC): numbers and phenotype. (A) Absolute numbers of CD8<sup>+</sup> T-cells counted in individual CRC punches ( $n = 1082$ ) were correlated with the intensity of programmed cell death ligand 1 (PD-L1) specific staining, as detectable in the same specimen. (B and C) CRC surgical specimens were enzymatically digested and immediately stained with fluorochrome labelled mAbs recognising CD8 and PD-1. Panel B reports one representative staining, whereas panel C summarises results from the seven freshly excised specimens investigated for PD-1 expression on CD8<sup>+</sup> cells in this study. Data in panel B are expressed as percentages of the total number of cells in the digested specimen, whereas data in panel C are expressed as percentages of CD8<sup>+</sup> cells showing evidence of PD-1 expression. NM = normal mucosa.

normal epithelial cells of colon mucosa do express PD-L1. More importantly, we have observed that PD-L1 expression is markedly enhanced in tumour cells in over 30% of CRC.

Unexpectedly, strong PD-L1 expression in MMR-proficient CRC was found to be associated with early tumour stage, absence of lymph node metastases, lower tumour grade, absence of vascular invasion and a significantly improved 5-year survival. More remarkably, a strong PD-L1 expression in CRC appeared to be paradoxically associated with high numbers of tumour infiltrating CD8<sup>+</sup> T cells. These cells however, did not express the PD-1 co-receptor. High PD-L1 expression in non-cancerous interstitial cells, as detectable in a small number of cases (2.5%), was also found to be associated with a more favourable prognosis.

Cancers are frequently infiltrated by lymphocytes and TILs are widely considered to reflect host immune response against malignancy.<sup>38</sup> In defined cancer types, tumour-infiltration by lymphocytes has been shown to be associated with improved prognosis. In particular, CRC infiltration by CD3<sup>+</sup> T cells or by CD8<sup>+</sup> lymphocytes expressing the CD45RO activation marker has been suggested to be endowed with high prognostic value.<sup>1</sup>

However, tumour-immune system interaction is highly dynamic. Cancer cells might escape from destruction by immunocompetent cells by taking advantage of a range of different mechanisms.<sup>39</sup> Down-regulation of the expression of HLA determinants or tumour associated antigens or alterations in the antigen processing machinery might prevent tumour cell recognition by specific T cells.<sup>40</sup> Alternatively, production of immunosuppressive factors or intratumoural recruitment of immunosuppressive cell populations, including regulatory T-cells and myeloid derived suppressor cells,<sup>39</sup> might contribute to the generation of a tumour microenvironment unfavourable to the elicitation of effective antitumour immune responses.

Notably, it has been shown that cancer cells from solid tumours are able to up-regulate the expression of PD-1 ligands, thereby providing inhibitory signals down-modulating T-cell activation and ultimately shutting down immune responses<sup>41</sup> and inducing specific tolerance.<sup>42</sup> Expression of PD-1 ligands on tumour cells was also shown to suppress the cytolytic activity of CD8<sup>+</sup> T cells.<sup>12,13</sup> Indeed, PD-L1 has been shown to

Table 3  
Uni- and multivariate Cox-regression analysis in all colorectal cancers (CRCs) ( $n = 1420$ ).

Features	Univariate		Multivariate	
	Hazard ratio (HR) (95% confidence interval (CI))	P-value	HR (95% CI)	P-value
Programmed cell death ligand 1 (PD-L1)	0.85 (0.81–0.89)	0.0003	0.92 (0.88–0.96)	0.052
Age (continuous)	1.02 (1.02–1.02)	<0.0001	1.03 (1.02–1.04)	<0.0001
Sex (men–women)	1.16 (1.12–1.20)	0.0002	1.17 (1.13–1.21)	<0.0001
pT (pT: 1, 2, 3, 4)	3.14 (1.76–5.61)	<0.0001	1.79 (1.71–1.87)	<0.0001
Grade (1, 2, 3)	1.78 (1.67–1.88)	<0.0001	1.14 (1.02–1.26)	0.29
pN (pN: 0, 1, 2)	2.41 (2.36–2.46)	<0.0001	1.91 (1.85–1.97)	<0.0001
Vascular invasion	2.78 (2.69–2.86)	<0.0001	1.45 (1.36–1.54)	<0.0001
Invasive margins	2.50 (2.41–2.59)	<0.0001	1.63 (1.53–1.73)	<0.0001
Mismatch repair (MMR) status	1.74 (1.61–1.87)	<0.0001	1.72 (1.59–1.76)	<0.0001

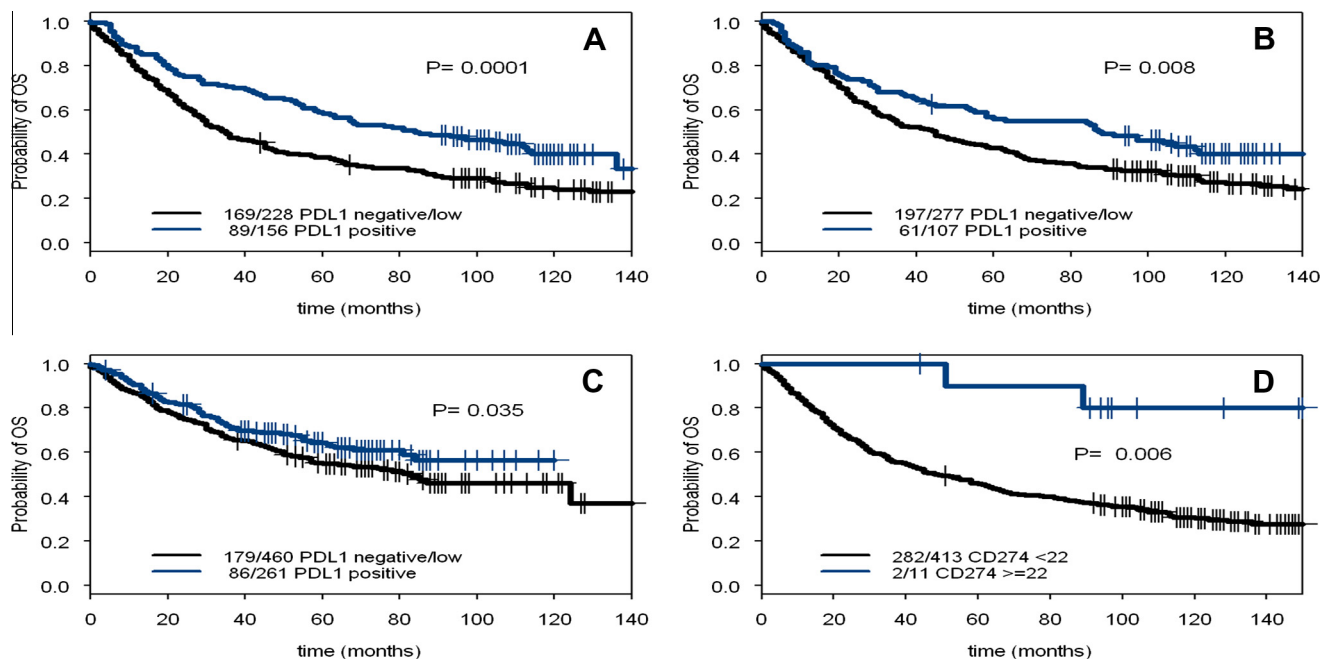


Fig. 3. Effect of programmed cell death ligand 1 (PD-L1) expression by cancer and tumour infiltrating cells on overall survival in patients with mismatch repair (MMR)-proficient colorectal cancer (CRC). Kaplan–Meier overall survival curves of patients bearing MMR-proficient CRC divided into training and validation set. Stratification occurs according to strong PD-L1 staining of tumour cells (blue line) and low to absent PD-L1 expression in tumour cells (black line). (A) Set 1, PD-L1 detection by monoclonal antibody. (B) Set 1, PD-L1 detection by polyclonal antibodies as scored by a second investigator. (C) Set 2: validation set. (D) Kaplan–Meier overall survival curves stratified according to PD-L1 expression in cancer infiltrating cells. Data refer to high (blue line) or low to absent (black line) infiltration by PD-L1+ cells. The threshold was defined at  $\geq 22$  cells per punch (see Section 2).

be expressed in different tumours, including glioblastoma, pancreas, ovarian, breast, renal cell carcinomas, head and neck squamous cell carcinomas as well as oesophageal, and non-small cell lung cancers.<sup>14–17,24,43,44</sup> Most importantly, a strong correlation between the expression of PD-1 ligands on tumour cells and severe prognosis has been observed.

Based on this background, the inhibition of PD-1/PD-L1 interaction has been proposed as a therapeutic target and PD-1 and PD-L1 specific monoclonal antibodies have been successfully developed and tested in phase I clinical trials.<sup>19–21</sup> In this context, our results are surprising and underline the specificities of tumour immune system interaction in CRC. Importantly however, no clinical responses have been observed to date in patients with CRC treated with therapeutic antibodies against PD-1 or PD-L1.<sup>20,21</sup>

What are the possible mechanisms underlying the favourable effect of PD-L1 over-expression in MMR-proficient CRC? Our data clearly indicate that CD8<sup>+</sup> T cell infiltration is unexpectedly increased in MMR-proficient CRC with high PD-L1 expression. These TILs do not express PD-1.

It is of note that in our study, overexpression of PD-L1 in tumour cells was not associated with an improved survival in MMR-deficient CRC. These tumours are known to be infiltrated by higher numbers of lymphocytes and to be characterised by a more favourable

prognosis as compared to MMR proficient tumours.<sup>26</sup> Thus, we might hypothesise that the association between PD-L1 expression in CRC cells and favourable prognosis in MMR proficient tumours could be related to the concomitant increase in CD8<sup>+</sup> T cell infiltration.

Interestingly, IFN- $\gamma$  gene expression in CRC tissues has been reported to be associated with a favourable prognosis.<sup>2</sup> This cytokine, typically produced by activated T cells has been shown to promote the expression of PD-1 ligands in different cell types, thus suggesting that the association of PD-L1 overexpression in MMR proficient CRC with a favourable prognosis might mirror tumour infiltration by IFN- $\gamma$  producing T cells.<sup>37</sup> Indeed, we found that PDL-1 and IFN- $\gamma$  gene expression are significantly ( $r = 0.33$ ,  $P = 0.03$ ) correlated in CRC. However, since PDL-1 gene expression was also observed in the absence of detectable IFN- $\gamma$  gene expression, other, presently undefined mechanisms are also likely to be involved in the elicitation of the favourable prognostic effects associated with PDL-1 expression by CRC cells.

On the other hand, the intestinal immune system is shaped by a continuous interaction with commensal microbiota.<sup>45</sup> Possibly, as a consequence of this specific microenvironment, CRC infiltration by immunocompetent cells is associated with paradoxically peculiar features.<sup>46</sup> Indeed, we and others<sup>26,47</sup> have previously demonstrated that, in contrast to a wide range of human

cancers, CRC infiltration by FOXP3<sup>+</sup> regulatory T cells, is associated with an improved prognosis. Furthermore, it has been observed that CRC infiltration by myeloid cells is also associated with a favourable prognosis.<sup>48,49</sup>

The results of this study contribute to the characterisation of the complex features inherent with gut micro-environment and with CRC-immune system interaction. Further research is warranted to clarify molecular mechanisms underlying increased CD8<sup>+</sup> T cell infiltration in PD-L1-high CRC. Nevertheless, PD-L1 expression in MMR-proficient CRC appears to play a conspicuously different role, as compared to a large variety of other solid tumours. Indeed, our data suggest that the role of immunological checkpoint markers could be different in different anatomical districts.

### Conflict of interest statement

None declared.

### Acknowledgements

Financial support was provided by the Swiss National Fund for scientific research (SNF) Grant No. PP00P3-133699 and 31003A-122235 and by the Italian Association for Cancer Research (AIRC) IG Grant No. 10555.

### References

- Galon J, Costes A, Sanchez-Cabo F, et al. Type, density, and location of immune cells within human colorectal tumors predict clinical outcome. *Science* 2006;**313**:1960–4.
- Pages F, Berger A, Camus M, et al. Effector memory T cells, early metastasis, and survival in colorectal cancer. *N Engl J Med* 2005;**353**:2654–66.
- Khouri SJ, Sayegh MH. The roles of the new negative T cell costimulatory pathways in regulating autoimmunity. *Immunity* 2004;**20**:529–38.
- Okazaki T, Honjo T. The PD-1–PD-L pathway in immunological tolerance. *Trends Immunol* 2006;**27**:195–201.
- Curiel TJ, Wei S, Dong H, et al. Blockade of B7-H1 improves myeloid dendritic cell-mediated antitumor immunity. *Nat Med* 2003;**9**:562–7.
- Freeman GJ, Long AJ, Iwai Y, et al. Engagement of the PD-1 immunoinhibitory receptor by a novel B7 family member leads to negative regulation of lymphocyte activation. *J Exp Med* 2000;**192**:1027–34.
- Latchman Y, Wood CR, Chernova T, et al. PD-L2 is a second ligand for PD-1 and inhibits T cell activation. *Nat Immunol* 2001;**2**:261–8.
- Keir ME, Liang SC, Guleria I, et al. Tissue expression of PD-L1 mediates peripheral T cell tolerance. *J Exp Med* 2006;**203**:883–95.
- Keir ME, Butte MJ, Freeman GJ, Sharpe AH. PD-1 and its ligands in tolerance and immunity. *Annu Rev Immunol* 2008;**26**:677–704.
- Shin T, Yoshimura K, Shin T, et al. In vivo costimulatory role of B7-DC in tuning T helper cell 1 and cytotoxic T lymphocyte responses. *J Exp Med* 2005;**201**:1531–41.
- Zhang L, Gajewski TF, Kline J. PD-1/PD-L1 interactions inhibit antitumor immune responses in a murine acute myeloid leukemia model. *Blood* 2009;**114**:1545–52.
- Hirano F, Kaneko K, Tamura H, et al. Blockade of B7-H1 and PD-1 by monoclonal antibodies potentiates cancer therapeutic immunity. *Cancer Res* 2005;**65**:1089–96.
- Iwai Y, Ishida M, Tanaka Y, Okazaki T, Honjo T, Minato N. Involvement of PD-L1 on tumor cells in the escape from host immune system and tumor immunotherapy by PD-L1 blockade. *Proc Natl Acad Sci U S A* 2002;**99**:12293–7.
- Konishi J, Yamazaki K, Azuma M, Kinoshita I, Dosaka-Akita H, Nishimura M. B7-H1 expression on non-small cell lung cancer cells and its relationship with tumor-infiltrating lymphocytes and their PD-1 expression. *Clin Cancer Res* 2004;**10**:5094–100.
- Ohgashi Y, Sho M, Yamada Y, et al. Clinical significance of programmed death-1 ligand-1 and programmed death-1 ligand-2 expression in human esophageal cancer. *Clin Cancer Res* 2005;**11**:2947–53.
- Strome SE, Dong H, Tamura H, et al. B7-H1 blockade augments adoptive T-cell immunotherapy for squamous cell carcinoma. *Cancer Res* 2003;**63**:6501–5.
- Thompson RH, Gillett MD, Cheville JC, et al. Costimulatory B7-H1 in renal cell carcinoma patients: indicator of tumor aggressiveness and potential therapeutic target. *Proc Natl Acad Sci U S A* 2004;**101**:17174–9.
- Wintterle S, Schreiner B, Mitsdoerffer M, et al. Expression of the B7-related molecule B7-H1 by glioma cells: a potential mechanism of immune paralysis. *Cancer Res* 2003;**63**:7462–7.
- Brahmer JR, Drake CG, Wollner I, et al. Phase I study of single-agent anti-programmed death-1 (MDX-1106) in refractory solid tumors: safety, clinical activity, pharmacodynamics, and immunologic correlates. *J Clin Oncol* 2010;**28**:3167–75.
- Brahmer JR, Tykodi SS, Chow LQ, et al. Safety and activity of anti-PD-L1 antibody in patients with advanced cancer. *N Engl J Med* 2012;**366**:2455–65.
- Topalian SL, Hodi FS, Brahmer JR, et al. Safety, activity, and immune correlates of anti-PD-1 antibody in cancer. *N Engl J Med* 2012;**366**:2443–54.
- Kallioniemi OP, Wagner U, Kononen J, Sauter G. Tissue microarray technology for high-throughput molecular profiling of cancer. *Hum Mol Genet* 2001;**10**:657–62.
- Sauter G, Simon R, Hillan K. Tissue microarrays in drug discovery. *Nat Rev Drug Discov* 2003;**2**:962–72.
- Hamanishi J, Mandai M, Iwasaki M, et al. Programmed cell death 1 ligand 1 and tumor-infiltrating CD8<sup>+</sup> T lymphocytes are prognostic factors of human ovarian cancer. *Proc Natl Acad Sci U S A* 2007;**104**:3360–5.
- Loos M, Langer R, Schuster T, et al. Clinical significance of the costimulatory molecule B7-H1 in Barrett carcinoma. *Ann Thorac Surg* 2011;**91**:1025–31.
- Frey DM, Droezer RA, Viehl CT, et al. High frequency of tumor-infiltrating FOXP3(+) regulatory T cells predicts improved survival in mismatch repair-proficient colorectal cancer patients. *Int J Cancer* 2010;**126**:2635–43.
- Zlobec I, Karamitopoulou E, Terracciano L, et al. TIA-1 cytotoxic granule-associated RNA binding protein improves the prognostic performance of CD8 in mismatch repair-proficient colorectal cancer. *PLoS One* 2010;**5**:e14282.
- Lugli A, Zlobec I, Baker K, et al. Prognostic significance of mucins in colorectal cancer with different DNA mismatch-repair status. *J Clin Pathol* 2007;**60**:534–9.
- Baker KM, Zlobec I, Tornillo L, Terracciano L, Jass JR, Lugli A. Differential significance of tumour infiltrating lymphocytes in sporadic mismatch repair deficient versus proficient colorectal cancers: a potential role for dysregulation of the transforming growth factor-beta pathway. *Eur J Cancer* 2007;**43**:624–31.
- Feder-Mengus C, Schultz-Thater E, Oertli D, et al. Nonreplicating recombinant vaccinia virus expressing CD40 ligand enhances APC capacity to stimulate specific CD4<sup>+</sup> and CD8<sup>+</sup> T cell responses. *Hum Gene Ther* 2005;**16**:348–60.

31. Martin I, Jakob M, Schafer D, Dick W, Spagnoli G, Heberer M. Quantitative analysis of gene expression in human articular cartilage from normal and osteoarthritic joints. *Osteoarthritis Cartilage* 2001;**9**:112–8.
32. Livak KJ, Schmittgen TD. Analysis of relative gene expression data using real-time quantitative PCR and the 2(-Delta Delta C(T)) method. *Methods* 2001;**25**:402–8.
33. Barlow RE, Bartholomew DJ, Bremner JM. *Statistical inference under order restrictions: theory and application of isotonic regression*. London: John Wiley & Sons Ltd.; 1972.
34. Breiman L, Friedman J, Stone CJ. *Classification and regression trees*. Chapman & Hall/CRC; 1984.
35. McShane LM, Altman DG, Sauerbrei W, Taube SE, Gion M, Clark GM. Reporting recommendations for tumor marker prognostic studies (REMARK). *J Natl Cancer Inst* 2005;**97**:1180–4.
36. Kanavaros P, Boulland ML, Petit B, Arnulf B, Gaulard P. Expression of cytotoxic proteins in peripheral T-cell and natural killer-cell (NK) lymphomas: association with extranodal site, NK or Tgammadelta phenotype, anaplastic morphology and CD30 expression. *Leuk Lymphoma* 2000;**38**:317–26.
37. Taube JM, Anders RA, Young GD, et al. Colocalization of inflammatory response with B7-h1 expression in human melanocytic lesions supports an adaptive resistance mechanism of immune escape. *Sci Transl Med* 2012;**4**:127ra37.
38. Mantovani A, Romero P, Palucka AK, Marincola FM. Tumour immunity: effector response to tumour and role of the microenvironment. *Lancet* 2008;**371**:771–83.
39. Schreiber RD, Old LJ, Smyth MJ. Cancer immunoediting: integrating immunity's roles in cancer suppression and promotion. *Science* 2011;**331**:1565–70.
40. Ferris RL, Whiteside TL, Ferrone S. Immune escape associated with functional defects in antigen-processing machinery in head and neck cancer. *Clin Cancer Res* 2006;**12**:3890–5.
41. Zou W. Immunosuppressive networks in the tumour environment and their therapeutic relevance. *Nat Rev Cancer* 2005;**5**:263–74.
42. Francisco LM, Salinas VH, Brown KE, et al. PD-L1 regulates the development, maintenance, and function of induced regulatory T cells. *J Exp Med* 2009;**206**:3015–29.
43. Parsa AT, Waldron JS, Panner A, et al. Loss of tumor suppressor PTEN function increases B7-H1 expression and immunoresistance in glioma. *Nat Med* 2007;**13**:84–8.
44. Pardoll D, Drake C. Immunotherapy earns its spot in the ranks of cancer therapy. *J Exp Med* 2012;**209**:201–9.
45. Kau AL, Ahern PP, Griffin NW, Goodman AL, Gordon JI. Human nutrition, the gut microbiome and the immune system. *Nature* 2011;**474**:327–36.
46. Ladoire S, Martin F, Ghiringhelli F. Prognostic role of FOXP3+ regulatory T cells infiltrating human carcinomas: the paradox of colorectal cancer. *Cancer Immunol Immunother* 2011;**60**:909–18.
47. Salama P, Phillips M, Grieu F, et al. Tumor-infiltrating FOXP3+ T regulatory cells show strong prognostic significance in colorectal cancer. *J Clin Oncol* 2009;**27**:186–92.
48. Sconocchia G, Zlobec I, Lugli A, et al. Tumor infiltration by FcgammaRIII (CD16)+ myeloid cells is associated with improved survival in patients with colorectal carcinoma. *Int J Cancer* 2011;**128**:2663–72.
49. Roxburgh CS, McMillan DC. The role of the in situ local inflammatory response in predicting recurrence and survival in patients with primary operable colorectal cancer. *Cancer Treat Rev* 2012;**38**:451–66.

## GM-CSF Production by Tumor Cells Is Associated with Improved Survival in Colorectal Cancer

Christian A. Nebiker<sup>1</sup>, Junyi Han<sup>1,8,9</sup>, Serenella Eppenberger-Castori<sup>2</sup>, Giandomenica Iezzi<sup>1</sup>, Christian Hirt<sup>1</sup>, Francesca Amicarella<sup>1</sup>, Eleonora Cremonesi<sup>1</sup>, Xaver Huber<sup>1,3</sup>, Elisabetta Padovan<sup>1</sup>, Basilio Angrisani<sup>2</sup>, Raoul A. Droscher<sup>1,3</sup>, Raffaele Rosso<sup>4</sup>, Martin Bolli<sup>5</sup>, Daniel Oertli<sup>3</sup>, Urs von Holzen<sup>3</sup>, Michel Adamina<sup>6</sup>, Manuele G. Muraro<sup>1</sup>, Chantal Mengus<sup>1</sup>, Paul Zajac<sup>1</sup>, Giuseppe Sconocchia<sup>10</sup>, Markus Zuber<sup>7</sup>, Luigi Tornillo<sup>2</sup>, Luigi Terracciano<sup>2</sup>, and Giulio C. Spagnoli<sup>1</sup>

### Abstract

**Purpose:** Colorectal cancer infiltration by CD16<sup>+</sup> myeloid cells correlates with improved prognosis. We addressed mechanistic clues and gene and protein expression of cytokines potentially associated with macrophage polarization.

**Experimental Design:** GM-CSF or M-CSF-stimulated peripheral blood CD14<sup>+</sup> cells from healthy donors were cocultured with colorectal cancer cells. Tumor cell proliferation was assessed by <sup>3</sup>H-thymidine incorporation. Expression of cytokine genes in colorectal cancer and autologous healthy mucosa was tested by quantitative, real-time PCR. A tumor microarray (TMA) including >1,200 colorectal cancer specimens was stained with GM-CSF- and M-CSF-specific antibodies. Clinicopathological features and overall survival were analyzed.

**Results:** GM-CSF induced CD16 expression in 66% ± 8% of monocytes, as compared with 28% ± 1% in cells stimulated by M-CSF ( $P = 0.011$ ). GM-CSF but not M-CSF-stimulated macrophages significantly ( $P < 0.02$ ) inhibited colorectal cancer cell proliferation. GM-CSF gene was expressed to significantly ( $n = 45$ ,  $P < 0.0001$ ) higher extents in colorectal cancer than in healthy mucosa, whereas M-CSF gene expression was similar in healthy mucosa and colorectal cancer. Accordingly, *IL1 $\beta$*  and *IL23* genes, typically expressed by M1 macrophages, were expressed to significantly ( $P < 0.001$ ) higher extents in colorectal cancer than in healthy mucosa. TMA staining revealed that GM-CSF production by tumor cells is associated with lower T stage ( $P = 0.02$ ), "pushing" growth pattern ( $P = 0.004$ ) and significantly ( $P = 0.0002$ ) longer survival in mismatch-repair proficient colorectal cancer. Favorable prognostic effect of GM-CSF production by colorectal cancer cells was confirmed by multivariate analysis and was independent from CD16<sup>+</sup> and CD8<sup>+</sup> cell colorectal cancer infiltration. M-CSF expression had no significant prognostic relevance.

**Conclusions:** GM-CSF production by tumor cells is an independent favorable prognostic factor in colorectal cancer. *Clin Cancer Res*; 20(12); 3094–106. ©2014 AACR.

**Authors' Affiliations:** <sup>1</sup>Department of Biomedicine, Institute for Surgical Research; <sup>2</sup>Institute of Pathology, University of Basel; <sup>3</sup>Department of Surgery, University Hospital, Basel; <sup>4</sup>Ospedale Regionale, Lugano; <sup>5</sup>Ospedale Regionale "San Giovanni," Bellinzona; <sup>6</sup>Department of Surgery, Kantonsspital, St. Gallen; <sup>7</sup>Department of Surgery, Kantonsspital, Olten, Switzerland; Departments of <sup>8</sup>General Surgery and <sup>9</sup>Gastroenterology, Shanghai East Hospital, Tongji University, Shanghai, P.R. China; and <sup>10</sup>Institute of Translational Pharmacology, National Research Council, Rome, Italy

**Note:** Supplementary data for this article are available at Clinical Cancer Research Online (<http://clincancerres.aacrjournals.org/>).

C. Nebiker, J. Han, S. Eppenberger-Castori, L. Terracciano, and G.C. Spagnoli contributed equally to this article.

**Corresponding Authors:** Giulio C. Spagnoli, Departments of Surgery and Biomedicine, Basel University Hospital, ICFS, Laboratory 401, Hebelstrasse 20, 4031 Basel, Switzerland. E-mail: giulio.spagnoli@usb.ch; and Luigi Terracciano, Institute of Pathology, University of Basel, Schonbeinstrasse 40, 4003 Basel, Switzerland. E-mail: lterracciano@uhbs.ch

doi: 10.1158/1078-0432.CCR-13-2774

©2014 American Association for Cancer Research.

### Introduction

Chronic inflammation is known to play a decisive role in cancer outgrowth and progression by powerfully shaping tumor microenvironment (1, 2). Tumor cells may produce factors promoting maturation and functional differentiation of resident pro-inflammatory cells. In turn, these cells may favor tumor angiogenesis and enhance cancer cell invasiveness. However, chemokine production within cancerous tissues may selectively chemoattract circulating cells expressing specific receptors, resulting in a peculiar composition of the cancer microenvironment, potentially affecting tumor progression and, ultimately, clinical prognosis (3–5). In particular, tumor infiltration by myeloid cells has frequently been associated with poor prognosis in different types of cancer, including, among others, breast, thyroid, and renal cell carcinoma and melanoma (6).



### Translational Relevance

GM-CSF is a powerful activator of myeloid cells. However, its role in cancer immunobiology is debated because it was shown to promote the generation of myeloid-derived suppressor cells. Here, we report that GM-CSF induces in human macrophages the ability to inhibit the proliferation of colorectal cancer cells *in vitro*. GM-CSF gene is expressed to significantly higher extents in colorectal cancer than in autologous healthy mucosa. By using a large (>1,200) number of specimens, we demonstrate that in mismatch repair proficient (MMRp) cancers, GM-CSF production by colorectal cancer cells is associated with improved survival in univariate and multivariate analyses. The favorable prognostic relevance of GM-CSF production by colorectal cancer cells is particularly evident in MMRp cancers in which poor CD8<sup>+</sup> T-cell infiltration is detectable. These data underline specificities of colorectal cancer immunobiology and indicate that prognostic significance of defined tumor microenvironmental features critically depends on tumor types and related anatomic districts.

Colorectal cancer represents a major cause of cancer-related death in different geographic areas. A variety of current experimental models of colorectal cancer induction do support the notion of an important causal role of inflammation (6, 7). Indeed, chronic inflammation, as observed in different types of inflammatory bowel diseases (IBD), is known to be associated with increased colorectal cancer incidence in humans (6, 7).

However, in sporadic colorectal cancer, accounting for a large majority of these tumors, evidence of a clinically significant inflammatory state, possibly associated with cancer outgrowth, is infrequently observed. While questioning the pertinence of several murine models to sporadic human colorectal cancer, these common clinical observations urge addressing the issue of the role of innate and adaptive immune responses in these cancers.

A number of studies have convincingly demonstrated that colorectal cancer infiltration by T cells, and, in particular, by CD8<sup>+</sup> lymphocytes, is associated with improved survival. These cells usually display a memory (8, 9) and activated (10) phenotype. Colorectal cancer infiltration by FOXP3<sup>+</sup> T cells has also been shown to be paradoxically associated with good prognosis (11, 12).

In contrast, the functional relevance of colorectal cancer infiltration by cells of the innate immune system is still unclear. NK-cell infiltration is relatively rarely detectable and it is devoid of prognostic significance (13). Instead, at difference with a variety of cancers of diverse histologic origin (14), colorectal cancer infiltration by macrophages has been shown to be associated with favorable prognosis (15). Therefore, in this context, colorectal cancer seems to represent an important exception.

In the same line, we have observed that infiltration by myeloid CD16<sup>+</sup> cells represents a novel, independent, favorable prognostic factor in colorectal cancer (16).

In this study we have attempted to unravel mechanistic clues possibly underlying these effects, and to address the expression at the gene and protein level of cytokines and chemokines associated with chemoattraction and functional polarization of macrophage subsets possibly endowed with antitumor potential.

### Materials and Methods

#### Generation and phenotypic and functional characterization of polarized macrophages

Monocytes were isolated from peripheral blood mononuclear cells (PBMC) of healthy donors to a >98% purity by using anti-CD14-coated magnetic beads (Miltenyi). Purified cells were cultured for 6 to 7 days in the presence of recombinant GM-CSF (Laboratorio Pablo Cassarà) or M-CSF (R&D Systems) at 50 to 5 ng/mL concentrations in RPMI 1640 medium supplemented with antibiotics, glutamine, nonessential aminoacids, sodium pyruvate, HEPES, β-mercaptoethanol and 10% fetal calf serum (FCS; all from Invitrogen Life Sciences), thereafter referred to as complete medium, according to previously published protocols (17).

Freshly isolated or cultured cells were stained with CD16-, CD163-, and CD204-specific fluorochrome-conjugated antibodies (Becton Dickinson), and analyzed by using a 2-laser FACSCalibur flow cytometer (Becton Dickinson). Propidium iodide (PI) positive cells were excluded from the analysis. Results were analyzed by Cell Quest (Becton Dickinson) and Flow Jo (Tree Star) computer softwares.

Authenticated, established human colorectal cancer cell lines Colo205 and HCT116 were purchased from the European Collection of Cell Cultures (ECACC) and cultured in complete medium. To evaluate their cytostatic capacity, 6 to 7 days cytokine-stimulated macrophages (see above) were cocultured in 96-well plates (Falcon) at different effector:target ratios with 3,000 tumor cells for 2 days. 3H-Thymidine (Amersham GE) was then added (1 μCi/well) for overnight incubation. Cultures were then harvested and tracer incorporation was measured by β-counting.

#### Gene expression analysis

Total cellular RNA was extracted from surgical specimens of colorectal cancer and autologous healthy mucosa sampled at distance from the tumor and reverse transcribed. Predeveloped Taqman assays (Applied Biosystems) were used to quantitatively evaluate the expression of a panel of cytokine and chemokine genes by using ABI Prism 7300 PCR system (Applied Biosystems). Data are reported as relative expression normalized to GAPDH house-keeping gene amplification. Expression of individual genes was analyzed by using the  $2^{-\Delta\Delta C_T}$  method (18).

#### Tumor microarray construction

The tumor microarray (TMA) utilized in this study has been described in detail in previous reports (19, 20).

Briefly, it includes 1,420 unselected, nonconsecutive, primary sporadic colorectal cancers, treated between 1987 and 1996, and 71 normal mucosa specimens. These samples were collected from the Tissue Biobank of the Institute of Pathology, University Hospital Basel, performing translational research with the approval of the Ethical Committee Beider Basel (EKBB), in compliance with ethical standards and patient confidentiality. Tissue cylinders with a 0.6-mm diameter from formalin-fixed, paraffin-embedded tissue blocks from resected colorectal cancer were punched from representative tissue areas and brought into 1 recipient paraffin block (30 × 25 mm), using a semiautomated tissue arrayer. Punches were made from the center of the tumor to guarantee that each TMA spot included at least 50% tumor cells.

Clinicopathological annotation included patient age, tumor diameter, location, pT/pN stage, grade, histologic subtype, vascular invasion, border configuration, presence of peritumoral lymphocytic inflammation at the invasive tumor front and disease-specific survival (Table 1). Tumor border configuration and peritumoral lymphocytic inflammation were evaluated by using the original hematoxylin

and eosin (H&E) slides of the resection specimens corresponding to microarray punches, as previously described (20). Numbers of lymph nodes evaluated ranged between 1 and 61 with mean and median of 12 and 11, respectively. MMR status was evaluated by immunohistochemistry according to MLH1, MSH2, and MSH6 expression (20), as previously described. The TMA under evaluation included 1,031 MMR-proficient and 194 MMR-deficient tumors. Follow-up data were available for 1,379 patients with mean/median and interquartile range (IQR) event-free follow-up time of 67.7/68 and 45 to 97 months.

#### Immunohistochemistry

Indirect immunoperoxidase protocol was used for immunohistochemistry (ABC-Elite, Vector Laboratories). Following slide dewaxing and rehydration endogenous peroxidase activity was blocked using 0.5% H<sub>2</sub>O<sub>2</sub>. Epitope retrieval was achieved by incubation in Epitope Retrieval Reagent 2 (EDTA buffer, pH 9; Leica Biosystems) at 100°C for 30 minutes, as previously described (20), before staining. The sections were treated with 10% normal goat serum

**Table 1.** Association of GM-CSF staining and clinicopathological features in colorectal cancer (*n* = 1,239)

Clinicopathological features		Histoscore <sup>a</sup>		<i>P</i>
		Low <i>N</i> = 475 (38.3%)	High <i>N</i> = 764 (61.7%)	
Age ( <i>n</i> = 1,239), y	Mean, range	69.4 (39–95)	69.8 (30–96)	0.537 <sup>b</sup>
Tumor diameter ( <i>n</i> = 1,235), mm	Median, mean, range	50, 49.7 (4–150)	45, 48.6 (5–160)	0.146 <sup>c</sup>
Gender ( <i>n</i> = 1,239)	Female	248 (52.2)	407 (53.3)	0.760 <sup>c</sup>
	Male	227 (47.8)	357 (46.7)	
Tumor location ( <i>n</i> = 1,225)	Left-sided	297 (63.6)	502 (66.2)	0.380 <sup>d</sup>
	Right-sided	170 (35.4)	256 (33.8)	
pT stage ( <i>n</i> = 1,213)	pT1-2	76 (16.5)	166 (22.1)	<b>0.020<sup>d</sup></b>
	pT3-4	386 (83.5)	585 (77.9)	
pN stage ( <i>n</i> = 1,197)	pN0	230 (50.2)	406 (54.9)	0.126 <sup>d</sup>
	pN1-2	228 (49.8)	333 (45.1)	
Tumor grade ( <i>n</i> = 1,212)	G <sub>1</sub> -G <sub>2</sub>	400 (87.5)	658 (87.2)	0.9195 <sup>d</sup>
	G <sub>3</sub>	57 (12.5)	97 (12.8)	
Vascular invasion ( <i>n</i> = 1,212)	Absent	324 (70.7)	559 (74.1)	0.222 <sup>d</sup>
	Present	134 (29.3)	195 (25.9)	
Tumor growth pattern ( <i>n</i> = 1,212)	Pushing/expanding	150 (32.8)	310 (41.1)	<b>0.004<sup>d</sup></b>
	Infiltrating	308 (67.2)	444 (58.9)	
Peritumoral lymphocyte infiltration ( <i>n</i> = 1,213)	Absent	357 (77.9)	598 (79.2)	0.655 <sup>d</sup>
	Present	101 (22.1)	157 (20.8)	
Local recurrence ( <i>n</i> = 433)	Absent	69 (55.2)	185 (60.1)	0.410 <sup>d</sup>
	Present	56 (44.8)	123 (39.9)	
Distant metastasis ( <i>n</i> = 440)	Absent	110 (85.3)	252 (81.0)	0.356 <sup>d</sup>
	Present	19 (14.7)	59 (19.0)	
Postoperative therapy ( <i>n</i> = 437)	None	97 (75.7)	250 (80.9)	0.282 <sup>d</sup>
	Treated	31 (24.3)	59 (19.1)	
Overall survival ( <i>n</i> = 1,206)	5-y (95% CI)	51.3 (46.7–56.4)	62.1 (58.4–66)	<b>0.0002<sup>e</sup></b>

<sup>a</sup>GM-CSF staining intensity (0–3) multiplied by frequency (%) of stained cells. Based on ROC curves analysis, a value of 115 was used to discriminate between samples with low or high histoscore. <sup>b</sup>t Test was used for age analysis because of normal distribution; <sup>c</sup>Wilcoxon (Mann–Whitney test) was used for tumor diameter analysis. <sup>d</sup>Discrete/qualitative variables:  $\chi^2$  test; <sup>e</sup>log-rank test was used to compare overall survival rates. Statistically significant *P* values are reported in boldface.

(DakoCytomation) for 20 minutes and incubated for 60 minutes at room temperature with monoclonal antibodies recognizing M-CSF (110-57176; Novus Biologicals) or CX3CL1/fractalkine (89229; Abcam) or overnight at 4°C (21) with a GM-CSF-specific reagent (100-65022; Novus Biologicals). Slides were then incubated with peroxidase-labeled secondary antibody (DakoCytomation) for 30 minutes at room temperature, immersed in 3-amino-9-ethyl-carbazole plus substrate-chromogen (DakoCytomation) for 30 minutes, and counterstained with Gill's hematoxylin.

#### Evaluation of immunohistochemistry

Percentages of positive tumor cells and staining intensities in each punch were evaluated and samples were classified as negative (0), weakly positive (1), moderately positive (2), and highly positive (3). A histoscore was calculated by multiplying staining intensity (0–3) by percentages of positive cells, as previously described (22). Immunohistochemical slides were independently examined by 3 experienced pathologists (L. Terracciano, L. Tornillo, B. Angrisani) blinded to any prior information on clinicopathological features of the patients' samples, with excellent correlation between measurements.

#### Statistical analysis

Gene expression data from different tissues were compared by using the nonparametric Wilcoxon test for paired samples.

For outcome assessment, cut-off values used to classify colorectal cancer with low or high parameters of interest were obtained by ROC curves based on histoscore analyses, evaluating sensitivity and false-positive rate for the discrimination of survivors and nonsurvivors, on all tumor samples. Threshold values thus obtained were compared with the expression levels in nonmalignant and malignant colon tissues and final threshold values were set according to biologic significance.  $\chi^2$  or Fisher exact tests were used to determine the association of GM-CSF expression and clinicopathological features. Survival curves were constructed according to the Kaplan–Meier method. Log ranks were calculated to test for differences between survival curves. Multivariate regression analysis was performed according to Cox proportional hazard models including CD16<sup>+</sup> and CD8<sup>+</sup> cell infiltration, age, gender, T and N stage, tumor grade, vascular invasion, invasive margin, and MMR status. Wald tests statistic was used to test the hypothesis that GM-CSF provides significant information to the model. Subsequently, data obtained from multivariate Cox regression analysis were tabulated including hazard ratios (HR) and 95% confidence intervals (CI). Multivariate Cox regression analysis was performed by using 955 cases because missing values were excluded from the model. M-CSF and CX3CL1 were not integrated in the Cox hazard regression model because specific staining did not show significant prognostic relevance in univariate analysis.

Spearman's rank correlation was used to analyze the association between GM-CSF, M-CSF, CX3CL1, and CD16<sup>+</sup> and CD8<sup>+</sup> cell infiltration. Two-tailed *P* values

<0.05 were considered significant for all analyses. Statistical analyses were performed using R i386 Version 2.15.2 (<http://www.R-project.org>).

## Results

### Phenotypes of GM-CSF- and M-CSF-activated monocytes

Human CD14<sup>+</sup> peripheral blood monocytes were cultured in the presence of GM-CSF or M-CSF. Consistent with the M1/M2 polarization model (5, 17), we observed that following a 6- to 7-day culture in the presence of 25 to 6.25 ng/mL GM-CSF, a significantly higher percentage of cells expressed CD16, as compared with cultures performed in the presence of the same concentrations of M-CSF (average  $\pm$  SE: 66%  $\pm$  8.7% vs. 28%  $\pm$  11.4%, *n* = 6, *P* = 0.011; Fig. 1A and B). In contrast, percentages of cells expressing CD204 molecular scavenger were significantly increased in M-CSF cells, as compared with GM-CSF-stimulated cells (average  $\pm$  SE: 85%  $\pm$  6.5% vs. 41%  $\pm$  10%, *n* = 6, *P* = 0.008). Percentages of cells expressing CD163 did not significantly differ in cells cultured in the presence of M-CSF or GM-CSF (average  $\pm$  SE: 78%  $\pm$  6.5% vs. 65%  $\pm$  10.1%, *n* = 6, *P* = 0.27). Representative histograms and cumulative data derived from 6 experiments with cells from different donors are reported in Fig. 1A and B.

### Cytostatic activity of GM-CSF-activated macrophages against colorectal cancer cells

We then tested the effects of GM-CSF- and M-CSF-stimulated macrophages on the proliferation of MMR proficient (MMRp) Colo 205 colorectal cancer cells.

Following 6 to 7 days stimulation in the presence of 25 to 6.25 ng/mL GM-CSF, monocytes were able to significantly inhibit colorectal cancer cell proliferation (Fig. 1C). This effect was dependent on effector:target (E:T) ratios and on GM-CSF doses used in the initial stimulation phase. In sharp contrast, monocytes cultured in the presence of the same concentrations of M-CSF, were devoid of antiproliferative ability, irrespective of E:T ratios (Fig. 1C). Effects of GM-CSF-stimulated monocytes were not mediated by soluble factors. Indeed, neither recombinant GM-CSF nor culture supernatants did inhibit colorectal cancer cell proliferation. Moreover, macrophages did not induce apoptosis of target cells, as indicated by lack of annexin V binding, but rather exerted cytostatic effects. Interestingly, GM-CSF-stimulated monocytes at 10:1 E:T ratios were as effective as a 30  $\mu$ g/mL concentration of the pyrimidin analog 5FU in inhibiting colorectal cancer proliferation (data not shown).

Comparable results were observed upon culture in the presence of GM-CSF but not M-CSF-stimulated monocytes by using MMR-deficient (MMRd) HCT116 colorectal cancer cells as targets (data not shown).

### GM-CSF and M-CSF gene expression in colorectal cancer and in corresponding, autologous healthy mucosa

To obtain an insight into local tumor microenvironment conditions, we then addressed the expression of GM-CSF

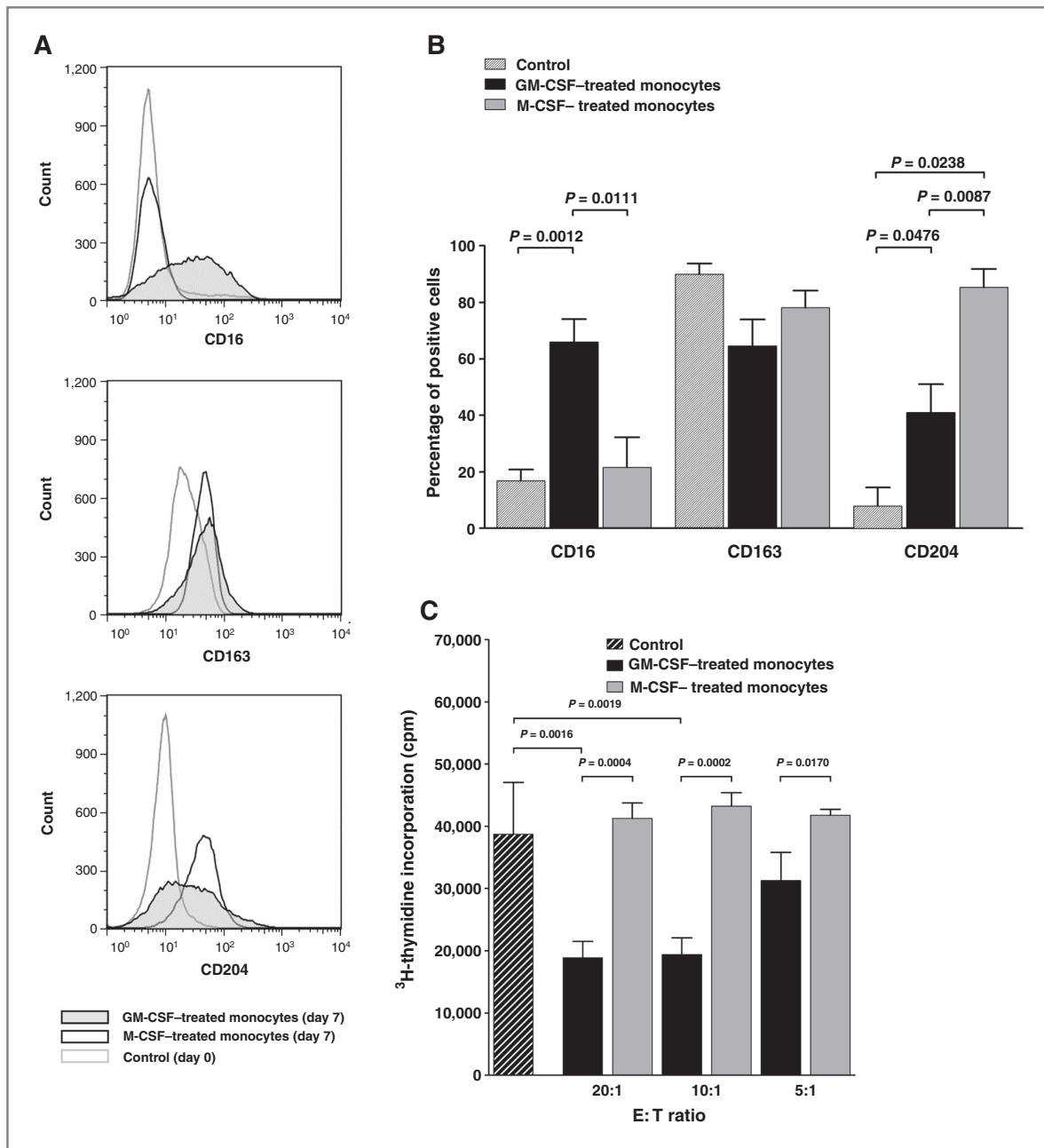


**Figure 1.** Phenotypic and functional differentiation of GM-CSF- and M-CSF-stimulated monocytes. Peripheral blood CD14<sup>+</sup> monocytes from healthy donors were magnetically sorted and cultured in the presence of GM-CSF or M-CSF (12.5 ng/mL). Cells were then washed and stained with mAbs recognizing the indicated markers (A and B). Representative results referring to uncultured monocytes (gray lines), M-CSF treated (black lines), and GM-CSF treated (shaded profiles) are shown in A, whereas B reports cumulative data from 6 independent experiments. GM-CSF or M-CSF-stimulated (12.5 ng/mL) cells were then cocultured with Colo205 cells at the indicated E:T ratios in flat bottom 96-well plates in triplicates. Tumor cell proliferation was assessed by <sup>3</sup>H-thymidine incorporation on day 3. Control data refer to Colo205 cells cultured in the absence of myeloid cells (C). Data refer to 1 representative experiment out of 4 performed with cells from different donors with similar results.

and M-CSF genes in surgically excised paired specimens of colorectal cancer and autologous healthy mucosa sampled at distance from the cancerous tissue (23).

GM-CSF gene was expressed to significantly higher extents in colorectal cancer tissue, as compared with corresponding autologous healthy mucosa [median, IQR: 6.167E10<sup>-5</sup>,



$2.7E10^{-5}$ – $2.6E10^{-4}$  vs.  $4.03E10^{-6}$ ,  $0$ – $1.91E10^{-5}$ ,  $n = 45$ ,  $P < 0.0001$ ]. In contrast, *M-CSF* gene expression was similar in healthy colon mucosa and in the corresponding colorectal cancer tissues (median, IQR:  $1.8E10^{-2}$ ,  $5.6E10^{-3}$ – $5.2E10^{-2}$  vs.  $3.8E10^{-2}$ ,  $2.3E10^{-2}$ – $1E10^{-1}$ ,  $n = 46$ ,  $P = 0.25$ ). Accordingly, *GM-CSF/M-CSF* gene expression ratio was significantly higher in tumor tissue than in the corresponding autologous mucosa ( $0.025$  vs.  $0.0014$ ,  $P < 0.0001$ ; Fig. 2A).

### Expression of genes predominantly associated with M1 and M2 macrophages in colorectal cancer and in corresponding, autologous healthy mucosa

To obtain insights into specific gene signatures eventually detectable in clinical specimens, we assessed *IL23* and *IL1 $\beta$*  gene expression in paired colorectal cancer and autologous healthy mucosa samples. We found that these genes were expressed to significantly higher extents in colorectal cancer than in matched healthy mucosa (median, IQR: *IL23*:  $2E10^{-3}$ ,  $9E10^{-4}$ – $5.1E10^{-3}$  vs.  $5E10^{-4}$ ,  $1.4E10^{-4}$ – $1.1E10^{-3}$ ,  $n = 47$ ,  $P < 0.0001$ ; *IL1 $\beta$* :  $2E10^{-2}$ ,  $7.7E10^{-3}$ – $5.2E10^{-2}$  vs.  $7.5E10^{-3}$ ,  $2.3E10^{-3}$ – $1.6E10^{-2}$ ,  $n = 48$ ,  $P = 0.001$ ; Fig. 2B). However, expression of *IL12p35* gene, reportedly typically observed in M1 cells, was detectable to significantly higher extents in healthy mucosa than in matched tumor tissues (median, IQR:  $9.3E10^{-4}$ ,  $3E10^{-4}$ – $2.2E10^{-3}$  vs.  $3.5E10^{-4}$ ,  $1.9E10^{-4}$ – $8.5E10^{-4}$ ,  $n = 46$ ,  $P = 0.01$ ; Fig. 2B).

M2 polarized macrophages are characterized by the ability to produce IL10 (5). Indeed, we did not observe significant differences in *IL10* gene expression between healthy mucosa and tumor tissue (median, IQR:  $6.4E10^{-4}$ ,  $3.1E10^{-4}$ – $1.2E10^{-3}$  vs.  $3.4E10^{-4}$ ,  $1E10^{-4}$ – $1E10^{-3}$ ,  $n = 46$ ,  $P = 0.41$ ).

Furthermore, expression of *TNF $\alpha$* , *IL6*, and *IL12p40* genes was also similarly detectable in healthy mucosa and corresponding colorectal cancer tissue (median, IQR: *TNF $\alpha$* :  $6.7E10^{-4}$ ,  $1.7E10^{-4}$ – $1.6E10^{-3}$  vs.  $8E10^{-4}$ ,  $3.1E10^{-4}$ – $1.8E10^{-3}$ ,  $n = 47$ ,  $P = 0.089$ ; *IL6*:  $5.1E10^{-5}$ ,  $8.6E10^{-6}$ – $6.1E10^{-4}$  vs.  $2.7E10^{-4}$ ,  $5.9E10^{-5}$ – $9.6E10^{-4}$ ,  $n = 45$ ,  $P = 0.17$ ; *IL12p40*:  $6.8E10^{-5}$ ,  $3.19E10^{-5}$ – $2.7E10^{-4}$  vs.  $7.5E10^{-5}$ ,  $1.8E10^{-5}$ – $2.1E10^{-4}$ ,  $n = 46$ ,  $P = 0.7$ ; Fig. 2B).

Thus, conventional patterns of polarized macrophage gene expression do not seem to fully fit gene signatures detectable in colorectal cancer (4, 5). However, consistent with gene expression profiles commonly attributed to polarized macrophages (5), *M-CSF* and *IL10* and *GM-CSF* and *TNF $\alpha$*  gene expression in colorectal cancer tissues were highly significantly correlated ( $r = 0.63$ ,  $P < 0.0001$  and  $r = 0.49$ ,  $P < 0.0001$ , respectively; Fig. 2C).

### Prognostic relevance of GM-CSF expression in colorectal cancer

We then explored GM-CSF and M-CSF expression, at the protein level, by using a TMA including 50 healthy mucosa tissues and 1,239 different colorectal cancer specimens annotated with clinicopathological data. Specific staining was evaluated by multiplying staining intensity (0–3) by percentages of positive cells (22).

In 60% of colorectal cancer, a diffuse and strong GM-CSF-specific staining involving a large majority of tumor cells with a negligible contribution of interstitial cells could be observed. In the remaining 40% of cases, similarly to healthy mucosa specimens, GM-CSF-specific staining of tumor cells was weak or negative (Fig. 3A and B). GM-CSF-specific histoscore median values were 140, 170, 105, and 170 in healthy mucosa, total colorectal cancer, and MMRd and MMRp colorectal cancer, respectively (Supplementary Fig. S1). Thus, colorectal cancer MMRp expressed significantly more GM-CSF protein ( $P = 0.0001$ ) than MMRd colorectal cancer. In the latter cancers, histoscore values were even lower than in healthy mucosa.

Based on this analysis, and on results of ROC curves and regression trees, we established GM-CSF threshold histoscore value for survival analyses at 115. Analysis of TMA data (Table 1) indicates that colorectal cancer displaying high GM-CSF-specific staining are characterized by a significantly lower pT stage ( $P = 0.02$ ), and a significantly ( $P = 0.004$ ) more frequently detectable pushing/expanding, as opposed to infiltrating (20), growth pattern. Overall survival, as evaluated in the whole TMA seemed to be correlated with GM-CSF expression ( $P = 0.0002$  at 5 years,  $n = 1206$ ), as detectable at the protein level. In particular, this effect was specifically observed in MMRp colorectal cancer ( $n = 1014$ ;  $P < 0.0001$ ). In contrast, GM-CSF expression had no effect on overall survival of patients with MMRd colorectal cancer ( $n = 192$ ;  $P = 0.927$ ; Fig. 3E and F).

GM-CSF maintained its prognostic significance ( $P = 0.036$ ) also in multivariate Cox regression analysis (Table 2), together with high CD16<sup>+</sup> ( $P = 0.002$ ) and CD8<sup>+</sup> ( $P = 0.04$ ) cell infiltration, age ( $P < 0.00001$ ), gender ( $P < 0.0001$ ), pT/N stage, vascular invasion, tumor border configuration, and microsatellite instability.

Detection of M-CSF could only be performed in a subset of the TMA including 37 healthy mucosa and 743 colorectal cancer. M-CSF staining was usually diffuse with different intensity (Fig. 3C and D). Absent or very low intensity (below the score of 115) was observed in 48.6% (19/37) of healthy mucosa and in 82% (614/743) of the colorectal cancer ( $P = 0.002$ ). No differential M-CSF expression was detectable MMRp and MMRd tissues ( $P = 0.6$ ; Supplementary Fig. S1). In the patients with colorectal cancer with higher M-CSF expression (129/743, 17%), we did not observe improved survival neither in MMRp ( $P = 0.124$ ) nor in MMRd ( $P = 0.283$ ) cases (Fig. 3G and H).

### Correlations between GM-CSF production and colorectal cancer infiltration by immunocompetent cells

We explored the relationship eventually occurring between GM-CSF production by colorectal cancer cells and cancer infiltration by CD16<sup>+</sup> or CD8<sup>+</sup> cells, significantly associated with favorable prognosis (8–10, 16, 20).

Surprisingly, GM-CSF staining did not seem to be associated with CD16<sup>+</sup> cell infiltration ( $P = 0.59$ ).

Combined Kaplan–Meier survival analysis (Fig. 4A and B) indicates that patients with CD16<sup>+</sup> cell infiltration of MMRp

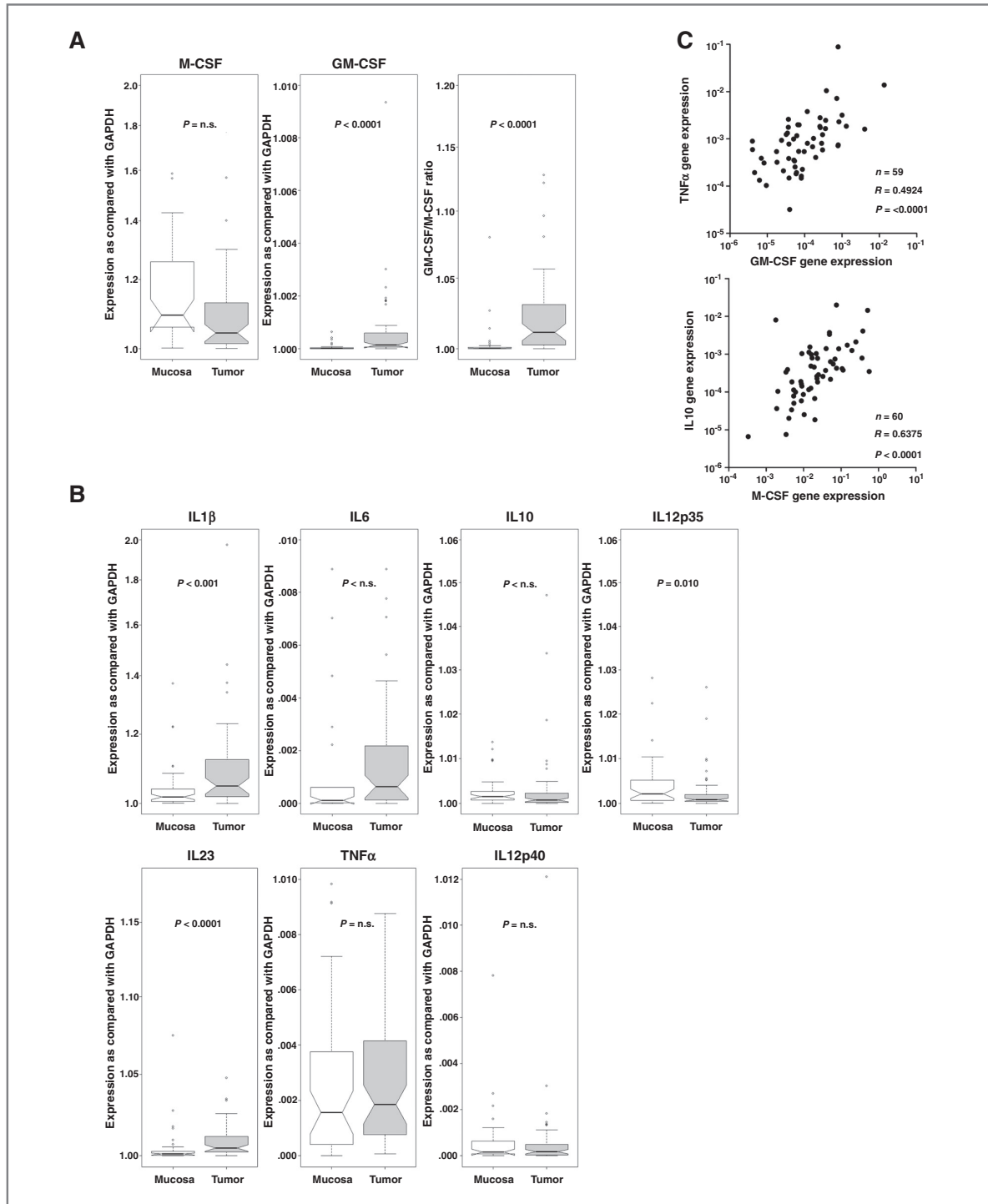


**Figure 2.** Cytokine gene expression in freshly excised colorectal cancer and corresponding healthy mucosa. Total cellular RNA was purified from freshly excised colorectal cancer and autologous healthy mucosa specimens and reverse transcribed. Expression of *GM-CSF* and *M-CSF* genes was assessed by quantitative RT-PCR, by using *GAPDH* house-keeping gene, as reference. *GM-CSF/M-CSF* gene expression ratios were also calculated (A). The expression of additional cytokine genes was similarly evaluated (B), and the correlation between *GM-CSF* and *TNF $\alpha$* , and *M-CSF* and *IL10* gene expression was analyzed (C). n.s., nonsignificant.

**Figure 3.** Prognostic significance of GM-CSF and M-CSF protein expression in colorectal cancer. A colorectal cancer TMA was stained with GM-CSF (A and B) or M-CSF (C and D) specific reagents. Representative samples with low or high specific histoscores are shown in A and C and B and D, respectively (magnification:  $\times 20$ ). Based on ROC curves derived from histoscore data, the prognostic significance of GM-CSF (E and F) and M-CSF (G and H) could then be analyzed in MMRp (E and G) and MMRd (F and H) colorectal cancer. In both panels, red lines and black lines refer to cases with high and low cytokine expression, respectively. Number of events (= deaths) and total number of cases are also reported.

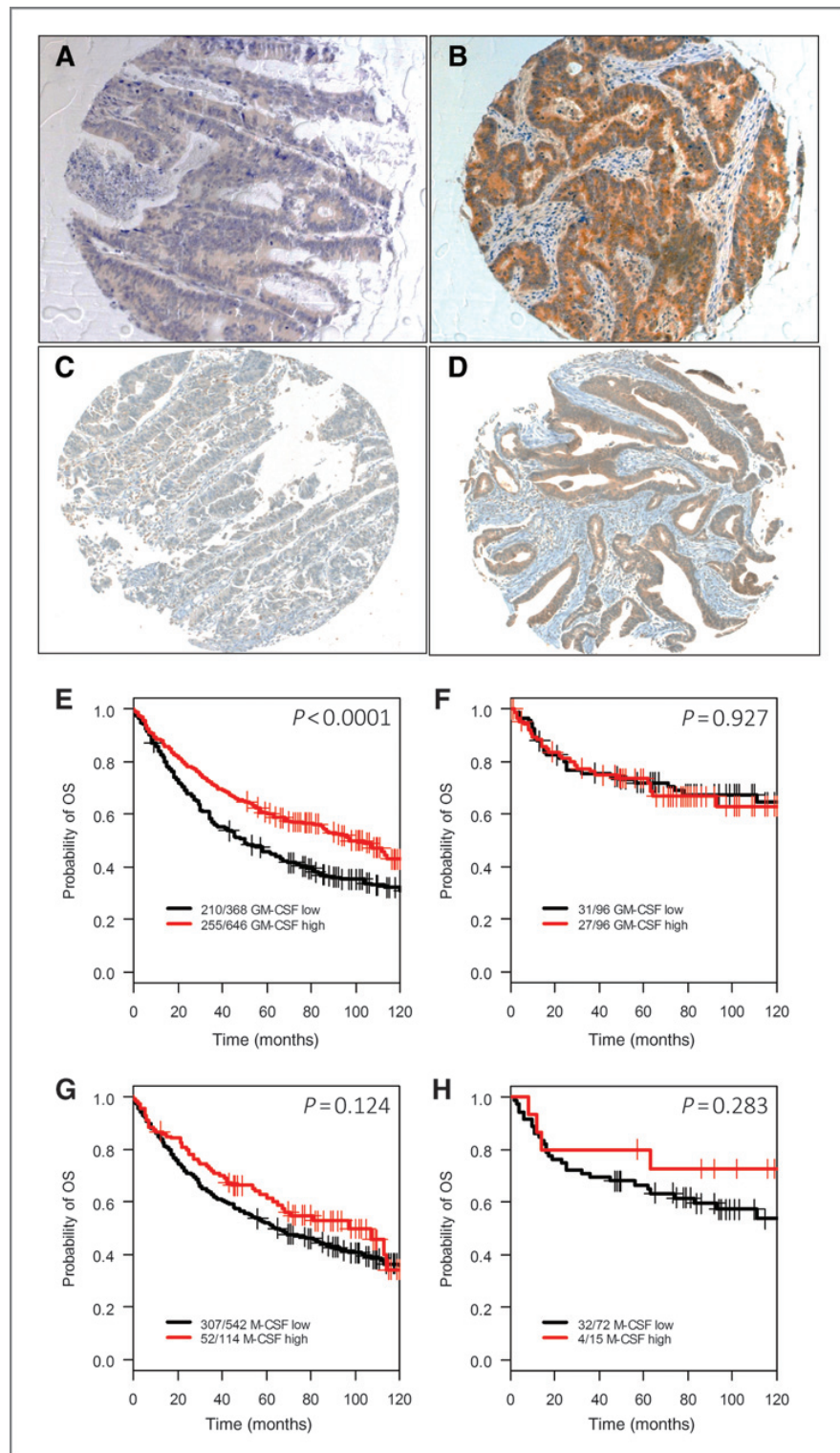


**Table 2.** Multivariate hazard Cox regression survival analysis

	HR (95% CI)	P
GM-CSF (low vs. high)	0.808 (0.706–0.909)	0.036
CD8 (low vs. high)	0.763 (0.626–0.899)	0.048
CD16 (low vs. high)	0.716 (0.608–0.824)	0.002
Age (continuous)	1.033 (1.028–1.038)	<0.00001
Gender (women vs. men)	0.656 (0.554–0.757)	<0.0001
pT stage (1, 2, 3, 4)	1.900 (1.807–1.993)	<0.00001
pN stage (0, 1, 2)	1.882 (1.809–1.954)	<0.00001
Tumor grade (1, 2, 3)	1.259 (1.114–1.403)	0.11
Vascular invasion (0, 1) <sup>a</sup>	1.413 (1.300–1.525)	0.002
Tumor border configuration (0, 1) <sup>b</sup>	1.429 (1.302–1.556)	0.005
Microsatellite stability (deficient vs. proficient)	1.692 (1.534–1.849)	0.0009

NOTE: Multivariate analysis showing HRs and P values for all colorectal cancer (n = 975, because of missing values, see "Materials and Methods"), as conferred by high GM-CSF expression, CD8<sup>+</sup> and CD16<sup>+</sup> infiltrating cell density, age, gender, tumor size, nodal status, tumor grade, vascular invasion, tumor border configuration, and microsatellite stability.

<sup>a</sup>0: absent, 1: present.

<sup>b</sup>0: pushing, 1: infiltrating.

colorectal cancer and high GM-CSF production have a significantly better prognosis than those with low CD16<sup>+</sup> cell infiltration and low GM-CSF production (P = 0.000193).

However, in CD16<sup>+</sup> cell infiltrated colorectal cancer, GM-CSF production did not seem to significantly influence overall survival. No effects were detectable in MMRd cancers.

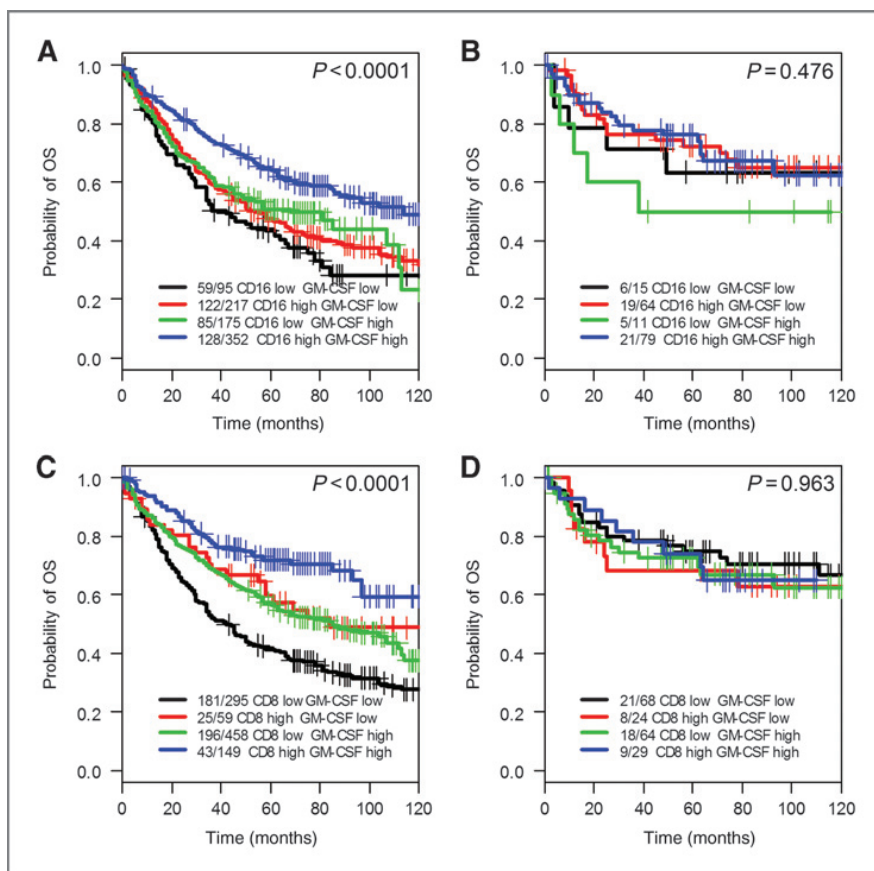


**Figure 4.** Prognostic significance of GM-CSF in colorectal cancer as related to levels of infiltration by immunocompetent cells. The prognostic significance of GM-CSF production was analyzed in tumors stratified according to their high or poor infiltration by CD8<sup>+</sup> or CD16<sup>+</sup> cells (10, 15, 20) in MMRp and MMRd colorectal cancer. Kaplan-Meier curves in A and B display the combined effects of GM-CSF expression (score threshold at 115) and CD16<sup>+</sup> cell infiltration (16) in MMRp and MMRd colorectal cancer, respectively. Black lines: both markers low; blue lines: both markers elevated; red lines: high CD16<sup>+</sup> cell infiltration and low GM-CSF expression; green lines: low CD16<sup>+</sup> cell infiltration and high GM-CSF expression. Number of events (= deaths)/total number of cases are also reported. Similarly, Kaplan-Meier curves in C and D display the combined effects of GM-CSF expression and CD8<sup>+</sup> infiltration (10, 20) in MMRp and MMRd colorectal cancer, respectively. Black lines: both markers low; blue lines: both markers elevated; red lines: high CD8<sup>+</sup> cell infiltration and low GM-CSF expression; green lines: low CD8<sup>+</sup> cell infiltration and high GM-CSF expression. Number of events (= deaths)/total number of cases are also reported.



GM-CSF staining was also unrelated with colorectal cancer infiltration by CD8<sup>+</sup> cells ( $r$  Spearman: 0.09). However, most interestingly, in colorectal cancer characterized by poor CD8<sup>+</sup> T cell infiltration, a condition known to be associated with severe prognosis (8–10, 20), GM-CSF production by cancer cells was highly significantly correlated with improved overall survival in MMRp ( $P = 0.00004$ ) but not in MMRd colorectal cancer (Fig. 4C and D).

### Expression of CX3CL1/fractalkine gene in colorectal cancer

CX3CL1/fractalkine has been shown to selectively attract CD16<sup>+</sup> monocytes, which do express cognate CX3CR1 receptor (24) and CX3CL1/fractalkine gene expression has been suggested to associate with favorable prognosis in colorectal cancer (25).

We observed that CX3CL1/fractalkine gene is expressed to significantly higher extents in colorectal cancer than in corresponding healthy mucosa (median, IQR:  $1.8E10^{-2}$ ,  $9.3E10^{-3}$ – $8.5E10^{-2}$  vs.  $9.2E10^{-3}$ ,  $4.6E10^{-3}$ – $4.7E10^{-2}$ ,  $n = 22$ ,  $P = 0.0028$ ) and that the specific gene product is detectable by ELISA in supernatants from established colorectal cancer cell lines (Supplementary Fig. S2A and B). Most interestingly, CX3CL1/fractalkine protein is also detectable in colorectal cancer (Supplementary Fig. S2C and D). TMA analysis indicates that this protein is detectable to significantly higher extents in colorectal cancer than in healthy mucosa ( $P = 0.0045$ ). However, its expression was devoid of prognostic significance and unrelated to colorectal cancer infiltration by CD16<sup>+</sup> myeloid cells (data not shown).

### Discussion

In previous work we showed that colorectal cancer infiltration by CD16<sup>+</sup> myeloid cells is associated with improved prognosis (16). Here we have addressed mechanistic clues possibly underlying these effects, by analyzing the antitumor potential of *in vitro* polarized macrophages. Furthermore, and most importantly, we have explored the expression at the gene and protein level of cytokines and chemokines associated with functional polarization and chemoattraction of macrophage subsets possessing antitumor capacity and their prognostic significance.

M-CSF and GM-CSF are known to be involved in the polarization of anti-inflammatory/pro-angiogenic M2 and pro-inflammatory/antitumor M1 macrophages, respectively (5, 17). Here we show that upon GM-CSF but not M-CSF *in vitro* stimulation, peripheral blood monocytes from healthy donors become capable of exerting cytostatic effects on colorectal cancer cells. However, the analysis of >40 matched pairs of colorectal cancer and autologous healthy mucosa clearly indicates that malignant tissues are typically characterized by an increased expression of GM-CSF gene, as compared with autologous healthy mucosa. Accordingly, colorectal cancer tissues are characterized by a cytokine gene expression signature reminiscent, although not fully matching, of that observed in activated M1 cells, including high *IL1 $\beta$*  and *IL23* gene expression (5).

*Per se*, these data might still be consistent with a pathogenic role of local inflammation in colorectal cancer, as suggested by a number of experimental models (6). However, by using a large number of surgical specimens (>1,000) annotated with an exhaustive clinical database, we report here that high GM-CSF expression at the protein level in colorectal cancer is associated with favorable prognosis, although only in MMRp cases. In contrast, M-CSF protein expression, as detectable in our TMA, does not seem to be significantly associated with clinicopathological features or overall survival. Importantly, TMA analysis reveals that GM-CSF is predominantly produced by tumor cells.

GM-CSF plays a key role in the differentiation and functional maturation of different myeloid populations.

Because of its ability to activate antigen-presenting cells, this cytokine has been widely used in cancer immunotherapy (26, 27). GM-CSF-transfected primary tumor cells and established tumor cell lines have been used for vaccination purposes (27). Moreover, recombinant GM-CSF has been utilized as supportive cytokine to supplement immunization targeting tumor-associated antigens (TAA) implemented through administration of peptides, antigen-pulsed dendritic cells or recombinant viruses.

GM-CSF has also widely been used in combination with IL4 or IFN type I (28) in the *in vitro* dendritic cell generation. A number of studies indicate that treatment of peripheral blood monocytes with GM-CSF leads to polarization toward a M1 pro-inflammatory phenotypic and functional profile, whereas M-CSF promotes the differentiation of alternatively activated M2 macrophages possessing pro-angiogenic and anti-inflammatory properties (17).

However, GM-CSF has also been shown to promote the generation of myeloid-derived suppressor cell (MDSC; refs. 29 and 30), characterized by a powerful ability to inhibit T-cell proliferation and to promote the expansion of CD4<sup>+</sup>/FOXP3<sup>+</sup> regulatory T cells. Notably, increased numbers of myeloid cells with phenotypic and functional profiles closely overlapping those of MDSC have been detected in peripheral blood of patients bearing cancers following treatment with GM-CSF (31).

Myeloid cell colony-stimulating factors have been found to be produced by different types of carcinoma cells. In particular, GM-CSF production by tumor cells has been shown to be associated with increased recurrence rate and metastasis formation in head and neck cancers (32). Furthermore, GM-CSF production by breast cancer cells was suggested to enhance tumor growth and to promote the formation of bone metastases, possibly by stimulating resident macrophages or by inducing osteoclast differentiation and activation (33). Lung cancer cells have also been shown to produce GM-CSF and their proliferation may be enhanced by exogenous GM-CSF (34).

We and others have previously shown that colorectal cancer cells do produce GM-CSF (21, 35). Interestingly, colorectal cancer cell lines producing GM-CSF have been suggested to be highly aggressive *in vivo* (36), possibly because of the activation of macrophages, promoting stromal reactivity. In addition, GM-CSF production by colorectal

cancer cells from liver metastases has been suggested to promote tumor growth by a paracrine loop implying heparin-binding EGF production by activated tumor-infiltrating macrophages (37).

Most recently however, immune-dependent and immune-independent antitumor activities of GM-CSF in human colorectal cancer have been suggested (38). In a group of 124 patients, association with favorable prognosis was detectable in 8 patients bearing tumors concomitantly expressing genes encoding GM-CSF and both receptor subunits (38). However, MMR status of colorectal cancer was not analyzed, GM-CSF protein expression was not investigated and the association with macrophage and T-cell infiltration or with the expression of additional cytokines promoting their polarization was not explored.

Within this frame our data provide important novel information on the role of GM-CSF in colorectal cancer microenvironment. First, we show here that GM-CSF is predominantly produced by MMRp colorectal cancer cells. Despite their higher genomic stability, these cancers are characterized by a more severe prognosis, as compared with MMRd colorectal cancer. Furthermore, we report that although recombinant GM-CSF is *per se* ineffective, colorectal cancer cell lines are sensitive to the cell-cell contact-dependent cytostatic effects of GM-CSF-activated macrophages. However, although previously published data from our groups indicate that colorectal cancer infiltration by cells expressing CD16 is associated with improved prognosis (16), we did not observe any significant correlation between GM-CSF-specific staining and CD16<sup>+</sup> cell infiltration in the TMA under investigation.

We reasoned that tumor infiltration by CD16<sup>+</sup> myeloid cells might result from the functional maturation/differentiation of cells residing into colonic tissues promoted by factors present in local microenvironment or from the selective chemoattraction of circulating cells endowed with specific phenotypic and functional features (24).

Therefore, we explored the potential prognostic role of CX3CL1/fractalkine, a chemokine selectively attracting CD16<sup>+</sup> peripheral monocytes (24) in colorectal cancer. This chemokine has been found to be expressed in colorectal cancer cells and, based on the analysis of a small ( $n = 80$ ) number of specimens, it has been suggested to be associated with favorable prognosis in colorectal cancer (25, 39). Our data show that CX3CL1/fractalkine gene expression can indeed be observed to significantly higher extents in colorectal cancer than in matched healthy mucosa. However, protein detection in colorectal cancer tissue sections is infrequent and devoid of clinical significance.

Taken together, these data suggest that colorectal cancer microenvironment contains factors promoting both local CD16<sup>+</sup> myeloid cell differentiation and specific chemoattraction, such as GM-CSF and CX3CL1/fractalkine. However, although neither of these factors correlates significantly with CD16<sup>+</sup> myeloid cell infiltration in colorectal cancer, GM-CSF detection is associated with favorable prognosis in a large colorectal cancer subset.

Most obviously, other CD16<sup>-</sup> cell types possibly favoring tumor progression might be responsive to GM-CSF (40). Indeed, their activities might eventually "mask" or modulate the favorable effects of this cytokine promoting the expansion of CD16<sup>+</sup> myeloid cells at the tumor site. Alternatively, in defined subgroups of patients, myeloid cells might be hypo-responsive to GM-CSF. Interestingly, a decreased expression of GM-CSF receptor  $\alpha$  chain CD116, accompanied by hypo-responsiveness to cytokine stimulation, has recently been observed in peripheral blood monocytes and granulocytes from patients with IBD (41). However, recruitment, differentiation, and elicitation of antitumoral effects of CD16<sup>+</sup> myeloid cells might require other factors in addition to GM-CSF. It is tempting to speculate that bacterial products possibly deriving from gut lumen might be of relevance in this context, possibly through TLRs triggering.

Indeed, GM-CSF-transduced murine CT-26 colorectal cancer cells have been repeatedly tested in experimental models in the past. Dranoff and colleagues originally reported that irradiated, GM-CSF-transduced, CT-26 are more effective than wild-type cells in inducing antitumor immunity upon subcutaneous administration. However, live transduced CT-26 cells were not tested (42). Colombo and colleagues have reported (43) that subcutaneous injection of live GM-CSF-transduced cells resulted in rapid tumor growth, similarly to wild-type cells. In both series of studies, cells were injected subcutaneously. Therefore, the role of mucosal immune response and gut microbiome could not be addressed. This aspect might represent a major difference between the above-cited experimental models and clinical reality. Furthermore, importantly, paradoxical effects of GM-CSF used as adjuvant for tumor-specific vaccination were more recently reviewed (44). These data suggest that low doses injected locally might be helpful, whereas systemic administration of high doses could be ineffective or detrimental.

Although further research is warranted to clarify underlying molecular mechanisms, our data emphasize the prognostic significance of GM-CSF production by colorectal cancer cells. In this context, it is particularly interesting that GM-CSF seems to possess a major favorable prognostic significance in colorectal cancer, which are not infiltrated by CD8<sup>+</sup> T cells. Therefore, although adaptive immunity seems to play an important role in the control of colorectal cancer progression, other mechanisms, possibly related to innate immune system activation, might still be significantly active in its absence. Thus, GM-CSF might *bona fide* be included in the hierarchy of cell subsets and soluble factors of relevance in shaping the clinical course of colorectal cancer.

Cytokine and chemokine gene expression has been extensively investigated in colorectal cancer tissues (9, 45). However, to the best of our knowledge, this is one of the first studies addressing the prognostic significance of cytokine and chemokine expression at the protein level in a large number of patients.

It has been highlighted that a number of conventional assumptions related to cancer-immune system interaction

do not seem to apply to colorectal cancer (46). For instance, at difference with a large number of cancer types, we and others have shown that colorectal cancer infiltration by FOXP3<sup>+</sup> cells is associated to improved prognosis (11, 12). Accordingly, in keeping with the proposed colorectal cancer paradoxical scenario, we and others have previously observed that colorectal cancer infiltration by myeloid cells is also associated with relatively good prognosis (15, 16). Our data unravel a further important paradoxical colorectal cancer feature, represented by the favorable prognostic role of GM-CSF.

Most interestingly, our data reveal that CD8<sup>+</sup> and CD16<sup>+</sup> cell infiltration and GM-CSF production by tumor cells play independent antitumor roles. While underlining the complexity of colorectal cancer microenvironment, these findings suggest that the peculiar immunobiology of these cancers could provide important hints for the development of innovative treatments.

Colorectal cancer treatment options, including curative or palliative surgical resection, neoadjuvant, adjuvant, and palliative chemotherapy are currently largely based on tumor–node–metastasis (TNM) staging. However, conventional staging seems to be relatively inefficient in daily clinical practice, frequently leading to overtreatment or undertreatment (47, 48). In this respect, analysis of colorectal cancer immunotexture (49) seems to identify a set of markers largely independent from TNM staging but also associated with a high prognostic relevance, as detectable in large cohorts of patients. It is tempting to speculate that, in a next future, relatively limited constellations of markers, possibly including GM-CSF production by colorectal cancer cells, might be integrated into novel staging procedures, helping to identify subsets of patients eligible for effective therapies while sparing them unnecessary treatments and improving their quality of life.

## References

- Hanahan D, Weinberg RA. Hallmarks of cancer: the next generation. *Cell* 2011;144:646–74.
- Hanahan D, Coussens LM. Accessories to the crime: functions of cells recruited to the tumor microenvironment. *Cancer Cell* 2012;21:309–22.
- Allavena P, Sica A, Garlanda C, Mantovani A. The Yin–Yang of tumor-associated macrophages in neoplastic progression and immune surveillance. *Immunol Rev* 2008;222:155–61.
- Biswas SK, Mantovani A. Macrophage plasticity and interaction with lymphocyte subsets: cancer as a paradigm. *Nat Immunol* 2010;11:889–96.
- Mantovani A, Sozzani S, Locati M, Allavena P, Sica A. Macrophage polarization: tumor-associated macrophages as a paradigm for polarized M2 mononuclear phagocytes. *Trends Immunol* 2002;23:549–55.
- Terzic J, Grivennikov S, Karin E, Karin M. Inflammation and colon cancer. *Gastroenterology* 2010;138:2101–14.
- Danese S, Malesci A, Vetrano S. Colitis-associated cancer: the dark side of inflammatory bowel disease. *Gut* 2011;60:1609–10.
- Galon J, Costes A, Sanchez-Cabo F, Kirilovsky A, Mlecnik B, Lagorce-Pages C, et al. Type, density, and location of immune cells within human colorectal tumors predict clinical outcome. *Science* 2006;313:1960–4.
- Pages F, Berger A, Camus M, Sanchez-Cabo F, Costes A, Molitor R, et al. Effector memory T cells, early metastasis, and survival in colorectal cancer. *N Engl J Med* 2005;353:2654–66.
- Zlobec I, Karamitopoulou E, Terracciano L, Piscuoglio S, Iezzi G, Muraro MG, et al. TIA-1 cytotoxic granule-associated RNA binding protein improves the prognostic performance of CD8 in mismatch repair-proficient colorectal cancer. *PLoS ONE* 2010;5:e14282.
- Frey DM, Droeser RA, Viehl CT, Zlobec I, Lugli A, Zingg U, et al. High frequency of tumor-infiltrating FOXP3(+) regulatory T cells predicts improved survival in mismatch repair-proficient colorectal cancer patients. *Int J Cancer* 2010;126:2635–43.
- Salama P, Phillips M, Grieu F, Morris M, Zeps N, Joseph D, et al. Tumor-infiltrating FOXP3+ T regulatory cells show strong prognostic significance in colorectal cancer. *J Clin Oncol* 2009;27:186–92.
- Sconocchia G, Arriga R, Tornillo L, Terracciano L, Ferrone S, Spagnoli GC. Melanoma cells inhibit NK cell functions. *Cancer Res* 2012;72:5428–9.
- Allavena P, Mantovani A. Immunology in the clinic review series; focus on cancer: tumour-associated macrophages: undisputed stars of the inflammatory tumour microenvironment. *Clin Exp Immunol* 2012;167:195–205.
- Nagorsen D, Voigt S, Berg E, Stein H, Thiel E, Loddenkemper C. Tumor-infiltrating macrophages and dendritic cells in human

## Disclosure of Potential Conflicts of Interest

No potential conflicts of interest were disclosed.

## Authors' Contributions

**Conception and design:** C.A. Nebiker, J. Han, G. Iezzi, R.A. Droeser, D. Oertli, M. Adamina, G. Sconocchia, G.C. Spagnoli

**Development of methodology:** C.A. Nebiker, J. Han, G. Iezzi, X. Huber, C. Mengus, L. Terracciano, G.C. Spagnoli

**Acquisition of data (provided animals, acquired and managed patients, provided facilities, etc.):** C.A. Nebiker, J. Han, C. Hirt, F. Amicarella, E. Cremonesi, E. Padovan, R.A. Droeser, R. Rosso, M. Bolli, M. Adamina, M.G. Muraro, M. Zuber, L. Tornillo, G.C. Spagnoli

**Analysis and interpretation of data (e.g., statistical analysis, biostatistics, computational analysis):** C.A. Nebiker, J. Han, S. Eppenberger-Castori, G. Iezzi, B. Angrisani, D. Oertli, U. von Holzen, M. Adamina, C. Mengus, P. Zajac, G. Sconocchia, L. Terracciano, G.C. Spagnoli

**Writing, review, and/or revision of the manuscript:** C.A. Nebiker, J. Han, C. Hirt, F. Amicarella, R.A. Droeser, D. Oertli, U. von Holzen, M. Adamina, M.G. Muraro, C. Mengus, P. Zajac, G. Sconocchia, G.C. Spagnoli

**Administrative, technical, or material support (i.e., reporting or organizing data, constructing databases):** J. Han, B. Angrisani, R.A. Droeser, M.G. Muraro, M. Zuber

**Study supervision:** D. Oertli, G.C. Spagnoli

## Acknowledgments

The authors thank Dr. I. Zlobec (Institute of Pathology, University of Bern, Switzerland) for the statistical analysis of data in the initial phases of this study.

## Grant Support

J. Han has been supported by the "Academic Leaders Training Program of Pudong Health Bureau" (Shanghai, P.R. China, Grant No. PEWd2010-05); G. Iezzi and F. Amicarella are partially supported by a Swiss National Fond Professorship grant to G. Iezzi. R.A. Droeser is partially supported by a grant from the Dr. Hans-Altschüler Stiftung and the Werner und Hedy Berger-Janser Stiftung. G. Sconocchia is supported by the Italian Association for Cancer Research (AIRC), Grant No. IG10555. L. Terracciano and L. Tornillo are partially funded by a Swiss National Fond grant to L. Terracciano.

The costs of publication of this article were defrayed in part by the payment of page charges. This article must therefore be hereby marked *advertisement* in accordance with 18 U.S.C. Section 1734 solely to indicate this fact.

Received October 9, 2013; revised March 5, 2014; accepted March 25, 2014; published OnlineFirst April 15, 2014.

- colorectal cancer: relation to local regulatory T cells, systemic T-cell response against tumor-associated antigens and survival. *J Transl Med* 2007;5:62.
16. Sconocchia G, Zlobec I, Lugli A, Calabrese D, Iezzi G, Karamitopoulou E, et al. Tumor infiltration by Fcγ<sub>3</sub> (CD16)<sup>+</sup> myeloid cells is associated with improved survival in patients with colorectal carcinoma. *Int J Cancer* 2011;128:2663–72.
  17. Verreck FA, de Boer T, Langenberg DM, Hoeve MA, Kramer M, Vaisberg E, et al. Human IL-23-producing type 1 macrophages promote but IL-10-producing type 2 macrophages subvert immunity to (myco) bacteria. *Proc Natl Acad Sci U S A* 2004;101:4560–5.
  18. Livak KJ, Schmittgen TD. Analysis of relative gene expression data using real-time quantitative PCR and the 2<sup>−ΔΔC(T)</sup> method. *Methods* 2001;25:402–8.
  19. Baker K, Zlobec I, Tornillo L, Terracciano L, Jass JR, Lugli A. Differential significance of tumour infiltrating lymphocytes in sporadic mismatch repair deficient versus proficient colorectal cancers: a potential role for dysregulation of the transforming growth factor-beta pathway. *Eur J Cancer* 2007;43:624–31.
  20. Lugli A, Karamitopoulou E, Panayiotides I, Karakitsos P, Rallis G, Peros G, et al. CD8<sup>+</sup> lymphocytes/tumour-budding index: an independent prognostic factor representing a 'pro-/anti-tumour' approach to tumour host interaction in colorectal cancer. *Br J Cancer* 2009;101:1382–92.
  21. Trutmann M, Terracciano L, Noppen C, Kloth J, Kaspar M, Peterli R, et al. GM-CSF gene expression and protein production in human colorectal cancer cell lines and clinical tumor specimens. *Int J Cancer* 1998;77:378–85.
  22. Ruiz C, Holz DR, Oeggerli M, Schneider S, Gonzales IM, Kiefer JM, et al. Amplification and overexpression of vinculin are associated with increased tumour cell proliferation and progression in advanced prostate cancer. *J Pathol* 2011;223:543–52.
  23. Le Gouvello S, Bastuji-Garin S, Aloulou N, Mansour H, Chaumette MT, Berrehar F, et al. High prevalence of Foxp3 and IL17 in MMR-proficient colorectal carcinomas. *Gut* 2008;57:772–9.
  24. Ancuta P, Rao R, Moses A, Mehle A, Shaw SK, Luscinskas FW, et al. Fractalkine preferentially mediates arrest and migration of CD16<sup>+</sup> monocytes. *J Exp Med* 2003;197:1701–7.
  25. Ohta M, Tanaka F, Yamaguchi H, Sadanaga N, Inoue H, Mori M. The high expression of Fractalkine results in a better prognosis for colorectal cancer patients. *Int J Oncol* 2005;26:41–7.
  26. Dougan M, Dranoff G. Immune therapy for cancer. *Annu Rev Immunol* 2009;27:83–117.
  27. Dranoff G. GM-CSF-based cancer vaccines. *Immunol Rev* 2002;188:147–54.
  28. Figdor CG, de Vries IJ, Lesterhuis WJ, Melief CJ. Dendritic cell immunotherapy: mapping the way. *Nat Med* 2004;10:475–80.
  29. Gabrilovich DI, Nagaraj S. Myeloid-derived suppressor cells as regulators of the immune system. *Nat Rev Immunol* 2009;9:162–74.
  30. Sica A, Bronte V. Altered macrophage differentiation and immune dysfunction in tumor development. *J Clin Invest* 2007;117:1155–66.
  31. Filipazzi P, Valenti R, Huber V, Pilla L, Canese P, Iero M, et al. Identification of a new subset of myeloid suppressor cells in peripheral blood of melanoma patients with modulation by a granulocyte-macrophage colony-stimulation factor-based antitumor vaccine. *J Clin Oncol* 2007;25:2546–53.
  32. Young MR, Wright MA, Lozano Y, Prechel MM, Benefield J, Leonetti JP, et al. Increased recurrence and metastasis in patients whose primary head and neck squamous cell carcinomas secreted granulocyte-macrophage colony-stimulating factor and contained CD34<sup>+</sup> natural suppressor cells. *Int J Cancer* 1997;74:69–74.
  33. Steeg PS, Theodorescu D. Metastasis: a therapeutic target for cancer. *Nat Clin Pract Oncol* 2008;5:206–19.
  34. Uemura Y, Kobayashi M, Nakata H, Kubota T, Bandobashi K, Saito T, et al. Effects of GM-CSF and M-CSF on tumor progression of lung cancer: roles of MEK1/ERK and AKT/PKB pathways. *Int J Mol Med* 2006;18:365–73.
  35. Lahm H, Wyniger J, Hertig S, Yilmaz A, Fischer JR, Givel JC, et al. Secretion of bioactive granulocyte-macrophage colony-stimulating factor by human colorectal carcinoma cells. *Cancer Res* 1994;54:3700–2.
  36. Bretscher V, Andreutti D, Neuville P, Martin M, Martin F, Lefebvre O, et al. GM-CSF expression by tumor cells correlates with aggressivity and with stroma reaction formation. *J Submicrosc Cytol Pathol* 2000;32:525–33.
  37. Rigo A, Gottardi M, Zamo A, Mauri P, Bonifacio M, Krampera M, et al. Macrophages may promote cancer growth via a GM-CSF/HB-EGF paracrine loop that is enhanced by CXCL12. *Mol Cancer* 2010;9:273.
  38. Urdinguio RG, Fernandez AF, Moncada-Pazos A, Huidobro C, Rodriguez RM, Ferrero C, et al. Immune-dependent and independent antitumor activity of GM-CSF aberrantly expressed by mouse and human colorectal tumors. *Cancer Res* 2013;73:395–405.
  39. Lucas AD, Chadwick N, Warren BF, Jewell DP, Gordon S, Powrie F, et al. The transmembrane form of the CX3CL1 chemokine fractalkine is expressed predominantly by epithelial cells *in vivo*. *Am J Pathol* 2001;158:855–66.
  40. Qian BZ, Pollard JW. Macrophage diversity enhances tumor progression and metastasis. *Cell* 2010;141:39–51.
  41. Goldstein JI, Kominsky DJ, Jacobson N, Bowers B, Regalia K, Austin GL, et al. Defective leukocyte GM-CSF receptor (CD116) expression and function in inflammatory bowel disease. *Gastroenterology* 2011;141:208–16.
  42. Dranoff G, Jaffee E, Lazenby A, Golumbek P, Levitsky H, Brose K, et al. Vaccination with irradiated tumor cells engineered to secrete murine granulocyte-macrophage colony-stimulating factor stimulates potent, specific, and long-lasting anti-tumor immunity. *Proc Natl Acad Sci U S A* 1993;90:3539–43.
  43. Chiodoni C, Paglia P, Stoppacciaro A, Rodolfo M, Parenza M, Colombo MP. Dendritic cells infiltrating tumors cotransduced with granulocyte/macrophage colony-stimulating factor (GM-CSF) and CD40 ligand genes take up and present endogenous tumor-associated antigens, and prime naive mice for a cytotoxic T lymphocyte response. *J Exp Med* 1999;190:125–33.
  44. Parmiani G, Castelli C, Pilla L, Santinami M, Colombo MP, Rivoltini L. Opposite immune functions of GM-CSF administered as vaccine adjuvant in cancer patients. *Ann Oncol* 2007;18:226–32.
  45. Mlecnik B, Tosolini M, Charoentong P, Kirilovsky A, Bindea G, Berger A, et al. Biomolecular network reconstruction identifies T-cell homing factors associated with survival in colorectal cancer. *Gastroenterology* 2010;138:1429–40.
  46. Ladoire S, Martin F, Ghiringhelli F. Prognostic role of FOXP3<sup>+</sup> regulatory T cells infiltrating human carcinomas: the paradox of colorectal cancer. *Cancer Immunol Immunother* 2011;60:909–18.
  47. Greene FL, Sobin LH. The staging of cancer: a retrospective and prospective appraisal. *CA Cancer J Clin* 2008;58:180–90.
  48. Poston GJ, Figueras J, Giulianti F, Nuzzo G, Sobrero AF, Gigot JF, et al. Urgent need for a new staging system in advanced colorectal cancer. *J Clin Oncol* 2008;26:4828–33.
  49. Fridman WH, Pages F, Sautes-Fridman C, Galon J. The immune contexture in human tumours: impact on clinical outcome. *Nat Rev Cancer* 2012;12:298–306.

# Clinical Cancer Research

## GM-CSF Production by Tumor Cells Is Associated with Improved Survival in Colorectal Cancer

Christian A. Nebiker, Junyi Han, Serenella Eppenberger-Castori, et al.

*Clin Cancer Res* 2014;20:3094-3106. Published OnlineFirst April 15, 2014.

**Updated version** Access the most recent version of this article at:  
doi:[10.1158/1078-0432.CCR-13-2774](https://doi.org/10.1158/1078-0432.CCR-13-2774)

**Supplementary Material** Access the most recent supplemental material at:  
<http://clincancerres.aacrjournals.org/content/suppl/2014/04/15/1078-0432.CCR-13-2774.DC1.html>

**Cited articles** This article cites 49 articles, 14 of which you can access for free at:  
<http://clincancerres.aacrjournals.org/content/20/12/3094.full.html#ref-list-1>

**Citing articles** This article has been cited by 1 HighWire-hosted articles. Access the articles at:  
<http://clincancerres.aacrjournals.org/content/20/12/3094.full.html#related-urls>

**E-mail alerts** [Sign up to receive free email-alerts](#) related to this article or journal.

**Reprints and Subscriptions** To order reprints of this article or to subscribe to the journal, contact the AACR Publications Department at [pubs@aacr.org](mailto:pubs@aacr.org).

**Permissions** To request permission to re-use all or part of this article, contact the AACR Publications Department at [permissions@aacr.org](mailto:permissions@aacr.org).





## Bioreactor-engineered cancer tissue-like structures mimic phenotypes, gene expression profiles and drug resistance patterns observed “in vivo”



Christian Hirt<sup>a, b, 1</sup>, Adam Papadimitropoulos<sup>a, b, 1</sup>, Manuele G. Muraro<sup>a, b</sup>,  
Valentina Mele<sup>a, b</sup>, Evangelos Panopoulos<sup>a, b</sup>, Eleonora Cremonesi<sup>a, b</sup>, Robert Ivanek<sup>b</sup>,  
Elke Schultz-Thater<sup>a, b</sup>, Raoul A. Droeser<sup>a</sup>, Chantal Mengus<sup>a, b</sup>, Michael Heberer<sup>a, b</sup>,  
Daniel Oertli<sup>a</sup>, Giandomenica Iezzi<sup>a, b</sup>, Paul Zajac<sup>a, b</sup>, Serenella Eppenberger-Castori<sup>c</sup>,  
Luigi Tornillo<sup>c</sup>, Luigi Terracciano<sup>c</sup>, Ivan Martin<sup>a, b, \*</sup>, Giulio C. Spagnoli<sup>a, b, \*</sup>

<sup>a</sup> Department of Surgery, University Hospital Basel, Switzerland

<sup>b</sup> Department of Biomedicine, University of Basel, Switzerland

<sup>c</sup> Institute of Pathology, University of Basel, Switzerland

### ARTICLE INFO

#### Article history:

Received 18 February 2015

Received in revised form

8 May 2015

Accepted 18 May 2015

Available online 20 May 2015

#### Keywords:

Bioreactors

Tri-dimensional cultures

Tumor tissue-like structures

Colorectal cancer

Drug resistance

### ABSTRACT

Anticancer compound screening on 2D cell cultures poorly predicts “in vivo” performance, while conventional 3D culture systems are usually characterized by limited cell proliferation, failing to produce tissue-like-structures (TLS) suitable for drug testing. We addressed engineering of TLS by culturing cancer cells in porous scaffolds under perfusion flow. Colorectal cancer (CRC) HT-29 cells were cultured in 2D, on collagen sponges in static conditions or in perfused bioreactors, or injected subcutaneously in immunodeficient mice. Perfused 3D (p3D) cultures resulted in significantly higher ( $p < 0.0001$ ) cell proliferation than static 3D (s3D) cultures and yielded more homogeneous TLS, with morphology and phenotypes similar to xenografts. Transcriptome analysis revealed a high correlation between xenografts and p3D cultures, particularly for gene clusters regulating apoptotic processes and response to hypoxia. Treatment with 5-Fluorouracil (5-FU), a frequently used but often clinically ineffective chemotherapy drug, induced apoptosis, down-regulation of anti-apoptotic genes (*BCL-2*, *TRAF1*, and *c-FLIP*) and decreased cell numbers in 2D, but only “nucleolar stress” in p3D and xenografts. Conversely, BCL-2 inhibitor ABT-199 induced cytotoxic effects in p3D but not in 2D cultures. Our findings advocate the importance of perfusion flow in 3D cultures of tumor cells to efficiently mimic functional features observed “in vivo” and to test anticancer compounds.

© 2015 Elsevier Ltd. All rights reserved.

### 1. Introduction

Established cell lines play a central role in tumor cell biology investigations and in the development of novel anticancer treatments [1,2]. Their availability in large quantities and their relatively stable phenotypes, transcriptomes and functional characteristics represent obvious advantages. Screening of novel antitumor compounds is currently based on the assessment of their ability to

inhibit proliferation or to induce cytotoxicity in human cancer cell lines cultured in high-throughput formats. Frequently however, “in vitro” behavior of established cell lines poorly mirrors “in vivo” cancer cell features [3].

Based on this background, a variety of innovative “in vitro” technologies are currently being developed to provide the scientific community with advanced models potentially overcoming limitations of current assays and eventually improving their predictive performance [4,5]. A series of studies have underlined that culture in bi-dimensional (2D) or tri-dimensional (3D) systems differentially affects sensitivity of cancer cells to compounds used in cancer treatment [6–9] or to immune effector cells specific for human tumor associated antigens [10]. These findings have been related to a variety of mechanisms, including differential drug penetration

\* Corresponding authors. Department of Surgery, Basel University Hospital, ICFS, Hebelstrasse 20, 4031, Basel, Switzerland.

E-mail addresses: [ivan.martin@usb.ch](mailto:ivan.martin@usb.ch) (I. Martin), [giulio.spagnoli@usb.ch](mailto:giulio.spagnoli@usb.ch) (G.C. Spagnoli).

<sup>1</sup> Christian Hirt and Adam Papadimitropoulos contributed equally to this article.

and cell proliferation in different cell layers and modulation of defined signaling pathways, in 2D cultures and in 3D tumor-like structures.

3D cancer cell culture technologies have been suggested to mimic, at least in part, “in vivo” tumor microenvironmental conditions such as cell-to-cell contact and cell-extracellular matrix (ECM) interactions, or generation of hypoxic-necrotic areas, potentially playing a role in tumor metabolism and progression and in metastasis formation [11,12]. Alternative models, based on seeding and culture of tumor cells within porous 3D scaffolds composed of different materials with potentially tunable architectural complexity, have also been described [13,14].

Notably however, although 3D cultures may share morphological and biochemical features of “in vivo” growing tumors, they are usually characterized by poor cell proliferation and display only scattered areas of clustered tumor cells, with limited resemblance to xenografts and human malignant tissues [13,14], possibly due to mass transport limitations associated with tissue growth [15].

The use of bioreactor devices has been proposed to provide a dynamic culture environment promoting tissue viability, maturation and availability of bioactive factors, thereby supporting the generation of uniform tissue-like structures (TLS) [16]. In the context of tumor cell cultures, most bioreactor-based approaches have introduced agitation techniques and microfluidic platforms [17–19], generating hydrodynamic conditions in the form of convectional fluid flow around cells and tissues. However, resulting superficial flows in those systems are of limited effectiveness to address internal transport limitations [20], which in turn critically affect cell behavior and function as well as drug penetration [21].

Bioreactor devices applying direct perfusion were shown to provide uniform cell distribution [22], allowing the development and maintenance of uniformly viable large tissues for prolonged culture times [22,23]. Perfusion flow velocities may be regulated to control flow-induced shear stress and local oxygen distributions within 3D constructs [24]. Such systems have been utilized in a variety of applications for tissue engineering [23,25], but their potential for tumor tissue formation “in vitro” has not been explored so far.

Colorectal cancer (CRC) is the third most common malignancy worldwide both in women and men [26]. Despite major progress in the understanding of its molecular pathogenesis and the development of new therapies over the last decade, cure rates remain low [27]. In this study, we comparatively analyzed morphology, cell phenotype, proliferation rates, gene expression profiles and sensitivity to drug treatment in CRC cells growing in 2D cell cultures, in tumor TLS generated in perfusion-based bioreactors and in xenografts in immunodeficient mice. We here report that culture of CRC cells in perfused 3D (p3D) cultures results in the formation of tumor TLS characterized by high similarities with “in vivo” xenografts generated in immunodeficient mice.

## 2. Materials and methods

### 2.1. Cell lines and scaffolds

HT-29, SW480 and DLD-1 CRC cell lines and PC-3 (prostate cancer), A549 (non-small cell lung cancer) and BT474 (breast-cancer) cell lines were obtained from the American Type Culture Collection (ATCC) and authenticated by short tandem repeat (STR) DNA profiling. Cells were passaged for less than 6 months after resuscitation. HT-29 cells were maintained in McCoy's 5A medium (Sigma–Aldrich) containing 10% heat-inactivated fetal calf serum, GlutaMAX-I, and Kanamycin sulphate (all from Gibco, Life Technologies). All other cancer cell lines were cultured in RPMI-1640

(Sigma–Aldrich) containing 10% heat-inactivated fetal calf serum, 0.1% 2-β-Mercaptoethanol (Sigma–Aldrich), GlutaMAX-I, MEM non-essential aminoacids (NEAA), Sodium Pyruvate, HEPES buffer and Kanamycin sulphate. Collagen scaffolds (Ultrafoam, Avitene) obtained from Davol, were cut with 6–8 mm biopsy punches prior to cultures. A non-woven polyethylene (PET, 185 g/m<sup>2</sup>) scaffold mesh was obtained from Norafin Industries and silk scaffolds were a gift from Dr. Sourabh Ghosh, Indian Institute of Technology, Delhi, India [28]. Prior to use, PET and silk scaffolds were autoclaved and cut by a biopsy punch.

### 2.2. Cell culture in 2D, and in static and perfused 3D conditions

For standard 2D cell cultures we used 75 cm<sup>2</sup> culture flasks or 8-well-tissue chamber slides (Becton Dickinson) and 5 × 10<sup>5</sup>–10<sup>6</sup>/mL cell concentrations. For static 3D (s3D) cell cultures, 6-well-plates (Becton Dickinson) were coated with 1 mL of 1.5% Agar in DMEM (Sigma–Aldrich) at least one day before use and kept at 4 °C. Static seeding was achieved by resuspending 10<sup>6</sup> cells in 40 μL of medium and letting them attach to scaffolds for 1 h at 37 °C. Culture medium (5 mL) was then added. For perfused 3D (p3D) cultures, we used a commercially available (Cellego Biotek AG) perfusion bioreactor system [29]. Cells (10<sup>6</sup>) were seeded and perfused overnight at a superficial velocity of 400 μm/s. After a 24 h cell seeding phase, superficial velocity was reduced to 100 μm/s.

Cell seeding efficiency on different scaffolds was determined by analyzing DNA content in constructs harvested after overnight culture. Briefly, samples were digested with proteinase K solution (Sigma–Aldrich) for 16 h at 56 °C, as previously described [29], and DNA quantity was evaluated by CyQUANT Cell Proliferation Assay (Invitrogen) according to manufacturer's protocols. Fluorescence was measured by a Spectra-Max Gemini XS Microplate Spectrofluorometer (Molecular Devices), at 485 nm excitation and 538 nm emission wavelengths. Seeding efficiencies were calculated as percentages of the original cell input detectable in cultured constructs.

Cell proliferation was determined in constructs harvested at various time points using an MTT assay (Sigma–Aldrich), as previously described [28], and pH levels in culture supernatants were measured by standard methods.

### 2.3. Immunofluorescence, cytofluorimetry and immunohistochemistry

Constructs retrieved following 7 or 14 days cultures were fixed overnight in 1.5% paraformaldehyde at 4 °C and paraffin embedded (TPC15 Medite). Sections (5 μm) were deparaffinized, re-hydrated and stained with hematoxylin and eosin (H&E). Culture chamber slides used for 2D cultures were fixed with paraformaldehyde and directly stained with H&E.

Immunofluorescence analyses were performed following deparaffinization, re-hydration and antigen retrieval at 95 °C for 30 min with ready-to-use S1700 solution (DAKO). Proliferating cells were identified using a Ki67 specific rabbit monoclonal antibody (mAb) (ab27619, AbCAM) and apoptotic cells were identified using a cleaved caspase 3 specific rabbit mAb (cC13, Asp175, rabbit mAb #9664, Cell Signaling) [30]. As secondary reagent, we used an Alexa-Fluor 488 labeled goat-anti-rabbit polyclonal antibody (A-11034, Invitrogen) at a 1:400 final dilution. Nuclei were counterstained with DAPI (Invitrogen). Histological and immunofluorescence sections were analyzed using a BX-61 microscope (Olympus).

Alternatively, for cytofluorimetric analysis, cells were extracted from scaffolds by treatment with TrypLE (Gibco, Life Technologies) for 10 min, followed by incubation in 0.3% collagenase (Worthington) for 30 min at 37 °C, as previously described [31], and

stained with Annexin V FITC/PI according to manufacturer's protocol (Becton Dickinson) or with a Ki67 specific mAb (see above). Cells were analyzed by flow cytometry (FACScalibur, BD).

Standard procedures (ABC-Elite, Vector Laboratories) were used for immunohistochemical analysis of paraffin embedded sections from TLS. Briefly, 5  $\mu\text{m}$  slides were dewaxed and re-hydrated in distilled water. Endogenous peroxidase activity was blocked using 0.5%  $\text{H}_2\text{O}_2$ . Sections were treated with 10% normal goat serum (DakoCytomation) for 20 min and incubated with monoclonal mouse anti-human CDX2 (clone AMT28, 1:50, Abcam) and Cytokeratin 20 (clone Ks20.8, 1:50, DAKO) primary antibody for one hour at room temperature. Subsequently, sections were incubated with peroxidase-labelled secondary antibody (DakoCytomation) for 30 min at room temperature. For antigen visualization, sections were immersed in 3-amino-9-ethylcarbazole plus substrate-chromogen (DakoCytomation) for 30 min, and counterstained with Gill's hematoxylin.

#### 2.4. Quantification of gene expression by quantitative real-time PCR

Total cellular RNA was extracted by using NucleoSpin RNA II kit (Macherey–Nagel) and reverse transcribed, as previously described [32]. Quantitative Real-Time PCR (qRT-PCR) assays were performed in the presence of primers and probes specific for the indicated genes (Assays-on-demand, Applied Biosystems). Normalization of gene expression was performed using GAPDH as reference gene [33].

#### 2.5. RNA-sequencing and analysis

Purity of total cellular RNA was evaluated by a 2100 Bioanalyzer (Agilent Technologies). Non-stranded RNA libraries were prepared by using the Illumina TruSeq sample preparation kit and sequenced on Illumina HiSeq 2000 sequencer (Illumina).

Single-end RNA-seq reads (50-mers) were mapped to the human genome assembly, version hg19, with SpliceMap [34], implemented in Bioconductor's package QuasR. By using RefSeq mRNA coordinates from UCSC ([genome.ucsc.edu](http://genome.ucsc.edu), downloaded in January 2014) and the qCount function, we quantified gene expression as the number of reads that started within any annotated exon of a gene. Nucleotide sequences are deposited in the NCBI at GSE57961.

After quality control, we excluded from analysis a single sample from 2D cultures due to degraded RNA (reads obtained only at the end of transcripts) and poor correlation to other samples. Differentially expressed genes were identified using the edgeR package (version 3.4.2) [35]. Multidimensional scaling was used to visualize the relation between different cultures conditions. Differentially expressed genes, defined as having  $\text{FDR} \leq 0.05$  in any pairwise comparison, were clustered into 13 clusters using PAM algorithm [36]. Individual clusters were tested for enrichment in functional annotations using DAVID and REVIGO bioinformatics resources, as previously described [37,38].

#### 2.6. "In vitro" and "in vivo" drug-sensitivity assays

Chemotherapeutic agents were used at the following concentrations in "in vitro" assays: 5-Fluoruracil (5-FU, Teva Pharma), 1  $\mu\text{g}/\text{ml}$  and 10  $\mu\text{g}/\text{mL}$ ; Oxaliplatin (Sanofi-Aventis), 1  $\mu\text{g}/\text{mL}$  and 10  $\mu\text{g}/\text{mL}$ ; Irinotecan (Pfizer), 10  $\mu\text{g}/\text{mL}$  and 100  $\mu\text{g}/\text{mL}$ ; Sunitinib (LC Laboratories), 0.8  $\mu\text{g}/\text{mL}$  and 8  $\mu\text{g}/\text{mL}$ ; ABT-199 (Active Biochemicals), 2.2  $\mu\text{g}/\text{mL}$ .

"In vitro" tests were performed in standard 2D in 96 or 12 flat bottom wells trays (Falcon) following a one day pre-culture or in 3D perfused bioreactors following a four days pre-culture. In all conditions, a  $10^5$  cells/mL concentration was used. Effects of

chemotherapeutic agents were assessed after 48 or 96 h by DNA content analysis, as described above. Flow cytometric, histological and immunofluorescence studies were performed at the same times.

"In vivo" assays were performed at Oncotest GmbH. Briefly, NMRI-mice were injected with 400'000 HT-29 cells in Matrigel (Becton Dickinson). After reaching a tumor volume of 6  $\text{mm}^3$ , usually after 21 days, a 5-FU bolus (50  $\mu\text{g}/\text{kg}$ ) was administered and animals were sacrificed after 48 or 96 h. Xenografts were explanted and further analyses were performed in Basel, as for the "in vitro" conditions. In each experiment, four mice per time point and condition were used.

#### 2.7. Statistical analysis

Data are presented as mean values  $\pm$  standard deviations (SD). Statistical comparisons between groups were performed by one or two-way analysis of variance (ANOVA) followed by post-hoc Tukey or Bonferroni tests. In all cases, p values  $\leq 0.05$  were considered statistically significant. GraphPad Prism (Software Inc.) and R version 3.0.2 (<http://www.R-project.org>) softwares were used for statistical analysis.

### 3. Results

#### 3.1. Generation of tumor tissue-like structures on 3D scaffolds in perfused bioreactors

To evaluate the possibility to engineer "in vitro" TLS, we seeded cells from established tumor cell lines onto 3D porous scaffolds located within perfused bioreactor chambers (Fig. 1A) [23,31]. In this device, cells suspensions and culture media flow directly through the pores of the 3D scaffolds, resulting in efficient and uniform cell distribution [23], and allowing the subsequent development and maintenance of a uniformly viable tissue for prolonged culture times [22]. Different types of scaffolds were initially tested (Supplementary Fig. S1A). However, PET scaffolds were difficult to process for histological analysis and silk scaffolds underwent substantial structural modifications upon perfusion. Instead, collagen scaffolds were found to be compatible with perfusion, likely because of their natural composition, fiber structure, and simplicity of histological processing and cell retrieval by using commercially available enzymes. Therefore, this material was selected and used for the rest of our study.

Since we are particularly interested in the investigation of colorectal cancer (CRC) cell biology and microenvironmental features [39–41], we addressed in detail the generation of TLS upon 3D culture of cells from established CRC cell lines in p3D. HT-29, DLD-1 and SW480 CRC cell lines could be maintained in culture for over 7 days in the bioreactor system under investigation and developed TLS (Supplementary Fig. S1B). Mismatch repair proficient HT-29 cell line, yielding high-density tissue-constructs upon p3D culture (see below), was selected for additional studies.

The p3D cultures were characterized by a clearly more homogeneous cell seeding as compared to s3D ones, and by a higher cell density, as detectable by whole scaffold MTT uptake after a 7 days culture (Fig. 1B, upper and lower panels, respectively). Growth curves of cells cultured in 2D, s3D or p3D, displayed markedly different patterns (Fig. 1C). Standard monolayers reached a plateau after 3 days, whereas cells in p3D cultures displayed a significantly slower proliferation (Fig. 1C). Remarkably however, the lowest proliferation rate was observed in s3D cultures performed by using the same collagen scaffold as in p3D. In analogy with trends published using a variety of other cell types [25], this is possibly due to mass transport limitations, resulting in decreasing nutrient and



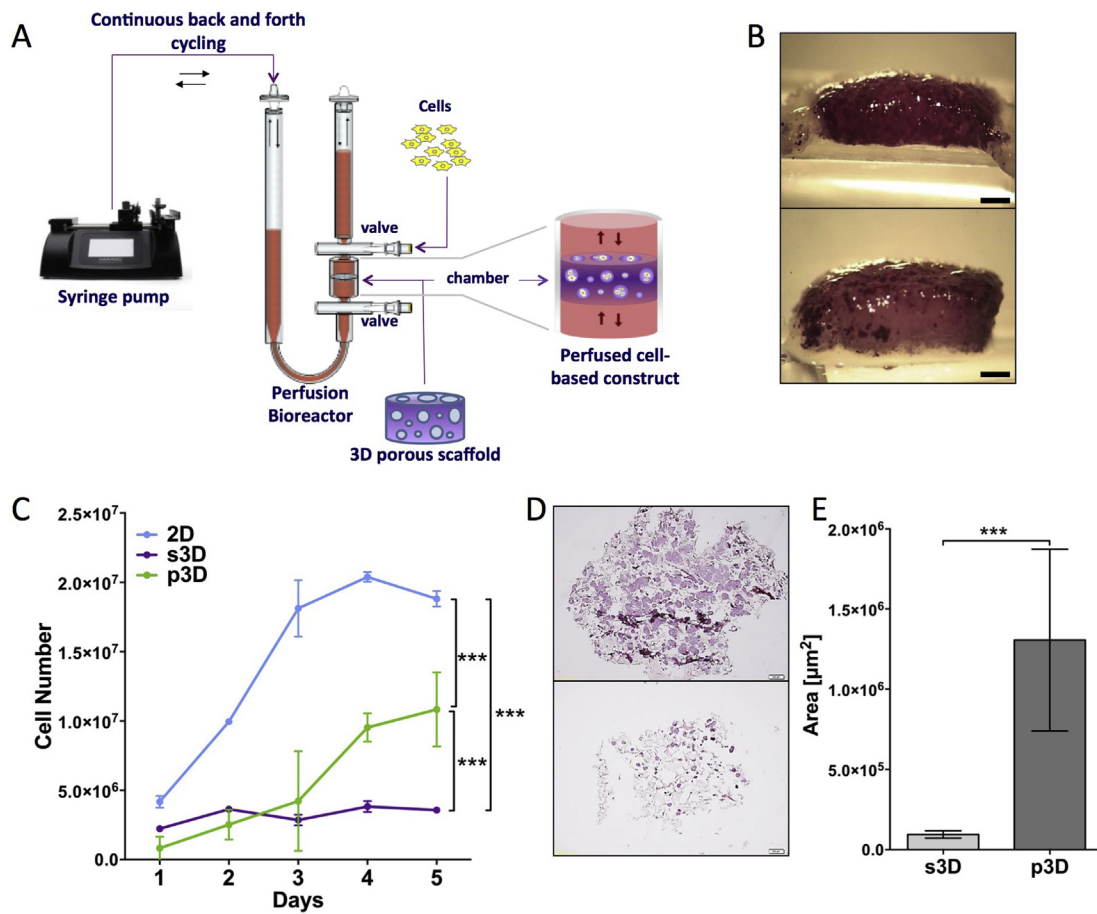


**Fig. 1.** Growth characteristics of perfused and static tridimensional cultures. A: A schematic view of the bioreactor utilized for the culture of tumor cells in perfused tridimensional (p3D) conditions. This device includes a perfusion chamber allocating a 3D porous scaffold. Cell suspensions or culture media may be introduced into the bioreactor through its valves. Fluid flow in alternate directions directly through the scaffold/resulting tissue is generated by using a pump connected with the bioreactor, programmed to deliver defined flow velocities. B: MTT staining of collagen scaffolds seeded with HT-29 cells in p3D (upper panel) or in s3D (lower panel) conditions, following a 7 days culture (scale bar: 1 mm). C: Proliferation kinetics of HT-29 cells under different culture conditions. D: H&E staining of whole scaffold sections from p3D (upper left panel) or s3D (lower left panel) cultures (scale bar: 200 μm). E: Histomorphometric assessment of tumor tissue areas in whole scaffold sections from s3D and p3D cultures of HT-29 cells (right panel) (\*\*\*:  $p < 0.001$ ).

oxygen availability. These growth patterns were mirrored by decreasing pH values over time (Supplementary Fig. S2).

H&E staining showed that perfusion promoted the generation of high density, homogeneous TLS (Fig. 1D, upper panel). In contrast, and consistent with previous studies [13,14], in s3D cultures small tumor areas were only detectable on the outer rims of the scaffolds while inner parts were largely free of tumor cells (Fig. 1D, lower panel). Average cross-sectional areas covered by tumor tissues in p3D cultures were over 10-fold larger than those measured in s3D conditions (Fig. 1E).

To address the broad applicability of p3D tumor cell culture, we tested a variety of cell lines of different histological origin, including PC-3 (prostate cancer), A549 (non-small cell lung cancer) and BT474 (breast cancer), in the bioreactor system under investigation. Different cell lines showed slightly different growth patterns in p3D cultures. For example, whereas HT-29 cells were growing as tumor nodules, DLD-1 cells formed tissue-like structures oriented by the scaffold-fibers. In all cases, however, p3D cultures resulted in the expansion of higher cell numbers, as compared to s3D cultures, and in the generation of larger TLS (Supplementary Fig. S3).

### 3.2. Histological and transcriptional profiles of p3D tumor cultures

Histological characteristics of HT-29 CRC cells cultured in

monolayers and of tissue-like 3D structures generated in p3D or s3D were then evaluated in comparison with xenografts obtained “in vivo” upon subcutaneous (s.c.) injection in immunodeficient mice (Fig. 2A). HT-29 cells cultured in 2D showed homogeneous cell shape and nodular-like growth upon H&E staining. Culture in s3D conditions resulted in the generation of small tissue nodules (Fig. 2A). HT-29 cell culture in p3D conditions promoted the formation of large, anaplastic tumor TLS integrating into the collagen scaffold. Interestingly, HT-29 cells from p3D cultures and xenografts displayed a high grade of mitotic figures and atypical mitoses, as well as signet ring cells and acini-like structures (Supplementary Fig. S4A, B).

Cytokeratin 20 (CK20) was consistently expressed in all culture conditions and in xenografts, whereas CDX2 [42] was undetectable in cells from 2D cultures and expressed to different extents in HT-29 cells from s3D and p3D cultures and xenografts (Fig. 2A).

In agreement with the observed proliferation rates (Fig. 2B), Ki67 positive cells were ubiquitously detectable in monolayer cultures, rare in s3D cultures and detectable to higher extents in both p3D cultures and xenografts (Fig. 2A). Conversely, cCl3 positive, apoptotic HT-29 cells were rare in monolayer cultures, but detectable to significantly higher extents in TLS from s3D than in p3D cultures or xenografts (Fig. 2A, C).

Transcriptional profiles of cells cultured in the different

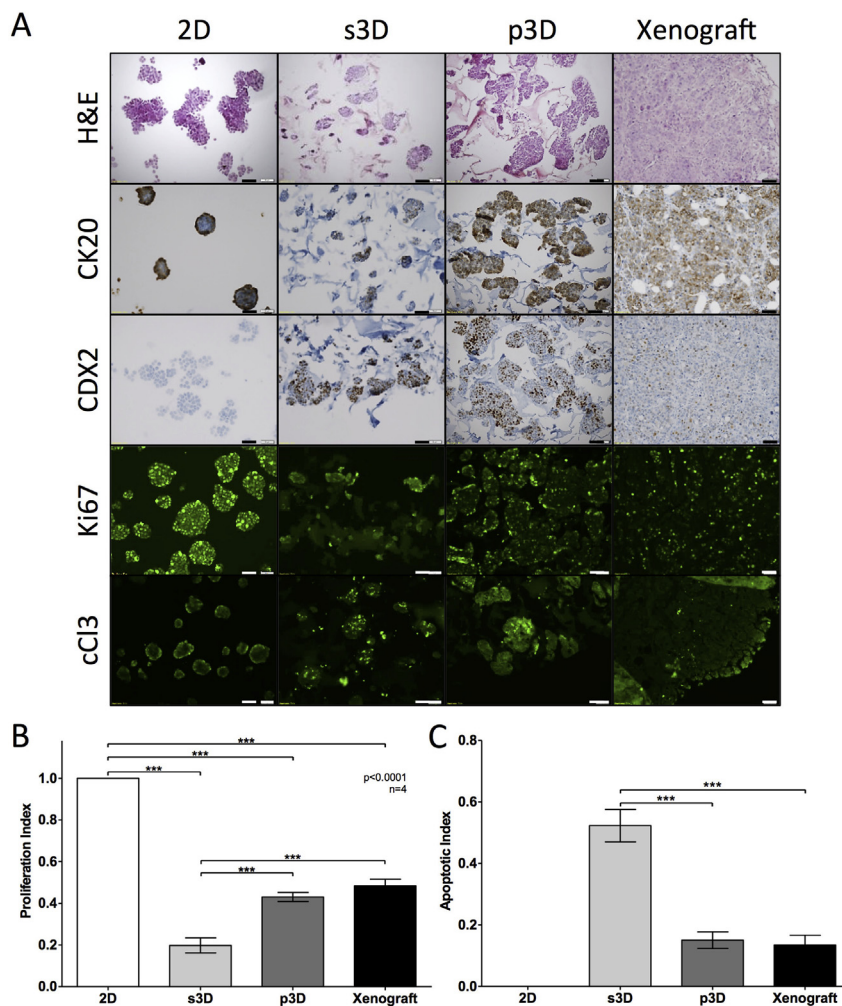


**Fig. 2.** Comparative analysis of phenotype and proliferation potential of HT-29 cells cultured in different conditions. A: HT-29 cells cultured in the indicated conditions or injected subcutaneously in NMRI-mice (xenografts) were stained by H&E or by Cytokeratin 20 (CK20) or CDX2 specific mAbs. Specific binding was visualized by standard immunohistochemical techniques. In parallel experiments, cells were stained by using fluorochrome labeled Ki67 and Cleaved Caspase 3 (cCl3) specific mAbs (scale bar: 50  $\mu$ m). B: Proliferation index was calculated as ratio of Ki67 + cells to total cell number. C: Apoptotic index was calculated as ratio of cCl3+ cells to total cell number. (\*\*\*:  $p < 0.001$ ).

conditions under investigation and growing in xenografts were investigated by RNA sequencing. A comparative analysis revealed high similarities between all “in vitro” cultures and xenografts ( $r > 0.97$ ). However, the expression of defined gene clusters appeared to be differentially regulated in 2D, s3D and p3D cultures and xenografts (Fig. 3). In particular, genes from cluster #2 controlling, among other functions, ribosome biogenesis and translation were highly expressed in 2D cultures. In contrast, genes from cluster #12, associated with cell cycle control and DNA transcription and repair, were expressed to higher extents in 3D cultures and xenografts, as compared to 2D cultures. On the other hand, expression of gene clusters controlling, among other processes, apoptosis and response to hypoxia (i.e., #10 and #4), was more similar to xenografts in p3D than in 2D or s3D cultures. Instead, gene clusters regulating cell adhesion and migration, as well as immune-related processes (i.e., #1 and #11), were expressed to uniquely high extents in xenografts, possibly due to the interaction with murine stromal and innate immune system cellular components “in vivo”.

Taken together, these data clearly indicate that p3D culture of HT-29 CRC cells promotes the formation of relatively large tumor TLS, characterized by proliferation, and apoptotic rates as well as gene expression and phenotypic profiles similar to tumor tissues “in vivo”.

### 3.3. Response of HT-29 p3D culture to chemotherapeutic treatment

We then explored responsiveness to current chemotherapy treatments in p3D cultures and xenografts, using, as control, currently utilized, standard 2D cultures. As s3D cultures failed to induce the generation of TLS of sizes amenable to drug testing and were characterized by negligible cell proliferation and high apoptotic rates, they were not further considered as experimental group.

We treated p3D cultured cells and xenografts with 5-Fluoruracil (5-FU), which is included in standard neo-adjuvant and adjuvant protocols for CRC treatment. For “in vitro” studies, 5-FU was used at a 1  $\mu$ g/mL concentration, whereas for xenograft treatment we chose a 50  $\mu$ g/kg dose, which has been reported to produce plasma levels similar to those used “in vitro” [43].

Following a 48 h treatment, signs of cellular “stress” were detectable to different extents in all cultures and in xenografts (Fig. 4A) [44]. In 2D cultures, nucleoli became prominently visible in all cells, whereas in p3D cultures and xenografts this effect was significantly reduced (Fig. 4B, left panel).

Remarkably, in 2D cultures total cell number was decreased by about 50% following a 48 or 96 h exposure to 5-FU (Fig. 4B, middle panel). In contrast, in p3D cultures and xenografts no significant

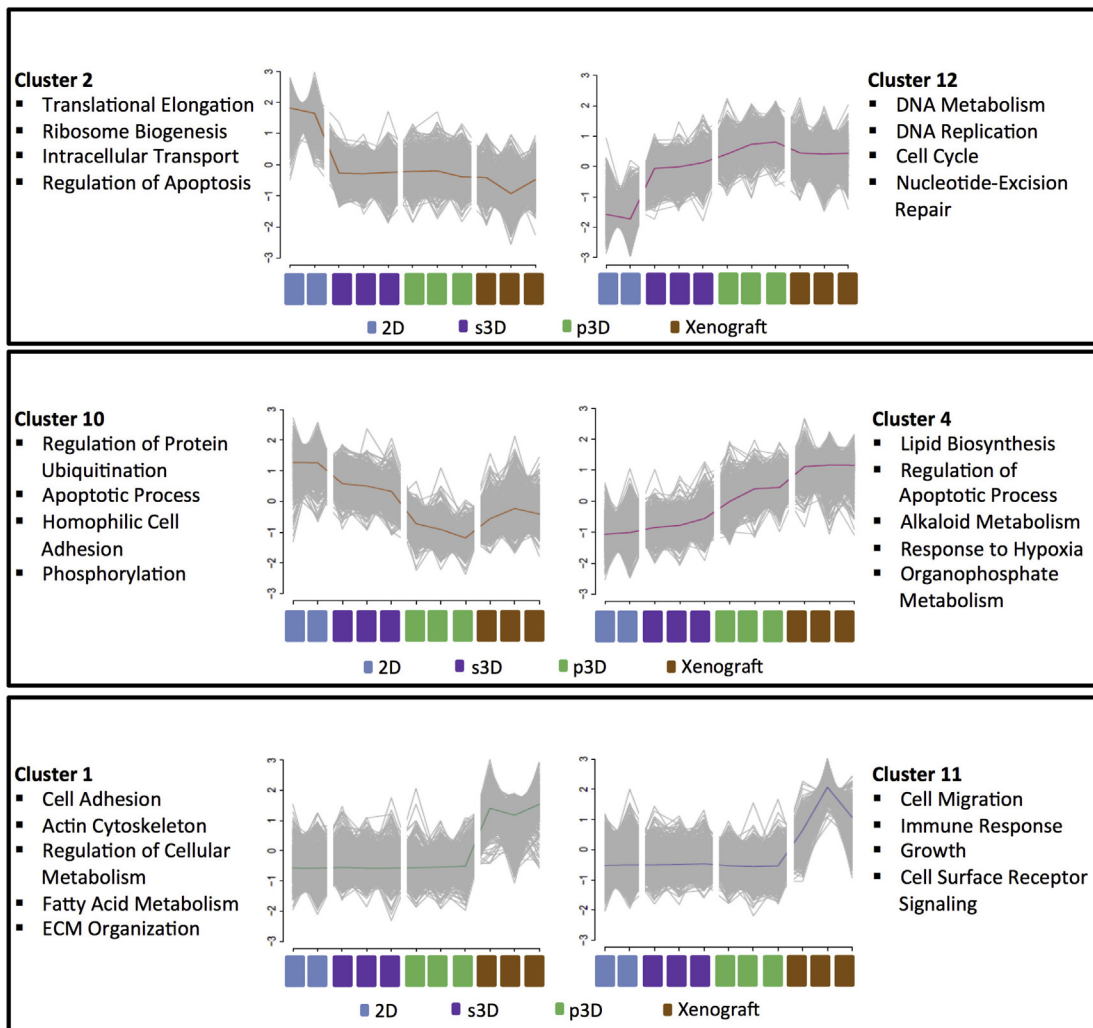


**Fig. 3.** Next generation sequencing transcriptome analysis of HT-29 cells cultured in 2D, s3D and p3D conditions or growing as xenografts. Total cellular RNA was extracted from cells cultured according to the indicated conditions or growing as xenografts. Expression profiles and enriched pathways in selected gene clusters were analyzed based on DAVID Functional Annotation and REVIGO using GO Biological Processes.

reduction of total cell numbers or tumor volumes could be observed (Fig. 4B). Similar trends were also observed by using other drugs commonly utilized in CRC treatment (Supplementary Fig. S5). In agreement with these data, a significant increase in apoptotic cell numbers upon treatment was observed in 2D, but not in p3D cultures or xenografts after 96 h of treatment (Fig. 4B, right panel).

To obtain a more detailed insight into the effects of 5-FU treatment on cells cultured in different conditions and in xenografts, we analyzed by qRT-PCR the expression of a large panel of genes potentially regulating defined tumor environmental features, cell cycle and apoptosis induction. Expression of PD-L1 [45] and CCL22 chemokine genes was similarly increased upon 5-FU treatment in 2D, p3D cultures and in xenografts (Supplementary Fig. S6A, B). In contrast, IL-8 gene expression was exclusively increased in 5-FU treated HT-29 cells cultured in 2D, but not in p3D cultures or xenografts (Supplementary Fig. S6C). Most importantly, the expression of genes associated to anti-apoptotic effects, such as BCL-2, TRAF-1 and c-FLIP, was significantly down regulated upon 5-FU treatment in 2D cultures (Fig. 4C). In contrast, c-FLIP and TRAF-1 gene expression was unaffected in p3D cultures or xenografts. Regarding BCL-2 expression, marginal, non-significant, decreases were observed in p3D cultures and similarly non-significant increases were detected in treated xenografts. Taken together, our

data suggest that responsiveness to 5-FU treatment appears to follow similar patterns in p3D cultures and xenografts.

Based on data emerging from 5-FU treatment of HT-29 cells, we reasoned that inhibition of anti-apoptotic proteins could potentially represent a viable treatment strategy in CRC. Interestingly, a BCL-2 inhibitor (ABT-199) has recently been developed for leukemia treatment [46]. This drug had no effect on HT-29 cells cultured in 2D, whereas a significant reduction in the number of HT-29 cells cultured in p3D was detectable upon 48 h treatment (Fig. 5A). Annexin V-PI staining showed that ABT-199 treatment led to a two-fold (46.6% vs. 22.4%) increase in the percentage of HT-29 cells undergoing apoptosis, as compared to untreated or 5-FU treated cells. Accordingly, H&E staining of ABT-199 treated p3D cultures documented a marked reduction in size of HT-29 tissue-like structures (Fig. 5B).

#### 4. Discussion

In this study we have used a perfused bioreactor system previously utilized for the culture of different mesenchymal cell types [20,31] to address the generation of TLS from established cancer cell lines and to explore their functional characteristics. We observed that p3D culture of established human tumor cell lines resulted in



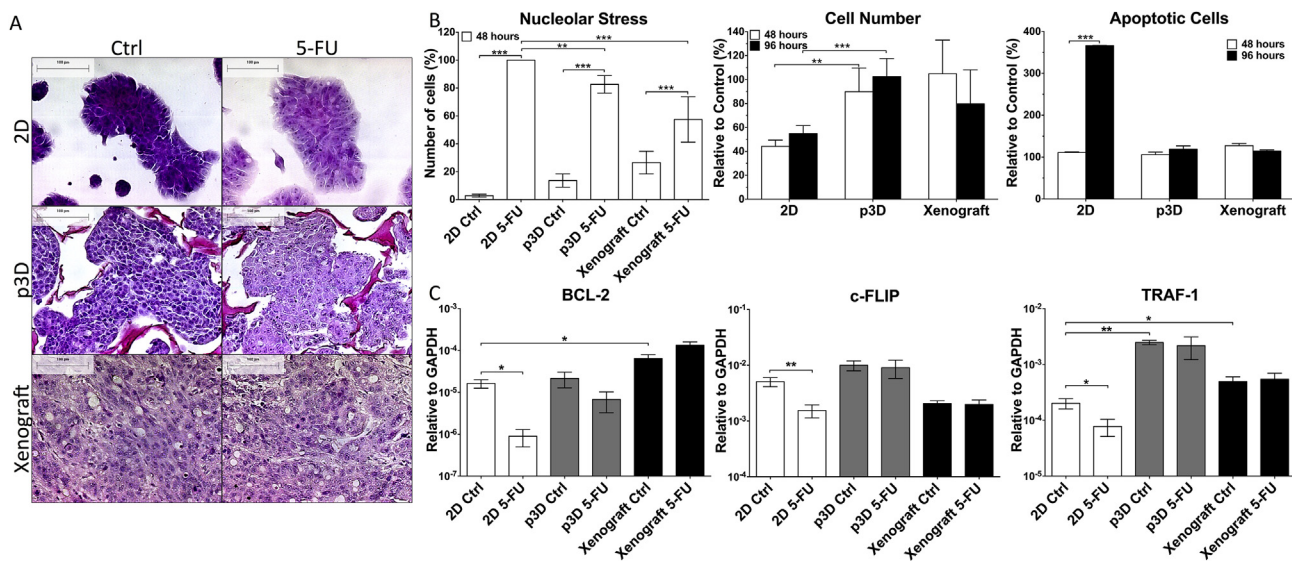


**Fig. 4.** Responsiveness of HT-29 cells cultured in different conditions to 5-FU treatment. A: HT-29 cells were cultured in the indicated conditions or injected subcutaneously in NMRI-mice. Cultures and experimental animals were then treated by 5-FU (1  $\mu\text{g}/\text{mL}$  and 50  $\mu\text{g}/\text{kg}$ , respectively), for 48 h, as detailed in “Materials and methods”. Cells and tissue sections were stained by H&E according to standard methods (scale bar: 100  $\mu\text{m}$ ). B: Percentages of cells showing evidence of nucleolar stress in untreated cultures and animals or following a 48 h 5-FU treatment (left panel). Effects of 48 and 96 h 5-FU treatment on total tumor cell number or tumor volume as assessed by DNA staining, as compared to untreated controls (middle panel). Increases in apoptotic tumor cell percentages upon 5-FU treatment in comparison to untreated controls, as measured by Annexin V-PI staining (right panel). C: Total cellular RNA was also extracted from HT-29 cells cultured according to the indicated conditions or growing as xenografts in NMRI-mice following a 24 h treatment with 5-FU, and reverse transcribed. Expression of BCL-2 (left panel), c-FLIP (middle panel) and TRAF-1 (right panel) genes was measured by qRT-PCR, using GAPDH gene expression as reference. (\*:  $p < 0.05$ ; \*\*:  $p < 0.01$ ; \*\*\*:  $p < 0.001$ ).

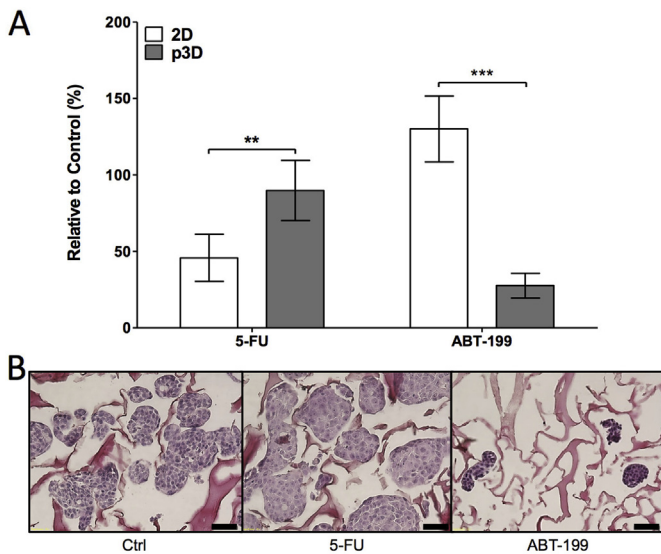


**Fig. 5.** Differential responsiveness to 5-FU and BCL-2 inhibition by HT-29 cells in 2D and p3D cultures. A: Effects of 48 h treatment with 5-FU or ABT-199 on total numbers of HT-29 cells cultured in 2D or in p3D cultures, as measured by DNA dye staining. B: H&E staining of p3D cultures of HT-29 cells untreated (Ctrl) or following treatment with 5-FU or ABT-199. Scale bar: 50  $\mu\text{m}$  (\*\*:  $p < 0.01$ ; \*\*\*:  $p < 0.001$ ).

the rapid generation of TLS characterized by more homogeneous cellular organization and significantly higher cell yields, as compared to s3D cultures. Most importantly, apoptosis, proliferation rates and response to 5-FU in p3D cultures matched those detectable in xenografts of the same cells in immunodeficient mice.

We have studied in detail the HT-29 CRC cell line. Culture of these cells in collagen sponges under perfusion flow resulted in the generation of acini-like formations, reminding histological features of differentiated colorectal mucosa. Interestingly, the formation of

these structures was previously attributed to cellular polarization associated with modifications of culture medium and, possibly, related to glutamine deprivation [47]. CDX2 homeobox gene has been shown to be highly expressed in colonic adenocarcinomas, typically displaying a high intensity specific staining in 90% of cases [42]. In our study, HT-29 cells cultured in 2D did not express CDX2. However, specific staining was readily observed, to different intensities, upon culture in 3D, irrespective of perfusion, or upon injection in immunodeficient animals, thereby further supporting the notion of the high similarity between 3D cultures of established cancer cell lines and xenograft specimens.

These data prompted us to perform a comparative analysis by next generation sequencing of the whole transcriptome of HT-29 cells cultured in different conditions or growing as xenografts. This study indicates that gene expression profiles of cultured or xenografted HT29 cells are highly similar. However, defined gene clusters appeared to be differentially expressed in cells cultured in 2D, s3D, and p3D cultures or xenografts. In particular, it is remarkable that clusters of genes regulating apoptotic process and response to hypoxia appeared to be similarly expressed in p3D cultures and in xenografts. These findings might be related to the maintenance of inner tissue structures in p3D cultures and to their exposure to oxygenation gradients, thereby mimicking the presence of hypovascularized areas in “in vivo” xenografts.

We then addressed the sensitivity to drug treatment of tumor TLS generated in p3D, in comparison with xenografts, and conventional HT-29 monolayers, the current standard. While HT-29 cells in 2D cultures were highly sensitive to 5-FU treatment, p3D cultures and xenografts were similarly characterized by a partial sensitivity, as indicated by cell “stress” signs in the absence of significant cytotoxicity. These effects were accompanied by typical gene signatures. In particular, 5-FU induced BCL-2, c-FLIP and TRAF-1 gene down-regulation in treated HT-29 cell monolayers. However, the expression of these genes was not significantly affected in “stressed” HT-29 cells from treated xenografts or p3D cultures. Our

results underline that the same CRC cell line cultured in p3D and xenografts not only shares similar functional, phenotypic and gene expression profiles, but is also characterized by a similar unresponsiveness to drug treatment.

These data, concurrently underlining the major role potentially played by the expression of anti-apoptotic genes in the resistance to 5-FU treatment, have urged us to investigate the effects of newly developed anti BCL-2 pharmacological treatments. Intriguingly, ABT-199, a promising BCL-2 inhibitor currently being tested in clinical trials for chronic lymphocytic leukemia [46], did not impact on viability of HT-29 cells cultured in monolayers. In sharp contrast, ABT-199 treatment of p3D cultures led to substantial decreases in total cell numbers. Further research is warranted to clarify molecular mechanisms underlying differential sensitivity to BCL-2 inhibition in different culture systems and with additional cell lines. Nevertheless, collectively, these findings indicate that standard 2D assays not only overestimated the antitumor effectiveness of 5-FU, but dramatically underestimated the therapeutic potential of unrelated compounds [48], which was, instead, revealed by p3D cultures.

Thus, p3D cultures may represent “in vitro” models of CRC of potentially high significance in drug screening and to address drug resistance mechanisms or basic tumor biology issues under controlled conditions by taking advantage of human cells. Moreover, the p3D culture system described here may be used to efficiently mimic phenotypic and functional features observed in animal models and clinical specimens. Similar technologies could also be used to generate primary tumor cultures from clinical specimens for personalized treatment assessment.

Our study has several limitations. In particular, molecular mechanisms underlying differential phenotypic, transcriptional and functional profiles detectable in monolayers, s3D and p3D cultures are largely unclear. Furthermore, most obviously, p3D cultures fail to account for the huge complexity of cancer microenvironment and for tumor cell heterogeneity. In order to partially address the latter issues, the p3D culture system could also be extended to include the co-culture of a variety of tumor cells with additional, non-transformed cell types such as mesenchymal stromal cells, tumor-associated fibroblasts or endothelial and immunocompetent cells, in order to explore tumor specific microenvironmental features [4]. On the other hand, the use of tumor TLS generated in p3D, eventually produced in miniaturized systems [18,49], properly adapted for the application of direct perfusion, could help to overcome limitations inherent in the use of human cell lines xenografts for drug screening. This could be especially relevant regarding costs, time requirements and confounding effects of murine stromal and innate immune system cells.

## Acknowledgments

Funding by the Lichtenstein-Stiftung of the University of Basel (CH) DMS2209, the Kommission für Technologie und Innovation (KTI, Bern, Switzerland) (GCS) and the Department of Surgery of the University Hospital Basel is gratefully acknowledged.

## Appendix A. Supplementary data

Supplementary data related to this article can be found at <http://dx.doi.org/10.1016/j.biomaterials.2015.05.037>.

## References

- [1] M.J. Garnett, E.J. Edelman, S.J. Heidorn, et al., Systematic identification of genomic markers of drug sensitivity in cancer cells, *Nature* 483 (2012) 570–575.

- [2] J.L. Wilding, W.F. Bodmer, Cancer cell lines for drug discovery and development, *Cancer Res.* 74 (2014) 2377–2384.
- [3] C.H. Lieu, A.C. Tan, S. Leong, J.R. Diamond, S.G. Eckhardt, From bench to bedside: lessons learned in translating preclinical studies in cancer drug development, *J. Natl. Cancer Inst.* 105 (2013) 1441–1456.
- [4] D.W. Huttmacher, R.E. Horch, D. Loessner, et al., Translating tissue engineering technology platforms into cancer research, *J. Cell. Mol. Med.* 13 (2009) 1417–1427.
- [5] M. Wu, M. Swartz, Modeling tumor microenvironments in vitro, *J. Biomech. Eng.* (2014), BIO 13-1492.
- [6] M.J. Bissell, D. Radisky, Putting tumours in context, *Nat. Rev. Cancer* 1 (2001) 46–54.
- [7] D. Herrmann, J.R. Conway, C. Vennin, et al., Three-dimensional cancer models mimic cell-matrix interactions in the tumour microenvironment, *Carcinogenesis* 35 (2014) 1671–1679.
- [8] R.E. Horch, A.M. Boos, Y. Quan, et al., Cancer research by means of tissue engineering—is there a rationale? *J. Cell. Mol. Med.* 17 (2013) 1197–1206.
- [9] K.M. Yamada, E. Cukierman, Modeling tissue morphogenesis and cancer in 3D, *Cell* 130 (2007) 601–610.
- [10] C. Feder-Mengus, S. Ghosh, A. Reschner, I. Martin, G.C. Spagnoli, New dimensions in tumor immunology: what does 3D culture reveal? *Trends Mol. Med.* 14 (2008) 333–340.
- [11] R.A. Cairns, I.S. Harris, T.W. Mak, Regulation of cancer cell metabolism, *Nat. Rev. Cancer* 11 (2011) 85–95.
- [12] J.A. Joyce, J.W. Pollard, Microenvironmental regulation of metastasis, *Nat. Rev. Cancer* 9 (2009) 239–252.
- [13] C. Fischbach, R. Chen, T. Matsumoto, et al., Engineering tumors with 3D scaffolds, *Nat. Methods* 4 (2007) 855–860.
- [14] E.L. Fong, S.E. Lamhamedi-Cherradi, E. Burdett, et al., Modeling Ewing sarcoma tumors in vitro with 3D scaffolds, *Proc. Natl. Acad. Sci. U. S. A.* 110 (2013) 6500–6505.
- [15] S.E. Lamhamedi-Cherradi, M. Santoro, V. Ramamoorthy, et al., 3D tissue-engineered model of Ewing’s sarcoma, *Adv. Drug Deliv. Rev.* 79–80C (2014) 155–171.
- [16] D.W. Huttmacher, D. Loessner, S. Rizzi, D.L. Kaplan, D.J. Mooney, J.A. Clements, Can tissue engineering concepts advance tumor biology research? *Trends Biotechnol.* 28 (2010) 125–133.
- [17] S. Breslin, L. O’Driscoll, Three-dimensional cell culture: the missing link in drug discovery, *Drug Discov. Today* 18 (2013) 240–249.
- [18] Y. Wen, X. Zhang, S.T. Yang, Microplate-reader compatible perfusion micro-bioreactor array for modular tissue culture and cytotoxicity assays, *Biotechnol. Prog.* 26 (2010) 1135–1144.
- [19] J.J. Winkenwerder, P.L. Palechek, J.S. Reece, et al., Evaluating prostate cancer cell culturing methods: a comparison of cell morphologies and metabolic activity, *Oncol. Rep.* 10 (2003) 783–789.
- [20] V.I. Sikavitsas, G.N. Bancroft, A.G. Mikos, Formation of three-dimensional cell/polymer constructs for bone tissue engineering in a spinner flask and a rotating wall vessel bioreactor, *J. Biomed. Mater. Res.* 62 (2002) 136–148.
- [21] G. Mehta, A.Y. Hsiao, M. Ingram, G.D. Luker, S. Takayama, Opportunities and challenges for use of tumor spheroids as models to test drug delivery and efficacy, *J. Control Release* 164 (2012) 192–204.
- [22] D. Wendt, S. Stroebel, M. Jakob, G.T. John, I. Martin, Uniform tissues engineered by seeding and culturing cells in 3D scaffolds under perfusion at defined oxygen tensions, *Biorheology* 43 (2006) 481–488.
- [23] D. Wendt, A. Marsano, M. Jakob, M. Heberer, I. Martin, Oscillating perfusion of cell suspensions through three-dimensional scaffolds enhances cell seeding efficiency and uniformity, *Biotechnol. Bioeng.* 84 (2003) 205–214.
- [24] M. Cioffi, J. Kuffer, S. Strobel, G. Dubini, I. Martin, D. Wendt, Computational evaluation of oxygen and shear stress distributions in 3D perfusion culture systems: macro-scale and micro-structured models, *J. Biomech.* 41 (2008) 2918–2925.
- [25] I. Martin, D. Wendt, M. Heberer, The role of bioreactors in tissue engineering, *Trends Biotechnol.* 22 (2004) 80–86.
- [26] D.M. Parkin, F. Bray, J. Ferlay, P. Pisani, Global cancer statistics, 2002, *CA Cancer J. Clin.* 55 (2005) 74–108.
- [27] D. Cunningham, W. Atkin, H.J. Lenz, et al., Colorectal cancer, *Lancet* 375 (2010) 1030–1047.
- [28] M. Bhattacharjee, S. Miot, A. Gorecka, et al., Oriented lamellar silk fibrous scaffolds to drive cartilage matrix orientation: towards annulus fibrosus tissue engineering, *Acta Biomater.* 8 (2012) 3313–3325.
- [29] N. Sadr, B.E. Pippenger, A. Scherberich, et al., Enhancing the biological performance of synthetic polymeric materials by decoration with engineered, decellularized extracellular matrix, *Biomaterials* 33 (2012) 5085–5093.
- [30] S. Mazumder, D. Plesca, A. Almasan, Caspase-3 activation is a critical determinant of genotoxic stress-induced apoptosis, *Methods Mol. Biol.* 414 (2008) 13–21.
- [31] A. Braccini, D. Wendt, C. Jaquiere, et al., Three-dimensional perfusion culture of human bone marrow cells and generation of osteoinductive grafts, *Stem Cells* 23 (2005) 1066–1072.
- [32] E. Schultz-Thater, D.M. Frey, D. Margelli, et al., Whole blood assessment of antigen specific cellular immune response by real time quantitative PCR: a versatile monitoring and discovery tool, *J. Transl. Med.* 6 (2008) 58.
- [33] K.J. Livak, T.D. Schmittgen, Analysis of relative gene expression data using real-time quantitative PCR and the 2<sup>-</sup>(Delta Delta C(T)) Method, *Methods* 25

- (2001) 402–408.
- [34] K.F. Au, H. Jiang, L. Lin, Y. Xing, W.H. Wong, Detection of splice junctions from paired-end RNA-seq data by SpliceMap, *Nucleic Acids Res.* 38 (2010) 4570–4578.
- [35] M.D. Robinson, D.J. McCarthy, G.K. Smyth, edgeR: a Bioconductor package for differential expression analysis of digital gene expression data, *Bioinformatics* 26 (2010) 139–140.
- [36] A.P. Reynolds, G. Richards, B. de la Iglesia, V.J. Rayward-Smith, Clustering rules: a comparison of partitioning and hierarchical clustering algorithms, *J. Math. Model. Algorithms* 5 (2006) 475–504.
- [37] dW. Huang, B.T. Sherman, Q. Tan, et al., DAVID Bioinformatics Resources: expanded annotation database and novel algorithms to better extract biology from large gene lists, *Nucleic Acids Res.* 35 (2007) W169–W175.
- [38] F. Supek, M. Bosnjak, N. Skunca, T. Smuc, REVIGO summarizes and visualizes long lists of gene ontology terms, *PLoS One* 6 (2011) e21800.
- [39] R.A. Droeser, C. Hirt, C.T. Viehl, et al., Clinical impact of programmed cell death ligand 1 expression in colorectal cancer, *Eur. J. Cancer* 9 (2013) 2233–2342.
- [40] V. Mele, M.G. Muraro, D. Calabrese, et al., Mesenchymal stromal cells induce epithelial-to-mesenchymal transition in human colorectal cancer cells through the expression of surface-bound TGF-beta, *Int. J. Cancer* 11 (2013) 2583–2594.
- [41] C.A. Nebiker, J. Han, S. Eppenberger-Castori, et al., GM-CSF production by tumor cells Is Associated with Improved Survival in Colorectal Cancer, *Clin. Cancer Res.* 20 (2014) 3094–3106.
- [42] C.A. Moskaluk, H. Zhang, S.M. Powell, L.A. Cerilli, G.M. Hampton, H.F. Frierson Jr., Cdx2 protein expression in normal and malignant human tissues: an immunohistochemical survey using tissue microarrays, *Mod. Pathol.* 16 (2003) 913–919.
- [43] G. Codacci-Pisanelli, C.L. van der Wilt, H.M. Pinedo, et al., Antitumour activity, toxicity and inhibition of thymidylate synthase of prolonged administration of 5-fluorouracil in mice, *Eur. J. Cancer* 31A (1995) 1517–1525.
- [44] S. Boulon, B.J. Westman, S. Hutten, F.M. Boisvert, A.I. Lamond, The nucleolus under stress, *Mol. Cell.* 40 (2010) 216–227.
- [45] P. Zhang, D.M. Su, M. Liang, J. Fu, Chemopreventive agents induce programmed death-1-ligand 1 (PD-L1) surface expression in breast cancer cells and promote PD-L1-mediated T cell apoptosis, *Mol. Immunol.* 45 (2008) 1470–1476.
- [46] A.J. Souers, J.D. Levenson, E.R. Boghaert, et al., ABT-199, a potent and selective BCL-2 inhibitor, achieves antitumor activity while sparing platelets, *Nat. Med.* 19 (2013) 202–208.
- [47] V.M. Weaver, S. Lelievre, J.N. Lakins, et al., Beta4 integrin-dependent formation of polarized three-dimensional architecture confers resistance to apoptosis in normal and malignant mammary epithelium, *Cancer Cell* 2 (2002) 205–216.
- [48] R.M. Phillips, M.C. Bibby, J.A. Double, A critical appraisal of the predictive value of in vitro chemosensitivity assays, *J. Natl. Cancer Inst.* 82 (1990) 1457–1468.
- [49] S.B. Huang, S.S. Wang, C.H. Hsieh, Y.C. Lin, C.S. Lai, M.H. Wu, An integrated microfluidic cell culture system for high-throughput perfusion three-dimensional cell culture-based assays: effect of cell culture model on the results of chemosensitivity assays, *Lab. Chip* 13 (2013) 1133–1143.

## OX40 expression enhances the prognostic significance of CD8 positive lymphocyte infiltration in colorectal cancer

Benjamin Weixler<sup>1</sup>, Eleonora Cremonesi<sup>2</sup>, Roberto Sorge<sup>3</sup>, Manuele Giuseppe Muraro<sup>2</sup>, Tarik Delko<sup>1</sup>, Christian A. Nebiker<sup>1</sup>, Silvio Däster<sup>1</sup>, Valeria Governa<sup>2</sup>, Francesca Amicarella<sup>2</sup>, Savas D. Soysal<sup>1,2</sup>, Christoph Kettelhack<sup>1</sup>, Urs W. von Holzen<sup>1,4</sup>, Serenella Eppenberger-Castori<sup>5</sup>, Giulio C. Spagnoli<sup>2</sup>, Daniel Oertli<sup>1</sup>, Giandomenica Iezzi<sup>2</sup>, Luigi Terracciano<sup>5</sup>, Luigi Tornillo<sup>5</sup>, Giuseppe Sconocchia<sup>6,\*</sup> and Raoul A. Droeser<sup>1,2,\*</sup>

<sup>1</sup> Department of Surgery, University Hospital Basel, Basel, Switzerland

<sup>2</sup> Institute of Surgical Research and Hospital Management (ICFS) and Department of Biomedicine, University Hospital Basel, Basel, Switzerland

<sup>3</sup> Department of Systems Medicine, University of Rome "Tor Vergata", Rome, Italy

<sup>4</sup> IU Health Goshen Center for Cancer Care, Goshen, IN, USA

<sup>5</sup> Institute of Pathology, University Hospital Basel, Basel, Switzerland

<sup>6</sup> Institute of Translational Pharmacology, National Research Council, Rome, Italy

\* These authors have contributed equally to this work

**Correspondence to:** Raoul A. Droeser, **email:** Raoul.Droeser@usb.ch

**Keywords:** OX40, CD8, colorectal cancer, prognosis, microenvironment

**Received:** August 15, 2015

**Accepted:** September 18, 2015

**Published:** September 29, 2015

This is an open-access article distributed under the terms of the Creative Commons Attribution License, which permits unrestricted use, distribution, and reproduction in any medium, provided the original author and source are credited.

### ABSTRACT

**Background:** OX40 is a TNF receptor family member expressed by activated T cells. Its triggering by OX40 ligand promotes lymphocyte survival and memory generation. Anti-OX40 agonistic monoclonal antibodies (mAb) are currently being tested in cancer immunotherapy. We explored the prognostic significance of tumor infiltration by OX40+ cells in a large colorectal cancer (CRC) collective.

**Methods:** OX40 gene expression was analyzed in 50 freshly excised CRC and corresponding healthy mucosa by qRT-PCR. A tissue microarray including 657 clinically annotated CRC specimens was stained with anti-OX40, -CD8 and -FOXP3 mAbs by standard immunohistochemistry. The CRC cohort was randomly split into training and validation sets. Correlations between CRC infiltration by OX40+ cells alone, or in combination with CD8+ or FOXP3+ cells, and clinical-pathological data and overall survival were comparatively evaluated.

**Results:** OX40 gene expression in CRC significantly correlated with FOXP3 and CD8 gene expression. High CRC infiltration by OX40+ cells was significantly associated with favorable prognosis in training and validation sets in univariate, but not multivariate, Cox regression analysis. CRC with OX40<sup>high</sup>/CD8<sup>high</sup> infiltration were characterized by significantly prolonged overall survival, as compared to tumors with OX40<sup>low</sup>/CD8<sup>high</sup>, OX40<sup>high</sup>/CD8<sup>low</sup> or OX40<sup>low</sup>/CD8<sup>low</sup> infiltration in both uni- and multivariate analysis. In contrast, prognostic significance of OX40+ and FOXP3+ cell infiltration was not enhanced by a combined evaluation. Irrespective of TNM stage, CRC with OX40<sup>high</sup>/CD8<sup>high</sup> density infiltrates showed an overall survival similar to that of all stage I CRC included in the study.

**Conclusions:** OX40<sup>high</sup>/CD8<sup>high</sup> density tumor infiltration represents an independent, favorable, prognostic marker in CRC with an overall survival similar to stage I cancers.



## INTRODUCTION

Colorectal cancer (CRC) represents the second most common cause of cancer-related death [1]. Surgical resection remains the mainstay of CRC therapy, and complete removal of the tumor may be achieved in a majority of patients. Radiotherapy, and chemotherapy represent additional standard treatments, currently administered according to histological findings, using the TNM staging system [2].

Histological staging however, fails to account for recurrences observed in patients treated for early stage CRC or for long term survival of patients bearing advanced stage CRC [3]. A variety of reports convincingly indicate that the composition of the tumor microenvironment is critical for CRC progression and that the immune system plays a pivotal prognostic role [4-6].

High densities of infiltrating CD8+ T cells are associated with improved disease-free and overall survival in CRC [4-8] and the analysis of tumor infiltration by immune cells has been suggested to outperform the prognostic significance of TMA staging [5, 6]. Molecular mechanisms underlying the anti-tumor effects of the immune infiltrate are largely unclear [4, 9]. Nevertheless, the expression of activation markers by CRC infiltrating CD8+ T cells has been shown to improve their predictive potential [8]. Unexpectedly, CRC infiltration by FOXP3+ regulatory T cells (Treg) and myeloid cells was also found to be associated with improved prognosis [10-12], at difference with a variety of cancers of different histological origin [13, 14].

OX40 (CD134) is a co-stimulatory, trans-membrane molecule of the tumor necrosis factor-receptor superfamily [15, 16] expressed by activated CD4+ and CD8+ T cells [17-19]. Engagement of OX40 by OX40-ligand expressed by antigen presenting cells (APC) enhances CD4+ and CD8+ cell proliferation, stimulates cytokine production and promotes survival of antigen-specific memory T cells [20-22]. Based on this background, OX40 targeted immunotherapy treatments are being tested in patients with advanced cancers [23, 24].

A previous study, based on the analysis of 72 patients with CRC, suggests that OX40 expression by CRC infiltrating cells correlates with favorable prognosis [25]. This information could be of potentially high clinical relevance since it might contribute to the definition of a constellation of markers allowing a more precise identification of patients with CRC who might benefit from current therapies, while sparing unnecessary treatment to others. Furthermore, patients potentially taking advantage of OX40 targeted immunotherapy might also be characterized.

We used a tumor microarray (TMA) including >600 clinically annotated CRC to address the prognostic significance of CRC infiltration by OX40+ cells, as evaluated in combination with CD8+ and FOXP3+ cell

infiltration.

## RESULTS

### OX40 gene expression in CRC and healthy mucosa

We comparatively addressed OX40 gene expression in CRC tissues and in corresponding healthy mucosa sampled at distance from the tumor ( $n = 49$ ). We found (Figure 1A) that OX40 gene is expressed to similar extents ( $P = 0.3$ ) in cancerous and healthy colon tissues. These results were matched by publicly available data indicating that in five out of seven databases OX40 gene expression did not significantly differ in CRC and healthy tissues [29, 32] (data not shown),

### Expression of OX40 gene and genes associated with favorable clinical course in CRC

Expression of a variety of immune cell markers within CRC tissues has been shown to be associated with defined clinical outcomes [4-6]. Based on this background, we assessed the correlation between OX40 gene expression and that of a panel of genes of known prognostic significance.

In our cohort of CRC tissues ( $n = 49$ ) OX40 gene expression was very strongly (Spearman  $r = 0.8$ ,  $P < 0.0001$ ) associated with FOXP3 [10, 11] gene expression (Figure 1B). Strong associations were also evident between OX40 and IRF1 (Spearman  $r = 0.67$ ,  $P < 0.0001$ ) or TBET (Spearman  $r = 0.57$ ,  $P < 0.0001$ ) genes [5, 6]. Furthermore, OX40 gene expression was also moderately associated with CD8 gene expression (Spearman  $r = 0.33$ ,  $P < 0.02$ ). In contrast, no significant associations were detected between OX40 and CD16, IL17A or IFN- $\gamma$  gene expression [12, 37] (Figure 1B). These data were largely consistent with those emerging from TCGA database (Supplementary Figure 1), although in this cohort ( $n = 380$ ) OX40 gene expression was also significantly associated with CD16 and IFN- $\gamma$  gene expression. Taken together these data urged the evaluation of the prognostic significance of OX40+ infiltrate in CRC.

### TMA analysis

A total of 657 CRC tissues were analyzed. Median age was 71 years (range: 36-96), 54.6% of the patients were female, and 45.4% were male. 65% of the tumors were located in the left hemicolon, and the remaining 35% in the right hemicolon. Median tumor size was 50mm (range: 5-170). Most patients presented T3 lesions (63.3%), and 50.7% were node negative (N0). 85.5%



**Table 1: Clinical-pathological characteristics of the overall CRC patient cohort and their association with levels of OX40+ infiltrate.**

Characteristics	Total N=657*		OX40 <sup>low</sup> N=440*		OX40 <sup>high</sup> N=217*		OX40 <sup>low</sup> vs high
	N or mean	(% or range)	N or mean	(% or range)	N or mean	(% or range)	P**
Age, years (median, mean)	71, 69.9	(36-96)	72, 70.5	(36-96)	70, 68.6	(40-90)	0.02
Tumor size in mm (median, mean)	50, 51.7	(5-170)	45, 51.5	(5-170)	50, 50.2	(7-160)	0.827
Sex							0.539
Female (%)	359	(54.6)	247	(56.1)	112	(51.6)	
Male (%)	298	(45.4)	193	(43.9)	105	(48.4)	
Anatomic site of the tumor							0.037
Left-sided (%)	425	(64.7)	272	(61.8)	153	(70.5)	
Right-sided (%)	228	(34.7)	165	(37.5)	63	(29.0)	
T stage							
T1 (%)	29	(4.4)	11	(2.5)	18	(8.3)	<0.0001
T2 (%)	103	(15.7)	62	(14.1)	41	(18.9)	
T3 (%)	416	(63.3)	284	(64.5)	132	(60.8)	
T4 (%)	91	(13.8)	74	(16.8)	17	(7.8)	
N stage							
N0 (%)	333	(50.7)	203	(46.1)	130	(59.9)	0.002
N1 (%)	174	(26.5)	127	(28.9)	47	(21.7)	
N2 (%)	128	(19.5)	97	(22.0)	31	(14.3)	
Tumor grade							0.739
G1 (%)	15	(2.2)	9	(2.0)	6	(2.8)	
G2 (%)	562	(85.5)	377	(85.7)	185	(85.2)	
G3 (%)	60	(9.1)	42	(9.6)	18	(8.3)	
UICC							
Stage IA (%) T1N0	21	(3.2)	9	(2.0)	12	(5.5)	0.0003
Stage IB (%) T2N0	73	(11.1)	44	(10.0)	29	(13.4)	
Stage IIA (%) T3N0	202	(30.7)	123	(30.0)	79	(36.4)	
Stage IIB-C (%) T4N0	30	(4.6)	25	(5.7)	5	(2.3)	
Stage III (%) N+	296	(45.1)	220	(50.0)	76	(35.0)	
Tumor border configuration							
Infiltrative (%)	418	(63.6)	285	(64.8)	133	(61.3)	0.568
Pushing (%)	218	(33.2)	143	(32.5)	75	(34.6)	
Vascular invasion							
No (%)	462	(70.3)	300	(68.2)	162	(74.7)	0.044
Yes (%)	175	(26.6)	129	(29.3)	46	(21.2)	

Microsatellite Stability							
Proficient (%)	552	(84.0)	362	(82.3)	190	(87.6)	0.104
Deficient (%)	105	(16.0)	78	(17.7)	27	(12.4)	
Rectal cancers (%)	219	(33.3)	131	(29.8)	88	(40.6)	0.013
Rectosigmoid cancers (%)	41	(6.2)	33	(7.5)	8	(3.7)	
Median overall survival time (months)	92	0-152	77	0-152	101	0-150	<0.0001
5-year overall survival % (95%CI)	55.4	51.6 – 59.6	49.9	45.2 – 55.1	66.1	59.9 – 72.9	0.0003

\*Percentages may not add to 100% due to missing values of defined variables.

\*\*Age and tumor size were evaluated using the Mann–Whitney test. Gender, anatomical site, T stage, N stage, grade, vascular invasion, and tumor border configuration were analyzed using the  $\chi^2$  or Fisher exact test depending on the number of observations. Survival analysis was performed using the Kaplan-Meier method and comparatively analyzed with the log-rank test.

were grade 2 tumors and 61.3% showed infiltrative tumor border configuration. Vascular invasion was absent in the majority of cases (70%). TMA included 552 MMR-proficient tumors and 105 MMR-deficient tumors (16%), as defined according to MLH1, MSH2 and MSH6 expression [38]. Median overall survival was of 92 months (0-152) (Table 1). This collective was randomly splitted into two similar training and validation subsets (Table 1s).

### Prognostic significance of CRC infiltration by OX40/CD134 cells

CRC included in the TMA under investigation were infiltrated to different extents by OX40+ cells (Figure 2A). Clinical-pathological characteristics of training and a validation subset did not significantly differ (supplementary Table 1). Cut-off score of OX40+ CRC infiltrating cells for the assessment of their clinical relevance ( $n = 40$ ) was defined by survival ROC curves in the training set (see above). Table 1 shows data related to each clinical-pathological feature, reported as absolute numbers and percentages. Dropouts due to missing information or to loss of punches during TMA staining and preparation represented < 10% of data.

Kaplan-Meier plots indicate that in both training and validation groups high OX40+ infiltration in CRC is significantly associated with favorable prognosis (Figure 2B). However, the good survival impact of high OX40+ infiltrating cells, failed to reach the threshold of statistical significance in multivariate analysis ( $P = 0.8$ ).

### Synergistic prognostic significance of CRC infiltration by OX40+ and CD8+ cells

OX40 is expressed upon activation by FOXP3+ and CD8+ human T cells [17, 39]. CRC infiltration by cells expressing either marker, known to correlate with favorable clinical course [5, 6, 8, 10, 11], was also associated with favorable prognosis in our cohort of patients (data not shown). Importantly, gene expression data support a significant correlation between OX40 and FOXP3 and CD8 gene expression (see above). Therefore, we explored the potentially synergistic prognostic significance of the expression of these markers.

Kaplan-Meier plots revealed that combination of high OX40+ and CD8+ infiltration (Figure 3C) was highly significantly associated with increasingly favorable clinical course, as compared to CRC displaying high CD8+ but low OX40+ cell infiltration or CD8+ low but OX40+ high cell infiltration ( $P = 0.0001$ ). In contrast, prognostic significance of OX40+ cell infiltration in CRC was not significantly improved if data were analyzed in combination with FOXP3+ cell infiltration (Figure 3B). However, poor CRC infiltration by OX40+ and FOXP3+ cells was indeed associated with severe prognosis. These findings were confirmed in the “training” and “validation” subsets (data not shown).

Univariate Cox regression analysis of CRC subgroups identified according to high or low OX40+ and/or CD8+ infiltration (supplementary Table 2), revealed that T and N stage and 5 year overall survival rate were associated with OX40+ and CD8+ density. CRC of pT3-4 or pN1-2 stage did show significantly poorer infiltration by OX40+ and CD8+ cells ( $P = 0.00005$  and  $P = 0.00004$ , respectively). Mean survival time for patients bearing tumors with OX40+ and CD8+ high, OX40+ low and

CD8+ high, OX40+ high and CD8+ low and OX40+ low and CD8+ low infiltrate was 53.8 ( $\pm 16.5$ ), 45.7 ( $\pm 21.4$ ), 43.2 ( $\pm 21.3$ ) and 38.6 ( $\pm 22.5$ ) months, respectively. Five year overall survival rate was 82% (CI: 72-94%) for patients presenting with high OX40+ and CD8+ tumor infiltration, and 48% (CI: 43-54%) for patients bearing tumors with poor OX40+ and CD8+ density ( $P = 0.0001$ ).

Multivariate Hazard Cox regression survival analysis revealed that the combination of high density OX40+ and CD8+ cell infiltration (HR = 0.95; 95%CI

= 93-97;  $P = 0.006$ ) represents an independent positive prognostic factor for overall survival in CRC. Age (HR = 1.03; 95%CI = 1.01-1.04;  $P < 0.00001$ ), gender (HR = .65; 95%CI = .53-.77;  $P = 0.0003$ ), T-stage (HR = 1.94; 95%CI = 1.82-2.05;  $P < 0.00001$ ), N-stage (HR = 1.88; 95%CI = 1.80-1.97;  $P < 0.00001$ ) and microsatellite instability (HR = 1.82; 95%CI = 1.64-2.01;  $P = 0.001$ ) were also independently associated with favorable prognosis in multivariate survival analysis (Table 2).

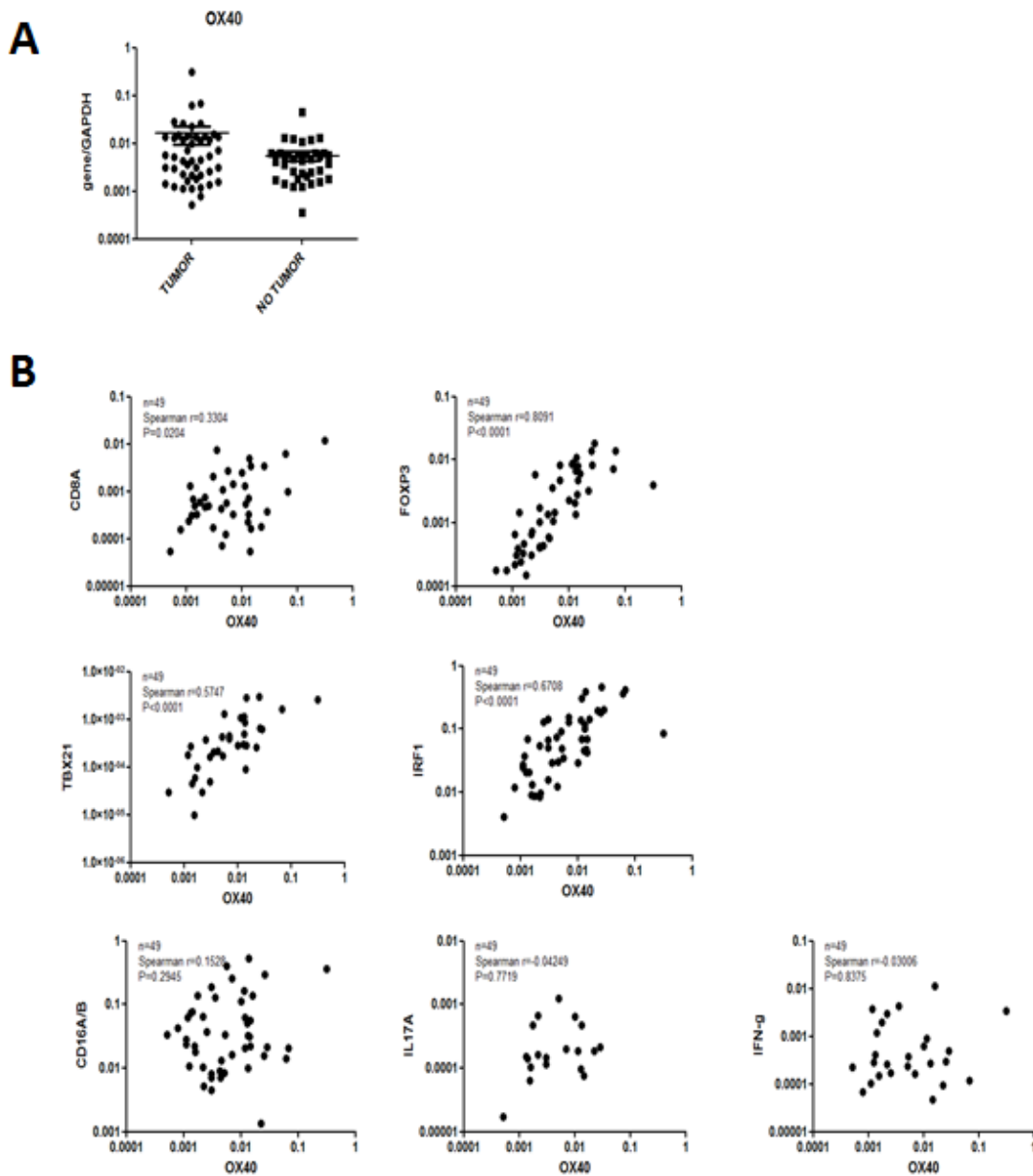


**Figure 1: Gene expression profiles in CRC.** Total cellular RNA was extracted from freshly excised CRC tissues ( $n = 48$ ) and corresponding healthy mucosa sampled at distance from the tumor and reverse transcribed. Specific gene expression was analyzed by qRT-PCR, using, as reference, GAPDH house-keeping gene expression.

**Table 2: Uni and Multivariate Hazard Cox regression survival analysis**

	Univariate			Multivariate		
	HR	95% CI	p-values	HR	95% CI	p-values
OX40 (continuous)	0.99	0.99-0.99	<0.0001	n.i.		
CD8 (continuous)	0.99	0.98-0.99	0.007	n.i.		
FoxP3 (continuous)	0.88	0.81-0.94	0.049	n.i.		
OX40 <sup>high/low</sup>	0.63	0.51-0.75	0.0001	n.i.		
CD8 <sup>high/low</sup>	0.54	0.37-0.70	0.0002	n.i.		
OX40 <sup>high</sup> CD8 <sup>high</sup>	0.93	0.92-0.95	<0.0001	0.95	0.93-0.97	0.006
FoxP3 <sup>high/low</sup>	0.77	0.66-0.88	0.02	0.84	0.72-0.96	0.15
Age	1.02	1.01-1.03	0.0001	1.03	1.02-1.04	<0.00001
Gender (men vs women)	0.67	0.67-0.67	0.0002	0.65	0.53-0.77	0.0003
pT stage	2.25	2.16-2.34	<0.000001	1.94	1.82-2.05	<0.00001
Tumor grade	1.51	1.36-1.67	0.008	1.22	1.03-1.41	0.28
pN stage	2.28	2.21-2.35	<0.000001	1.88	1.80-1.97	<0.00001
Vascular invasion	2.46	2.35-2.58	<0.000001	1.48	1.35-1.62	0.004
Tumor border configuration	2.03	1.90-2.16	<0.000001	1.39	1.24-1.54	0.029
Microsatellite stability (deficient vs. proficient)	1.55	1.38-1.72	0.01	1.82	1.64-2.01	0.001

Uni- and multivariate Cox-regression analyses showing Hazard Ratios and P-values. The multivariate model included 556 patients, due to missing values related to CD8+ and FOXP3+ density, age, sex, tumor size, tumor grade, vascular invasion, tumor border configuration and microsatellite stability. n.i.: not included in the final multivariate model.

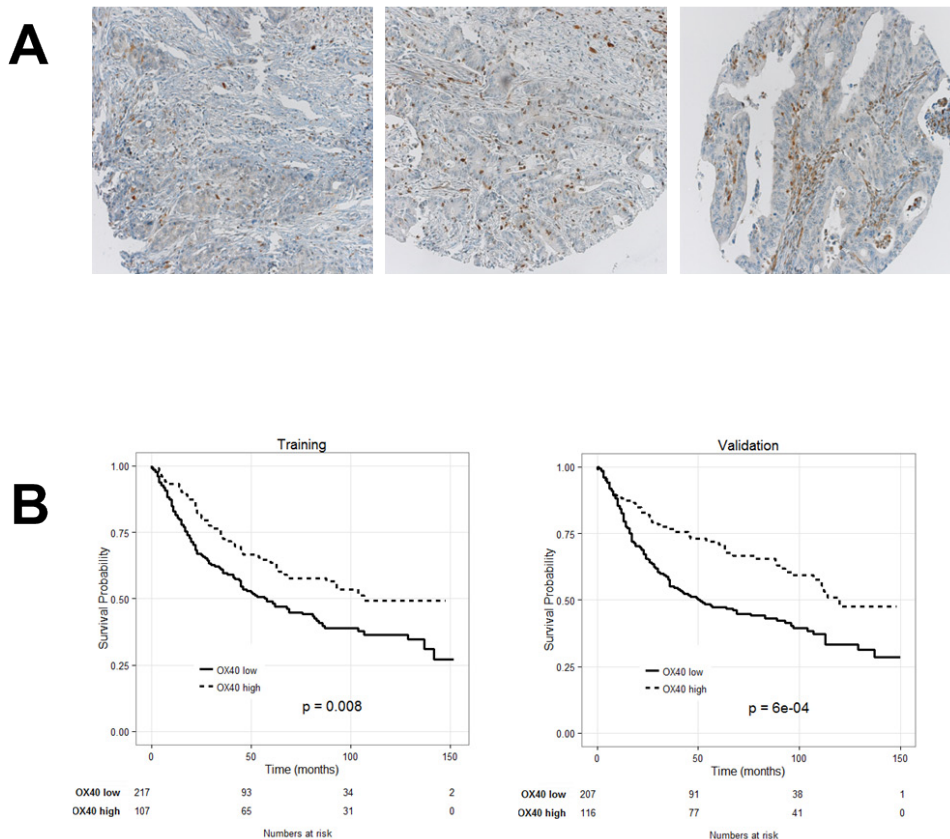


**Figure 2: Prognostic significance of OX40 expression by CRC infiltrating cells.** A. CRC TMA was stained with OX40 specific reagents, as detailed in “materials and methods”. Panel A shows representative punches with different extents of OX40+ cell infiltration (magnification 20X). Kaplan-Meier plots depicting the prognostic significance in randomly generated training and validation cohorts (panel B). Number of events (= deaths) and total number of cases in each cohort are reported.

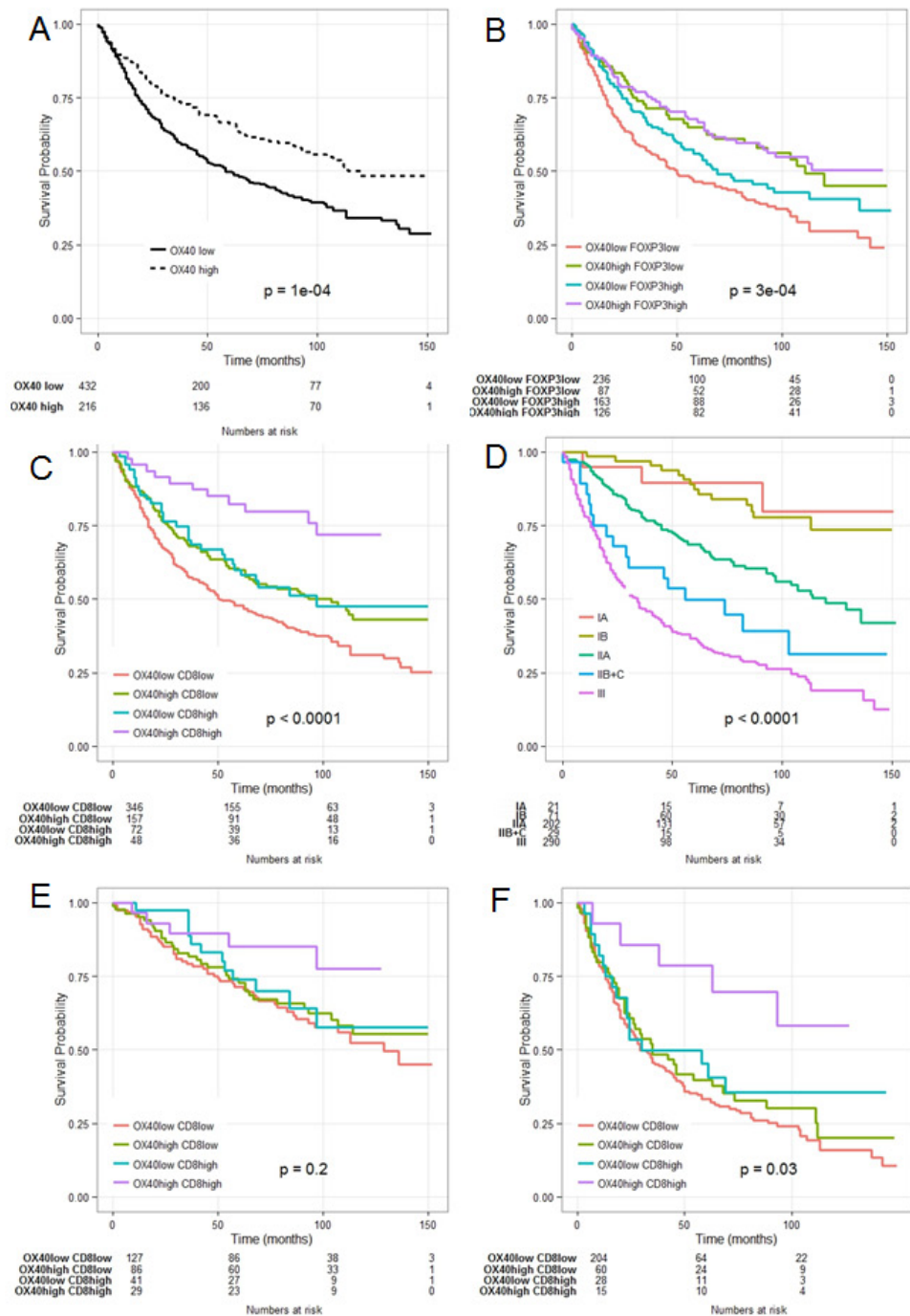


**Figure 3: Combined Kaplan- Meier analysis of OX40+ and CD8+ infiltration results in enhanced prognostic significance in CRC.** OX40+ in the overall collective (panel A.); OX40+ combined with FOXP3+ (panel B.); OX40+ combined with CD8+ cell infiltration (panel C.); comparative evaluation with conventional TNM staging (panel D.); OX40+/CD8+ in low stage CRC(panel E.) and in high grade (panel F.).



## Comparative analysis of the prognostic significance of OX40+ and CD8+ infiltration and AJCC staging

Previous studies suggest that infiltration by immune cells might outperform conventional tumor staging in CRC prognostic assessment (4). Therefore, we comparatively evaluated the prognostic significance of OX40+ and CD8+ infiltration and AJCC staging (Figure 3 panel C, D). Survival probability at five years was 85.2% (C.I. 72.6%-99.9%) for patients with low (IA, IB and IIA) AJCC stage and 78.6% (C.I. 59.8%-100%) for patients with high stage (IIB, IIC and III) (Figure 3, panel E, F). Prognostic impact of OX40/CD8 high density infiltration did not reach significance threshold ( $P = 0.2$ ) for patients with low stages, since the overall survival in this cohort is inherently good and analysis of a larger number of patients would be required. However, of peculiar clinical importance is the significant ( $P = 0.03$ ) favorable prognostic impact of high density OX40+ and CD8+ cell infiltration in high AJCC stage CRC. Thus, irrespective of their AJCC staging, CRC highly infiltrated by OX40+ and CD8+ cells are characterized by a prognosis similar to that of stage I patients CRC (Figure 3, panel C-F).

## DISCUSSION

Experimental models show that signaling through OX40 co-stimulatory molecule promotes the generation of T cell memory thereby significantly enhancing antigen specific re-call responses [22, 40]. Furthermore, administration of agonistic OX40 specific mAbs enhances anti-tumor immune responses “*in vivo*” in different models [41]. Responsiveness to treatment is accompanied by increasing densities of OX40+ CD8+ T cells within the tumor tissue and decreasing FOXP3+ Treg infiltration [24]. Based on this background, similar reagents are currently being tested in clinical immunotherapy trials [23, 42].

Although analysis of CRC immune-contexture is increasingly gaining clinical relevance [4-6], prognostic significance of OX40 expression in CRC infiltrating cells has only been explored in one study evaluating a cohort of 72 patients [25].

Here, we report that in CRC OX40 gene expression is significantly correlated to that of CD8, FOXP3, TBET and IRF1 genes, typically expressed in tumors with favorable prognosis [5, 6].

Indeed, the analysis of >600 clinically annotated CRC specimens indicates that OX40+ cell infiltration is significantly associated with increased overall survival, although this favorable prognostic effect could not be confirmed in multivariate analysis.

Most importantly however, a combined evaluation shows for the first time that CRC infiltration by high

density OX40+ and CD8+ cells is highly significantly associated with favorable clinical course, as also evident upon multivariate analysis. Strikingly, CRC with high OX40+ and CD8+ cell infiltration, irrespective of their TNM stage, are characterized by a prognosis similar to that of low (IA-IB) stage cancers within the whole cohort under investigation.

In contrast, interestingly, no such effects were observed upon combined analysis of both OX40+ and FOXP3+ cell CRC infiltration.

These data do not provide obvious mechanistic insights. However, it has been shown in “*in vivo*” models that effects of OX40 triggering are enhanced in the presence of “danger” signals [22]. Indeed, CRC carcinogenesis is typically characterized by early loss of the barrier function of intestinal mucosa [43]. Thus, a variety of TLR agonists might provide adequate “danger” signals potentially supporting the induction of antitumor effects associated with OX40 stimulation.

Besides activated T lymphocytes, OX40 expression has also been observed in natural killer T cells and neutrophils [17]. However, in our gene expression studies we did not observe a significant correlation between expression of OX40 and expression of CD16 gene, typically detectable in these cell types.

Our study has limitations, including its retrospective nature. However, data emerging from large retrospective analyses may help in the development of targeted prospective studies, currently being planned by our groups. Furthermore, the cohort investigated in this study includes patients bearing CRC surgically treated between 1985 and 1998, e.g. prior to a widespread use of neoadjuvant treatment regimens. Therefore, although our results may not be fully representative of current clinical treatment, they are more likely to faithfully mirror CRC immunobiology, in the absence of chemo-irradiation treatments.

On the other hand, TMA technology may insufficiently represent tumor tissue heterogeneity. However, punches included in the TMA under investigation are derived from the tumor center and do include at least 50% cancer cells. Furthermore, the number of CRC considered (>600) is likely to compensate at least in part for the diversity of immune contexture within different areas of individual biopsies.

Nevertheless, our data indicate that OX40 and CD8 specific staining may outperform TNM staging, thus potentially contributing to clinical decision making in sizeable groups of patients. On the other hand, they underline the critical relevance of OX40 in CRC immunobiology. Further research is warranted to unravel underlying molecular mechanisms.

## MATERIALS AND METHODS

### Gene expression analysis

Total cellular RNA was extracted from surgical specimens of CRC and autologous healthy mucosa (HM) sampled at distance from the tumor and reverse transcribed [26]. Pre-developed Taqman<sup>®</sup> assays (Applied Biosystems) were used to quantitatively evaluate the expression of a panel of cytokine and chemokine genes by using ABI Prism 7300 PCR system (Applied Biosystems). Data are reported as relative expression normalized to GAPDH house-keeping gene amplification. Expression of individual genes was analyzed by using the  $2^{-\Delta\Delta C_T}$  method [27].

### Public databases

Gene expression databases included in Oncomine databank [28] were used to analyze OX40 gene expression in CRC in comparison with normal tissues. Seven databases, including a total of 812 samples, were identified. Skrzypczak [29], Hong [30] and Kaiser [31] databases utilized Human Genome U133 Plus 2.0 technology (Affymetrix), whereas Gaedcke [32] used Agilent platform. Instead, TCGA data were obtained by using next generation sequencing (NGS) technology and Ki [33] data are based on a not pre-defined platform.

### Tissue microarray construction

657 unselected, non-consecutive, clinically annotated, primary CRC specimens were included in the TMA following approval by the Regional Ethical Committee (EKBB, Basel Stadt and Basel Land). Formalin-fixed, paraffin-embedded tissue blocks were prepared according to standard procedures. Tissue cylinders with a diameter of 0.6 mm were punched from morphologically representative areas of each donor block and brought into one recipient paraffin block (30x25mm), using a semi-automated tissue arrayer. Each punch was made from the center of the tumor so that each TMA spot consisted of at least 50% tumor cells.

### Clinical-pathological features

Clinical-pathological data for the patients included in the TMA are listed in Table 1. Briefly, data were collected retrospectively in a non-stratified and non-matched manner. Annotation included patient age, tumor diameter, location, pT/pN stage, grade, histologic subtype, vascular invasion, border configuration, presence of peritumoral lymphocytic inflammation at the invasive

tumor front and disease-specific survival. Tumor border configuration and peritumoral lymphocytic inflammation were evaluated using the original H&E slides of the resection specimens corresponding to each tissue microarray punch [34].

### Immunohistochemistry

Standard indirect immunoperoxidase procedures were used for immunohistochemistry (IHC; ABC-Elite, Vector Laboratories, Burlingame, CA). Slides were dewaxed and rehydrated in distilled water. Endogenous peroxidase activity was blocked using 0.5% H<sub>2</sub>O<sub>2</sub>. Sections were incubated with 10% normal goat serum (DakoCytomation, Carpinteria, CA) for 20 min and incubated with primary antibody at room temperature. Primary antibodies used were specific for OX40 (polyclonal anti-CD134/OX40, ab119904, Abcam, Cambridge, UK), CD8 (clone C8/144B, DakoCytomation, Switzerland) and FOXP3 (clone 236A/E7, Abcam, Cambridge, UK) [7, 10]. Subsequently, sections were incubated with peroxidase-labelled secondary antibody (DakoCytomation) for 30 min at room temperature. To visualize the antigen, sections were immersed in 3-amino-9-ethylcarbazole plus substrate-chromogen (DakoCytomation) for 30 min, and counterstained with Gill's hematoxylin.

### Evaluation of immunohistochemistry

Immunohistochemical readings were performed by trained research fellows [B.W. or R.D.] and data were independently validated by an additional investigator [L.To.]. Tumor infiltrating cells were counted for each punch (approximately one high power [20x] field). Data regarding CRC infiltration by FOXP3+ and CD8+ were available from our previous publications [7, 8, 10].

### Statistical analysis

Data were analyzed using the Statistical Package Software R (Version 3.1.3, www.r-project.org). Following confirmation histogram and the Kolmogorov-Smirnov test, descriptive statistic included mean  $\pm$  standard deviation for parameters with Gaussian distribution or percentage of frequencies for occurrences.

The TMA collective of 657 CRC was randomly split into training and validation subsets with approximately equal numbers of patients ( $n = 329$  and  $n = 328$ , respectively). Associations with survival were explored using the Cox proportional hazards regression model. Cut-off values used to classify CRC with low or high immune cell infiltration were obtained by ROC curves (survival ROC package), evaluating sensitivity and false positive

rate for the discrimination of survivors and non-survivors with respect to the Kaplan-Meier method, on the training subset and validated on the validation subset [35, 36]. The threshold value for OX40+ infiltration, calculated in the training test was 40 cells/TMA-punch. This value was reconfirmed in the validation set. Further specific scores were set at 10 cells/TMA-punch for CD8 and 17 cells/TMA-punch for FOXP3, as previously calculated in larger collectives by our team [8, 10].

Chi-Square, Fisher's Exact, and Kruskal-Wallis tests were used to determine the association of OX40+ and CD8+ infiltration and clinical-pathological features. Univariate survival analysis was performed by the Kaplan-Meier method and log rank test. The assumption of proportional hazards was verified for all markers by analyzing correlation of Schoenfeld residuals and ranks of individual failure times. Any missing clinical-pathological information was assumed to be missing at random. Subsequently, OX40, CD8, and FOXP3 cell infiltration data were entered into multivariate Cox regression analysis and hazard ratios (HR) and 95% confidence intervals (CI) were used to determine prognostic effects on survival time. *P*-values < 0.05 were considered statistically significant.

## SOURCES OF FINANCIAL SUPPORT

GS was supported by the Italian Association for Cancer Research (AIRC), grant 10555 and PRIN, the Ministry of Education, University and Research (PRIN), grant 2010AX2JX7\_005. GI was supported by SNF (CH) grant no. PP00P3-133699. GCS was supported by SNF (CH) grant no. 310030\_149745.

## ACKNOWLEDGEMENTS

All authors have agreed to the submission of this manuscript and have participated in the study to a sufficient extent to be named as authors. The authors have no conflicts of interest to disclose for the present study.

## CONFLICTS OF INTEREST

There is no conflict of interest.

## REFERENCES

1. Ferlay J, Soerjomataram I, Dikshit R, Eser S, Mathers C, Rebelo M, Parkin D M, Forman D D, Bray F. Cancer incidence and mortality worldwide: sources, methods and major patterns in GLOBOCAN 2012. *Int J Cancer* 2014;136:E359-86.
2. Cunningham D, Atkin W, Lenz H-J, Lynch HT, Minsky B, Nordlinger B, Starling N. Colorectal cancer. *Lancet* (London, England) 2010;375:1030-47.
3. Zlobec I, Lugli A. Prognostic and predictive factors in colorectal cancer. *Postgrad Med J* 2008;84:403-11.
4. Fridman WH, Pagès F, Sautès-Fridman C, Galon J. The immune contexture in human tumours: impact on clinical outcome. *Nat Rev Cancer* 2012;12:298-306.
5. Galon J, Costes A, Sanchez-Cabo F, Kirilovsky A, Mlecnik B, Lagorce-Pagès C, Tosolini M, Camus M, Berger A, Wind P, Zinzindohoué F, Bruneval P, Cugnenc PH, et al. Type, density, and location of immune cells within human colorectal tumors predict clinical outcome. *Science* 2006;313:1960-4.
6. Pagès F, Berger A, Camus M, Sanchez-Cabo F, Costes A, Molitor R, Mlecnik B, Kirilovsky A, Nilsson M, Damotte D, Meatchi T, Brunveval P, Cugnenc PH, et al. Effector memory T cells, early metastasis, and survival in colorectal cancer. *N Engl J Med* 2005;353:2654-66.
7. Lugli A, Karamitopoulou E, Panayiotides I, Karakitsos P, Rallis G, Peros G, Iezzi G, Spagnoli G, Bihl M, Terracciano L, Zlobec I. CD8+ lymphocytes/ tumour-budding index: an independent prognostic factor representing a "pro-/anti-tumour" approach to tumour host interaction in colorectal cancer. *Br J Cancer* 2009;101:1382-92.
8. Zlobec I, Karamitopoulou E, Terracciano L, Piscuoglio S, Iezzi G, Muraro MG, Spagnoli G, Baker K, Tzankow A, Lugli A. TIA-1 cytotoxic granule-associated RNA binding protein improves the prognostic performance of CD8 in mismatch repair-proficient colorectal cancer. *PLoS One* 2010;5:e14282.
9. Reissfelder C, Stamova S, Gossmann C, Braun M, Bonertz A, Walliczek U, Grimm M, Rahbari N, Koch M, Saadati M, Benner A, Buechler MW, Jaeger D, et al. Tumor-specific cytotoxic T lymphocyte activity determines colorectal cancer patient prognosis. *J Clin Invest* 2015;125:739-51.
10. Frey DM, Drosner RA, Viehl CT, Zlobec I, Lugli A, Zingg U, Oerli D, Kettelhack C, Terracciano L, Tornillo L. High frequency of tumor-infiltrating FOXP3(+) regulatory T cells predicts improved survival in mismatch repair-proficient colorectal cancer patients. *Int J Cancer* 2010;126:2635-43.
11. Salama P, Phillips M, Grieco F, Morris M, Zeps N, Joseph D, Platell C, Iacopetta B. Tumor-infiltrating FOXP3+ T regulatory cells show strong prognostic significance in colorectal cancer. *J Clin Oncol* 2009;27:186-92.
12. Sconocchia G, Zlobec I, Lugli A, Calabrese D, Iezzi G, Karamitopoulou E, Patsouris E, Peros G, Horcic M, Tornillo L, Zuber M, Drosner R, Muraro MG, et al. Tumor infiltration by FcγRIII (CD16)+ myeloid cells is associated with improved survival in patients with colorectal carcinoma. *Int J Cancer* 2011;128:2663-72.
13. Condeelis J, Pollard JW. Macrophages: obligate partners for tumor cell migration, invasion, and metastasis. *Cell* 2006;124:263-6.
14. Curiel TJ. Tregs and rethinking cancer immunotherapy. *J Clin Invest* 2007;117:1167-74.
15. Gough MJ, Weinberg AD. OX40 (CD134) and OX40L. *Adv Exp Med Biol* 2009;647:94-107.



16. Taraban VY, Rowley TF, O'Brien L, Chan HTC, Haswell LE, Green MHA, Tutt AL, Glennie MJ, Al-Shamkhani A. Expression and costimulatory effects of the TNF receptor superfamily members CD134 (OX40) and CD137 (4-1BB), and their role in the generation of anti-tumor immune responses. *Eur J Immunol* 2002;32:3617-27.
17. Croft M. Control of immunity by the TNFR-related molecule OX40 (CD134). *Annu Rev Immunol* 2010;28:57-78.
18. Sugamura K, Ishii N, Weinberg AD. Therapeutic targeting of the effector T-cell co-stimulatory molecule OX40. *Nat Rev Immunol* 2004;4:420-31.
19. Weinberg AD, Evans DE, Thalhofer C, Shi T, Prell RA. The generation of T cell memory : a review describing the molecular and cellular events following OX40 ( CD134 ) engagement 2004;40.
20. Bansal-Pakala P, Halteman BS, Cheng MH-Y, Croft M. Costimulation of CD8 T cell responses by OX40. *J Immunol* 2004;172:4821-5.
21. De Smedt T, Smith J, Baum P, Fanslow W, Butz E, Maliszewski C. Ox40 costimulation enhances the development of T cell responses induced by dendritic cells *in vivo*. *J Immunol* 2002;168:661-70.
22. Maxwell JR, Weinberg A, Prell RA, Vella AT. Danger and OX40 receptor signaling synergize to enhance memory T cell survival by inhibiting peripheral deletion. *J Immunol* 2000;164:107-12.
23. Curti BD, Kovacsovics-Bankowski M, Morris N, Walker E, Chisholm L, Floyd K, Walker J, Gonzalez I, Meeuwssen T, Fox B, Moudgil T, Miller W, Haley D, et al. OX40 is a potent immune-stimulating target in late-stage cancer patients. *Cancer Res* 2013;73:7189-98.
24. Gough MJ, Ruby CE, Redmond WL, Dhungel B, Brown A, Weinberg AD. OX40 agonist therapy enhances CD8 infiltration and decreases immune suppression in the tumor. *Cancer Res* 2008;68:5206-15.
25. Petty JK, D M, He K, Corless CL, Ph D, Vetto JT, Weinberg AD. Survival in human colorectal cancer correlates with expression of the T-cell costimulatory molecule OX-40 ( CD134 ) 2002;183:512-8.
26. Nebiker CA, Han J, Eppenberger-Castori S, Iezzi G, Hirt C, Amicarella F, Cremonesi E, Huber X, Padovan E, Angrisani B, Drosner R, Rosso R, Bolli M, et al. GM-CSF Production by Tumor Cells Is Associated with Improved Survival in Colorectal Cancer. *Clin Cancer Res* 2014;20:3094-106.
27. Livak KJ, Schmittgen TD. Analysis of relative gene expression data using real-time quantitative PCR and the 2(-Delta Delta C(T)) Method. *Methods* 2001;25:402-8.
28. Rhodes DR, Yu J, Shanker K, Deshpande N, Varambally R, Ghosh D, Barrette T, Pandey A, Chinnaiyan AM. ONCOMINE: a cancer microarray database and integrated data-mining platform. *Neoplasia* 6:1-6.
29. Skrzypczak M, Goryca K, Rubel T, Paziewska A, Mikula M, Jarosz D, Pachlewski J, Oledzki J, Ostrowski J, Ostrowski J, et al. Modeling oncogenic signaling in colon tumors by multidirectional analyses of microarray data directed for maximization of analytical reliability. *PLoS One* 2010;5.
30. Hong Y, Downey T, Eu KW, Koh PK, Cheah PY. A "metastasis-prone" signature for early-stage mismatch-repair proficient sporadic colorectal cancer patients and its implications for possible therapeutics. *Clin Exp Metastasis* 2010;27:83-90.
31. Kaiser S, Park Y-K, Franklin JL, Halberg RB, Yu M, Jessen WJ, Freudenberg J, Chen X, Haigis K, Jegga AG, Kong S, Sakthivel B, Xu H, Reichling T, et al. Transcriptional recapitulation and subversion of embryonic colon development by mouse colon tumor models and human colon cancer. *Genome Biol* 2007;8:R131.
32. Gaedcke J, Grade M, Jung K, Camps J, Jo P, Emons G, Gehoff A, Sax U, Schirmer M, Becker H, Beissbarth T, Ried T, Ghadimi BM. Mutated KRAS results in overexpression of DUSP4, a MAP-kinase phosphatase, and SMYD3, a histone methyltransferase, in rectal carcinomas. *Genes Chromosomes Cancer* 2010;49:1024-34.
33. Ki DH, Jeung H-C, Park CH, Kang SH, Lee GY, Lee WS, Kim NK, Chung HC, Rha SJ. Whole genome analysis for liver metastasis gene signatures in colorectal cancer. *Int J Cancer* 2007;121:2005-12.
34. Jass JR, Atkin WS, Cuzick J, Bussey HJ, Morson BC, Northover JM, Todd IP. The grading of rectal cancer: historical perspectives and a multivariate analysis of 447 cases. *Histopathology* 1986;10:437-59.
35. Blanche P, Dartigues J-F, Jacquemin-Gadda H. Estimating and comparing time-dependent areas under receiver operating characteristic curves for censored event times with competing risks. *Stat Med* 2013;32:5381-97.
36. Zlobec I, Steele R, Terracciano L, Jass JR, Lugli A. Selecting immunohistochemical cut-off scores for novel biomarkers of progression and survival in colorectal cancer. *J Clin Pathol* 2007;60:1112-6.
37. Tosolini M, Kirilovsky A, Mlecnik B, Fredriksen T, Mauger S, Bindea G, Berger A, Bruneval P, Fridman WH, Pages F, Galon J. Clinical Impact of Different Classes of Infiltrating T Cytotoxic and Helper Cells (Th1, Th2, Treg, Th17) in Patients with Colorectal Cancer. *Cancer Res* 2011;71:1263-71.
38. Hampel H, Stephens JA, Pukkala E, Sankila R, Aaltonen LA, Mecklin J-P, de la Chapelle A. Cancer risk in hereditary nonpolyposis colorectal cancer syndrome: later age of onset. *Gastroenterology* 2005;129:415-21.
39. Piconese S, Timperi E, Pacella I, Schinzari V, Tripodo C, Rossi M, Guglielmo N, Mennini G, Grazi GL, Di Filippo S, Brozzetti S, Fazzi K, Antonelli G, et al. Human OX40 tunes the function of regulatory T cells in tumor and nontumor areas of hepatitis C virus-infected liver tissue. *Hepatology* 2014;60:1494-507.

40. Ruby CE, Redmond WL, Haley D, Weinberg AD. Anti-OX40 stimulation *in vivo* enhances CD8 + memory T cell survival and significantly increases recall responses 2007;157-66.
41. Weinberg a D, Rivera MM, Prell R, Morris a, Ramstad T, Vetto JT, Urba WJ, Alvord G, Bunce C, Shields J. Engagement of the OX-40 receptor *in vivo* enhances antitumor immunity. J Immunol 2000;164:2160-9.
42. Weinberg AD, Morris NP, Kovacovics-Bankowski M, Urba WJ, Curti BD. Science gone translational: the OX40 agonist story. Immunol Rev 2011;244:218-31.
43. Abreu MT. Toll-like receptor signalling in the intestinal epithelium: how bacterial recognition shapes intestinal function. Nat Rev Immunol 2010;10:131-44.



OPEN ACCESS

ORIGINAL ARTICLE

# Dual role of tumour-infiltrating T helper 17 cells in human colorectal cancer

F Amicarella,<sup>1</sup> M G Muraro,<sup>1</sup> C Hirt,<sup>1</sup> E Cremonesi,<sup>1</sup> E Padovan,<sup>1</sup> V Mele,<sup>1</sup> V Governa,<sup>1,2</sup> J Han,<sup>1,3</sup> X Huber,<sup>1,4</sup> R A Drosler,<sup>4</sup> M Zuber,<sup>5</sup> M Adamina,<sup>6</sup> M Bolli,<sup>7</sup> R Rosso,<sup>8</sup> A Lugli,<sup>9</sup> I Zlobec,<sup>9</sup> L Terracciano,<sup>2</sup> L Tornillo,<sup>2</sup> P Zajac,<sup>1</sup> S Eppenberger-Castori,<sup>2</sup> F Trapani,<sup>2</sup> D Oertli,<sup>4</sup> G Iezzi<sup>1</sup>

► Additional material is published online only. To view please visit the journal online (<http://dx.doi.org/10.1136/gutjnl-2015-310016>).

<sup>1</sup>Department of Biomedicine, Institute of Surgical Research, University of Basel, Basel, Switzerland

<sup>2</sup>Institute of Pathology, University of Basel, Basel, Switzerland

<sup>3</sup>Department of General Surgery, Shanghai East Hospital, Tongji University, Shanghai, China

<sup>4</sup>Department of General Surgery, University Hospital Basel, Basel, Switzerland

<sup>5</sup>Department of Visceral Surgery, Kantonsspital Olten, Olten, Switzerland

<sup>6</sup>Department of Visceral Surgery, Kantonsspital St Gallen, St. Gallen, Switzerland

<sup>7</sup>Department of Visceral Surgery, St Claraspital, Basel, Switzerland

<sup>8</sup>Department of Visceral Surgery, Ospedale Civico Lugano, Lugano, Switzerland

<sup>9</sup>Institute of Pathology, University of Bern, Bern, Switzerland

## Correspondence to

Dr Giandomenica Iezzi, Department of Biomedicine, Institute of Surgical Research (ICFS), Basel University Hospital, Hebelstrasse 20, Basel 4031, Switzerland; [giandomenica.iezzi@usb.ch](mailto:giandomenica.iezzi@usb.ch)

Received 19 May 2015

Revised 11 November 2015

Accepted 30 November 2015

## ABSTRACT

**Background** The immune contexture predicts prognosis in human colorectal cancer (CRC). Whereas tumour-infiltrating CD8+ T cells and myeloid CD16+ myeloperoxidase (MPO)+ cells are associated with favourable clinical outcome, interleukin (IL)-17-producing cells have been reported to correlate with severe prognosis. However, their phenotypes and functions continue to be debated.

**Objective** To investigate clinical relevance, phenotypes and functional features of CRC-infiltrating, IL-17-producing cells.

**Methods** IL-17 staining was performed by immunohistochemistry on a tissue microarray including 1148 CRCs. Phenotypes of IL-17-producing cells were evaluated by flow cytometry on cell suspensions obtained by enzymatic digestion of clinical specimens. Functions of CRC-isolated, IL-17-producing cells were assessed by in vitro and in vivo experiments.

**Results** IL-17+ infiltrates were not themselves predictive of an unfavourable clinical outcome, but correlated with infiltration by CD8+ T cells and CD16+ MPO+ neutrophils. Ex vivo analysis showed that tumour-infiltrating IL-17+ cells mostly consist of CD4+ T helper 17 (Th17) cells with multifaceted properties. Indeed, owing to IL-17 secretion, CRC-derived Th17 triggered the release of protumorigenic factors by tumour and tumour-associated stroma. However, on the other hand, they favoured recruitment of beneficial neutrophils through IL-8 secretion and, most importantly, they drove highly cytotoxic CCR5+CCR6+CD8+ T cells into tumour tissue, through CCL5 and CCL20 release. Consistent with these findings, the presence of intraepithelial, but not of stromal Th17 cells, positively correlated with improved survival.

**Conclusions** Our study shows the dual role played by tumour-infiltrating Th17 in CRC, thus advising caution when developing new IL-17/Th17 targeted treatments.

## INTRODUCTION

The tumour immune contexture—that is, type, location, density and functional orientation of tumour-infiltrating immune cells,<sup>1</sup> predicts clinical outcome in human colorectal cancer (CRC). In particular, CD45RO+ memory T lymphocytes, cytotoxic CD8+ T cells (CTLs) and interferon (IFN)- $\gamma$ -producing T helper 1 cells (Th1) have been found to be associated with prolonged survival,

## Significance of this study

### What is already known on this subject?

- Infiltration of colorectal cancers (CRCs) by defined populations of immune cells predicts clinical outcome irrespective of tumour stage.
- CRC-infiltrating CD8+ T cells and CD16+ myeloperoxidase (MPO)+ neutrophils have been found to be associated with prolonged survival, whereas infiltration by interleukin (IL)-17-producing cells, as evaluated in a limited number of cases, has been suggested to correlate with more severe prognosis.
- IL-17 is a proinflammatory cytokine mediating protumorigenic and proangiogenic effects.
- Monoclonal antibodies targeting IL-17/IL-17-receptor or impairing expansion of IL-17-producing cells may represent a new therapeutic option in CRC.

### What are the new findings?

- Analysis of a large cohort of CRCs shows that tumour-infiltrating IL-17-producing cells are not themselves predictive of poor clinical outcome.
- Intraepithelial localisation of CRC-infiltrating IL-17+ cells is associated with improved survival.
- CRC infiltration by IL-17+ cells correlates with the presence of beneficial CD8+ T cells and CD16+ MPO+ neutrophils.
- CRC-infiltrating IL-17+ cells, mostly consisting of polyfunctional T helper 17 cells (Th17), can recruit highly cytotoxic CD8+ T cells into tumour nests through CCL5 and CCL20 release.

### How might it impact on clinical practice in the foreseeable future?

- By disclosing the dual role played by CRC-Th17, our findings question therapeutic approaches aimed at inhibiting Th17 development or expansion, possibly resulting in impaired tumour infiltration by beneficial effector cells. The positive contribution of Th17 to anti-tumour immune responses should not be disregarded when developing new IL-17/Th17 targeted treatments in CRC.

irrespective of tumour stage (5–7). Unexpectedly, Foxp3+ regulatory T cells (Tregs),<sup>2,3</sup> CD16+ and myeloperoxidase (MPO)+ myeloid cells,<sup>4–6</sup> also

**To cite:** Amicarella F, Muraro MG, Hirt C, *et al.* *Gut* Published Online First: [please include Day Month Year] doi:10.1136/gutjnl-2015-310016

correlate with favourable clinical outcome. In contrast, tumour infiltration by interleukin (IL)-17A-producing cells, evaluated so far in a limited number of cases (50–200), appears to be associated with unfavourable prognosis.<sup>7 8</sup>

IL-17A (hereafter referred to as IL-17) is an inflammatory cytokine, secreted by different cell types, including CD4+ T helper cells (Th17),<sup>9 10</sup> CTLs,  $\gamma\delta$ T cells, Tregs,<sup>11–13</sup> natural killer (NK) cells, NKT cells, lymphoid tissue inducer (LTI)-like cells and neutrophils.<sup>14 15</sup> IL-17 plays a prominent role in protective immune responses against bacterial and fungal infections and in the pathogenesis of inflammatory disorders.<sup>9 10 16</sup>

Experimental models indicate that IL-17 promotes intestinal tumorigenesis,<sup>17–22</sup> either by favouring proliferation of aberrant epithelial cells<sup>21</sup> or by inducing IL-6 release by tumour-associated stroma.<sup>18</sup> Furthermore, IL-17 promotes angiogenesis through vascular endothelial growth factor (VEGF) production,<sup>18 20</sup> thus mediating tumour resistance to antiangiogenic treatments.<sup>18</sup>

Monoclonal antibodies targeting IL-17/IL-17-receptor, or cytokines, such as IL-23, supporting Th17 development, have been recently developed and their clinical application in several inflammatory and autoimmune diseases is being evaluated.<sup>23–25</sup> These reagents may provide a new therapeutic option in CRC.<sup>26</sup> However, before testing IL-17/Th17-targeted treatments, a more comprehensive analysis of CRC-infiltrating, IL-17-producing cells is required.<sup>27</sup>

We evaluated the prognostic significance of IL-17 in a tissue micro-array (TMA) including 1148 CRC cases and we investigated phenotypes and functions of CRC-derived IL-17+ cells. Here we show that CRC-infiltrating IL-17-producing cells, mainly consisting of polyfunctional Th17, do not themselves predict clinical outcome, but rather play a dual role. On the one hand, owing to IL-17 secretion, they favour release of protumorigenic factors by tumour and tumour-associated stroma. However, on the other hand, they promote recruitment of beneficial neutrophils and CTLs by secreting specific chemokine and cytokine patterns. Interestingly, the presence of intraepithelial Th17 was significantly associated with patient survival, consistent with the ability of Th17 to drive beneficial immune cells into the tumour. The potential contribution of tumour-infiltrating Th17 to anti-tumour immune responses should not be disregarded when considering new IL-17/Th17 targeted treatments.

## MATERIALS AND METHODS

### Immunohistochemistry

A previously described TMA, including 1420 non-consecutive primary CRCs and 71 normal colonic mucosa samples,<sup>2 4–6 28</sup> was stained with a goat polyclonal anti-human IL-17 antibody (R&D Systems; staining I). IL-17 expression was evaluable in 1151 CRCs and 39 healthy mucosa samples. A randomised subgroup, including 746 CRCs and 27 healthy mucosa cases, was stained with a rabbit polyclonal anti-human IL-17 antibody (H-132, Santa Cruz Biotechnology; staining II). Secondary stainings and negative controls were performed as described.<sup>29</sup>

Protein markers were scored by three observers (AL, FA and FT). Cases were classified in four groups, according to numbers of positive cells/punch (0, 1–10, 11–50, >50). Staining protocols for CD8, CD16 and MPO have been previously reported.<sup>4 6 28</sup> Clinical information (see online supplementary table S1) was retrieved from patient records. The use of this information was approved by local ethical authorities.

### Clinical specimen collection and processing

Clinical specimens were collected from consenting patients undergoing surgical treatment at Basel University Hospital,

St Claraspital Basel, Kantonsspital Olten, Kantonsspital St Gallen and Ospedale Civico Lugano. Tumour and corresponding tumour-free mucosa fragments were snap-frozen for RNA extraction or enzymatically digested (2 mg/mL collagenase IV, Worthington Biochemical Corporation and 0.2 mg/mL DNase I, Sigma-Aldrich, for 1 h at 37°C) to obtain single cell suspensions.

### Flow cytometry and cell sorting

Cell suspensions from CRCs and tumour-free mucosa, and peripheral blood mononuclear cells (PBMC) of healthy donors (HDs) or patients with CRC, were incubated with 50 ng/mL phorbol 12-myristate 13-acetate, 1  $\mu$ g/mL ionomycin and 5  $\mu$ g/mL brefeldin A (Sigma-Aldrich) for 5 h. Cells were fixed and surface stained with fluorochrome-conjugated antibodies specific for human CD3, CD4, CD8, CD45RO, CD56, CD127, CCR6, HLA-DR,  $\gamma\delta$ TCR (all from BD Biosciences), V  $\alpha$  24 J  $\alpha$  18 TCR (eBioscience) and CD66b (BioLegend). Intracellular staining was then performed with antibodies specific for human IL-17 (eBioscience), IFN- $\gamma$ , tumour necrosis factor (TNF)- $\alpha$ , IL-22, IL-21, IL-8 (all from BD Biosciences) or granulocyte-macrophage colony stimulating factor (GM-CSF) and Foxp3 (BioLegend).

Chemokine receptor expression on CD8+ T cells was evaluated in CRC samples and autologous PBMC by surface staining with anti-human CCR5, CCR6 and CXCR3 antibodies (BD Biosciences). Stained cells were analysed by FACSCalibur flow cytometer (BD Biosciences) and FlowJo software (Tree Star).

Tumour, endothelial and mesenchymal cells were sorted from CRC cell suspensions using a BD Influx (BD Biosciences), upon staining with EpCAM-, CD31- and CD90-specific antibodies (BD Biosciences), respectively.

### T cell expansion and cloning

CRC-isolated T lymphocytes were stimulated with 1  $\mu$ g/mL of phytohaemagglutinin (Sigma-Aldrich) and expanded in medium supplemented with 100 IU/mL IL-2 (Roche Applied Science) and 5% of pooled human AB serum (provided by Blutspendenzentrum Beider Basel, Basel University Hospital) for 20 days. Th17 cells, identified based on CD4+ CXCR3-CCR4+CCR6+ phenotype,<sup>30</sup> were sorted by flow cytometry and further expanded as bulk populations. Th17 clones (hereafter referred to as CRC-Th17) were subsequently generated from bulk populations by limiting dilution. Supernatants from Th17 bulk populations and clones were obtained by T cell activation with plate bound anti-CD3 (10  $\mu$ g/mL, clone UCHT1, eBioscience) and soluble anti-CD28 antibodies (1  $\mu$ g/mL, clone CD28.2, BD Biosciences). After overnight culture, supernatants were collected and used for determination of cytokine contents by ELISA and for migration assays.

### Real-time reverse-transcription PCR

Total RNA was extracted from tissues or sorted cells using the RNeasy Mini Kit protocol (Qiagen), treated with DNase I (Invitrogen) and reverse transcribed using the Moloney murine leukemia virus reverse transcriptase (M-MLV RT, Invitrogen). Quantitative real-time PCR was performed in the ABI prism 7700 sequence detection system, using TaqMan Universal Master Mix and No AmpErase UNG (both from Applied Biosystems). Commercially available primers and probes specific for human IL-17A (Hs99999082\_m1), CCL5 (Hs00982282\_m1), CXCL9 (Hs00171065\_m1) and CXCL10 (Hs99999049\_m1, all from Applied Biosystems) were used.



### Cell lines

Human CRC cell lines LS180, COLO205 and HT29, purchased from the European Collection of Cell Cultures, were maintained in RPMI 1640 (GIBCO) or, for HT29, McCoy's 5A medium (Sigma-Aldrich), supplemented with 10% fetal bovine serum, GlutaMAX-I and kanamycin (GIBCO). HMEC cells (provided by Professor T Resink, University of Basel) were cultured in EBM-2 medium (Lonza). Tumour-associated stromal cells (TASC) were expanded from CRC samples in  $\alpha$ -MEM (GIBCO) supplemented with 10% fetal bovine serum and 5 ng/mL FGF-2 (R&D Systems).

### In vitro migration assay

Migration of neutrophils, isolated from PBMC of HDs by magnetic beads (EasyStep enrichment kit, StemCell Technologies), was assessed in transwell plates (5  $\mu$ m pore size, Corning Costar), towards Th17 supernatants or recombinant cytokines (IL-17, R&D Systems, 50 ng/mL; IL-8, R&D Systems, 100 ng/mL; GM-CSF, R&D Systems, 100 ng/mL), for 90 min at 37°C. In specific experiments, anti-IL-8 or anti-GM-CSF antibodies (10  $\mu$ g/mL, R&D Systems) were added to Th17 supernatants.

Migration of CD8+ T cells, sorted from PBMC of HDs by magnetic microbeads (Miltenyi Biotec) and pre-activated overnight with anti-CD3/CD28 antibodies, was evaluated in transwell plates (5  $\mu$ m pore size) towards Th17 supernatants, supernatants of HMEC cells, untreated, or exposed overnight to Th17 supernatants or recombinant proteins (IL-17, 50 ng/mL; TNF- $\alpha$ , 1 ng/mL, R&D Systems; IFN- $\gamma$ , 1 ng/mL, Biolegend; or their combination), or towards CCL5 (60 and 200 ng/mL, R&D Systems) and/or CCL20 (300 and 1000 ng/mL, R&D Systems). Depletion of CCL5 and/or CCL20 from Th17-derived supernatants was obtained by specific capture antibodies (R&D Systems). Cell migration was quantified by flow cytometry.

### ELISA

Cytokine/chemokine contents in supernatants were assessed by ELISA using CCL5, CCL20, CXCL10 and VEGF DuoSet ELISA (all from R&D Systems) and IL-6-specific reagents (BD Biosciences).

### T cell migration into engineered tumours

Tridimensional tumour tissues were engineered in a previously described bioreactor system.<sup>31</sup> HT29 cells ( $1 \times 10^6$ ) were injected and perfused through a collagen scaffold (Ultrafoam Avitene Collagen Hemostat, Davol Inc). At day 7,  $5 \times 10^6$  CRC-Th17 cells were injected and, after overnight incubation, were activated by CytoStim (Miltenyi Biotec) for 3 h. After extensive washing, perfusion was stopped and CD8+CD45RO+, sorted from PBMC of HDs, were then injected and allowed to spontaneously migrate overnight. Tissues were enzymatically digested and analysed by flow cytometry. Additionally, paraffin-embedded or cryosections were collected for H&E staining and immunofluorescence analysis.

### Histological and immunofluorescence analysis

Paraffin sections (5  $\mu$ m) were stained with H&E and analysed by light microscopy. Cryosections (10  $\mu$ m) were incubated with rabbit polyclonal anti-human CD8 (Abcam) and mouse monoclonal anti-human CD4 (DakoCytomation) antibodies, or with rabbit polyclonal anti-human IL-17 (H-132, Santa Cruz Biotechnology) and mouse monoclonal EpCAM (Cell Signalling), followed by secondary species-specific Alexa Fluor 488- or Alexa Fluor 547-conjugated antibodies (Invitrogen).

Nuclei were counterstained with 4,6-diamidino-2-phenylindole. Sections were examined under an Olympus BX61 fluorescence microscope (Olympus) and images captured with 10 $\times$  and 20 $\times$  magnifications using a F-VIEW II camera (Olympus) and AnalySIS software (Soft Imaging System GmbH).

### In vivo migration assay

LS180 cells were inoculated subcutaneously in 8-week-old NSG mice (Charles River, Germany). CRC-Th17 and CD8+ T cells, isolated from PBMC of HDs, were activated overnight with anti-CD3/CD28 antibodies. Carboxyfluorescein succinimidyl ester-labelled CD8+ T cells were adoptively transferred by intravenous injection in tumour-bearing mice (maximum tumour volume 1 cm<sup>3</sup>) alone or together with Th17 ( $5 \times 10^6$  cells/subset/mouse). After 48 h, tumours were harvested and frequencies of CD8+CSFE+ T cells in tumour cell suspensions were evaluated by flow cytometry.

### Statistical analysis

CRC cases were classified into four categories according to numbers of IL-17+ cells/punch (0; 1–10; 11–50; >50). Specific cut-off values for CD8, CD16 and MPO (10, 50 and 60, respectively) were obtained by receiver operating curve (ROC) analysis.<sup>4 6 28</sup>

A  $\chi^2$  test was used to determine the significance of differences between dichotomous variables. Survival analysis was depicted by Kaplan–Meier method and compared with log-rank test. Statistical analyses were performed using R (V2.15.2, <http://www.r-project.org>).

Differences in frequencies of IL-17+ cells within PBMC of HDs or patients with CRC and between tumour and control tissues were evaluated by t test. Differences in migration rates and cytokine release were tested by one way analysis of variance using GraphPad Prism5 (GraphPad Software).

## RESULTS

### CRC-infiltrating IL-17+ cells do not predict clinical outcome

IL-17+ cells were evaluated by immunohistochemistry upon staining of a characterised TMA (38–39 and see online supplementary table S1) with two different polyclonal anti-IL-17 antibodies (staining I, [figure 1A](#) and staining II, see online supplementary figure S1A). Results obtained from the two stainings showed good and significant correlation ( $r=0.436$   $p<0.00001$ , weighted Cohen  $\kappa=0.284$ ). IL-17+ cells were detectable within epithelial and stromal compartments. Numbers of intraepithelial IL-17+ cells were significantly higher in tumour samples than in normal colonic mucosa ([figure 1B](#)). Accordingly, higher IL-17 mRNA levels in CRC than in corresponding control tissues were detected (see online supplementary figure S1B).

No association between IL-17+ infiltrates and tumour location, mismatch repair status or tumour border configuration was seen ([table 1](#)). In a limited group of cases for which additional clinical information was available, no correlation between numbers of IL-17+ cells and local recurrences ( $n=446$ ), or distant metastasis ( $n=452$ ) was seen ([table 1](#)). In contrast, IL-17+ cells strongly correlated with peritumoral lymphocytic infiltration ( $p<0.001$ ). A slight increase in IL-17+ cell numbers was seen in tumours characterised by early T and N stage, low grade and absence of vascular invasion. Unexpectedly, no significant impact of IL-17+ cells on overall survival ([figure 1C](#) left panel,  $n=1151$  and see online supplementary figure S1C,  $n=649$ ) or relapse-free survival ([figure 1C](#) right panel,  $n=443$ ) was seen.

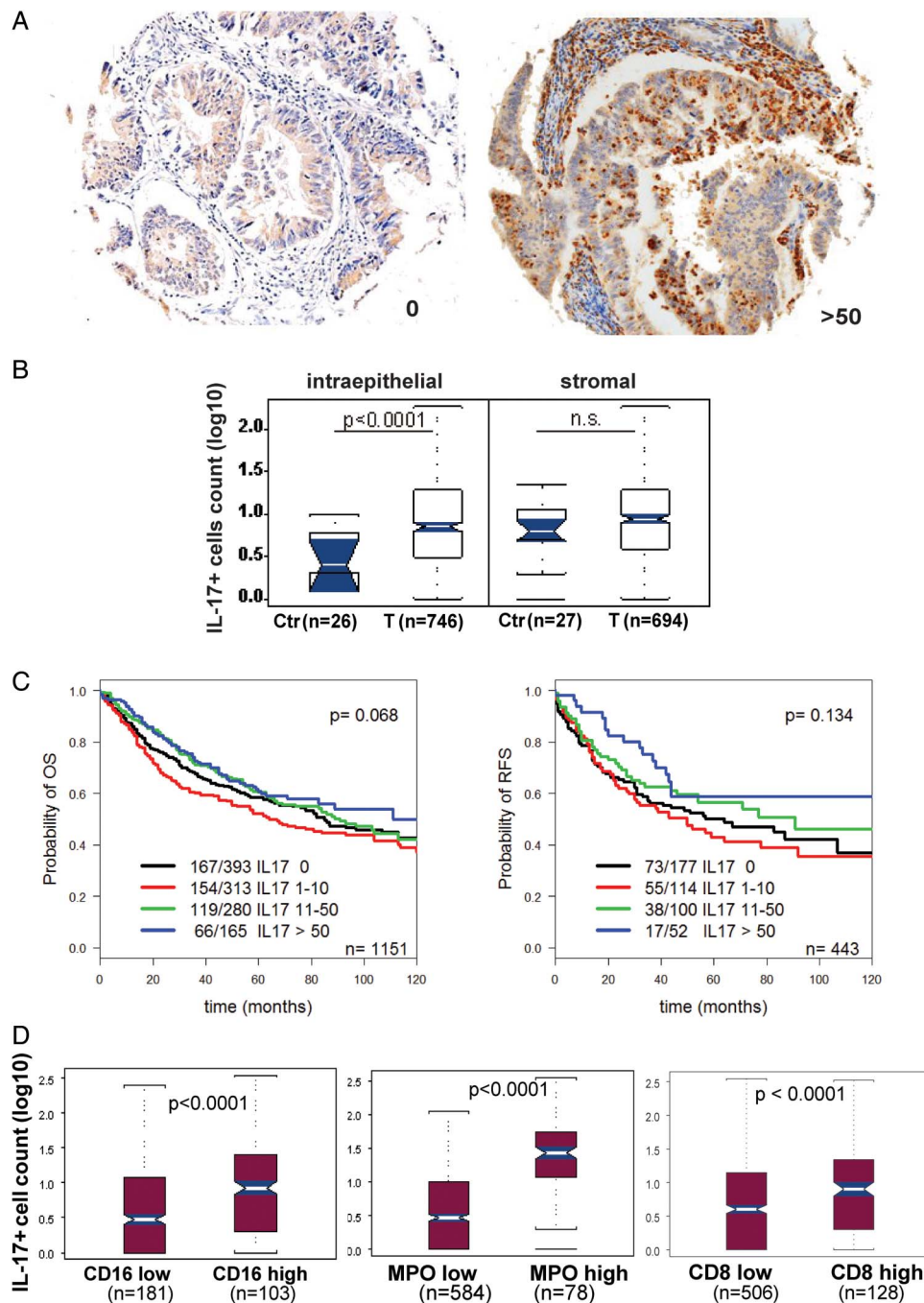


**Figure 1** Tumour infiltration by interleukin-17 (IL-17)-producing cells does not predict survival in colorectal cancer (CRC). IL-17 expression was evaluated by immunohistochemistry on a tissue microarray (TMA) including 1151 cases of primary CRC. (A) Representative pictures of IL-17 staining I (see 'Materials and methods'). Numbers of IL-17+ cells per punch are indicated. (B) Distribution of IL-17+ cells within the epithelial or stromal fraction of healthy colonic tissues (Ctr) or tumour samples (T). Statistical significance was assessed by  $\chi^2$  test. (C) Kaplan–Meier curves illustrating overall survival (OS, left panel) and relapse-free survival (RFS, right panel) probability according to IL-17+ cell density. Numbers of deaths/total cases within each category are indicated. Statistical significance was assessed by log-rank test. (D) Numbers of IL-17+ cells within CRC cases characterised by low or high infiltration of CD16+, MPO+ and CD8+ cells, according to cut-off scores identified by receiver operating characteristic curve analysis, as described in 'Materials and methods'. Statistical significance was assessed by  $\chi^2$  test. MPO, myeloperoxidase.

#### Tumour infiltration by IL-17+ cells is associated with the presence of CTLs and neutrophils

Interestingly, IL-17 was found to correlate significantly with CD16, MPO and CD8 markers (figure 1D), predictive of improved survival in the same TMA.<sup>4 6 32</sup> CD16 and MPO are expressed in a subset of HLA-DR- CD15+ CD66b+ myeloid cells, mostly including activated neutrophils.<sup>4 6</sup> Indeed, numbers

of IL-17+ cells also correlated with those of infiltrating polymorphonuclear cells (see online supplementary figure S1D).

We wondered whether the positive impact of these populations might mask the negative prognostic significance of IL-17+ cells. However, also in cases stratified for CD16, MPO or CD8 expression, no effect of IL-17 on survival was found (see online supplementary figure S2).

**Table 1** Association of IL-17 lymphocyte count and clinicopathological features in CRC (n=1148)

Clinicopathological features	IL-17* lymphocyte count		p Value
	Median/mean	Min-max	
All	3/13.8	0-350	
Tumour location			
Right-sided	3/12.6	0-200	0.94†
Left-sided	3/14.3	0-332	0.13‡
Rectum	4/13.7	0-350	
MMR status			
Proficient	3/13.6	0-350	0.18
Deficient	4/14.5	0-167	
pT stage			
pT1-2	5.5/15.1	0-150	0.03
pT3-4	3/13.7	0-350	
pN stage			
pN0	4/15.5	0-350	0.03
pN1-2	3/12.3	0-350	
Tumour grade			
G1-2	4/14.2	0-350	0.01
G3	2/12.1	0-200	
Vascular invasion			
Absent	4/15.1	0-350	0.03
Present	3/10.7	0-250	
Tumour border			
Pushing	4/12.3	0-250	0.78
Infiltrating	3/14.9	0-350	
Peritumoral lymphocytic inflammation			
Absent	3/13.4	0-350	<0.001
Present	7.5/15.8	0-250	
Local recurrence			
Absent	1/8.5	0-350	0.35
Present	1/6.1	0-200	
Distant metastasis			
Absent	1/8.2	0-350	0.10
Present	1/3.8	0-30	
Death			
Censored	3/14.1	0-350	0.5
Present	4/13.8	0-332	

p Value calculated according to the Mann-Whitney test. Significant p values are shown in bold.

\*As assessed by staining I (see 'Materials and methods').

†Right-sided versus left-sided.

‡Right-sided or left-sided versus rectum.

CRC, colorectal cancers; IL, interleukin; MMR, mismatch repair.

### CRC-infiltrating IL-17+ cells consist of Th17 cells

We next assessed phenotypes of CRC-infiltrating IL-17+ cells, in freshly isolated clinical specimens, by flow cytometry (figure 2). IL-17 production was exclusively observed within CD3+ T cells, whose large majority expressed CD4, CD45RO and CCR6 (figure 2A, B). Interestingly, 27±24% of infiltrating IL-17+ cells also expressed Foxp3 (figure 2A, B). Sporadically, IL-17+ CD8+ T cells were detected (figure 2A, B).

Large proportions of  $\gamma\delta$ T cells and CD66b+ neutrophils (up to 24±5% and 13±9%, respectively) were detectable, but only a minor fraction (<1%) of those cell types showed evidence of IL-17 production. CD56+NK, V $\alpha$ 24/J $\alpha$ 18TCR+NKT and CD3-CD127+ LTi-like cells were detected in limited numbers and did not include significant fractions of IL-17+ cells (figure 2A, B). Evaluation of absolute cell numbers confirmed that the large majority of IL-17+ cells were CD3+ cells (see online

supplementary figure S3). Thus, CRC-infiltrating, IL-17-producing cells mainly consist of memory Th17.

Th17 frequencies were significantly higher in tumours than in corresponding healthy tissues or autologous PBMC, whereas no significant difference was observed between PBMC of patients with CRC and HD (figure 2C).

Importantly, a significant fraction of CRC-infiltrating Th17 also produced TNF- $\alpha$ , IL-21, IL-22, GM-CSF, IFN- $\gamma$ , and IL-8 (figure 2D, E). Th17 clones expanded from CRC-infiltrating CD4+ T cells (CRC-Th17) also released TNF- $\alpha$ , IL-21, IL-22, GM-CSF, IFN- $\gamma$  and IL-8, in addition to IL-17 (see online supplementary figure S4), thus indicating that CRC-infiltrating Th17 are polyfunctional effector cells.

### CRC-Th17 mediate protumorigenic effects in an IL-17-dependent manner

The lack of association between IL-17-producing cells and unfavourable clinical outcome was an unexpected finding considering the suggested protumorigenic activity of IL-17.<sup>7 8</sup>

This prompted us to investigate the functional properties of CRC-Th17.

We conditioned CRC, endothelial cells (EC) and TASC with supernatants obtained from CRC-Th17 clones or bulk populations. No significant effects on cell proliferation were detected (see online supplementary figure S5). VEGF production by CRC cells was slightly increased by Th17 supernatants and it was inhibited upon IL-17 neutralisation (figure 3A and see online supplementary figure S6A). IL-6 release by EC and TASC was strongly induced by Th17 supernatants in an IL-17-dependent manner (figure 3B and see online supplementary figure S6B). Thus, IL-17 released by CRC-Th17 cells appears to mediate protumorigenic effects mainly by acting on EC and TASC.

### CRC-Th17 promote neutrophil recruitment and activation

We next investigated the molecular background underlying the association between Th17 and CD16+MPO+ myeloid cells or CD8+CTLs. The phenotypic analysis ruled out the possibility that neutrophils or CTLs could be the IL-17 producers. Alternatively, we investigated whether Th17 cells may recruit these cell populations into tumour tissues either directly or by eliciting chemokine release by stromal cells.<sup>33 34</sup>

Neutrophils are known to migrate in response to IL-8. Indeed, supernatants from CRC-Th17 clones and bulk populations induced vigorous neutrophil migration in an IL-8-dependent manner (figure 4A and see online supplementary figure S7A, respectively), whereas other Th17 cytokines, including IL-17 and GM-CSF, appeared to play no role in this phenomenon (figure 4A and see online supplementary figure S7B). Interestingly, exposure of neutrophils to Th17 supernatants also significantly enhanced MPO release, independently of IL-17, IL-8 or GM-CSF (figure 4B and see online supplementary figure S7C). Thus, CRC-Th17 might directly promote neutrophil recruitment and activation into CRC.

### CRC-Th17 favour CTL recruitment by triggering chemokine release from EC

In line with previous findings,<sup>35</sup> circulating and tumour-infiltrating CTLs were found to express CCR5 and CXCR3 receptors (figure 5A), enabling them to respond to CCL5 and CXCL9/CXCL10, respectively.

These chemokines were all expressed on whole CRC tissues (figure 5B). Upon sorting of tumour, stromal and EC from specimens, CCL5 and CXCL10 were expressed at the highest level within the endothelial compartment (figure 5C), whereas no



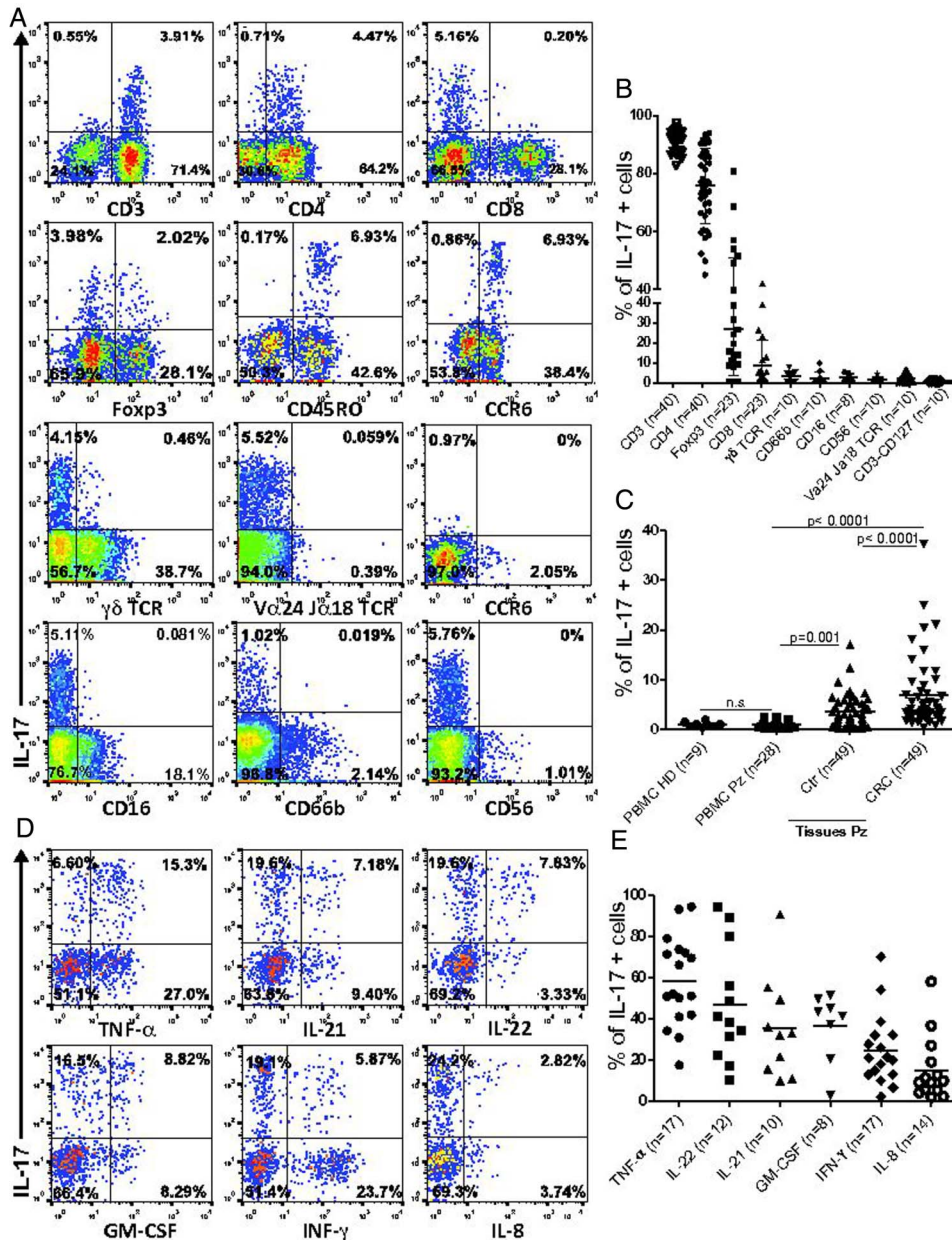


**Figure 2** Colorectal cancers (CRC)-infiltrating interleukin (IL)-17+ cells are polyfunctional Th17. Single cell suspensions from freshly excised clinical specimens of CRC and corresponding tumour-free colonic mucosa (Ctr) and peripheral blood mononuclear cells from healthy donors (PBMC HD) or patients with CRC (PBMC Pz), were incubated with phorbol 12-myristate 13-acetate (PMA)/ionomycin/brefeldin for 5 h. Surface staining for specific cell population markers and intracellular staining for Foxp3 and cytokines was then performed. (A) Representative flow cytometric analysis of CRC infiltrates stained for IL-17 and the indicated cell-specific markers. Tumour-infiltrating cells are gated based on physical parameters, as defined by analysis of autologous PBMC. (B) Frequencies of cells positive for the indicated markers within gated IL-17+ cells. Means are indicated by bars. Numbers of samples evaluated for each marker are indicated in parentheses. (C) Frequencies of IL-17+ cells on gated CD3+ T cells obtained from PBMC HD or PBMC CRC and single cell suspensions from freshly excised clinical specimens of Ctr and corresponding CRC. Means are indicated by bars. Numbers of samples evaluated for each marker are indicated in parentheses. Statistical significance was assessed by t test. (D) Representative flow cytometric analysis of intracellular cytokine staining on gated CRC-infiltrating CD3+CD4+ cells. (E) Frequencies of cells positive for the indicated cytokines gated on CD3+CD4+ IL-17+ T cells. Means are indicated by bars. Numbers of samples evaluated for each cytokine are indicated in parentheses. GM-CSF, granulocyte-macrophage colony stimulating factor; IFN, interferon; TNF, tumour necrosis factor.

CXCL9 was detected. EC exposure to CRC-Th17 supernatants strikingly enhanced their ability to release CCL5 and CXCL10 (figure 5D) and to promote CTL migration (figure 5E). Notably, these effects were not elicited by IL-17, nor were they inhibited after IL-17 neutralisation, but instead appeared to depend on Th17-derived TNF-α (figure 5F, G and see online supplementary figure S8). Thus, Th17 may favour CTL recruitment into CRC by triggering chemokine release from tumour-associated EC.

### CRC-Th17 directly attract CTLs in vitro

Intriguingly, we observed that supernatants from CRC-Th17 bulks and clones significantly induced CTL migration also in the absence of EC (figures 5E, 6A and see online supplementary figure S9A), thus suggesting that Th17 may release chemoattractants directly acting on CTLs.

In CRC-Th17 supernatants we detected significant amounts of CCL5, in addition to CCL20, a known Th17-derived



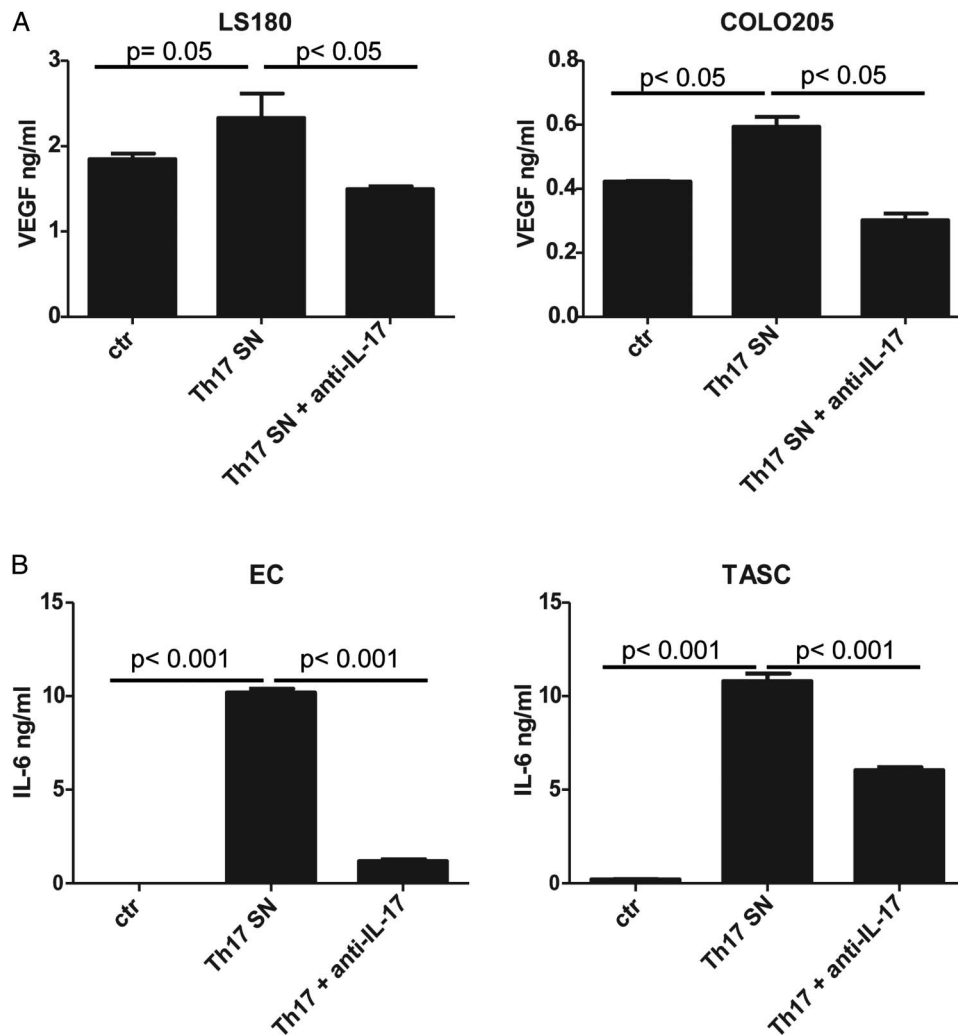


**Figure 3** Colorectal cancers (CRC)-Th17 mediate protumorigenic effects in an interleukin (IL)-17-dependent manner. Endothelial cells (EC), tumour-associated stromal cells (TASC) and CRC cell lines (LS180, COLO205) were conditioned for 24 h with CRC-Th17 supernatants untreated (Th17 SN) or pretreated with anti-IL-17 neutralising antibodies (Th17+ anti-IL-17). Vascular endothelial growth factor (VEGF) (A) or IL-6 (B) release was measured in culture supernatants by ELISA. Statistical significance was analysed by one-way analysis of variance. Data refer to experimental triplicates from two independent experiments performed with supernatants from two different clones. Ctr, healthy colonic tissue.

chemokine (figure 6B and see online supplementary figure S9B). CTL migration was marginally impaired by CCL5 depletion, whereas it was markedly reduced upon CCL20 removal (figure 6C). However, CCL5 increased CTL migration to low CCL20 concentrations (figure 6D), thus revealing a synergism between these two chemokines. CCR6, the receptor for CCL20, was expressed on a subset of CRC-infiltrating CTLs (figure 6E). Frequencies of CCR6+CTLs were significantly higher in CRC than in autologous control tissues or PBMC (figure 6E). Importantly, most CCR6+CTLs (up to  $62 \pm 10\%$ ) also expressed CCR5 (figure 6F). Furthermore, CCR5+CCR6+CTLs were positive for TIA-1 (figure 6F), a cytotoxic granule-associated, RNA-binding protein whose expression by CRC-infiltrating CTLs is associated with survival advantage.<sup>28</sup> Thus, through CCL5 and CCL20 CRC-Th17 target highly cytotoxic T cells.

#### CRC-Th17 cells promote CTL recruitment into CRC tissues

We next assessed whether Th17-mediated effects might be relevant for CTL recruitment into tumours.

We engineered tridimensional tumour-like tissues by culturing HT29 cells on collagen scaffolds in perfused bioreactors<sup>31 36</sup> (see online supplementary figure S10A, B). CRC-Th17 were

added into the system under perfusion, allowing their localisation in proximity of tumour nests (see online supplementary figure S10C) and were subsequently activated (figure 7A). Perfusion was then stopped and CTLs were applied. After an overnight incubation, tumour infiltration by CTLs was evaluated (figure 7B, C and see online supplementary figure S10D). CTLs were found in tumour-like tissues, in proximity of tumour cells (figure 7B) and their frequencies were significantly higher in the presence of activated CRC-Th17 (figure 7C).

Accordingly, when CTLs were adoptively transferred in tumour-bearing mice together with Th17, significantly higher numbers of tumour-infiltrating CTLs were detected as compared with mice transferred with CTLs alone (figure 7D). Thus, CRC-Th17 directly attract CTLs into tumours.

These findings suggested that CRC-Th17 localised into the tumour nests might play a beneficial role by recruiting CTLs close to tumour cells. Indeed, when we evaluated the prognostic significance of IL-17+ cells according to their localisation, the presence of intraepithelial, but not of stromal IL-17+ cells, positively correlated with absence of local recurrence and prolonged relapse-free survival (see online supplementary table S2 and figure 8).

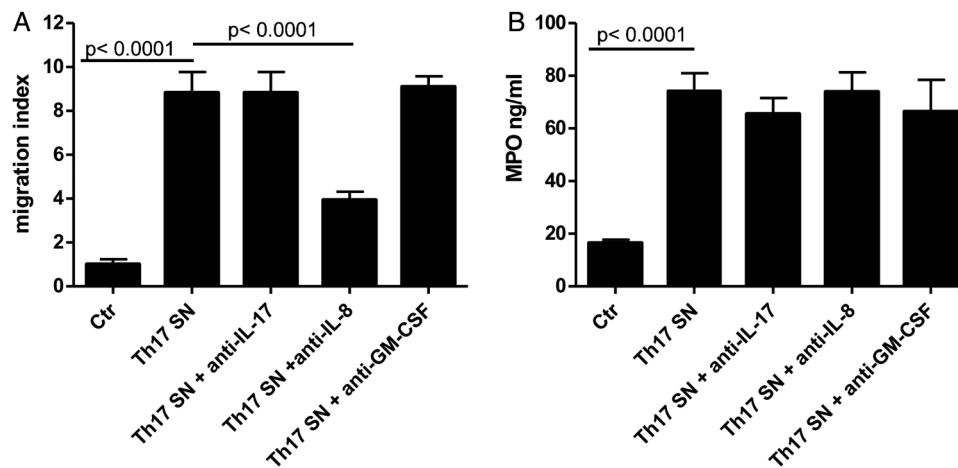


**Figure 4** Colorectal cancers (CRC)-infiltrating Th17 favour recruitment and activation of neutrophils. (A) Migration of neutrophils, purified from blood of healthy donors, towards control medium (Ctr), supernatants of Th17 clones expanded from CRC-infiltrating cells (Th17 SN) or Th17 supernatants pre-treated with anti-interleukin (IL)-17 (Th17 SN+ anti-IL-17), anti-IL-8 (Th17 SN+ anti-IL-8), or anti-granulocyte-macrophage colony stimulating factor (anti-GM-CSF antibodies) (Th17 SN+ anti-GM-CSF), was evaluated after 90 min incubation by flow cytometry. Data refer to experimental triplicates from three independent experiments performed with supernatants from three different clones. Means±SD are depicted. Statistical significance was assessed by one-way analysis of variance (ANOVA). (B) Myeloperoxidase (MPO) release by neutrophils exposed to control medium (Ctr), Th17 supernatants (Th17 SN) or Th17 supernatants pretreated with anti-IL-17, IL-8 or GM-CSF antibodies was assessed after 4 h incubation by ELISA. Means±SD are depicted. Data refer to experimental triplicates from three independent experiments performed with supernatants from three different clones. Statistical significance was assessed by one-way ANOVA.

## DISCUSSION

The goal of our study was to investigate the clinical relevance of CRC-infiltrating, IL-17-producing cells in a large patient cohort and to characterise in detail their phenotypes and functional properties. Upon analysis of >1000 primary CRC cases, we found that CRC-infiltrating IL-17+ cells are not themselves predictive of patient survival but, their prognostic significance rather appears to depend on their localisation within CRC tissue. Indeed, intraepithelial, but not stromal IL-17+ cells, were associated with improved prognosis. Ex vivo analysis showed that tumour-infiltrating, IL-17-producing cells mostly consist of polyfunctional Th17, releasing a spectrum of cytokines and chemokines, in addition to IL-17. Through IL-17, CRC-Th17 triggered the release of protumorigenic factors mainly by tumour-associated stroma. However, by releasing additional chemokines, they also appeared to contribute to the recruitment of beneficial effector cells into tumours. In particular, through IL-8 they promoted the recruitment of CD16+ MPO+ neutrophils. Most importantly, through CCL5 and CCL20, they attracted cytotoxic CTLs into tumour nests. Accordingly, in our patient cohort, CRC infiltration by Th17 cells correlated with that by neutrophils and CTLs.

Based on these findings, the lack of association between total numbers of Th17 cells and prognostic significance is not surprising. Indeed, the potentially negative impact of IL-17 is probably counterbalanced by recruitment of beneficial effector cells. In previous reports, however, an association between total IL-17+ infiltrates and unfavourable clinical outcome was observed.<sup>7 8</sup> Although a few differences in the protocol used in our study as compared with others must be acknowledged (ie, in our work IL-17 positivity was assessed by three independent observers, whereas in the study by Tosolini *et al*<sup>8</sup> the TMA staining was quantified by image software), the discrepancy between ours and previous studies probably relies on the different numbers of cases evaluated (52<sup>7</sup> and <200<sup>8</sup> vs 1148). Notably, we obtained comparable results upon TMA staining with two different IL-17-specific antibodies.<sup>7 8</sup>

Importantly, our study reveals a previously unrecognised positive prognostic significance of intraepithelial Th17 cells, suggesting a critical contribution of these cell subsets to the recruitment of CTLs and neutrophils into tumour nests.

IL-17-production by CD4+ cells has been previously reported in CRC.<sup>37–39</sup> However, whether other cell types may also contribute to IL-17 release within CRC tissues remained to be assessed. We observed that most IL-17+ cells are CD3+ CD4+ T cells, expressing CD45RO and CCR6 and including a subset of Foxp3+ cells. In contrast, no significant IL-17 production was seen within other cell subsets, including CTLs and innate lymphoid and myeloid cell populations.

IL-17-producing Foxp3+ cells were previously described within CRC tissues,<sup>37 38 40</sup> but their functional role remains unclear. Remarkably, CRC infiltration by Tregs correlates with prolonged patient survival.<sup>2 3</sup>

A recent study reported  $\gamma\delta$ T cells as a major IL-17 source in human CRC.<sup>41</sup> We also observed considerable percentages of  $\gamma\delta$ T cells within CRC infiltrates, but only a negligible fraction of them showed IL-17 production ability. However, the patients examined in the study by Wu *et al*<sup>41</sup> and in our study belong to two different ethnic and geographical groups (ie, China and Switzerland, respectively), therefore probably differing in the composition of their gut flora.<sup>42</sup> This may be of relevance when considering cell populations, such as  $\gamma\delta$ T and Th17 cells, whose function is modulated by defined microbiota.<sup>22 43 44</sup> Thus, this discrepancy may be due to the presence, in the patients evaluated, of distinct gut microbial species, possibly driving preferential expansion of IL-17-producing  $\gamma\delta$ T or Th17 cells.

The ability of Th17 to recruit effector cells appears to be dependent on their capacity to release cytokines other than IL-17. Indeed, Th17 supernatants promoted neutrophil recruitment in an IL-8-dependent fashion and enhanced secretion of MPO, a lysosomal enzyme possibly involved in the mechanisms underlying the favourable effect of MPO+ neutrophils in CRC.<sup>4</sup> In addition, CRC-Th17 supernatants activated tumour-associated EC to release CCL5 and CXCL10, attracting CTLs. Importantly, tumour-infiltrating Th17 proved capable of directly

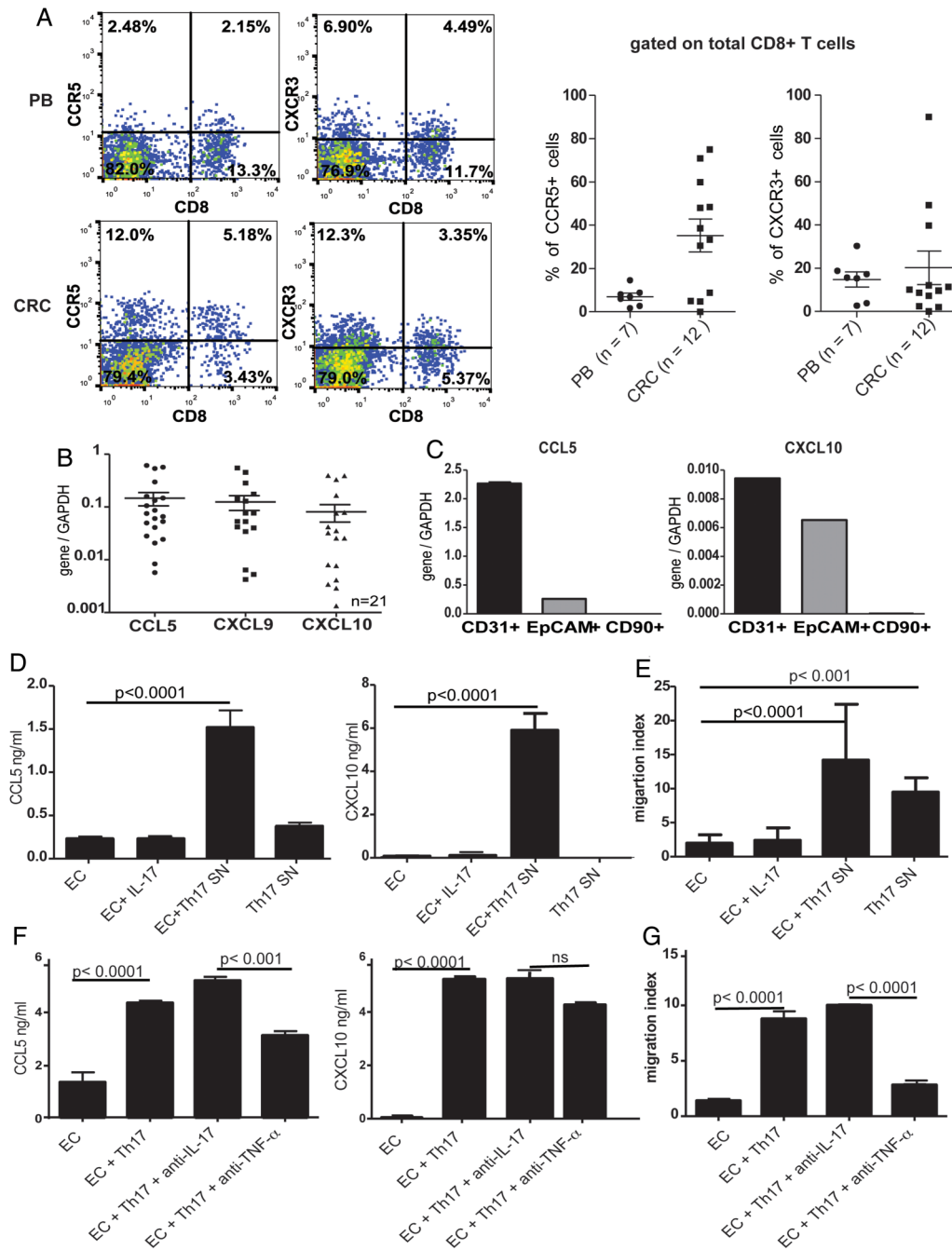
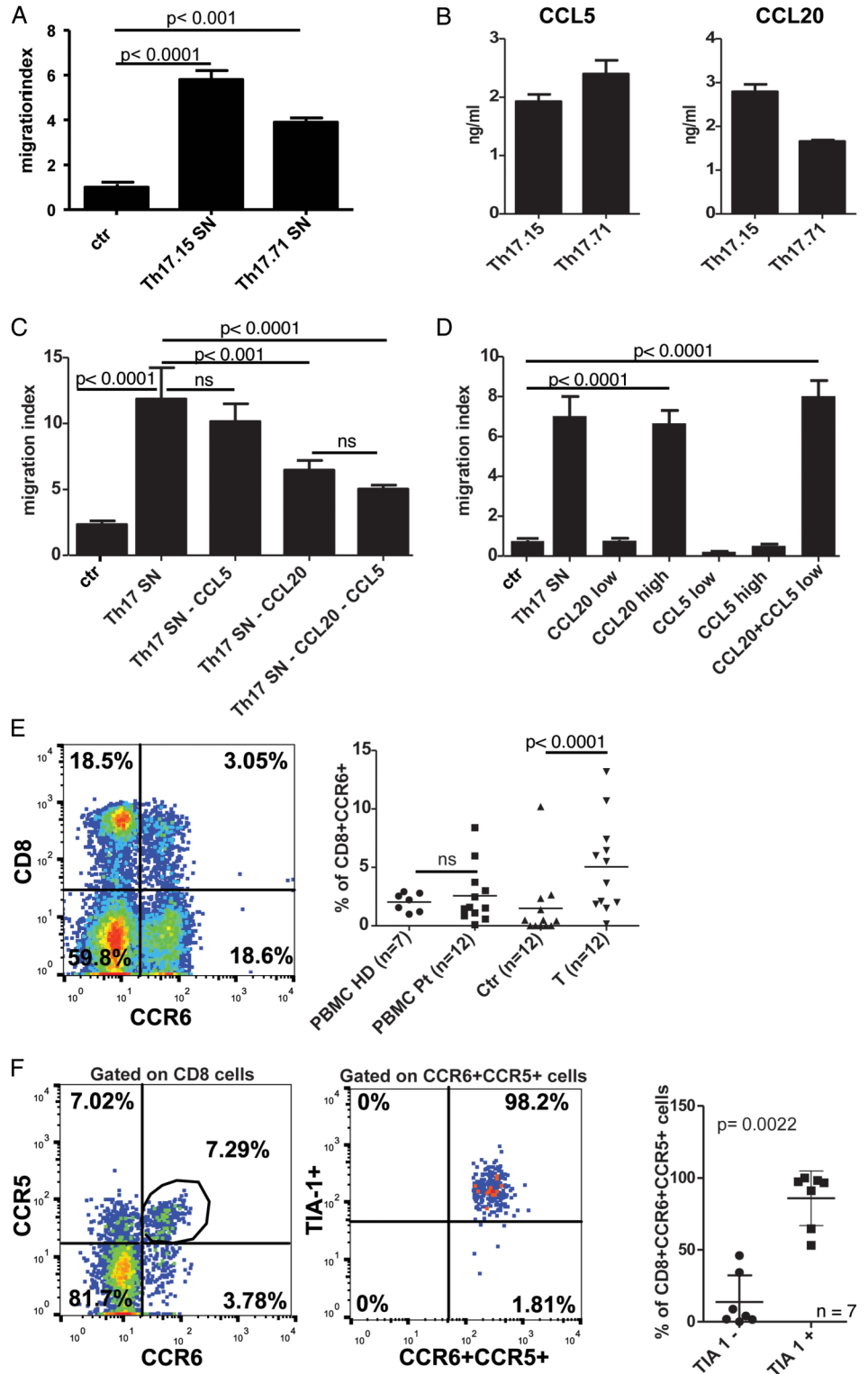


**Figure 5** Th17 cells favour recruitment of CD8<sup>+</sup> T cells by triggering chemokine release from endothelial cells (EC). (A) Peripheral blood cells (PB, n=7) and tumour cell suspensions from patients with colorectal cancer (CRC) (n=12) were surface stained for CD8 in combination with the indicated chemokine receptors. Left panels: representative flow cytometric analysis. Right panels: percentages of CD8<sup>+</sup> cells expressing the indicated chemokine receptors. Means $\pm$ SD are depicted. (B) The expression of the indicated chemokine genes was assessed on CRC samples (n=21) by quantitative PCR. Expression levels relative to glyceraldehyde-3-phosphate dehydrogenase (GAPDH) are depicted. (C) Endothelial, tumour and stromal cells were sorted from cell suspensions derived from CRC specimens by flow cytometry, based on CD31, EpCAM and CD90 expression, respectively. mRNA levels of the indicated chemokine genes were assessed in sorted cells by quantitative PCR. Gene expression levels relative to GAPDH are depicted. Data refer to analysis of one representative sample out of four. (D) Chemokine release by HMEC cells untreated (EC) or exposed overnight to recombinant interleukin-17 (rIL-17; 50 ng/mL) (EC+IL-17) or to Th17 clone supernatants (EC+Th17 SN), was measured by ELISA. Chemokine content in Th17 SN was also assessed as control. Data refer to experimental triplicates from three experiments performed with three different clones from one patient. Means $\pm$ SD are depicted. Statistical significance was assessed by one-way analysis of variance (ANOVA). (E) Migration of CD8<sup>+</sup> T cells, purified from peripheral blood mononuclear cells (PBMC) of healthy donors, towards supernatants of HMEC cells untreated (EC), or exposed to rIL-17 (50 ng/mL) (EC+IL17) or Th17 supernatants (EC+Th17), was assessed after 90 min of incubation by flow cytometry. Migration towards Th17 supernatants (Th17 SN) was also assessed as control. Data refer to experimental triplicates from three experiments performed with three different clones from one patient. Means $\pm$ SD are depicted. Statistical significance was assessed by one-way ANOVA. (F and G) Chemokine contents (F) and cytotoxic T lymphocyte (CTL) chemoattraction capacity (G) of supernatants from HMEC cells untreated (EC), exposed overnight to Th17 supernatants (EC+Th17 SN), or exposed to Th17 supernatants pretreated with anti-IL-17 (EC+Th17+anti-IL-17) or anti-tumour necrosis factor  $\alpha$  (anti-TNF- $\alpha$ ) antibodies (EC+Th17+anti-TNF- $\alpha$ ). Data refer to three experiments performed with supernatants of Th17 bulk populations derived from three different samples. Means $\pm$ SD are depicted. Statistical significance was assessed by one-way ANOVA.

GI cancer

**Figure 6** Th17 cells directly attract cytotoxic CD8+ T cells. (A) Migration of CD8+ T cells towards control medium (Ctr) or supernatants of two different colorectal cancer (CRC)-Th17 clones (Th17.15 SN and Th17.71 SN), was assessed after 90 min incubation by flow cytometry. (B) Chemokine release by Th17 clones (Th17.15 and Th17.71), activated with plate bound anti-CD3 and soluble anti-CD28 antibodies for an overnight period, was measured by ELISA. Means±SD of experimental triplicates are depicted. (C) Migration of CD8+ T cells towards Th17 clone supernatants depleted of CCL5 (Th17 SN–CCL5), CCL20 (Th17 SN–CCL20) or both (Th17 SN–CCL5–CCL20), relative to control (migration towards untreated Th17 supernatants). (D) Migration of CD8+ T cells towards Th17 clone supernatants (Th17 SN) or towards low or high doses of recombinant CCL20 (300 and 1000 ng/mL, respectively) and CCL5 (60 and 200 ng/mL, respectively). (A–D) Means ±SD from experimental triplicates are depicted. One representative experiment out of two is shown. Statistical significance was assessed by one-way analysis of variance (ANOVA). (E) Representative flow cytometric analysis of CRC infiltrates stained for CD8 and CCR6 markers (left panel). Frequencies of CCR6+CD8+ T cells were measured by flow cytometry in peripheral blood mononuclear cells of healthy donors (PBMC HD n=7) or patients with CRC (PBMC Pz n=12) and in single cell suspensions of tumour-free colonic mucosa (Ctr) and corresponding CRC (n=12). Means are indicated by bars. Statistical significance was assessed by t test. (F) Left and middle panels: representative flow cytometric analysis of CRC-infiltrating CD8+ T cells stained for CCR6, CCR5 and TIA-1. Right panel: frequencies of CCR6+ CCR5+ cells within TIA-1- or TIA-1+ CRC-infiltrating CD8+ T cells (n=7).



recruiting highly cytotoxic TIA-1+ CCR5+ CCR6+ CTLs through own production of CCL5 and CCL20. Interestingly, CCL5 and CCL20 appeared to synergise. Although CCL5 could not itself induce CTL migration, it could increase CTL response to low CCL20 concentrations.

In a melanoma mouse model, Th17 have been previously shown to favour tumour infiltration by CTLs, ultimately mediating tumour eradication.<sup>45 46</sup> These in vivo models, however, could not discriminate between direct and indirect effects of Th17 on CTL recruitment. Therefore, to assess the relevance of

the direct Th17-mediated effects on CTLs, we took advantage of an engineered tridimensional tumour tissue infiltrated by Th17 cells, in the absence of EC. Furthermore, we adoptively transferred human CTLs and Th17 in immunodeficient mice bearing human tumour xenografts. Strikingly, in both experimental systems, the presence of activated Th17 cells markedly enhanced CTL recruitment into the tumour.

These data suggest that Th17 cells may promote tumour infiltration by CTLs through a double axis: on the one hand, they might favour EC activation leading to CTL recruitment from the

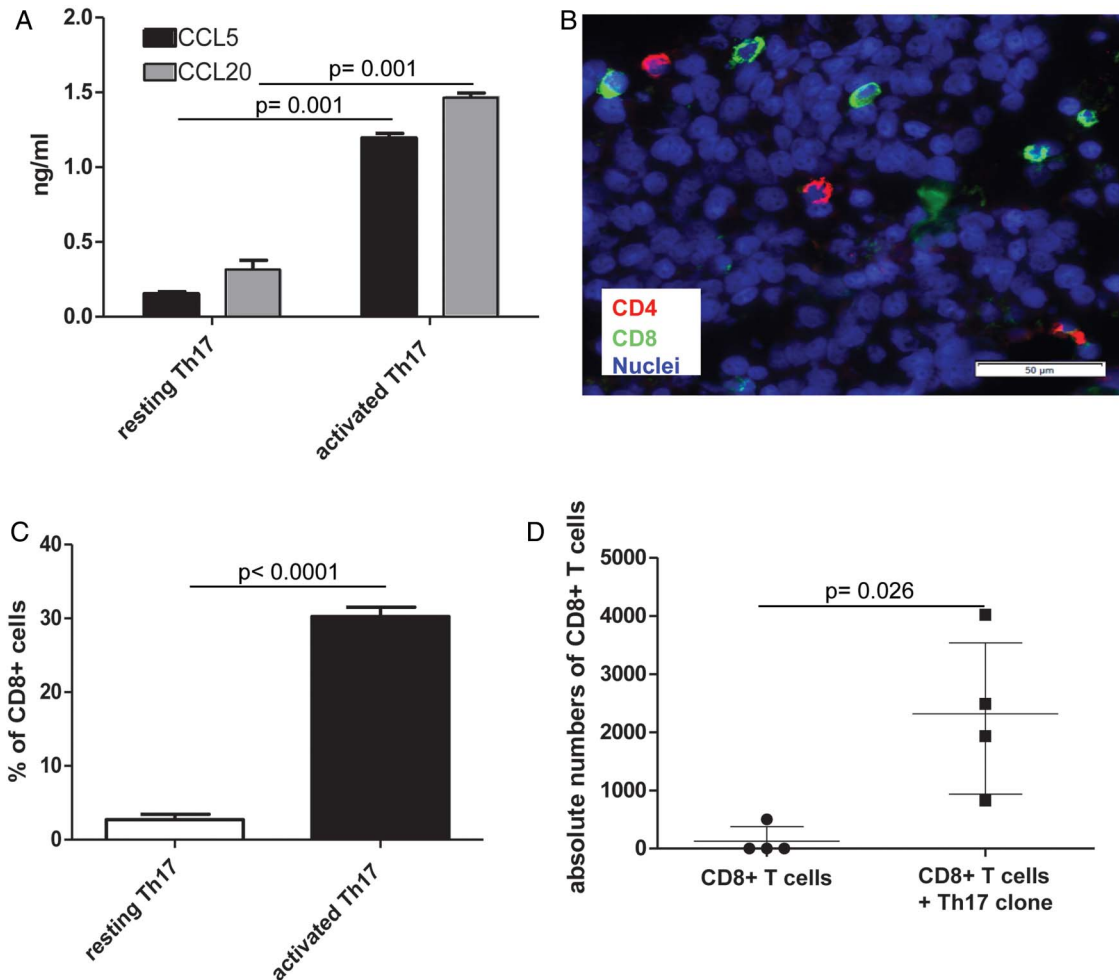


**Figure 7** Th17 cells promote recruitment of cytotoxic CD8+ T cells into colorectal cancer (CRC) tissues. (A) CRC-Th17-infiltrating engineered tumour tissues (see online supplementary figure S10) were left untreated or were activated by adding CytoStim to the perfusion medium. Culture media were collected 20 h later and chemokine contents were assessed by ELISA. Statistical significance was assessed by Mann–Whitney test. (B and C) Three hours after Th17 activation, the perfusion in the bioreactor was stopped and CD8+ T cells were added to the system. After an overnight period, scaffolds were removed and tumour infiltration by CD8+ T cells was evaluated by immunofluorescence analysis upon staining with CD4- and CD8-specific antibodies (B) and by flow cytometry upon staining of single cell suspensions with EpCAM-, CD4- and CD8-specific antibodies (C). Percentages of CD8+ cells in tumour tissues infiltrated by resting or activated Th17 cells are reported. Means $\pm$ SD from three experimental replicates performed with one Th17 clone are depicted. Statistical significance was assessed by Mann–Whitney test. (D) CSFE+CD8+ T cells were adoptively transferred in tumour bearing mice alone or together with equal numbers of CRC-Th17 (four mice/condition). Absolute numbers of CD8+CSFE+ T cells were evaluated by flow cytometry upon staining of tumour and Th17 cells with anti-EpCAM and anti-CD4 antibodies, respectively. Statistical significance was assessed by Mann–Whitney test.

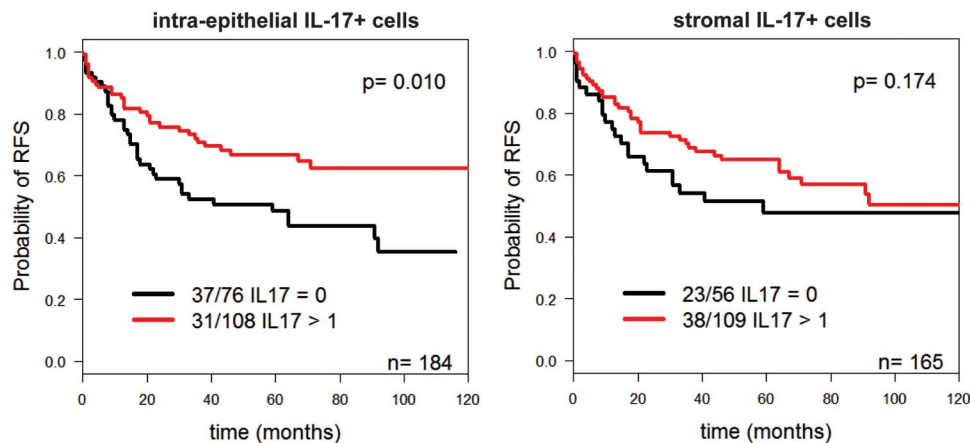


**Figure 8** Intra-epithelial localisation of interleukin (IL)-17+ cells correlates with prolonged relapse-free survival (RFS) survival. Kaplan–Meier curves illustrating RFS probability according to infiltration by IL-17+ cells within the epithelial (left panel) or stromal (right panel) compartment. Numbers of deaths/total cases within each category are indicated. Statistical significance was assessed by log-rank test.



blood stream, on the other, they might directly guide the positioning of CTLs in proximity of tumour cells. Altogether our data reveal a positive contribution of Th17 cells to beneficial anti-tumour immune responses developing in CRC and underline their pleiotropic function resulting from the production of a broad spectrum of cytokines and chemokines beyond IL-17.

This may, at least partially, explain the discrepancies between results obtained from studies evaluating the effects of IL-17 or IL-17 signalling only and those examining functions of the whole Th17 cell subset.<sup>47–50</sup>

Our findings have important clinical implications. Indeed, the positive contribution of Th17 to anti-tumour immune responses should not be disregarded when developing new IL-17/Th17 targeted treatments in CRC, possibly resulting in impaired tumour infiltration by beneficial effector cells.

**Acknowledgements** We thank Giulio C Spagnoli, Ed Palmer, Daniela Finke, Michael Heberer, Marco Lepore and Mariacarla Andreozzi for critical discussion and review of the manuscript; Thèrese J Resink for human microvascular endothelial cells (HMEC); Diego Calabrese for his advice on immunofluorescence studies; and Ivan Martin for his support with bioreactor-based cultures.

**Contributors** FA and GI conceived and designed the experiments, analysed and interpreted results, obtained funding, wrote the manuscript. FA, MGM, CH, EC, VM, VG, and JH performed and analysed the experiments. XH, RAD, MZ, MA, MB and RR contributed to the conception of research and data collection. AL, IZ, LTe, LTo, PZ, SE-C and FT contributed to the conception of research, and collection, analysis and interpretation of data. IZ and SE-C performed the statistical analysis. EP contributed to the conception of research, experimental design, data analysis and interpretation and writing of the manuscript. DO contributed to the conception of research, data collection and financial support.

**Funding** Swiss National Science Foundation (SNF 310030-127490, PP00P3-133699, and PP00P3-159262), Freiwillige Akademische Gesellschaft Basel and Department of Surgery, Basel University Hospital.

**Competing interests** MGM is employed at Cellec-Biotek AG.

**Patient consent** Obtained.

**Ethics approval** Ethikkommission Beider Basel/Ethik Kommission Nord-West Schweiz (EKBB/EKNZ).

**Provenance and peer review** Not commissioned; externally peer reviewed.

**Open Access** This is an Open Access article distributed in accordance with the Creative Commons Attribution Non Commercial (CC BY-NC 4.0) license, which permits others to distribute, remix, adapt, build upon this work non-commercially, and license their derivative works on different terms, provided the original work is properly cited and the use is non-commercial. See: <http://creativecommons.org/licenses/by-nc/4.0/>

## REFERENCES

- 1 Fridman WH, Pagès F, Sautès-Fridman C, *et al.* The immune contexture in human tumours: impact on clinical outcome. *Nat Rev Cancer* 2012;12:298–306.
- 2 Frey DM, Droezer RA, Viehl CT, *et al.* High frequency of tumor-infiltrating FOXP3+ regulatory T cells predicts improved survival in mismatch repair-proficient colorectal cancer patients. *Int J Cancer* 2010;126:2635–43.
- 3 Salama P, Phillips M, Griew F, *et al.* Tumor-infiltrating FOXP3+ T regulatory cells show strong prognostic significance in colorectal cancer. *J Clin Oncol* 2009;27:186–92.
- 4 Droezer RA, Hirt C, Eppenberger-Castori S, *et al.* High myeloperoxidase positive cell infiltration in colorectal cancer is an independent favorable prognostic factor. *PLoS ONE* 2013;8:e64814.
- 5 Hirt C, Eppenberger-Castori S, Sconocchia G, *et al.* Colorectal carcinoma infiltration by myeloperoxidase-expressing neutrophil granulocytes is associated with favorable prognosis. *Oncimmunology* 2013;2:e25990.
- 6 Sconocchia G, Zlobec I, Lugli A, *et al.* Tumor infiltration by FcγRIII (CD16)+ myeloid cells is associated with improved survival in patients with colorectal carcinoma. *Int J Cancer* 2011;128:2663–72.
- 7 Liu J, Duan Y, Cheng X, *et al.* IL-17 is associated with poor prognosis and promotes angiogenesis via stimulating VEGF production of cancer cells in colorectal carcinoma. *Biochem Biophys Res Commun* 2011;407:348–54.
- 8 Tosolini M, Kirilovsky A, Mlecnik B, *et al.* Clinical impact of different classes of infiltrating T cytotoxic and helper cells (Th1, th2, treg, th17) in patients with colorectal cancer. *Cancer Res* 2011;71:1263–71.
- 9 Weaver CT, Hatton RD, Mangan PR, *et al.* IL-17 family cytokines and the expanding diversity of effector T cell lineages. *Annu Rev Immunol* 2007;25:821–52.
- 10 Korn T, Bettelli E, Oukka M, *et al.* IL-17 and Th17 cells. *Annu Rev Immunol* 2009;27:485–517.
- 11 Beriou G, Costantino CM, Ashley CW, *et al.* IL-17-producing human peripheral regulatory T cells retain suppressive function. *Blood* 2009;113:4240–9.
- 12 Voo KS, Wang YH, Santori FR, *et al.* Identification of IL-17-producing FOXP3+ regulatory T cells in humans. *Proc Natl Acad Sci U S A* 2009;106:4793–8.
- 13 Koenen HJ, Smeets RL, Vink PM, *et al.* Human CD25<sup>high</sup>Foxp3<sup>pos</sup> regulatory T cells differentiate into IL-17-producing cells. *Blood* 2008;112:2340–52.
- 14 Cua DJ, Tato CM. Innate IL-17-producing cells: the sentinels of the immune system. *Nat Rev Immunol* 2010;10:479–89.
- 15 Spits H, Artis D, Colonna M, *et al.* Innate lymphoid cells—a proposal for uniform nomenclature. *Nat Rev Immunol* 2013;13:145–9.
- 16 Steinman L. A brief history of T(H)17, the first major revision in the T(H)1/T(H)2 hypothesis of T cell-mediated tissue damage. *Nat Med* 2007;13:139–45.
- 17 Chae WJ, Gibson TF, Zelterman D, *et al.* Ablation of IL-17A abrogates progression of spontaneous intestinal tumorigenesis. *Proc Natl Acad Sci USA* 2010;107:5540–4.
- 18 Chung AS, Wu X, Zhuang G, *et al.* An interleukin-17-mediated paracrine network promotes tumor resistance to anti-angiogenic therapy. *Nat Med* 2013;19:1114–23.
- 19 Grivnenkov SI, Wang K, Mucida D, *et al.* Adenoma-linked barrier defects and microbial products drive IL-23/IL-17-mediated tumour growth. *Nature* 2012;491:254–8.
- 20 Numasaki M, Fukushi J, Ono M, *et al.* Interleukin-17 promotes angiogenesis and tumor growth. *Blood* 2003;101:2620–7.
- 21 Wang K, Kim MK, Di Caro G, *et al.* Interleukin-17 receptor signaling in transformed enterocytes promotes early colorectal tumorigenesis. *Immunity* 2014;41:1052–63.
- 22 Wu S, Rhee KJ, Albesiano E, *et al.* A human colonic commensal promotes colon tumorigenesis via activation of T helper type 17 T cell responses. *Nat Med* 2009;15:1016–22.
- 23 Garber K. Anti-IL-17 mAbs herald new options in psoriasis. *Nat Biotechnol* 2012;30:475–7.
- 24 Niederreiter L, Adolph TE, Kaser A. Anti-IL-12/23 in Crohn's disease: bench and bedside. *Curr Drug Targets* 2013;14:1379–84.
- 25 Tse MT. IL-17 antibodies gain momentum. *Nat Rev Drug Discov* 2013;12:815–16.
- 26 Wang K, Grivnenkov SI, Karin M. Implications of anti-cytokine therapy in colorectal cancer and autoimmune diseases. *Ann Rheum Dis* 2013;72(Suppl 2):ii100–3.
- 27 Middleton GW, Annels NE, Pandha HS. Are we ready to start studies of Th17 cell manipulation as a therapy for cancer? *Cancer Immunol Immunother* 2012;61:1–7.
- 28 Zlobec I, Karamitopoulou E, Terracciano L, *et al.* TIA-1 cytotoxic granule-associated RNA binding protein improves the prognostic performance of CD8 in mismatch repair-proficient colorectal cancer. *PLoS One* 2010;5:e14282.
- 29 Zlobec I, Steele R, Terracciano L, *et al.* Selecting immunohistochemical cut-off scores for novel biomarkers of progression and survival in colorectal cancer. *J Clin Pathol* 2007;60:1112–16.
- 30 Acosta-Rodríguez EV, Rivino L, Geginat J, *et al.* Surface phenotype and antigenic specificity of human interleukin 17-producing T helper memory cells. *Nat Immunol* 2007;8:639–46.
- 31 Hirt C, Papadimitropoulos A, Muraro MG, *et al.* Bioreactor-engineered cancer tissue-like structures mimic phenotypes, gene expression profiles and drug resistance patterns observed “in vivo”. *Biomaterials* 2015;62:138–46.
- 32 Lugli A, Karamitopoulou E, Panayiotides I, *et al.* CD8+ lymphocytes/ tumour-budding index: an independent prognostic factor representing a ‘pro-anti-tumour’ approach to tumour host interaction in colorectal cancer. *Br J Cancer* 2009;101:1382–92.
- 33 Hot A, Lenief V, Miossec P. Combination of IL-17 and TNFα induces a pro-inflammatory, pro-coagulant and pro-thrombotic phenotype in human endothelial cells. *Ann Rheum Dis* 2012;71:768–76.
- 34 Onishi RM, Gaffen SL. Interleukin-17 and its target genes: mechanisms of interleukin-17 function in disease. *Immunology* 2010;129:311–21.
- 35 Musha H, Ohtani H, Mizoi T, *et al.* Selective infiltration of CCR5(+)/CXCR3(+) T lymphocytes in human colorectal carcinoma. *Int J Cancer* 2005;116:949–56.
- 36 Braccini A, Wendt D, Jaquiere C, *et al.* Three-dimensional perfusion culture of human bone marrow cells and generation of osteoinductive grafts. *Stem Cells* 2005;23:1066–72.
- 37 Blatner NR, Bonertz A, Beckhove P, *et al.* In colorectal cancer mast cells contribute to systemic regulatory T-cell dysfunction. *Proc Natl Acad Sci USA* 2010;107:6430–5.
- 38 Kryczek I, Wu K, Zhao E, *et al.* IL-17+ Regulatory T Cells in the microenvironments of chronic inflammation and cancer. *J Immunol* 2011;186:4388–95.
- 39 Su X, Ye J, Hsueh EC, *et al.* Tumor microenvironments direct the recruitment and expansion of human Th17 cells. *J Immunol* 2010;184:1630–41.
- 40 Yang S, Wang B, Guan C, *et al.* Foxp3+IL-17+ T cells promote development of cancer-initiating cells in colorectal cancer. *J Leukoc Biol* 2011;89:85–91.

- 41 Wu P, Wu D, Ni C, *et al.* GammadeltaT17 cells promote the accumulation and expansion of myeloid-derived suppressor cells in human colorectal cancer. *Immunity* 2014;40:785–800.
- 42 Yatsunenko T, Rey FE, Manary MJ, *et al.* Human gut microbiome viewed across age and geography. *Nature* 2012;486:222–7.
- 43 Hooper LV, Littman DR, Macpherson AJ. Interactions between the microbiota and the immune system. *Science* 2012;336:1268–73.
- 44 Ivanov II, Atarashi K, Manel N, *et al.* Induction of intestinal Th17 cells by segmented filamentous bacteria. *Cell* 2009;139:485–98.
- 45 Ankathatti MM, Deng Y, Mulligan SJ, *et al.* Th17 and Th17-stimulated CD8(+) T cells play a distinct role in Th17-induced preventive and therapeutic antitumor immunity. *Cancer Immunol Immunother* 2011;60:1473–84.
- 46 Martin-Orozco N, Muranski P, Chung Y, *et al.* T helper 17 cells promote cytotoxic T cell activation in tumor immunity. *Immunity* 2009;31:787–98.
- 47 Murugaiyan G, Saha B. Protumor vs antitumor functions of IL-17. *J Immunol* 2009;183:4169–75.
- 48 Punt S, Langenhoff JM, Putter H, *et al.* The correlations between IL-17 vs. Th17 cells and cancer patient survival: a systematic review. *Oncoimmunology* 2015;4:e984547.
- 49 Wilke CM, Kryczek I, Wei S, *et al.* Th17 cells in cancer: help or hindrance? *Carcinogenesis* 2011;32:643–9.
- 50 Zou W, Restifo NP. T(H)17 cells in tumour immunity and immunotherapy. *Nat Rev Immunol* 2010;10:248–56.



## Dual role of tumour-infiltrating T helper 17 cells in human colorectal cancer

F Amicarella, M G Muraro, C Hirt, E Cremonesi, E Padovan, V Mele, V Governa, J Han, X Huber, R A Drosner, M Zuber, M Adamina, M Bolli, R Rosso, A Lugli, I Zlobec, L Terracciano, L Tornillo, P Zajac, S Eppenberger-Castori, F Trapani, D Oertli and G Iezzi

*Gut* published online December 30, 2015

---

Updated information and services can be found at:  
<http://gut.bmj.com/content/early/2015/12/30/gutjnl-2015-310016>

*These include:*

- Supplementary Material** Supplementary material can be found at:  
<http://gut.bmj.com/content/suppl/2015/12/30/gutjnl-2015-310016.DC1.html>
- References** This article cites 50 articles, 17 of which you can access for free at:  
<http://gut.bmj.com/content/early/2015/12/30/gutjnl-2015-310016#BIBL>
- Open Access** This is an Open Access article distributed in accordance with the Creative Commons Attribution Non Commercial (CC BY-NC 4.0) license, which permits others to distribute, remix, adapt, build upon this work non-commercially, and license their derivative works on different terms, provided the original work is properly cited and the use is non-commercial. See: <http://creativecommons.org/licenses/by-nc/4.0/>
- Email alerting service** Receive free email alerts when new articles cite this article. Sign up in the box at the top right corner of the online article.

---

**Topic Collections** Articles on similar topics can be found in the following collections

- [Open access](#) (245)
- [Colon cancer](#) (1513)

---

### Notes

---

To request permissions go to:  
<http://group.bmj.com/group/rights-licensing/permissions>

To order reprints go to:  
<http://journals.bmj.com/cgi/reprintform>

To subscribe to BMJ go to:  
<http://group.bmj.com/subscribe/>



## **CREMONESI ELEONORA**

Home address: Davidsbodenstrasse 42, 4056 Basel  
Telephone: +41766188117  
E-mail: ele.cremonesi@yahoo.it  
Date of birth: 07.10.1985

### **EDUCATION**

- 2009:** Degree in Medical and Pharmaceutical Biotechnology obtained at the Università degli Studi in Pavia (final mark: 110/110)
- 2007:** 3-year degree in Biotechnology obtained at the Università degli Studi in Pavia (final mark: 99/110)
- 2004:** Diploma of “Ragioniere Programmatore” obtained at the Institute “A. Bassi” in Lodi (final mark: 78/100)

### **TRAINING**

- 2007:** Course of Biotechnology and Medicine
- 2010:** Symposium about pandemic influenza

### **WORK EXPERIENCE**

Since 15.08.2011: PhD student at University Hospital of Basel investigating the Chemotactic factors underlying tumor infiltration by immunocompetent cells in Colorectal cancer (CRC).

From 1.07.2010 to 1.7.2011: Fellowship on “Role of peripheral and intrahepatic Natural Killer cells (NK) in hepatitis B pathogenesis and immune predictors to therapeutic response” at the “Laboratorio di Immunologia Cellulare e Molecolare dei laboratori di infettivologia”, I.R.C.C.S. Foundation, Policlinico S. Matteo di Pavia, Italy.

From 17.12.2009 to 1.7.2010: Internship at the “Laboratorio di Immunologia Cellulare e Molecolare dei laboratori di infettivologia”, I.R.C.C.S. Foundation, Policlinico S. Matteo di Pavia, Italy.

From 1.01.2009 to 16.12.2009: Degree training on analysis of the cytotoxic function of intrahepatic NK lymphocytes in chronic hepatitis C virus infection” at the “Laboratorio di Immunologia Cellulare e Molecolare dei laboratori di infettivologia”, I.R.C.C.S. Foundation, Policlinico S. Matteo di Pavia, Italy.

From 1.11.2008 to 06.2011: Molecular Biology Laboratory Technician for the “DNA chiavi in mano” project at the Institute “A. Bassi” in cooperation with IFOM (Fondazione Istituto Firc di Oncologia Molecolare).

From 1.09.2006 to 25.09.2007: 3-year degree training on the analysis of megakaryocyte and platelet differentiation by using a confocal and fluorescence microscopy at the Clinical Biochemical Laboratory.

## **SCIENTIFIC REPORTS**

### **PUBLICATIONS**

Varchetta S, Mele D, Mantovani S, Oliviero B, **Cremonesi E**, Ludovisi S, Michelone G, Alessiani M, Rosati R, Montorsi M, Mondelli MU. Impaired intrahepatic natural killer cell cytotoxic function in chronic hepatitis C virus infection. *Hepatology*. 2012

Raoul A, Drosier, Christian Hirt, Carsten T. Viehl, Daniel M. Frey, Christian Nebiker, Xaver Huber, Inti Zlobec, Serenella Eppenberger-Castori, Alexander Tzankov, Raffaele Rosso, Markus Zuber, Manuele Giuseppe Muraro, Francesca Amicarella, **Eleonora Cremonesi**, Michael Heberer, Giandomenica Iezzi, Alessandro Lugli, Luigi Terracciano, Giuseppe Sconocchia, Daniel Oertli, Giulio C. Spagnoli, Luigi Tornillo. Clinical impact of programmed cell death ligand 1 expression in colorectal cancer. *European Journal of Cancer* 2013

Oliviero B, Mele D, Degaspero E, Aghemo A, **Cremonesi E**, Grazia Rumi M, Tinelli C, Varchetta S, Mantovani S, Colombo M, Mondelli MU. Natural Killer Cell Dynamic Profile Is Associated with Treatment Outcome in Patients with Chronic HCV Infection. *J Hepatol*. 2013.

Nebiker C, Han J, Castori-Eppenberger S, Iezzi G, Hirt C, Amicarella F, **Cremonesi E**, Huber X, Padovan E, Angrisani B, Drosier RA, Rosso R, Bolli M, Oertli D, von Holzen U, Adamina M, Muraro MG, Mengus C, Zajac P, Sconocchia G, Zuber M, Tornillo L, Terracciano L, Spagnoli GC. GM-CSF production by tumor cells is associated with improved survival in colorectal cancer. *Clin Cancer Res*. 2014.

Hirt C, Papadimitropoulos A, Muraro MG, Mele V, Panopoulos E, **Cremonesi E**, Ivanek R, Schultz-Thater E, Drosier RA, Mengus C, Heberer M, Oertli D, Iezzi G, Zajac P, Eppenberger-Castori S, Tornillo L, Terracciano L, Martin I, Spagnoli GC. Bioreactor-engineered cancer tissue-like structures mimic phenotypes, gene expression profiles and drug resistance patterns observed "in vivo". *Biomaterials*. 2015.

Weixler B, **Cremonesi E**, Sorge R, Muraro MG, Delko T, Nebiker CA, Daester S, Governa V, Amicarella F, Soysal SD, Kettelhack C, von Holzen UW, Eppenberger-Castori S, Spagnoli GC, Oertli D, Iezzi G, Terracciano L, Tornillo L, Sconocchia G, Drosier RA. OX40 expression enhances the prognostic significance of CD8 positive lymphocyte infiltration in colorectal cancer. *Oncotarget*. 2015

Amicarella F, Muraro MG, Hirt C, **Cremonesi E**, Padovan E, Mele V, Governa V, Han J, Huber X, Drosier RA, Zuber M, Adamina M, Bolli M, Rosso R, Lugli A, Zlobec I, Terracciano L, Tornillo L, Zajac P, Eppenberger-Castori S, Trapani F, Oertli D, Iezzi G. Dual role of tumour-infiltrating T helper 17 cells in human colorectal cancer. *Gut*. 2015

### **ABSTRACTS**

S. Varchetta, B. Oliviero, E. Paudice, **E. Cremonesi**, G. Michelone, M. Zaramella, M.U. Mondelli. Defective cytotoxic function of intrahepatic Natural Killer cells in chronic hepatitis C virus infection. (Present to AASLD 2009, Boston)

B. Oliviero, D. Mele, E. Degaspero, **E. Cremonesi**, S. Varchetta, A. Aghemo, M. G. Rumi, C. Tinelli, M. Colombo, M. U. Mondelli. Early NK cell activation predicts successful treatment outcome in chronic HCV infection. (Present to A.I.S.F. Annual meeting, Nizza 2010)

Stefania Varchetta, Dalila Mele, **Eleonora Cremonesi**, Barbara Oliviero, Mario U. Mondelli. Sialic-acid-binding immunoglobulin-like lectins-7 (siglec-7) binds HCV-E2 and is downregulated on NK cell of HCV infected patient. (Present to HCV Symposium, Siattle 2011)

Amicarella Francesca, **Cremonesi Eleonora**, Adamina Michel, Zuber Markus, Huber Xaver, Oertli Daniel, Lugli Alessandro, Zlobec Inti Trapani Francesca, Eppenberger Serenella, Terracciano Luigi M., Zajac Paul, Spagnoli Giulio C. and Iezzi Giandomenica. IL-17 production by tumor-infiltrating Th17 cells favors inflammation and promotes survival in human colorectal cancer. (Present to WIRM 2012 Davos)

Amicarella Francesca, Trapani Francesca, **Cremonesi Eleonora**, Muraro Manuele G, Mele Valentina, Padovan Elisabetta Adamina Michel, Zuber Markus, Huber Xaver, Oertli Daniel, Droseser Raoul, Lugli Alessandro, Zlobec Inti, Terracciano Luigi M, Zajac Paul, Spagnoli Giulio C., Eppenberger Serenella and Iezzi Giandomenica. Tumor infiltrating Th-17 cells promotes the recruitment of cytotoxic CD8<sup>+</sup> T cells into human colorectal cancer. (Present to WIRM 2013, Davos)

**Cremonesi Eleonora**, Amicarella Francesca, Padovan Elisabetta, Muraro Manuele G., Zajac Paul Heberer Michael, Spagnoli Giulio C., Oertli Daniel, Droseser Raoul, Huber Xaver, Zuber Markus, Adamina Michel, Terracciano Luigi M. and Iezzi Giandomenica. Chemotactic factors underlying tumor infiltration by immunocompetent cells in Colorectal cancer (CRC). (Present to WIRM 2013 Davos)

Christian Hirt, Adam Papadimitropoulos, Evangelos Panopoulos, Valentina Mele, Manuele Muraro, **Eleonora Cremonesi**, Raoul Droseser, Chantal Mengus, Michael Heberer, Daniel Oertli, Giandomenica Iezzi, Paul Zajac, Serenella Eppenberger-Castori, Luigi Tornillo, Luigi Terracciano, Ivan Martin and Giulio Spagnoli Resistance of colorectal cancer cells to 5-FU treatment in three dimensional cell culture models under perfusion involves BCL-2. (Present to AACR 2014 San Diego)

Adam Papadimitropoulos, Christian Hirt, Evangelos Panopoulos, Valentina Mele, Manuele Muraro, **Eleonora Cremonesi**, Raoul Droseser, Chantal Mengus, Michael Heberer, Daniel Oertli, Giandomenica Iezzi, Paul Zajac, Serenella Eppenberger-Castori, Luigi Tornillo, Luigi Terracciano, Ivan Martin and Giulio Spagnoli. A three dimensional (3D) perfusion bioreactor-based model of colorectal cancer for chemotherapeutic assessment. (Present to TermisEU 2014)

**Eleonora Cremonesi**, Francesca Amicarella, Elisabetta Padovan, Manuele G Muraro, Paul Zajac, Christian Hirt, Raoul Droseser, Daniel Oertli, Christian Nebiker, Markus Zuber, Michel Adamina, Raffaele Rosso, Michael Heberer, Giulio C Spagnoli, and Giandomenica Iezzi. Chemotactic factors underlying tumor infiltration by immunocompetent cells in colorectal cancer (oral presentation to EuCc congress in Basel, 2014)

**Eleonora Cremonesi**, Francesca Amicarella, Elisabetta Padovan, Manuele G Muraro, Valentina Mele, Paul Zajac, Daniel Oertli, Jesus Glaus Garzón, Lubor Borsig, and Giandomenica Iezzi. Effects of gut microbiome on colorectal cancer infiltration by immunocompetent cells (Present to Sgai-SSAI congress, 2015).

**Eleonora Cremonesi**, Francesca Amicarella, Elisabetta Padovan, Manuele G Muraro, Valentina Mele, Paul Zajac, Christian Hirt, Raoul Droseser, Daniel Oertli, Markus Zuber, Michel Adamina, Raffaele Rosso, Jesus Glaus Garzón, Lubor Borsig, Giulio C Spagnoli, and Giandomenica Iezzi. Chemotactic factors underlying tumor infiltration by immunocompetent cells in colorectal cancer. (Present to AACR Philadelphia, 2015).

**Eleonora Cremonesi**, Francesca Amicarella, Elisabetta Padovan, Manuele G Muraro, Valentina Mele, Paul Zajac, Daniel Oertli, Jesus Glaus Garzón, Lubor Borsig, and Giandomenica Iezzi. The gut microbiome modulates colorectal cancer infiltration by beneficial immune cells. (Present to cell-symposia: cancer, inflammation and immunity, Sitges 2015).

**Eleonora Cremonesi**, Francesca Amicarella, Elisabetta Padovan, Manuele G Muraro, Valentina Mele, Valeria Governa, Paul Zajac, Daniel Oertli, Jesus Glaus Garzón, Lubor Borsig, and Giandomenica Iezzi. Modulation of immune cell trafficking into human colorectal cancer by gut microbiota (Present to WIRM X, 2016 Davos).

## **SKILLS AND COMPETENCES**

In vitro separation and stimulation of monocytes, B-lymphocytes, T-lymphocytes, NK cells hepatocytes; tumor cells and neutrophils;

Cell cultures: murine cells (P815), human erythroleukemia cells (K562), human hepatoma cells (Huh7), Human microvessicol endothelial cells (HMEC), colorectal cancer cell lines (HT29, HCT116, COLO205, LS180, DLD1, HCT15)

Digestion of liver and colorectal cancer tissue;

Methods for direct and indirect labelling of whole blood, frozen lymphocytes and cell suspension obtained from tissues digestion.

Analysis of cell proliferation by CFSE labelling

Acquisition and analysis of data by using the Facscalibur flow cytometer (Becton Dickinson).

PCR techniques;

ELISA techniques;

Migration assay;

Good knowledge of Flow Jo software analysis;

Good knowledge of English.

Good knowledge of Windows applications, Internet browsing tools.

**2004:** European computer driving licence (ECDL).

## **OTHER WORK EXPERIENCE**

- Clerk at UPIM department store (2005-2009)
- Clothing store clerk (2004-2005)
- Pastry shop co-worker (2003)
- Garden center co-worker (2002)

## **PERSONAL INTERESTS**

Reading  
Latin-American dances  
Cooking

I AUTHORIZE PERSONAL DATA TREATMENT (ART. 23 OF LAW 196/03)

Eleonora Cremonesi